



Universiteit  
Leiden  
The Netherlands

## **Mechanisms underlying success and failure of cancer immunotherapy**

Beyranvand Nejad, E.

### **Citation**

Beyranvand Nejad, E. (2019, September 10). *Mechanisms underlying success and failure of cancer immunotherapy*. Retrieved from <https://hdl.handle.net/1887/77741>

Version: Not Applicable (or Unknown)

License: [Licence agreement concerning inclusion of doctoral thesis in the Institutional Repository of the University of Leiden](#)

Downloaded from: <https://hdl.handle.net/1887/77741>

**Note:** To cite this publication please use the final published version (if applicable).

Cover Page



Universiteit Leiden



The handle <http://hdl.handle.net/1887/77741> holds various files of this Leiden University dissertation.

**Author:** Beyranvand Nejad, E.

**Title:** Mechanisms underlying success and failure of cancer immunotherapy

**Issue Date:** 2019-09-10

The background of the entire page is a fluorescence microscopy image of tissue. It shows a dense network of green-stained cells or structures, with several distinct red-stained areas scattered throughout, possibly representing specific cell types or regions of interest. The overall texture is granular and complex.

# **Mechanisms underlying success and failure of cancer immunotherapy**

**Elham Beyranvand Nejad**



# **Mechanisms underlying success and failure of cancer immunotherapy**

Elham Beyranvand Nejad

The research described in this thesis was performed at the Departments of Immunohematology and Blood Transfusion and Medical Oncology of the Leiden University Medical Center, Leiden, The Netherlands. This work was supported by a grant from Dutch Cancer Society (KWF UL 2015-7824), BW-plus PhD grant from Leiden University Medical Center.

Financial support for the publication of this thesis was partially provided by Greiner Bio-One B.V.

ISBN: 978-94-6323-708-6

Cover design: Camilla Labrie and Elham Beyranvand Nejad, based on a confocal microscopy of the tumor tissue of SLP vaccinated TC-1 tumor bearing mouse which stained for immune cells; CD3, CD4, CD8 and CD11b.

Layout and printing: Gilderprint

All rights reserved. No part of this publication may be reproduced, stored in a retrieval system, or transmitted, in any form or by any means, electronic, mechanical, photocopying, recording, or otherwise, without permission of the author.

Copyright © 2019 Elham Beyranvand Nejad

# **Mechanisms underlying success and failure of cancer immunotherapy**

Proefschrift

ter verkrijging van  
de graad van Doctor aan de Universiteit Leiden,  
op gezag van Rector Magnificus prof.mr. C.J.J.M. Stolker,  
volgens besluit van het College voor Promoties  
te verdedigen op

dinsdag 10 september 2019 klokke 15:00 uur

door

Elham Beyranvand Nejad  
geboren te Teheran, Iran in 1986



**Promotor**

Prof. dr. S.H. van der Burg

**Co-promotor**

Dr. R. Arens

**Leden promotiecommissie**

Prof. dr. T.D. de Gruijl (VU University Medical Center Amsterdam)

Prof. dr. V. Umansky (German Cancer Research Center)

Prof. dr. C. van Kooten



Dedicated to my dear parents  
and  
my brother Ashkan



## Table of contents

Chapter 1:	Introduction	9
Chapter 2:	Tumor eradication by cisplatin is sustained by CD80/86-mediated costimulation of CD8 <sup>+</sup> T cells.	25
Chapter 3:	The microenvironment of tumor cells resisting non-curative immunotherapy determines the type of immune escape.	65
Chapter 4:	Counteracting interleukin-6 associated resistance to immunotherapy and chemotherapy.	105
Chapter 5	Demarcated thresholds of tumor-specific CD8 T cells elicited by MCMV-based vaccine vectors provide robust correlates of protection.	139
Chapter 6	The importance of correctly timing cancer immunotherapy.	171
Chapter 7	Summary and general discussion	205
Appendix	Nederlandse samenvatting	217
	Acknowledgments	221
	List of publications	224
	Curriculum vitae	225



# Chapter **1**

## Introduction



## Cancer and the immune system

In 1893, William Coley reported the first observation on the important role of the immune system in the treatment of cancer by using live bacteria as immune stimulant to cure the cancer (1). Since then, tremendous numbers of studies have been performed to expand the knowledge on the role of the immune system to prevent and control cancer development, a process called cancer immunosurveillance. Currently, our increased understanding about the composition and function of the immune system polished that concept. It has been demonstrated that the immune system can eradicate tumor cells and prevent tumor development but when this process is not complete; the immune system may foster alteration in the tumor's immunogenicity and facilitate tumor progression. This is the basis of the cancer immunoediting concept (2). Cancer immunoediting consists of three distinct phases termed “elimination”, “equilibrium” and “escape” (**Figure 1A**). In the elimination phase, which could be considered as an updated version of cancer immunosurveillance, the innate immune system senses cancer cells via different mechanisms, including danger signals such as type I IFNs, damage-associated molecular pattern (DAMP) molecules like high mobility group box 1 (HMGB1) or the stress ligands that are expressed on the surface of tumor cells. All these signals activate receptors on innate immune cells and establish a platform to induce tumor-specific adaptive immunity (3, 4). Especially, the T cells of the adaptive immune system can recognize tumor-associated antigens (TAA) and tumor-specific antigens (TSA) presented by major histocompatibility complex (MHC) molecules, resulting in the activation of tumor-specific effector T cell populations. Effector T cells can directly eradicate malignant cells and subsequently form memory T cells that provide long-term protection against tumors. The increased susceptibility of immunodeficient mice, lacking either interferon-gamma ( $\text{IFN}\gamma$ ) responsiveness or adaptive immunity by lacking T cells, B cells and natural killer T (NKT) cells, to develop carcinogen-induced and spontaneous primary tumors underscores the importance of adaptive immunity at the elimination phase (5). If the immune system fails in eradicating all tumor cells in this phase, residual tumor cells enter the equilibrium phase, in which the adaptive immune system controls the tumor outgrowth and edits the immunogenicity of the tumor. At the tumor cell level, loss of antigen, downregulation of MHC I or of the antigen processing machinery as well as loss in  $\text{IFN}\gamma$  responsiveness could lead to decreased recognition of tumor cells by immune cells (2). In addition, tumor cells can upregulate the expression of anti-apoptotic molecules to increase resistance to the cytotoxic anti-tumor response. All these mechanisms could lead to the immunoselection of poorly immunogenic tumor cell variants. At the immune level, the production of immunosuppressive cytokines, expression of galectins, or expression of ligands for checkpoint molecules by tumor cells and the attraction of immunosuppressive leukocytes such as the regulatory T cells (Tregs), M2 macrophages and myeloid-derived suppressor cells (MDSCs) eventually lead to local and systemic immune suppression (6). Therefore, it is worth to design cancer immunotherapeutic

interventions that potentially can interfere with these different mechanisms negatively influencing a successful anti-tumor response.

## Cancer therapeutic strategies

Several cancer therapeutic strategies have been developed already. These strategies can be characterized as mechanisms to debulk the tumor mass or to boost the immune response to cancer. Surgery, radiotherapy and chemotherapy are the prototypic examples of conventional therapy aiming to debulk the tumor mass and inhibit tumor growth. Considering the key role of surgery and tumor dissection in diagnosing cancer type and stage, it might be the first treatment modality to reduce tumor mass. However, there is still a possibility that complete dissection of the tumor cannot be achieved by surgery. Therefore, surgery can be combined by other methods of conventional therapy. For example, if the tumor is localized to one area of the body, ionizing radiation by radiotherapy can additionally control or kill the tumor cells. Such a cancer treatment modality can also be considered as adjuvant therapy after surgery to inhibit the possible tumor recurrence of the residual tumor cells. However, in some cases due to the localization of the tumor, surgery or radiotherapy is not feasible. In this regard, chemotherapy alone or in combination with the aforementioned therapies is highly recommended. Notwithstanding that these conventional therapy modalities have been developed to reduce the tumor burden, several studies have shown that these therapies affect the immune system, and in many cases even rely on the immune system for their efficacy (7-12). In appreciation of the important role of the immune system in controlling cancer development, various immunotherapeutic approaches have been designed to induce or augment anti-tumor immune responses (13). In recent years, immunotherapy has become an important cancer therapeutic strategy. Given its success, it has become first line therapy for certain stages of tumors.

## Anti-tumor Immunity: APCs, T cells and their regulation

To induce proper anti-tumor responses that control tumor progression, different components of the immune systems need to interact with each other. In this regard, APCs play crucial roles in instructing T cells to induce antigen-specific T cells. Macrophages, dendritic cells (DCs) and B cells are the examples of APCs. B cells originate from common lymphoid progenitor cells in bone marrow and develop further in this organ. Macrophages and DCs originate from common myeloid progenitor and develop further in the bone marrow. These cells enter the blood in the form of monocytes and in the tissues differentiate further into macrophages and DCs. Basophils, neutrophils and eosinophils are the granulocytes, which also originate from myeloblasts. Beside the role of macrophages and DCs in antigen-presentation, granulocytes also function as phagocytic and cytokine producing cells. All



these cells serve in host defense mechanisms by recognizing pathogen-associated molecular patterns (PAMPs) and DAMPs. Upon ligation of PAMPs and DAMPs to Toll-like receptors (TLRs) and nucleotide oligomerization domain (NOD)-like receptors, APCs become activated. Following activation, APCs gain the capacity to activate lymphocytes and foster cytokine and chemokine production. To characterize the different subsets of the myeloid lineage, various markers have been recognized. However, in pathological conditions such as tumor development, myeloid cells can develop to functionally distinct populations such as MDSCs and tumor associated macrophages (TAMs). Although MDSCs and TAMs can still share similar markers as other myeloid cells, they have potent suppressive functions.

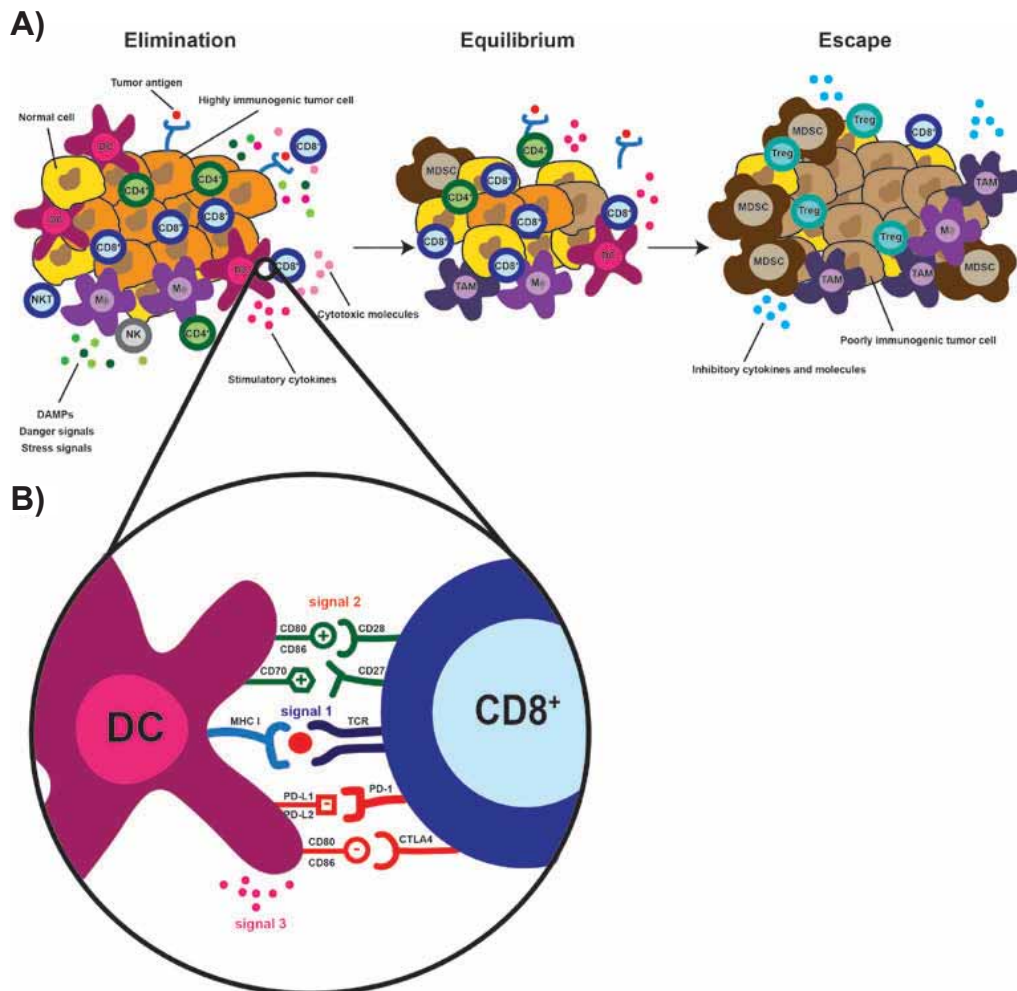
T cell precursors originate from hematopoietic stem cells in the bone marrow and further develop in the thymus (14). After development processes in the thymus, naïve T cells enter the periphery and circulate in blood and secondary lymphoid organs until they encounter their cognate antigen in the context of MHC molecules (15). For proper antigen-specific T cell induction and activation, three signals should be provided from APCs to T cells (**Figure 1B**) (16). The first signal is delivered by the presentation of antigen in the presence of MHC complex to the T cell receptor (TCR). For this signal, peptides originated from intracellular or extracellular sources need to be taken up by APCs, processed and presented on the MHC complex on these cells (16). In this regard, presentation of exogenous antigens by MHC

#### Figure 1 - Interaction of tumor cells and immune cells in the tumor microenvironment

**A) Three phases of cancer immunoediting.** Cancer immunoediting consists of three sequential phases: elimination, equilibrium and escape. In the first phase, the innate immune system senses tumor cells via different mechanisms including danger signals such as type I IFNs, damage-associated molecular patterns (DAMPs) like high mobility group box 1 (HMGB1) or the stress ligands that are expressed on the surface of tumor cells (i.e. RAE-1). Binding of these molecules to their receptors on immune cells initiate the T-cell specific anti-tumor response. These T cells can recognize tumor antigen and further eradicate the tumor cells by releasing cytotoxic molecules such as perforin or granzymes. If the immune system is not able to eradicate all the tumor cells at this step, the remnant tumor cells enter to the equilibrium phase. In this phase, the adaptive immune system controls the tumor outgrowth in a steady state. In the last phase, the residual tumor cells escape from the immune response by various mechanisms. All these steps could lead to immunoselection of poorly immunogenic tumor cell variants.

**B) Three signals for T cell activation.** For proper antigen-specific T cell induction and activation, three signals should be provided from APCs to T cells. The first signal is delivered by the presentation of peptide antigens by MHC complexes to the T cell receptor (TCR). For this signal, tumor antigens need to be taken up by APCs, processed and presented on MHC molecules (16). This leads to the priming of naïve CD8 T cells to become cytotoxic T lymphocytes (CTLs). The second signal is driven by costimulatory molecules expressed on APCs, which can bind to their unique receptors on T cells. Examples of such costimulatory molecules are CD80/CD86 and CD70 that can bind to CD28 and CD27, respectively. The third signal is delivered by cytokines produced by APCs that bind to cytokine receptors expressed by T cells. In this regard, IL-12 and type I interferons (IFNs) play important roles in the activation of CD8 T cells. All these signals lead to proper induction of tumor antigen-specific CTLs, which can potentially kill the tumor cells. The activation of T cells is controlled by inhibitory signals driven by inhibitory receptors expressed on activated T cells such as PD-1 and CTLA-4, which are triggered by PDL-1/2 and CD80/CD86, respectively.

class I molecules expressed by APCs, a process termed cross-presentation, leads to the priming of naïve CD8 T cells to become cytotoxic T lymphocytes (CTLs) (17). To induce fully activated T cells, two complementary signals are required. The second signal is driven by costimulatory molecules expressed on APCs, which can bind to their unique receptors on T cells (16). Two major groups of costimulatory receptors have been identified on T cells; the immunoglobulin (Ig) superfamily and the tumor necrosis factor receptor (TNFR) superfamily. Different examples of these receptors have been depicted in **Figure 1B**. The Ig superfamily CD28 and the TNFR family member CD27, which bind to CD80/CD86 (B7.1/B7.2) and CD70, respectively, are constitutively expressed on naïve T cells (18, 19). Other costimulatory receptors, such as ICOS, OX40, and 4-1BB are upregulated after activation



of T cells by TCR signaling (18). In addition to signal 1 and 2, the third signal is delivered by cytokines produced by APCs that bind to cytokine receptors expressed by T cells (20). In this regard, IL-12 and type I interferons (IFNs) play important roles in the activation of CD8 T cells. Eventually, all these signals lead to the induction of antigen-specific CTLs, which expand clonally and are able to migrate to the tumor and exert effector functions. CTLs induce their cytotoxic functions to eradicate tumor cells by a) releasing cytotoxic molecules such as perforin and granzyme B, b) producing cytokines like IFN $\gamma$  and tumor necrosis factor alpha (TNF $\alpha$ ), c) expressing apoptosis-inducing ligands such as TNF-related apoptosis-inducing ligand (TRAIL) and Fas (21). To prevent immune-mediated pathology T cell responses need to be controlled. This can be achieved by different mechanisms including the elimination of APCs or upregulation of coinhibitory receptors. Similar to stimulatory molecules, expression of a variety of coinhibitory receptors can be induced following T cell activation (**Figure 1B**). CTLA-4 is a coinhibitory receptor that competes with CD28 for interaction with CD80 and CD86, thereby dampening the T cell activation (22). Another example of an inhibitory pathway is the interaction of PD1 with its ligands PDL1 and PDL2/. PD-1 is upregulated on T cells upon activation, while PDL1 is broadly expressed on immune cells such as monocytes and macrophages but also on non-immune cells such as tumor cells (23). Other examples of coinhibitory molecules are T cell immunoglobulin and mucin domain 3 (TIM-3) and lymphocyte-activation gene 3 (LAG3), which are expressed on T cells following long-lasting activation. After the contraction of the T cell response, a small proportion of the antigen-specific T cells develop into memory T cells, which are capable of inducing recall responses upon encounter to the same antigen. Besides the induction of tumor specific CD8 T cells, subsets of CD4 T cells play also important roles. Based on the expression of transcription factors and cytokine profiles, CD4 T cells are sub categorized to T helper (Th1), Th2, Th17, T follicular helper cells (TFH) and Tregs. Th1 cells are differentiated by IL-2 and are characterized by the expression of the transcription factor T-bet and the production of TNF $\alpha$  and IFN $\gamma$ . Th1 cells can kill tumor cells directly via the TRAIL pathway or inhibit tumor cells growth and induce tumor senescence in combination with IFN $\gamma$  (24, 25). Th1 can also mediate indirect anti-tumor effect by IFN $\gamma$  via recruitment and activation of various immune cells, upregulation of class I and co-stimulatory molecules on APCs (26). In addition, these cells can promote anti-tumor activity of CTL by producing cytokines or activating APCs which can prime the CTL. CD4 T cells express CD40-ligand (CD40L) on their surface upon antigen recognition. Ligation of CD40L to the CD40 expressed on the surface of APCs increase antigen presentation and co-stimulatory capacity of these cells, thereby provide a license to CTL priming (27). Besides, Th1 cells can activate and recruit myeloid cells and CTLs to the tumor, thereby providing help to the establishment of an adequate tumor-specific CD8 T cell response (28). In contrast to Th1 cells, Tregs which are known as immunosuppressive cells can potentially dampen the adaptive immune response to tumors (29).

## Immunotherapy of cancer

Since the immune system is involved in the different phases of cancer immunoediting, several immunotherapeutic strategies have been designed to augment the anti-tumor immune response. These strategies can target different components of the immune system to induce or maintain the tumor-specific T cell response. Adoptive cell therapy (ACT) based on ex vivo isolation and expansion of antigen-specific T cells has been developed and shows promising results in multiple cancers (30). Another principle is based on providing antigenic stimulation. Vaccines including synthetic peptides, viral vectors, RNA or DNA vectors aim to enhance the magnitude of the tumor-specific T cell response. In the category of peptide vaccines, synthetic short-peptides (SSP) have been designed to encode minimal MHC class I molecule-binding epitopes. However, several problems including insufficient immunogenicity, structural and/or conformational instability and chemical instability due to degradation led to the invention of synthetic long-peptide (SLP) vaccines (31). In this case, SLPs can be designed as long and/or overlapping peptides. It is worthwhile to mention that overlapping HPV16 SLP vaccines containing the sequence of E6 and E7 oncogenes has shown partial and complete regression in patients with HPV-16 induced premalignant lesions of the vulva (32, 33). In addition, since these SLPs contain longer epitopes than minimal epitopes, they have to be taken up by the professional APCs, processed and presented in MHC class I or II molecules, thereby ensuring the presentation of tumor antigens by APCs and proper priming of T cells by these APCs. Moreover, adjuvants can be combined with SLP vaccines to improve the immune response. Different examples of such adjuvants are TLRs ligands, alum, oil and water emulsions and cytokines (34). From all these adjuvants, CpG, which is a TLR9 agonist, and IFA (Freund's incomplete adjuvant) are used widely in combination with peptide vaccines in mice. Beside peptide vaccines, RNA vaccines, plasmid DNA and viral vector-based vaccines are also used to activate the immune system. DNA vaccines are genetically modified to express the tumor antigen of interest by using viral promoter elements and transcriptional terminator sequences. Viral vector-based vaccines are engineered with an insertion of a gene encoding the protein of interest (e.g. tumor antigens) into the viral genome. Either direct priming or cross-priming of the antigen encoded by plasmid or virus can lead to the induction of antigen-specific T cell responses (35). All of these vaccine strategies have shown promising results in clinical trials (36, 37).

Another immunotherapeutic approach to improve the tumor specific T cell response is the application of agonistic antibodies that target costimulatory molecules. Examples of these costimulatory molecules that have been targeted for cancer immunotherapy are CD70/CD27, CD40L/CD40, 4-1BBL/4-1BB, OX40L/OX40 (38). The successful efficacy of these antibodies has been shown as stand-alone therapy or in combination with other immunotherapeutic approaches (39, 40).

T cell responses can also be augmented by other immunomodulatory compounds such as cytokines (41). Cytokines such as granulocyte-macrophage colony-stimulating factor (GM-CSF) can be used to stimulate the APCs, which causes proliferation of DCs and macrophages. On the other hand, some cytokines such as IL-2 and IL-12 can induce direct T cell activation and proliferation, and the use of these cytokines in the clinic as stand-alone therapy improved tumor immunity (42, 43). In addition, some cytokines such as type I interferons, known for their roles in innate immune response against viral infection, can affect both T cells and DCs leading to enhanced differentiation of Th1 cells and increased proliferation and survival of T cells (44, 45). Since, systemic administration of these cytokines may induce toxicity as these cytokines have very broad effects on the cells in body. Hence it should be taken into account to design more optimal immunotherapy approaches.

Considering the important role of the tumor microenvironment in controlling the anti-tumor response, another strategy is based on counteracting immune suppression. As mentioned before, coinhibitory receptors are expressed on T cells to dampen the T cell response following the activation of T cells. However, tumor cells as well as myeloid cells in the tumor microenvironment can take advantage of these inhibitory signals by expressing coinhibitory ligands for these receptors, thus dampening the anti-tumor induced T cell response. Therefore, these T cell inhibitory molecules called immune checkpoints are interesting targets for immunotherapy. In this regard, various blocking antibodies targeting CTLA-4, PD-1 or its ligand PD-L1, have been successfully developed to block the induction of the inhibitory signals (23). Since T cell inhibitory receptors are expressed on CD8 T cells as well as on CD4 T cells including Tregs, the blocking antibodies targeting the T cell inhibitory molecules can mediate their effects by both selective depletion of Tregs and by directly stimulating the expansion of T cells. Checkpoint blockade therapies targeting other coinhibitory molecules are currently being developed.

Besides coinhibitory receptors, immunosuppressive molecules or cytokines are also produced in the tumor microenvironment by tumor cells or immunosuppressive immune cells. An example of an inhibitory cytokine is IL-10. This cytokine is produced by various immune cells such as monocytes, Th2 cells, Tregs, and B cells. In addition, certain tumor cells can also produce IL-10. Effects of this cytokine include dampening the immune response by having direct immunosuppressive effects on T cells and APCs. Notably, IL-10 production is associated with the suppressive effect of Tregs and MDSCs (46). Another immunosuppressive cytokine is transforming growth factor beta (TGF- $\beta$ ), which is also produced by various cells including immune cells, epithelial cells, and endothelial cells (47). TGF $\beta$  not only inhibits T cell proliferation but also functions as a positive differentiation factor for Tregs and is a negative differentiation factor for Th1 and Th2 cells (48). Besides

these cytokines, tumor cells and immune cells in the tumor microenvironment can produce other immunosuppressive molecules that can be targeted for the immunotherapy. For example, Indoleamine 2,3-dioxygenase (IDO) and arginase 1 which are important in the regulation of immune cell reactivity such as T cell activation can be targeted to alleviate the immunosuppression (49, 50). Moreover, depleting the immunosuppressive cells such as Tregs and MDSCs can be beneficial to the anti-tumor induced response. This can be achieved by using depleting antibodies for the markers expressed on these cells such as CD25, which is expressed on the majority of Tregs.

## Immunological effects of chemotherapy

Chemotherapeutic drugs were originally developed to inhibit tumor cell growth and division. These agents impede cell mitosis by various mechanisms mainly by induction of DNA damage and impairment of the DNA repair processes, thereby inducing apoptosis in replicating cells. Due to the cytotoxic effects of these agents it was believed for a long time that chemotherapy has suppressive effects on the immune system. In spite of data from the late 1960s, indicating a role of the immune system in the clinical efficacy of chemotherapy, it was only recently that chemotherapeutic agents were shown to exert direct and indirect immunostimulatory effects. Studies showing the importance of myeloid cells as well as T cells in chemotherapy-induced anti-tumor responses underscore the impact of chemotherapy on the immune system (51, 52).

The types of chemotherapies causing a type of cancer cell death that elicits immunologic responses, is called immunogenic cell death (ICD). The immunological response is based on the induction of DAMPs including the exposure of endoplasmic reticulum chaperones such as calreticulin on the cell surface, the secretion of adenosine triphosphate (ATP) and the release of HMGB1 (53). Anthracyclines (e.g. doxorubicin) are chemotherapeutic agents known to improve tumor antigen uptake, processing and presentation by APCs to T cells, thereby improving the tumor specific T cell response (54). Furthermore, cyclophosphamide modulates the gene and protein expression of several immunomodulatory factors including danger signals, pattern recognition receptors, inflammatory mediators, growth factors, cytokines, chemokines, and chemokine receptors (55). It also induces Th17 related gene signature which is associated with an increase in Th17, Th1 and CD25<sup>+</sup> CD4<sup>+</sup> Foxp3<sup>-</sup> T cells (55). It has been shown that cyclophosphamide changes the composition of microbiota in small intestine which are important in generating a specific subset of pathogenic Th17 and memory Th1 immune response (56). Moreover, some chemotherapeutic agents such as 5-fluorouracil and gemcitabine have an ability to boost the antigenicity of tumors, for example by restoration of MHC I expression (57). In addition, oxaliplatin elevates the tumoricidal activity of macrophages and neutrophils (57). Another example is paclitaxel, which prompts DC maturation and cross priming as well as increases tumor infiltration by NK cells and



macrophages (58-60). Chemotherapies such as paclitaxel, cisplatin and doxorubicin can enhance the sensitivity of tumor cells to the CTL mediated killing by increasing the permeability of tumor cells to granzyme B in a perforin-independent manner (61). Cisplatin can also synergize with TNF $\alpha$  to enhance tumor cell death (62).

Considering the immunosuppressive features of the tumor microenvironment, some chemotherapy agents support the anti-tumor immune response by depleting or inhibiting the immunosuppressive activity of immunosuppressive cells. In this case, 5-fluorouracil, cyclophosphamide, gemcitabine and paclitaxel are examples of chemotherapies that can deplete tumor-infiltrating Tregs and/or circulating MDSCs (57). In addition, the combination of carboplatin and paclitaxel were shown to normalize the tumor-mediated alteration of the myeloid cell composition in mice and men, thereby increasing the effect of immunotherapy (63). Thus, chemotherapy as stand-alone therapy or in combination with immunotherapeutic approaches can enhance the induced anti-tumor immune response.

## Aim and scope of this thesis

In the clinic, several forms of immunotherapy are combined with the standard treatments, including chemotherapy, specific for the tumor type that is treated. Translational studies trying to understand the different outcomes in patients have led to new questions and hypotheses. The studies described in this thesis are to answer some of these questions and to test the associated hypotheses in order to lay the foundation for improved combination therapies. Cisplatin is often used to treat patients with immunogenic cancers and would be one of the standards of care treatments to be combined with immunotherapy. Therefore, in **chapter 1**, we focused on the immunological effects of cisplatin. We reveal that the maximum tolerated dose of cisplatin requires the immune system for definite cure of tumor-bearing mice. Cisplatin not only has a direct toxicity on tumor cells, greatly slowing down tumor cell growth, but it also stimulates the immune system. The immune-mediated tumor destruction of cisplatin requires myeloid cells and T cells and is associated with a much stronger infiltration of intratumoral inflammatory APCs, displaying higher expression of T cell costimulatory molecules following the release of DAMPs induced by tumor cell death.

Notably, immune monitoring of our therapeutic vaccination trials in patients with HPV-induced diseases showed that the vaccine-induced immune response is weaker in patients with advanced or late stage cancer. Therefore, in **chapter 2**, we made use of a suboptimal vaccination strategy for HPV16 SLP vaccination in mice to mimic this. We show that suboptimal vaccination initially still is able to induce tumor regression and to control the outgrowth of HPV-associated tumor cells but eventually tumors recur and progressively grow. We demonstrate that a suboptimal anti-tumor response results in immune editing and



secondary resistance. Recurring tumors displayed a deregulation in genes associated with the apoptosis pathways including P53 and genes involved in epithelial–mesenchymal transition (EMT) such as TGF $\beta$ ,  $\beta$ -catenin and a marked reduction in the number of infiltrating leukocytes, in particular CD8 T cells. Administration of the chemotherapeutic agent cisplatin or blocking antibody for TGF $\beta$  after initial regression could prevent the relapse. Importantly, these relapsed tumors, when transplanted to a naïve host, were not sensitive to immunotherapy anymore except when cisplatin was co-administered to increase immune infiltration, confirming the importance of tumor microenvironment in combination therapy to achieve the successful control of tumor burden.

Previous studies had shown that for many tumors the resistance to chemotherapy was associated with increased IL-6 production by tumor cells. Work of our group suggested that rather than a direct resistance of tumor cells to chemotherapy, the IL-6 induced differentiation of myeloid cells to an immune suppressive phenotype may underlie chemoresistance. In **chapter 3**, we show that IL-6 produced by tumor cells indeed impairs the anti-tumor efficacy of cisplatin chemotherapy but also that of HPV16 SLP vaccine mediated immunotherapy. Resistance was associated with a severely IL-6-mediated alteration of systemic and local myeloid cell phenotypes as well as an impaired tumor-specific T cell response. Several strategies to block this IL-6 mediated effect were studied, but they were complicated by the fact that IL-6 signaling was also required for the launch of an effective vaccine-induced tumor-specific T cell response and the optimal function of tumoricidal macrophages during initial tumor regression. Timing of the therapeutic strategy was key in this case since IL-6 blockade after initial tumor regression improved the response of IL-6 producing tumors to immunotherapy.

In order to induce a long-term sustained effector T cell response, we examined the potency of mouse cytomegalovirus to be used as a viral vector-based vaccine in **Chapter 4**. We demonstrated that the demarcated thresholds of vaccine-specific T cells correlate to tumor protection. Recognizing the fact that at each phase of the antitumor immune response a different type of help might have to be provided to obtain maximal therapeutic efficacy, the correct timing of various types of chemotherapeutic agents or immune modulators when used in combination with different T cell based immunotherapeutic approaches is discussed in **chapter 5**. This chapter also emphasizes on the importance of immunomonitoring as essential strategy to design the appropriate sequencing of the combination therapies.

Finally, **chapter 6** discusses the general aspects and relevance of the studies mentioned in this thesis in the content of combination therapies. The recent literature and future prospective of cancer therapeutic strategies will be argued.

## References

1. Coley WB. The treatment of malignant tumors by repeated inoculations of erysipelas. With a report of ten original cases. 1893. *Clin Orthop Relat Res*. 1991(262):3-11.
2. Schreiber RD, Old LJ, Smyth MJ. Cancer immunoediting: integrating immunity's roles in cancer suppression and promotion. *Science*. 2011;331(6024):1565-70.
3. Guerra N, Tan YX, Joncker NT, Choy A, Gallardo F, Xiong N, et al. NKG2D-deficient mice are defective in tumor surveillance in models of spontaneous malignancy. *Immunity*. 2008;28(4):571-80.
4. Sims GP, Rowe DC, Rietdijk ST, Herbst R, Coyle AJ. HMGB1 and RAGE in inflammation and cancer. *Annu Rev Immunol*. 2010;28:367-88.
5. Vesely MD, Kershaw MH, Schreiber RD, Smyth MJ. Natural innate and adaptive immunity to cancer. *Annu Rev Immunol*. 2011;29:235-71.
6. Gajewski TF, Fuertes M, Spaapen R, Zheng Y, Kline J. Molecular profiling to identify relevant immune resistance mechanisms in the tumor microenvironment. *Curr Opin Immunol*. 2011;23(2):286-92.
7. Campbell AM, Decker RH. Harnessing the Immunomodulatory Effects of Radiation Therapy. *Oncology (Williston Park)*. 2018;32(7):370-4, CV3.
8. Honeychurch J, Illidge TM. The influence of radiation in the context of developing combination immunotherapies in cancer. *Ther Adv Vaccines Immunother*. 2017;5(6):115-22.
9. Ghiringhelli F, Apetoh L. The interplay between the immune system and chemotherapy: emerging methods for optimizing therapy. *Expert Rev Clin Immunol*. 2014;10(1):19-30.
10. Ma Y, Kepp O, Ghiringhelli F, Apetoh L, Aymeric L, Locher C, et al. Chemotherapy and radiotherapy: cryptic anticancer vaccines. *Semin Immunol*. 2010;22(3):113-24.
11. Vacchelli E, Bloy N, Aranda F, Buque A, Cremer I, Demaria S, et al. Trial Watch: Immunotherapy plus radiation therapy for oncological indications. *Oncoimmunology*. 2016;5(9):e1214790.
12. Galluzzi L, Buque A, Kepp O, Zitvogel L, Kroemer G. Immunological Effects of Conventional Chemotherapy and Targeted Anticancer Agents. *Cancer Cell*. 2015;28(6):690-714.
13. Pham T, Roth S, Kong J, Guerra G, Narasimhan V, Pereira L, et al. An Update on Immunotherapy for Solid Tumors: A Review. *Ann Surg Oncol*. 2018.
14. Schwarz BA, Bhandoola A. Trafficking from the bone marrow to the thymus: a prerequisite for thymopoiesis. *Immunol Rev*. 2006;209:47-57.
15. Klein L, Hinterberger M, Wirmsberger G, Kyewski B. Antigen presentation in the thymus for positive selection and central tolerance induction. *Nat Rev Immunol*. 2009;9(12):833-44.
16. Williams MA, Bevan MJ. Effector and memory CTL differentiation. *Annu Rev Immunol*. 2007;25:171-92.
17. Joffre OP, Segura E, Savina A, Amigorena S. Cross-presentation by dendritic cells. *Nat Rev Immunol*. 2012;12(8):557-69.
18. Croft M. The role of TNF superfamily members in T-cell function and diseases. *Nat Rev Immunol*. 2009;9(4):271-85.
19. Sharpe AH, Freeman GJ. The B7-CD28 superfamily. *Nat Rev Immunol*. 2002;2(2):116-26.
20. Curtsinger JM, Mescher MF. Inflammatory cytokines as a third signal for T cell activation. *Curr Opin Immunol*. 2010;22(3):333-40.
21. Russell JH, Ley TJ. Lymphocyte-mediated cytotoxicity. *Annu Rev Immunol*. 2002;20:323-70.
22. Krummel MF, Allison JP. CD28 and CTLA-4 have opposing effects on the response of T cells to stimulation. *J Exp Med*. 1995;182(2):459-65.
23. Mahoney KM, Rennert PD, Freeman GJ. Combination cancer immunotherapy and new immunomodulatory targets. *Nat Rev Drug Discov*. 2015;14(8):561-84.

24. Knutson KL, Disis ML. Tumor antigen-specific T helper cells in cancer immunity and immunotherapy. *Cancer Immunol Immunother.* 2005;54(8):721-8.
25. Braumuller H, Wieder T, Brenner E, Assmann S, Hahn M, Alkhaled M, et al. T-helper-1-cell cytokines drive cancer into senescence. *Nature.* 2013;494(7437):361-5.
26. Parker BS, Rautela J, Hertzog PJ. Antitumour actions of interferons: implications for cancer therapy. *Nat Rev Cancer.* 2016;16(3):131-44.
27. Schoenberger SP, Toes RE, van der Voort EI, Offringa R, Melief CJ. T-cell help for cytotoxic T lymphocytes is mediated by CD40-CD40L interactions. *Nature.* 1998;393(6684):480-3.
28. Hung K, Hayashi R, Lafond-Walker A, Lowenstein C, Pardoll D, Levitsky H. The central role of CD4(+) T cells in the antitumor immune response. *J Exp Med.* 1998;188(12):2357-68.
29. Shevach EM. Regulatory T cells in autoimmunity\*. *Annu Rev Immunol.* 2000;18:423-49.
30. Gajewski TF. Cancer immunotherapy. *Mol Oncol.* 2012;6(2):242-50.
31. Hans D, Young PR, Fairlie DP. Current status of short synthetic peptides as vaccines. *Med Chem.* 2006;2(6):627-46.
32. Kenter GG, Welters MJ, Valentijn AR, Lowik MJ, Berends-van der Meer DM, Vloon AP, et al. Vaccination against HPV-16 oncoproteins for vulvar intraepithelial neoplasia. *N Engl J Med.* 2009;361(19):1838-47.
33. Welters MJ, Kenter GG, de Vos van Steenwijk PJ, Lowik MJ, Berends-van der Meer DM, Essahsah F, et al. Success or failure of vaccination for HPV16-positive vulvar lesions correlates with kinetics and phenotype of induced T-cell responses. *Proc Natl Acad Sci U S A.* 2010;107(26):11895-9.
34. Alving CR, Peachman KK, Rao M, Reed SG. Adjuvants for human vaccines. *Curr Opin Immunol.* 2012;24(3):310-5.
35. Anderson RJ, Schneider J. Plasmid DNA and viral vector-based vaccines for the treatment of cancer. *Vaccine.* 2007;25 Suppl 2:B24-34.
36. van der Burg SH. Correlates of immune and clinical activity of novel cancer vaccines. *Semin Immunol.* 2018.
37. van der Burg SH, Arens R, Ossendorp F, van Hall T, Melief CJ. Vaccines for established cancer: overcoming the challenges posed by immune evasion. *Nat Rev Cancer.* 2016;16(4):219-33.
38. Moran AE, Kovacsovics-Bankowski M, Weinberg AD. The TNFRs OX40, 4-1BB, and CD40 as targets for cancer immunotherapy. *Curr Opin Immunol.* 2013;25(2):230-7.
39. Bullock TN. TNF-receptor superfamily agonists as molecular adjuvants for cancer vaccines. *Curr Opin Immunol.* 2017;47:70-7.
40. Ward-Kavanagh LK, Lin WW, Sedy JR, Ware CF. The TNF Receptor Superfamily in Co-stimulating and Co-inhibitory Responses. *Immunity.* 2016;44(5):1005-19.
41. Arens R, van Hall T, van der Burg SH, Ossendorp F, Melief CJ. Prospects of combinatorial synthetic peptide vaccine-based immunotherapy against cancer. *Semin Immunol.* 2013;25(2):182-90.
42. Gollob JA, Mier JW, Veenstra K, McDermott DF, Clancy D, Clancy M, et al. Phase I trial of twice-weekly intravenous interleukin 12 in patients with metastatic renal cell cancer or malignant melanoma: ability to maintain IFN-gamma induction is associated with clinical response. *Clin Cancer Res.* 2000;6(5):1678-92.
43. Portielje JE, Kruit WH, Schuler M, Beck J, Lamers CH, Stoter G, et al. Phase I study of subcutaneously administered recombinant human interleukin 12 in patients with advanced renal cell cancer. *Clin Cancer Res.* 1999;5(12):3983-9.
44. Arico E, Belardelli F. Interferon-alpha as antiviral and antitumor vaccine adjuvants: mechanisms of action and response signature. *J Interferon Cytokine Res.* 2012;32(6):235-47.
45. Huber JP, Farrar JD. Regulation of effector and memory T-cell functions by type I interferon. *Immunology.* 2011;132(4):466-74.

46. Berti FCB, Pereira APL, Cebinelli GCM, Trugilo KP, Brajao de Oliveira K. The role of interleukin 10 in human papilloma virus infection and progression to cervical carcinoma. *Cytokine Growth Factor Rev.* 2017;34:1-13.
47. Blobel GC, Schiemann WP, Lodish HF. Role of transforming growth factor beta in human disease. *N Engl J Med.* 2000;342(18):1350-8.
48. Li MO, Flavell RA. Contextual regulation of inflammation: a duet by transforming growth factor-beta and interleukin-10. *Immunity.* 2008;28(4):468-76.
49. Brandacher G, Perathoner A, Ladurner R, Schneeberger S, Obrist P, Winkler C, et al. Prognostic value of indoleamine 2,3-dioxygenase expression in colorectal cancer: effect on tumor-infiltrating T cells. *Clin Cancer Res.* 2006;12(4):1144-51.
50. Kim SH, Roszik J, Grimm EA, Ekmekcioglu S. Impact of l-Arginine Metabolism on Immune Response and Anticancer Immunotherapy. *Front Oncol.* 2018;8:67.
51. Casares N, Pequignot MO, Tesniere A, Ghiringhelli F, Roux S, Chaput N, et al. Caspase-dependent immunogenicity of doxorubicin-induced tumor cell death. *J Exp Med.* 2005;202(12):1691-701.
52. DeNardo DG, Brennan DJ, Rexhepaj E, Ruffell B, Shiao SL, Madden SF, et al. Leukocyte complexity predicts breast cancer survival and functionally regulates response to chemotherapy. *Cancer Discov.* 2011;1(1):54-67.
53. Garg AD, More S, Rufo N, Mece O, Sassano ML, Agostinis P, et al. Trial watch: Immunogenic cell death induction by anticancer chemotherapeutics. *Oncoimmunology.* 2017;6(12):e1386829.
54. Gebremeskel S, Johnston B. Concepts and mechanisms underlying chemotherapy induced immunogenic cell death: impact on clinical studies and considerations for combined therapies. *Oncotarget.* 2015;6(39):41600-19.
55. Moschella F, Valentini M, Arico E, Macchia I, Sestili P, D'Urso MT, et al. Unraveling cancer chemotherapeutic mechanisms by gene and protein expression profiling of responses to cyclophosphamide. *Cancer Res.* 2011;71(10):3528-39.
56. Viaud S, Saccheri F, Mignot G, Yamazaki T, Daillere R, Hannani D, et al. The intestinal microbiota modulates the anticancer immune effects of cyclophosphamide. *Science.* 2013;342(6161):971-6.
57. Galluzzi L, Zitvogel L, Kroemer G. Immunological Mechanisms Underneath the Efficacy of Cancer Therapy. *Cancer Immunol Res.* 2016;4(11):895-902.
58. Demaria S, Volm MD, Shapiro RL, Yee HT, Oratz R, Formenti SC, et al. Development of tumor-infiltrating lymphocytes in breast cancer after neoadjuvant paclitaxel chemotherapy. *Clin Cancer Res.* 2001;7(10):3025-30.
59. Pfannenstiel LW, Lam SS, Emens LA, Jaffee EM, Armstrong TD. Paclitaxel enhances early dendritic cell maturation and function through TLR4 signaling in mice. *Cell Immunol.* 2010;263(1):79-87.
60. Geller MA, Bui-Nguyen TM, Rogers LM, Ramakrishnan S. Chemotherapy induces macrophage chemoattractant protein-1 production in ovarian cancer. *Int J Gynecol Cancer.* 2010;20(6):918-25.
61. Ramakrishnan R, Assudani D, Nagaraj S, Hunter T, Cho HI, Antonia S, et al. Chemotherapy enhances tumor cell susceptibility to CTL-mediated killing during cancer immunotherapy in mice. *J Clin Invest.* 2010;120(4):1111-24.
62. van der Sluis TC, van Duikeren S, Huppelschoten S, Jordanova ES, Beyranvand Nejad E, Sloots A, et al. Vaccine-induced tumor necrosis factor-producing T cells synergize with cisplatin to promote tumor cell death. *Clin Cancer Res.* 2015;21(4):781-94.
63. Welters MJ, van der Sluis TC, van Meir H, Loof NM, van Ham VJ, van Duikeren S, et al. Vaccination during myeloid cell depletion by cancer chemotherapy fosters robust T cell responses. *Sci Transl Med.* 2016;8(334):334ra52.





## Chapter 2

# Tumor Eradication by Cisplatin Is Sustained by CD80/86-Mediated Costimulation of CD8<sup>+</sup> T Cells

*Elham Beyranvand Nejad<sup>1</sup>, Tetje C. van der Sluis<sup>1</sup>, Suzanne van Duikeren<sup>1</sup>, Hideo Yagita<sup>2</sup>, George M. Janssen<sup>3</sup>, Peter A. van Veelen<sup>3</sup>, Cornelis J.M. Melief<sup>1,4</sup>, Sjoerd H. van der Burg<sup>5</sup>, and Ramon Arens<sup>1</sup>*

Cancer Res. 2016 Oct 15;76(20):6017-6029. Epub 2016 Aug 28.

1. Department of Immunohematology and Blood Transfusion, Leiden University Medical Center, Leiden, the Netherlands
2. Department of Immunology, Juntendo University School of Medicine, Tokyo, Japan
3. Center for Proteomics and Metabolomics, Leiden University Medical Center, Leiden, the Netherlands
4. ISA Pharmaceuticals, Leiden, the Netherlands
5. Department of Clinical Oncology, Leiden University Medical Center, Leiden, the Netherlands



## Abstract

Certain cytotoxic chemotherapeutic drugs are immunogenic, stimulating tumor immunity through mechanisms that are not completely understood. Here we show how the DNA-damaging drug cisplatin modulates tumor immunity. At the maximum tolerated dose (MTD), cisplatin cured 50% of mice with established murine TC-1 or C3 tumors, which are preclinical models of human papillomavirus (HPV)-associated cancer. Notably, the curative benefit of cisplatin relied entirely upon induction of tumor-specific CD8<sup>+</sup> T cells. Mechanistic investigations showed that cisplatin stimulated tumor infiltration of inflammatory antigen-presenting cells (APC) expressing relatively higher levels of the T-cell costimulatory ligands CD70, CD80, and CD86. Cell death triggered by cisplatin was associated with the release of at least 19 proteins in the tumor environment that could act as damage-associated molecular patterns and upregulate costimulatory molecules, either alone or in concert, but the responsible proteins remain unknown. Essentially, the curative effect of cisplatin was abrogated in mice lacking expression of CD80 and CD86 on APCs. Furthermore, cisplatin treatment was improved by CTLA-4 blockade, which increases the availability of CD80/86 to bind to CD28. In contrast, there was no effect of CD27 stimulation, which replaces CD70 interaction. At the cisplatin MTD, cure rates could also be increased by vaccination with synthetic long peptides, whereas cures could also be achieved at similar rates at 80% of the MTD with reduced side effects. Our findings reveal an essential basis for the immunogenic properties of cisplatin, which are mediated by the induction of costimulatory signals for CD8<sup>+</sup> T-cell-dependent tumor destruction.

*Cancer Res; 76(20); 6017–29. ©2016 AACR.*



## Introduction

The involvement of the immune system in controlling tumor progression is now well established (1). The adaptive immune system is not only capable of recognizing tumor-associated antigens (TAA) and tumor-specific antigens (TSA), but also has the ability to eliminate cancerous cells and to generate long-term memory that protects against tumor recurrence. However, despite immune recognition many tumors can still progress due to various immune evasion strategies, which dampen or circumvent the tumor-specific immune response (2–4).

Chemotherapy is frequently used as primary care to treat cancer, to prevent metastases and to debulk the tumor mass. In spite of evidence from the late 1960s pointing at a role of the immune system in the action of chemotherapeutic drugs (5–7), it was only recently shown that the therapeutic efficacy of certain chemotherapeutic agents was partially mediated via immune system activation (8). This resurgence of the role of the immune system in chemotherapy thus revisited the notion that, rather than the original idea of neutral or immunosuppressive effects of chemotherapeutic agents, certain of these agents given as monotherapy have direct and indirect effects on the immune system, leading to improved antitumor responses (9).

Chemotherapeutic agents, such as anthracyclines, can cause cancer cell death that provokes an immunologic response, which relies on the induction of damage-associated molecular patterns (DAMP) including the exposure of endoplasmic reticulum chaperones such as calreticulin on the cell surface, the secretion of ATP, and the release of the non-histone chromatin-binding protein high mobility group box 1 (HMGB1; refs. 10–12). This so-called immunogenic cell death improves tumor antigen uptake, processing, and presentation by APCs to T cells, thereby polarizing T cells towards IFN $\gamma$ -producing CD8<sup>+</sup> T cells. Other chemotherapeutic agents such as the widely used platinum-containing cisplatin do not induce upregulation of calreticulin (13, 14). However, immune-stimulating properties have been associated with cisplatin including increased susceptibility of tumor cells to CD8<sup>+</sup> T cells (15, 16) and synergy with TNF to induce tumor cell apoptosis (17). Thus, chemotherapeutic agents can trigger diverse immune-stimulating processes that contribute to enhanced antitumor immune responses and improved therapeutic effects. However, the immune-stimulating properties of chemotherapeutics are often researched in mouse models in which the MTD is not determined, while in the clinic chemotherapies are administered at the MTD (18). Potential effects may be therefore unexplored.

In this study, we aimed to explore in preclinical models of HPV-associated cancer the immune-associated mechanisms of cisplatin-mediated tumor destruction in settings in which the MTD was used to mimic the clinical setting. The MTD of cisplatin induces attraction of

inflammatory APCs with increased expression of costimulatory molecules mediated through the release of DAMPs in the local tumor microenvironment upon cisplatin-mediated tumor cell death. This phenomenon leads to subsequent induction of tumor-specific CD8<sup>+</sup> T cells and is an integral part of the mechanisms underlying the sustained curative action of this chemotherapeutic agent.

## Materials and Methods

### Mice

C57BL/6 mice were obtained from Charles River Laboratories and were used as wild-type mice. *Cd80/86*<sup>-/-</sup> (19) and *Cd70/80/86*<sup>-/-</sup> mice (20) were bred inhouse. *Tlr4*<sup>-/-</sup> mice were obtained from The Jackson Laboratory and bred inhouse. Pmel-1 TCR transgenic mice containing CD8<sup>+</sup> T cells expressing gp100<sub>25-33</sub>-specific TCRs (21) were a kind gift from Dr. N.P. Restifo (National Cancer Institute, Bethesda, MD) and were bred to express the congenic marker CD90.1 (Thy1.1). All used knock-out and transgenic mice were on a C57BL/6 background. At the start of the experiments, mice were 8 to 14 weeks old. Mice were housed in individually ventilated cages under specific pathogen-free conditions in the animal facility of Leiden University Medical Center (LUMC, Leiden, the Netherlands). All animal experiments were approved by the Animal Experiments Committee of LUMC and were executed according to the animal experimentation guidelines of LUMC in compliance with the guidelines of Dutch and European committees.

### Tumor challenge models and chemotherapy

The tumor cell line TC-1 was generated by retroviral transduction of C57BL/6 lung epithelial cells with the HPV16 E6/E7 and c-H-ras oncogenes (22) and cultured as described previously (23). The tumor cell line C3 was developed by transfection of mouse embryonic cells with the HPV16 genome and an activated ras oncogene (24). Cell line authentication was carried out by flow cytometry 4 months prior to the first submission of the manuscript. Treatment schedule of each experiment is indicated in the respective figures. In brief, female mice were inoculated subcutaneously with  $1 \times 10^5$  TC-1 or  $5 \times 10^5$  C3 tumor cells (both preclinical models of HPV-associated cancer) in 200- $\mu$ L PBS containing 0.2% BSA on day 0. Tumor size (horizontal dimension  $\times$  vertical dimension) was measured two times a week using a caliper. When a palpable tumor was present on day 7 (TC-1) or day 13 (C3) post-tumor injection, mice were divided into groups with comparable tumor sizes. On day 8 and 14 after TC-1 and C3 tumor challenge, respectively, mice were treated intraperitoneally (i.p.) with the indicated dosages of cisplatin. Treatments with 1, 2, 4, and 8 but not 10 mg/kg of cisplatin were followed by a second injection on day 15 in the TC-1 tumor model. Mice were routinely weighed 2–3 times per week. After cisplatin administration, mice were weighed 3–4 times per week until mice recovered. Exclusion criteria were ulceration of tumors and

insusceptibility for cisplatin treatment as evidenced by complete lack of weight loss. Mice were euthanized when tumor size reached  $>2,000 \text{ mm}^3$  in volume or when mice lost  $>20\%$  of their total body weight (relative to initial body mass).

### Statistical analysis

Statistical analyses were performed using Prism (GraphPad). Survival data were analyzed by Kaplan–Meier and the log-rank (Mantel–Cox) test. Statistical significance was determined using the Mann–Whitney test or Student t test as indicated in the legends. P values of  $\leq 0.05$  were considered statistically significant.

Additional methods are described in the Supplementary Information.

## Results

### Efficacy of the MTD of cisplatin to control tumor progression

To identify a clinically relevant dose of cisplatin in mice, the MTD was assessed. TC-1 tumor cells, expressing the HPV-16 oncoproteins E6 and E7, were injected into mice. When a palpable tumor was present on day 8, groups of mice were treated with increasing doses of cisplatin. Administration of 1, 2, and 4 mg/kg of cisplatin did not alter the weight of the mice significantly (Fig. 1A). However, substantial weight loss was observed after each administration of 8 or 10 mg/kg of cisplatin. Mice receiving 10 mg/kg of cisplatin displayed close to 20% weight loss, preventing a second administration of cisplatin because of ethical considerations. To analyze cisplatin-induced toxicity, the levels of aspartate transaminase (AST) and alanine transaminase (ALT) were measured 4 days after administration of cisplatin as clinical biomarkers for tissue and liver injury (Supplementary Fig. S1A). Even the highest dose (10 mg/kg) of cisplatin was not associated with significant changes in AST and ALT serum levels, indicating that cisplatin treatment at these doses is not accompanied with major tissue/liver damage in mice. In addition, blood counts also showed no significant difference in the number of white blood cells, red blood cells, and platelets (PLT; Supplementary Fig. S1B).

The tumor outgrowth in mice treated with 1 or 2 mg/kg of cisplatin was comparable with untreated mice. However, the groups of mice treated with 4 or 8 mg/kg displayed a better survival of 14% and 25%, respectively (Fig. 1B and C). Remarkably, a single dose of 10 mg/kg of cisplatin cured 50% of the mice. On the basis of the clinical outcome, the weight loss and the absence of changes in AST and ALT levels, a single dose of cisplatin at 10 mg/kg was defined as the MTD.

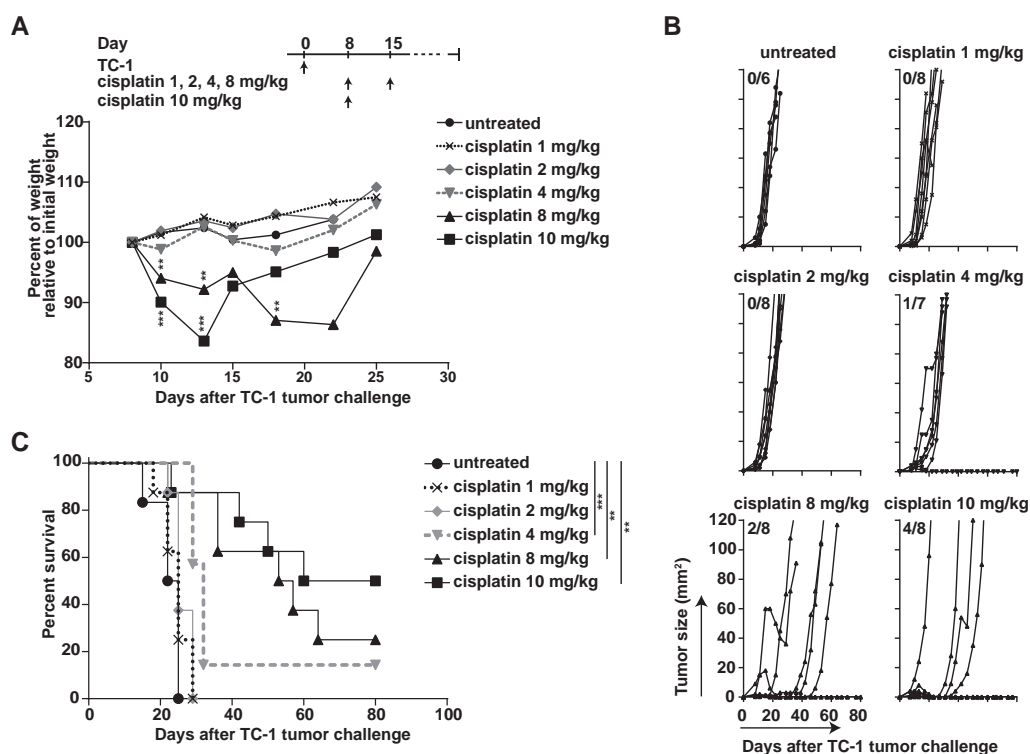


**Figure 1. The MTD of cisplatin induces the most efficacious tumor destruction**

**A**, weight loss of TC-1 tumor-bearing wild-type mice following treatment with different doses of cisplatin. The percentage of weight loss on each day was compared with untreated mice on the same day. Significance was determined by unpaired Student's *t* test. \*, *P* < 0.05; \*\*, *P* < 0.01; \*\*\*, *P* < 0.001. **B**, tumor growth curves of the mice shown in **A**. In each tumor outgrowth graph, the number of tumor-free mice from the total mice is indicated. **C**, survival graph of the TC-1 tumor-bearing mice. Significance was determined by a log-rank (Mantel-Cox) test (\*, *P* < 0.05; \*\*, *P* < 0.01; \*\*\*, *P* < 0.001).

## The antitumor effect of cisplatin treatment fully depends on the induction of tumor-specific CD8<sup>+</sup> T-cell responses

Next, we asked whether the efficacy of the MTD of cisplatin to cure half of the mice is solely determined by direct killing of tumor cells or whether also immune-associated mechanisms are implicated. To address this, we ablated several types of immune cells: that is, NK cells, CD4<sup>+</sup> T cells, and CD8<sup>+</sup> T cells (Supplementary Fig. S1C and S1D) *in vivo* through administration of depleting antibodies during cisplatin chemotherapy in TC-1 tumor-bearing mice. Clodronate liposomes were used to deplete phagocytic cells including macrophages and dendritic cells. Whereas treatment with the MTD of cisplatin was able to cure 50% of the immune-competent mice, cisplatin only delayed tumor progression until day 20 post-tumor challenge in mice depleted of CD8<sup>+</sup> T cells or phagocytic APCs, after which all tumors progressed rapidly (Fig. 2A–C). Depletion of CD4<sup>+</sup> T cells and NK cells had no effect. To

validate the importance of CD8<sup>+</sup> T cells in cisplatin-mediated tumor destruction in a second model, we used HPV16-transformed C3 tumors. Administration of cisplatin markedly delayed C3 tumor outgrowth and full eradication was observed in about half of the mice. Again the sustained clinical effect fully depended on the presence of CD8<sup>+</sup> T cells (Fig. 2D). Thus, tumor regression is a direct effect of cisplatin on tumor cells but cisplatin-induced cure, which means full tumor eradication, requires the presence of CD8<sup>+</sup> T cells, and phagocytic APCs.

Given the role of CD8<sup>+</sup> T cells in cisplatin-mediated tumor destruction, we determined the tumor-reactivity of circulating CD8<sup>+</sup> T cells after cisplatin treatment. Stimulation of splenic CD8<sup>+</sup> T cells isolated from mice that previously eradicated TC-1 tumors (day 60) resulted in the production of IFN $\gamma$  and TNF toward irradiated TC-1 tumor cells but not to unrelated tumor cells (Fig. 2E and Supplementary Fig. S2A and S2B). Splenic CD8<sup>+</sup> T cells isolated from mice with established TC-1 tumors (day 21) produced more IFN $\gamma$  and TNF in response to irradiated TC-1 tumor cells compared with untreated mice (Supplementary Fig. S2B), confirming the importance of tumor-specific CD8<sup>+</sup> T cells in tumor clearance. As a control, splenic CD8<sup>+</sup> T cells isolated from cisplatin-treated naïve (non tumor-bearing) mice stimulated with irradiated tumor cells were unable to produce IFN $\gamma$  (Supplementary Fig. S2C), indicating that the observed tumor-specific T-cell responses depends on cisplatin-treated tumor cells and are not caused by effects of cisplatin on other cells. Moreover, splenic CD8<sup>+</sup> T cells from cured mice showed higher production of IFN $\gamma$  compared with noncured mice in the C3 tumor model (Supplementary Fig. S2C).

To examine whether cisplatin treatment induced protective tumor-specific CD8<sup>+</sup> T-cell responses, we rechallenged mice that previously eradicated TC-1 tumors after cisplatin treatment and remained tumor free for at least one month. The majority of these mice were protected against TC-1 tumor rechallenge (Fig. 2F), indicating that cisplatin treatment can lead to the induction of tumor-specific immunologic memory. Thus, cisplatin treatment of tumor-bearing mice results in the induction of tumor-specific effector and memory CD8<sup>+</sup> T-cell responses.

### **Cisplatin treatment triggers enhanced levels of costimulatory molecules on intratumoral inflammatory APCs**

To dissect the underlying mechanisms of the cisplatin-mediated cure of tumor-bearing mice and the connection with the important role for APCs and the induction of tumor-specific CD8<sup>+</sup> T-cell responses, we performed a series of *in vitro* experiments. Cisplatin-treated tumor cells were unable to directly cause significant activation of CD8<sup>+</sup> T cells but when antigen-pulsed APCs such as BMDCs or D1 dendritic cells were present in the cultures, CD8<sup>+</sup> T-cell proliferation was clearly increased, confirming the importance of APCs in the cisplatin-

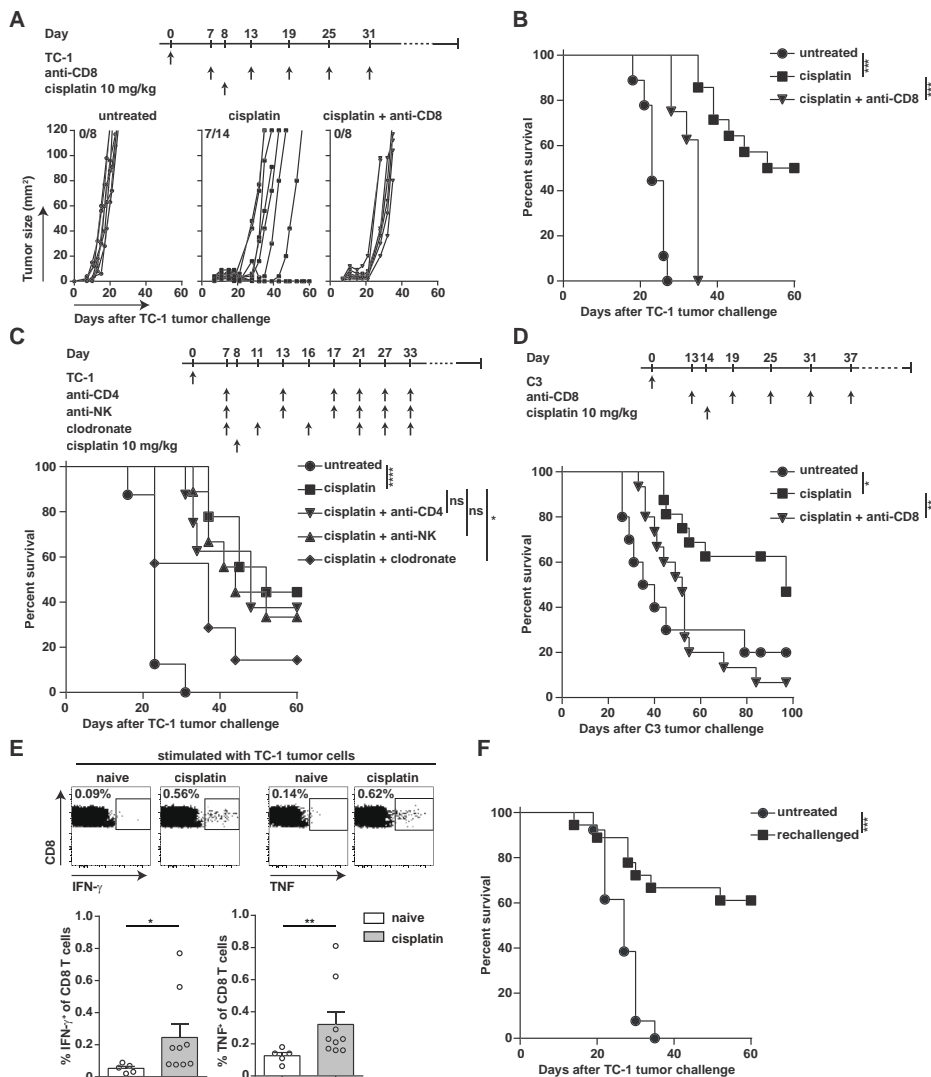


**Figure 2. Cisplatin-mediated tumor destruction is CD8<sup>+</sup> T-cell-dependent**

**A**, tumor growth curves of TC-1 tumor-bearing wild-type mice following treatment with cisplatin and CD8<sup>+</sup> T-cell depletion. The number of tumor-free mice from the total mice is indicated. **B**, survival curves of TC-1 tumor-bearing wild-type mice shown in **A**. Data are pooled of two independent experiments with 8–14 mice per group. **C**, survival curves of TC-1 tumor-bearing wild-type mice following treatment with cisplatin and depletion of CD4<sup>+</sup> T cells, NK cells, or phagocytic cells (macrophages/dendritic cells). **D**, survival curves of C3 tumor-bearing wild-type mice following treatment with cisplatin and CD8<sup>+</sup> T-cell depletion. Data are pool of two independent experiments with 10–16 mice per group. Significance was determined by a log-rank (Mantel–Cox) test. \*,  $P < 0.05$ ; \*\*,  $P < 0.01$ ; \*\*\*,  $P < 0.001$ ; \*\*\*\*,  $P < 0.0001$ . **E**, representative flow cytometry plots of IFN $\gamma$  and TNF-producing splenic CD8<sup>+</sup> T cells of naïve mice and of cisplatin-treated mice that survived tumor challenge and remained tumor free for 45 days following stimulation with irradiated TC-1 tumor cells. Data in bar graphs are expressed as the mean with SEM. Experiments were performed three times with similar outcomes. Significance was determined by a Mann–Whitney nonparametric test. \*,  $P < 0.05$ ; \*\*,  $P < 0.01$ . **F**, survival of wild-type mice rechallenged with TC-1 tumor cells. Approximately 60 days after first TC-1 tumor challenge, the cisplatin-treated mice that eradicated tumors and remained tumor free were rechallenged with TC-1 tumor cells. Data are pool of four independent experiments with 4–6 mice per group. Significance was determined by log-rank (Mantel–Cox) test. \*\*\*,  $P < 0.001$ .

induced immunologic response (Fig. 3A and Supplementary Fig. S3A). Moreover, the IFN $\gamma$  production in these cultures correlated with the level of T-cell proliferation (as evidenced by CFSE dilution; Fig. 3B and Supplementary Fig. S3B). Together, these data indicate that cisplatin treatment of tumor cells stimulate local APCs to activate CD8 $^{+}$  T cells.

Given the pivotal role of costimulatory signals provided by APCs in driving T-cell responses (25), we hypothesized that cisplatin treatment mediates induction of these molecules on APCs. To test this, we exposed dendritic cells to TC-1 tumor cells, which had been incubated with increasing amounts of cisplatin causing 20% to 50% cell death overnight (Supplementary Fig. S3C). In a dose-dependent fashion, cisplatin increased the expression of the costimulatory molecules CD70, CD80, and CD86 but not that of OX40L, 4-1BBL, and ICOSL (Fig. 3C and Supplementary Fig. S3D). In contrast, cisplatin treatment of D1 cells in the absence of tumor cells did not alter the expression of CD70 and CD86 while the expression of CD80 was slightly higher (Supplementary Fig. S3E). A similar result was observed in case of cisplatin treatment of TC-1 and C3 tumor cells without the presence of APCs. Together, these results indicate that cisplatin-mediated tumor cell death leads to upregulation of CD70, CD80, and CD86 on APCs.

To demonstrate the importance of the cisplatin-mediated induction of costimulatory molecule expression on APCs, the cytokine production of antigen-specific T cells was measured in cultures with cisplatin-treated tumor cells in the presence of dendritic cells from wild-type, *Cd70* $^{-/-}$ , *Cd80/86* $^{-/-}$ , and *Cd70/80/86* $^{-/-}$  mice. IFN $\gamma$  production of T cells was markedly lower when stimulated with APCs lacking the expression of CD70, CD80, and CD86 costimulatory molecules (Fig. 3D).

We hypothesized that factors released during cisplatin-induced cell death might be involved in the costimulatory molecule upregulation on APCs. First, we used cytokine multiplex assays to identify whether such factors are present in the supernatant of TC-1 tumor cells that were treated with 1 or 2.5 mg/mL cisplatin.

While most cytokines such as IL1, IL12, and TNF were not changed or below the detection limit, we were able to identify type I IFNs as factors that are elevated upon cisplatin treatment (Fig. 3E). Importantly, for our study, type I IFNs upregulated the expression of CD70, CD80, and CD86 on both BMDCs and D1 cells (Fig. 3F and Supplementary Fig. S3F). Preventing the effects of type I IFNs by using a blocking antibody for the IFN $\alpha/\beta$  receptor (IFNAR) abrogated the upregulation of these costimulatory molecules on dendritic cells treated with IFN $\alpha$  (Supplementary Fig. S3G), but failed to block the cisplatin-mediated upregulation of costimulatory molecules, indicating that the type I IFN pathway is not essential for this occurrence (Supplementary Fig. S3H).

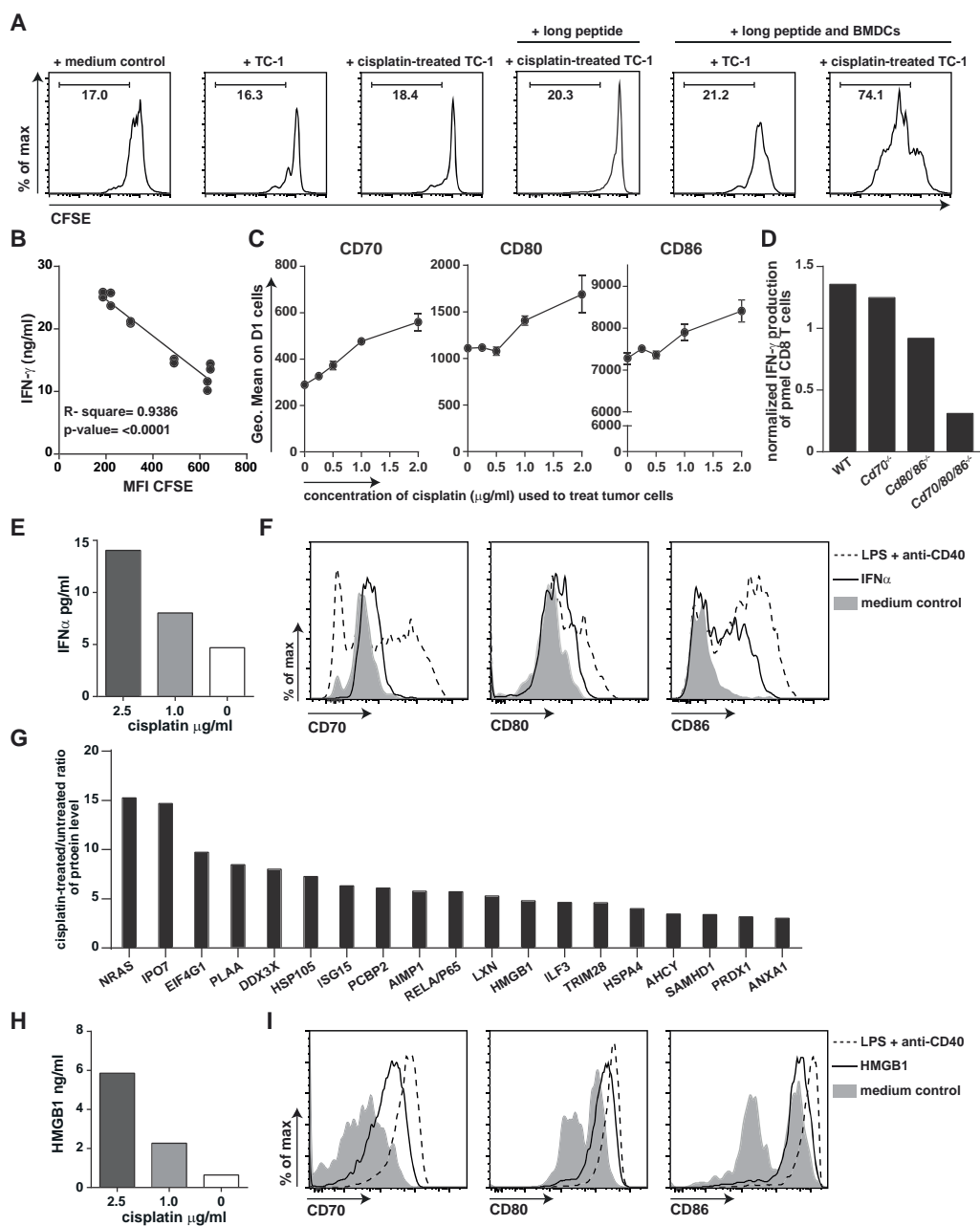


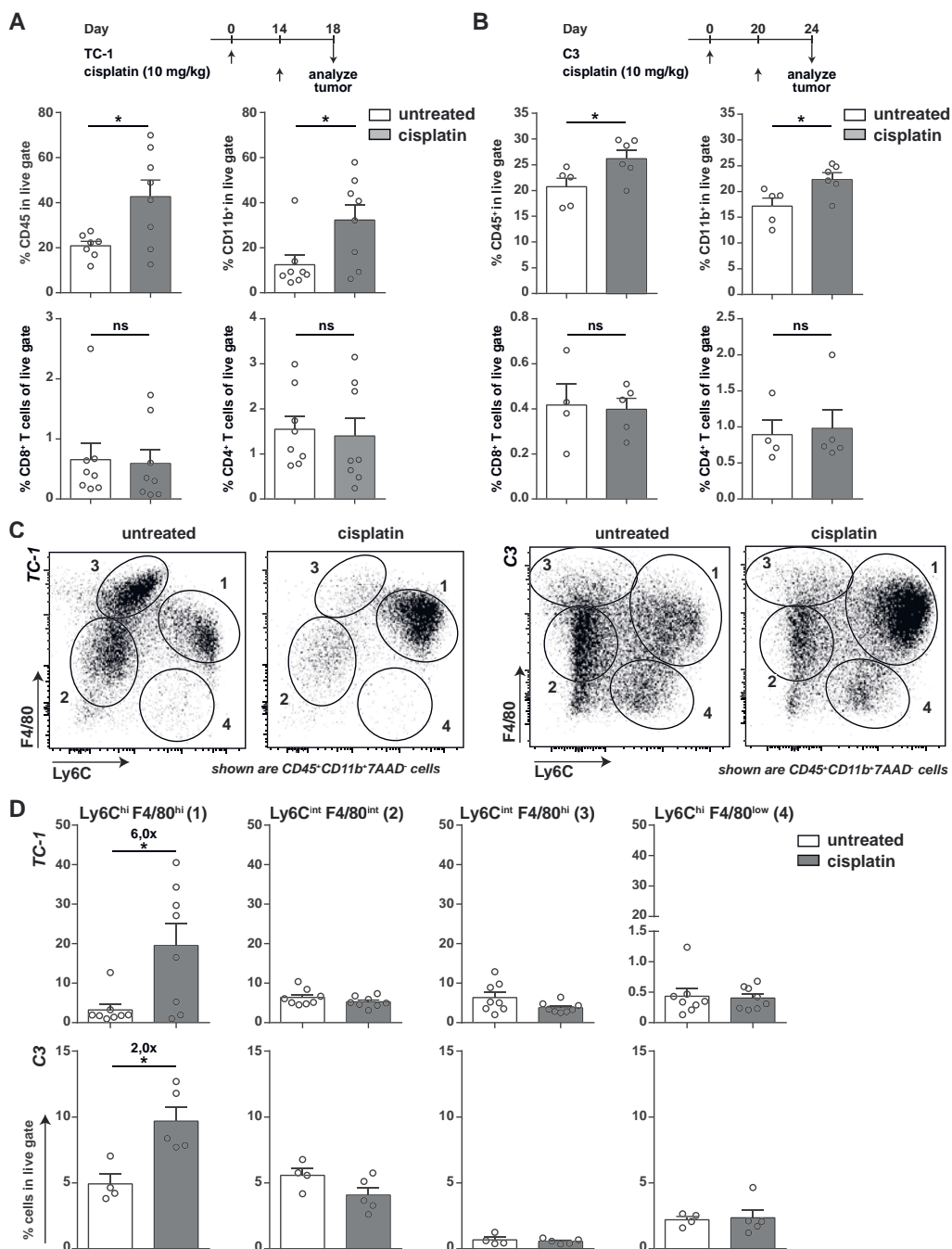
To further identify factors, we took a global proteomics approach using mass spectrometry allowing comprehensive analysis of induced proteins. Mass spectrometric analysis was performed to detect and quantify proteins released in the supernatant of cisplatin-treated tumor cells. In total, 2,239 unique proteins were found, of which 526 proteins were increased with a ratio of >3 by cisplatin treatment (Supplementary Fig. S4A). Protein classification using PANTHER revealed a variety of proteins with different functions (Supplementary Fig. S4B). In particular, we focused on those proteins involved in the defence response, and could act as DAMPs. In total, we found 19 of such proteins, including heat-shock proteins and HMGB1 (Fig. 3G). The latter protein is known to be released upon tumor cell death and to be capable of mediating inflammation (26, 27). To validate the mass spectrometry results, we performed an ELISA for HMGB1, revealing a similar 5-fold increase of this DAMP in the supernatant of cisplatin-treated tumor cells (Fig. 3H). Essentially, incubation of BMDCs and D1 cells with HMGB1 caused significant cell-surface upregulation of CD70, CD80, and CD86 (Fig. 3I and Supplementary Fig. S5A). However, BMDCs that are deficient in the HMGB1 receptor TLR4 did not show the abrogation of upregulation of costimulatory molecules induced by cisplatin-treated tumor cells (Supplementary Fig. S5B). Similarly, neutralizing HMGB1 with antibody in cisplatin-treated wild-type mice or cisplatin treatment of *Tlr4*<sup>-/-</sup> mice did not decrease the survival of treated mice (Supplementary Fig. S5C and S5D). Collectively, these data indicate that the release of a cocktail of DAMPs in the local microenvironment by cisplatin-induced tumor cell death is responsible for the upregulation of costimulatory molecules on APCs, which are required for optimal T-cell activation, and blocking of one DAMP pathway is redundant.

Next, we assessed whether similar mechanisms regarding the cisplatin-mediated induction of tumor-specific CD8<sup>+</sup> T-cell responses operate *in vivo*. First the potential effect of cisplatin on the composition of the intratumoral APCs was addressed. Tumors at day 4 after systemic

**Figure 3. Cisplatin-induced tumor cell death induces T-cell costimulation, leading to increased T-cell activation.** ►

**A**, representative flow cytometry plots for CD8<sup>+</sup> T-cell proliferation. Shown is the CFSE dilution of CFSE-labeled CD8<sup>+</sup> pmel-1 cells incubated with mentioned conditions. Percentages of proliferated cells are indicated. **B**, correlation of the IFN $\gamma$  production (ng/mL) of CD8<sup>+</sup> pmel-1 cells in the presence of peptide-loaded BMDCs and cisplatin-treated TC-1 tumor cells with the geometric mean of CFSE in each concentration. **C**, expression of the costimulatory molecules CD70, CD80, and CD86 on D1 cells in the presence of cisplatin-treated tumor cells. **D**, ELISA quantification of IFN $\gamma$  production by CD8<sup>+</sup> pmel-1 cells in the presence of cisplatin-treated TC-1 tumor cells and different BMDCs as described in the Supplementary Data. **E**, IFN $\alpha$  levels in supernatants of cisplatin-treated TC-1 tumor cells measured by multiplex immunoassays. **F**, expression of CD70, CD80, and CD86 on BMDCs in the presence of IFN $\alpha$ . **G**, protein level in supernatant of cisplatin-treated TC-1 tumor cells compared with untreated. Shown is the ratio of each protein in the supernatant of TC-1 tumor cells treated with 1 mg/mL cisplatin and without any treatment measured by mass spectrometry. Ratio of 3 was chosen as cut-off value. **H**, HMGB1 levels in supernatants of cisplatin-treated TC-1 tumor cells measured by ELISA. **I**, expression of CD70, CD80, and CD86 on BMDCs in the presence of HMGB1. LPS anti-CD40 was used as a positive control and medium alone as a negative control (**F** and **I**). All data shown is representative of three independent experiments.





treatment with 10 mg/kg cisplatin were dissected (Fig. 4A and B). This moment was chosen as the tumor sizes between cisplatin-treated and nontreated mice are comparable (Supplementary Fig. S6A), thereby excluding tumor size-related differences in immune parameters. We observed an increase in the percentage of the total CD45<sup>+</sup> leukocyte tumor-infiltrating population upon cisplatin treatment in TC-1 and C3 tumor models (Fig. 4A and B and Supplementary Fig. S6B). Especially the percentage of the CD11b<sup>+</sup> myeloid cells was elevated while the percentage of infiltrated T cells was not affected (Fig. 4A and B). Cisplatin treatment did not decrease the percentage of intratumoral regulatory CD4<sup>+</sup> CD25<sup>+</sup> Foxp3<sup>+</sup> T cells (Supplementary Fig. S6C).

Next, we gated on the CD3<sup>+</sup>CD11b<sup>+</sup> myeloid cells by using our previously described gating strategy to delineate four subsets (28): Ly6C<sup>hi</sup>F4/80<sup>hi</sup>, Ly6C<sup>int</sup>F4/80<sup>int</sup>, Ly6C<sup>int</sup>F4/80<sup>hi</sup>, and Ly6C<sup>hi</sup>F4/80<sup>low</sup> myeloid cells (Fig. 4C). The Ly6C<sup>int</sup>F4/80<sup>hi</sup> and Ly6C<sup>hi</sup>F4/80<sup>low</sup> populations express high levels of CD11c and Ly6G, respectively, resembling DC-like and granulocytic APCs. In both the TC-1 and C3 tumor models, cisplatin treatment induced a predominant increase in the inflammatory Ly6C<sup>hi</sup>F4/80<sup>hi</sup> APC population (Fig. 4C and D). Remarkably, cisplatin treatment not only increased the number of Ly6C<sup>hi</sup>F4/80<sup>hi</sup> APCs but also increased the percentage of CD11c<sup>hi</sup> cells within this subset (Supplementary Fig. S6D and S6E). Moreover, cisplatin treatment enhanced the levels of monocyte chemotactic protein 1 (MCP-1/CCL2) in the serum as compared with untreated and naïve mice (Supplementary Fig. S6F).

To analyze the effect of cisplatin on myeloid-derived suppressor cells (MDSC), we used a gating strategy based on CD11b and Gr-1, a myeloid differentiation antigen that consists of Ly6C and Ly6G. Cisplatin treatment did not alter the percentage of the CD11b<sup>+</sup>Gr-1<sup>hi</sup> MDSCs, nor that of CD11b<sup>+</sup>Gr-1<sup>neg</sup> cells while there was a significant increase in the CD11b<sup>+</sup>Gr-1<sup>int</sup> population upon cisplatin treatment (Supplementary Fig. S6G). The increase of the latter population reflects the Ly6C<sup>hi</sup>F4/80<sup>hi</sup> cells (population 1) (29) shown in Fig. 4C and D.

#### ◀ Figure 4. Induction of intratumoral inflammatory myeloid APCs by cisplatin treatment

**A and B**, the percentage of intratumoral leukocytes (CD45<sup>+</sup>), myeloid cells (CD11b<sup>+</sup>), and CD8<sup>+</sup> and CD4<sup>+</sup> T cells in TC-1 tumors on day 18 (**A**) and in C3 tumor cells on day 24 (**B**). The percentages of myeloid cells, CD8<sup>+</sup>, and CD4<sup>+</sup> T cells were determined on the basis of the following gated populations: 7AAD<sup>+</sup>CD45<sup>+</sup>CD11b<sup>+</sup>, 7AAD<sup>+</sup>CD3<sup>+</sup>CD8<sup>+</sup>class II<sup>+</sup>CD4<sup>+</sup>, and 7AAD<sup>+</sup>CD3<sup>+</sup>CD8<sup>+</sup>class II<sup>+</sup>CD4<sup>+</sup> cells. Data are expressed as mean with SEM (Mann–Whitney test; \*, *P* < 0.05). **C**, flow cytometry plots for F4/80 versus Ly6C staining of tumor-infiltrating myeloid cells in TC-1 (left) and C3 (right) tumors of untreated and cisplatin-treated animals. Flow cytometry plots show similar amounts of cells in each tumor model for both untreated and cisplatin conditions. **D**, percentages of the four different myeloid cell subsets were determined for both tumor types (shown in A and B). Experiments were performed twice with similar results. Data are expressed as the mean with SEM (Mann–Whitney test; \*, *P* < 0.05).

To dissect whether chemotherapy altered the costimulatory activation status of the intratumoral myeloid cells *in vivo*, the expression of the costimulatory molecules CD70, CD80, and CD86 was analyzed. A cisplatin-mediated increase in the expression of the costimulatory molecules CD80 and CD86 was observed for myeloid cells isolated from both TC-1 and C3 tumors, while CD70 was increased on myeloid cells from TC-1 tumors treated with cisplatin (Fig. 5A and B). When analyzed per subset, CD80 and CD86 were specifically increased on the inflammatory Ly6C<sup>hi</sup>F4/80<sup>hi</sup> APCs and not on the other subsets (Fig. 5C and D). The expression of CD70 increased on both inflammatory Ly6C<sup>hi</sup>F4/80<sup>hi</sup> and DC-like Ly6C<sup>int</sup>F4/80<sup>hi</sup> APCs in TC-1 tumors upon cisplatin treatment (Fig. 5D). Detailed analysis of the Ly6C<sup>hi</sup>F4/80<sup>hi</sup> population based on CD11c<sup>int/hi</sup> indicated that CD70, CD80, and CD86 were highly expressed on the CD11c<sup>hi</sup> cells of this population (Fig. 5E). Notably, the expression of these costimulatory molecules increased significantly on the CD11c<sup>hi</sup> Ly6C<sup>hi</sup>F4/80<sup>hi</sup> cells upon cisplatin treatment (Fig. 5E and Supplementary Fig. S7A). Importantly, cisplatin did not affect the expression of CD70, CD80, and CD86 costimulatory molecules on myeloid cells in spleen and tumor-draining lymph node (TDLN; Supplementary Fig. S7B and S7C), corroborating that upregulation of these costimulatory molecules is not a direct effect of cisplatin on myeloid cells but that the effect of cisplatin acts strictly locally in the tumor microenvironment where both tumor cells and APCs are present. Moreover, cisplatin treatment did not alter the expression of these costimulatory molecules on either TC-1 or C3 tumor cells *in vivo* (Supplementary Fig. S7D and S7E). Thus, cisplatin treatment specifically upregulates the expression of the costimulatory molecules CD70, CD80, and CD86 on intratumoral inflammatory APCs with a CD11c<sup>hi</sup>Ly6C<sup>hi</sup>F4/80<sup>hi</sup> phenotype.

### Cisplatin-mediated tumor destruction requires T-cell costimulation

In view of the upregulation of these costimulatory molecules on tumor-infiltrated APCs *in vivo*, their requirement for cisplatin-mediated tumor eradication was next determined. Wild-type, *Cd80/86*<sup>-/-</sup>, and *Cd70/80/86*<sup>-/-</sup> mice were challenged with TC-1 tumor cells and subsequently, when tumors were palpable, treated with 10 mg/kg cisplatin, or left untreated. When left untreated, the tumors in the wild-type and costimulation-deficient mice progressed rapidly with similar kinetics (Fig. 6A). Treatment with cisplatin resulted in significant tumor delay and eradication in 50% of the wild-type mice. In contrast, cisplatin treatment in *Cd80/86*<sup>-/-</sup> and *Cd70/80/86*<sup>-/-</sup> mice resulted only in a delay of tumor outgrowth and the vast majority of the cisplatin-treated costimulation-deficient mice did not survive (Fig. 6A and B). The survival of cisplatin-treated *Cd80/86*<sup>-/-</sup> and *Cd70/80/86*<sup>-/-</sup> mice is similar, suggesting that CD70, although upregulated on myeloid cells after cisplatin treatment, seems to play a minor role in comparison with the B7 molecules CD80 and CD86. To examine whether increment of CD70- or CD80/86- mediated costimulation could affect cisplatin-mediated tumor eradication, we used agonistic CD27 antibodies or CTLA-4– blocking antibodies, respectively. No increase in survival of cisplatin-treated TC-1 tumor-bearing mice was

observed when cotreated with CD27 agonistic antibody (Fig. 6C). On the other hand, blocking the inhibitory signal via CTLA-4, leading to enhanced capacity of CD80 and CD86 to bind CD28, slightly improved cisplatin-mediated tumor eradication (Fig. 6D). Taken together, these data show that T-cell costimulation via CD80/86 on host cells is required for the full efficacy of the cisplatin induced antitumor response.

### **The combination of cisplatin with therapeutic vaccination strongly improves clinical outcome and depends on costimulation**

Next, we assessed whether the clinical effect of tumor-specific vaccination with HPV16 SLP could be improved by combination treatment with cisplatin at different dosage levels, including the MTD. Wild-type mice were treated with HPV16 SLP vaccination on day 8 and day 22 combined with 0, 1, 2, 4, or 8 mg/kg of cisplatin on day 8 and 15 or once with 10 mg/kg only on day 8. SLP vaccination alone resulted in a delay of tumor outgrowth but after day 40 all mice succumbed. The combination of SLP vaccination with cisplatin enhanced the overall survival of mice, albeit with varying efficacy (Fig. 7A). Interestingly, the strong clinical effect (90% cure) obtained by the combination of SLP vaccination and the MTD of cisplatin, was retained in animals given vaccination and twice 80% of the MTD (8 mg/kg; Fig. 7A) while the side effects induced by cisplatin are reduced at this dose (Fig. 1A). Notably, lowering the dose of cisplatin to 4 mg/kg in combination with SLP vaccination resulted only in 50% tumor eradication, similar to what otherwise could be achieved only with cisplatin used at the MTD (Fig. 7A).

To show that also in this combined therapeutic setting costimulation is a central component, wild-type and *Cd70/80/86<sup>-/-</sup>* mice were treated by SLP vaccination and the MTD of cisplatin (Fig. 7B). When compared with the clinical response in wild-type mice, the absence of costimulation clearly abrogated the delay in tumor progression despite chemioimmunotherapy, and only 30% of the mice survived tumor challenge. Thus, chemioimmunotherapy strongly depends on T-cell costimulation.

## **Discussion**

In the current study, we show that the MTD of cisplatin results in complete tumor eradication in about half of the animals. While tumor regression was observed in all mice treated with the MTD of cisplatin, full eradication of established tumors requires the induction of tumor-specific CD8<sup>+</sup> T cells and the expression of the costimulatory molecules CD80 and CD86 on host APCs. By performing cytokine multiplex assays and mass spectrometry, we found that a cocktail of factors, which are released upon cisplatin-induced tumor cell death, have the capacity to enhance costimulatory molecule expression on inflammatory APCs. Cisplatin-mediated tumor destruction resulted not only in the induction of cytokine-producing tumor-specific effector CD8<sup>+</sup> T cells reactive to TC-1 tumor cells but also memory CD8<sup>+</sup> T-cell

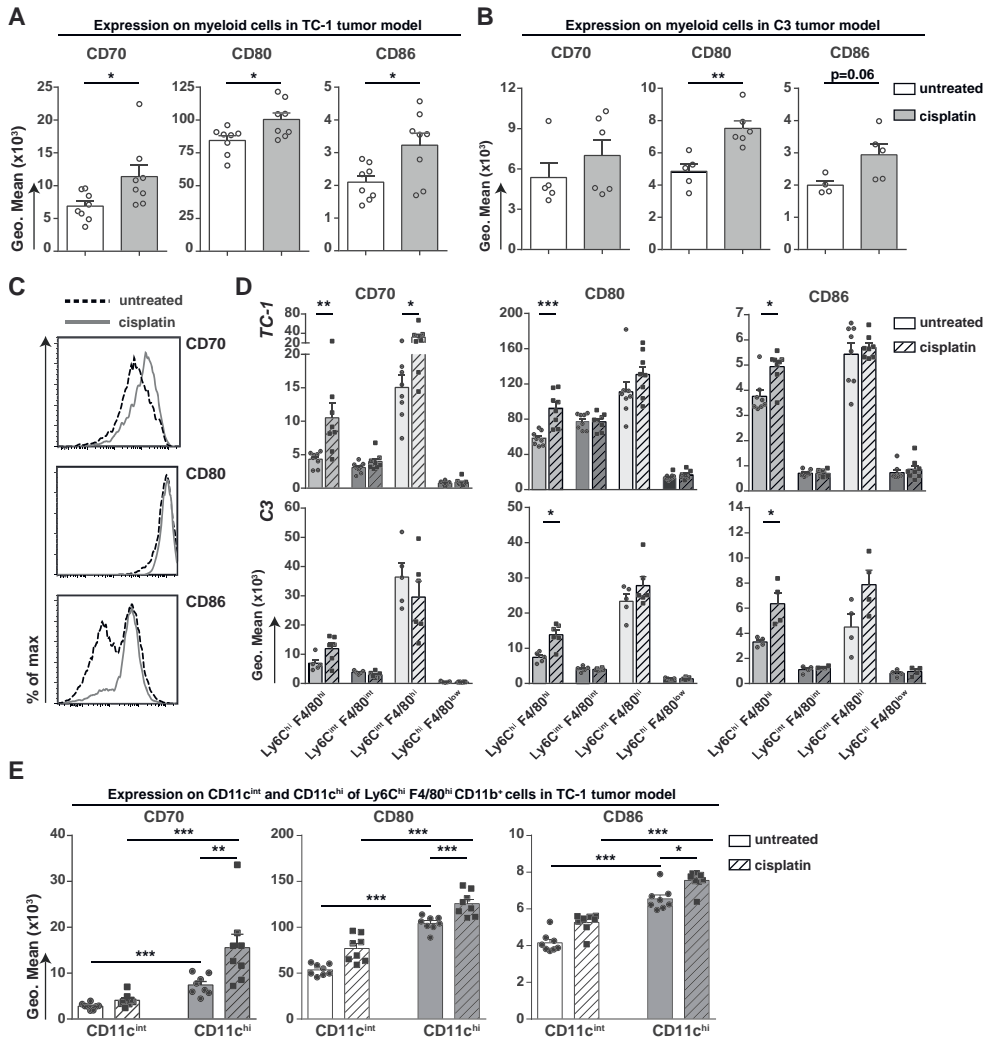


**Figure 5. Enhanced expression of costimulatory molecules on intratumoral myeloid subsets upon cisplatin treatment**

The expression of CD70, CD80, and CD86 was determined on total myeloid cells 4 days after cisplatin treatment as described in the Supplementary Data. Data shown are gated on 7AAD<sup>-</sup>CD45<sup>+</sup>CD3<sup>-</sup>CD11b<sup>+</sup> cells in TC-1 tumors (A) and C3 tumors (B). C, representative flow cytometry plots (based on median value) for CD70, CD80, and CD86 expression on 7AAD<sup>-</sup>CD45<sup>+</sup>CD3<sup>-</sup>CD11b<sup>+</sup> cells in TC-1 tumors. D, expression of CD70, CD80, and CD86 on the four indicated myeloid subsets isolated from TC-1 and C3 tumors. E, expression of CD70, CD80, and CD86 on CD11c<sup>int</sup> and CD11c<sup>hi</sup> cells of Ly6C<sup>hi</sup>F4/80<sup>hi</sup>CD11b<sup>+</sup> myeloid cells isolated from TC-1 tumor. Each dot represents data from an individual mouse. Bar graphs indicate mean values with SEM. Significance was determined by Mann-Whitney test. \*,  $P < 0.05$ ; \*\*,  $P < 0.01$ ; \*\*\*,  $P < 0.001$ . Experiments were performed twice with similar outcomes.



formation occurred, as cured mice were able to resist a secondary tumor challenge. Thus, the MTD of cisplatin mediates tumor cell death that both directly delays tumor growth and indirectly stimulates tumor-specific immunity to achieve full tumor regression and cure.

Chemotherapeutic agents such as vinblastine, paclitaxel, and etoposide are known to exert direct effects on the APC maturation including the increased expression of CD80 and CD86 (30). We showed that the enhanced expression of costimulatory molecules on APCs upon cisplatin treatment was only observed in the presence of tumor cells, indicating a strict requirement of cisplatin-induced tumor cell death for this type of APC maturation. Moreover, we found that cisplatin treatment *in vivo* resulted in an enhanced expression of costimulatory molecules exclusively on intratumoral APCs while it did not affect the expression of CD70, CD80, and CD86 in spleen and TDLN, suggesting that the costimulation-inducing factors released by cisplatin-mediated tumor cell death act only locally on neighboring APCs. Certain types of chemotherapeutic agents can induce immunogenic cell death that is demarcated by calreticulin exposure, HMGB1 release, and ATP secretion, thereby stimulating antitumor responses. Moreover, the immune-stimulatory effect of immunogenic cell death—inducing chemotherapy is abolished in mice deficient in TLR4 (31). Although cisplatin fails to meet all the proposed criteria of this immunogenic cell death as it does not induce the preapoptotic exposure of calreticulin (12), it induces HMGB1 release of tumor cells as shown by us and others (13). Notably, our data also demonstrated that HMGB1 induces the upregulation of costimulatory molecules on APCs. Consistent with this notion, it has been shown that in a type I diabetes model, HMGB1 potentially could induce CD11c<sup>+</sup>CD11b<sup>+</sup> DC maturation and macrophage activation in NOD mice (32). In addition to HMGB1, we found production of type I IFNs after cisplatin treatment of tumor cells. Reportedly, such type I IFN induction by cisplatin is important for the maturation and migration of DCs and subsequent T-cell priming (33). Like HMGB1, we also showed that type I IFNs can upregulate costimulatory molecules on APCs, indicating that multiple factors play a role in enhancement of costimulatory molecules on APCs upon cisplatin treatment. Moreover, using mass spectrometry analyses, we found that cisplatin induces the release of a cocktail of potential immune-stimulatory proteins (e.g., HSPs), which next to type I IFNs and HMGB1, can activate APCs and contribute to T-cell stimulation (34). This would fit with recent reports that type I IFNs can act *in cis* with other stimuli to induce DC maturation (35). Indeed, TLR4-deficient DCs still upregulated costimulatory molecules following stimulation with cisplatin-treated tumor cells and similarly blocking of type I IFN signaling did not affect the upregulation of costimulatory molecules by cisplatin. Moreover, cisplatin treatment of TLR4-deficient mice or during neutralization of HMGB1 was as efficient as in wild-type mice.

Previously, results from head and neck cancer patients receiving radiochemotherapy (5-FU and cisplatin) indicated that one of the immune-stimulatory mechanisms could be the



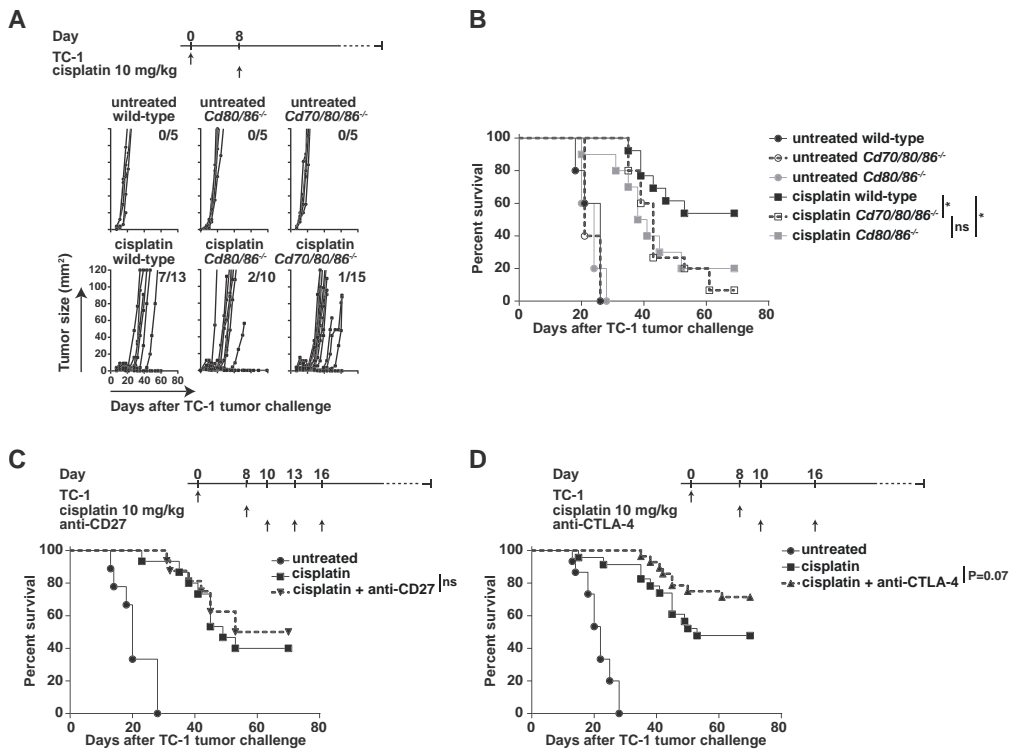


**Figure 6. Cisplatin treatment requires CD80 and CD86 costimulatory signals**

**A**, tumor growth curves in TC-1 tumor-bearing wild-type, *Cd80/86*<sup>-/-</sup>, and *Cd70/80/86*<sup>-/-</sup> mice following treatment with cisplatin. Numbers on the top right side represent the tumor-free mice from the total mice. Data are pool of two independent experiments. **B**, survival of TC-1 tumor-bearing wild-type, *Cd80/86*<sup>-/-</sup>, and *Cd70/80/86*<sup>-/-</sup> mice following treatment with cisplatin shown in **A**. **C**, survival of TC-1 tumor-bearing wild-type mice following treatment with cisplatin and agonistic CD27 antibody (anti-CD27). Data are pool of two independent experiments with 9–16 mice per group. **D**, survival of TC-1 tumor-bearing wild-type mice following treatment with cisplatin and CTLA-4-blocking antibody (anti-CTLA-4). Data are pool of three independent experiments with 15–25 mice per group. Significance was determined by log-rank (Mantel–Cox) test.

reduction of immune-suppressive cells in the tumor microenvironment (36). Study of the tumor microenvironment in cisplatin-treated animals, however, showed that cisplatin did not act via the reduction of intratumoral Tregs or MDSCs. Instead, an increase in a particular subset of APCs was found, which was important for the clinical effect of cisplatin as depletion of APCs by clodronate liposomes prevented the cisplatin-induced cure of tumor-bearing mice. In-depth analyses of the different subsets of APCs after cisplatin treatment showed alteration in number and composition of myeloid cells toward inflammatory Ly6<sup>hi</sup>CD11c<sup>+</sup> APCs. Analysis of the APC status revealed that cisplatin indirectly stimulated the expression of the costimulatory molecules CD70, CD80, and CD86 on intratumoral inflammatory APCs with a CD11c<sup>hi</sup>Ly6<sup>hi</sup>F4/80<sup>hi</sup> phenotype. The enhanced presence of these APCs in the

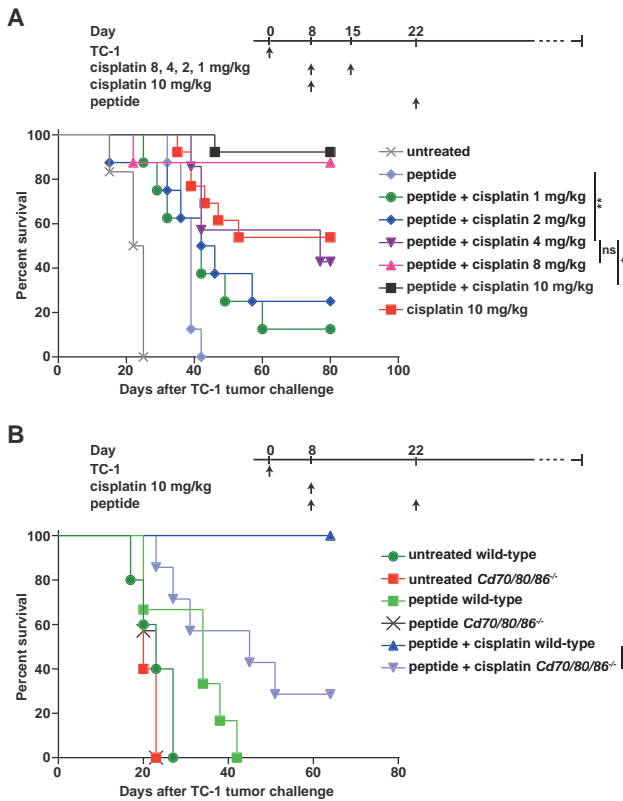


**Figure 7. Chemotherapy requires CD80 and CD86 costimulatory signals**

**A**, survival of TC-1 tumor-bearing wild-type mice following treatment with cisplatin and HPV16 E7<sub>43-77</sub> SLP vaccination. **B**, survival of TC-1 tumor-bearing wild-type and *Cd70/80/86*<sup>-/-</sup> mice following treatment with 10 mg/kg cisplatin and HPV16 E7<sub>43-77</sub> SLP vaccination. Significance was determined by a log-rank (Mantel-Cox) test. \*,  $P < 0.05$ ;  $n = 6-7$  mice per group.

tumor microenvironment upon cisplatin treatment may be related to enhanced production of MCP-1/CCL2. These myeloid cells are well equipped to engulf apoptotic tumor cells and subsequently present tumor-specific peptides to T cells, and our data suggest that this is one of the mechanisms. In this respect, it has been demonstrated that following anthracycline therapy, intratumoral CD11cCD11b<sup>+</sup>Ly6C<sup>hi</sup> cells have such properties as well (37), suggesting that this effect is not limited to cisplatin only. Therefore, it will be of interest to further investigate the particular characteristics of chemotherapy-induced APCs in antitumor responses.

To improve cisplatin treatment, we combined it with therapeutic vaccination. This almost doubled the response rate, leading to cure of almost all animals treated with the combination. In the past, cisplatin was shown to increase the cytotoxicity of lymphocytes against tumor

cells (15, 16) and we recently revealed that T-cell–derived TNF, through upregulation of several proapoptotic proteins, sensitized tumor cells to cisplatin-induced killing (17). In clinical settings, the side effects of cisplatin treatment often results in the administration of reduced doses as part of the standard clinical treatment. Our experiments revealed that at 80% of the MTD, chemotherapy can be given at least twice, without the loss in body weight seen when the MTD is used. Importantly, while the side effects are reduced, the clinical efficacy was retained. This provides ample opportunities to combine cisplatin chemotherapy at clinically relevant doses with immunotherapy.

In conclusion, cisplatin as single-agent chemotherapy results in an enhanced attraction of myeloid cells into the tumor, increases costimulatory molecules on the intratumoral myeloid APCs, and thereby fosters the stimulation of tumor-specific CD8<sup>+</sup> T cells. Because immune mechanisms are obviously essential for the antitumor effects by cisplatin, a cancer cell centric view of tumor cell destruction has to be abandoned. The powerful immune-stimulatory effects of cisplatin are important underlying mechanisms for the sustained clinical antitumor effect of cisplatin monotherapy and provide opportunities for new treatment options including in combination with other immunotherapy modalities such as therapeutic vaccination or immunomodulating antibodies.

### **Disclosure of Potential Conflicts of Interest**

C.J.M. Melief is a chief scientific officer at ISA Pharmaceuticals and is a consultant/advisory board member for Immatics. S.H. van der Burg reports receiving a commercial research grant and is a consultant/advisory board member for ISA Pharmaceuticals. No potential conflicts of interest were disclosed by the other authors.

### **Authors' Contributions**

**Conception and design:** E. Beyranvand Nejad, T.C. van der Sluis, C.J.M. Melief, S.H. van der Burg, R. Arens

**Development of methodology:** E. Beyranvand Nejad, T.C. van der Sluis, G.M. Janssen, C.J.M. Melief, S.H. van der Burg, R. Arens

**Acquisition of data (provided animals, acquired and managed patients, provided facilities, etc.):** E. Beyranvand Nejad, T.C. van der Sluis, S. van Duikeren, G.M. Janssen, P.A. van Veelen

**Analysis and interpretation of data (e.g., statistical analysis, biostatistics, computational analysis):** E. Beyranvand Nejad, T.C. van der Sluis, G.M. Janssen, P.A. van Veelen, C.J.M. Melief, S.H. van der Burg, R. Arens  
**Writing, review, and/or revision of the manuscript:** E. Beyranvand Nejad, T.C. van der Sluis, H. Yagita, P.A. van Veelen, C.J.M. Melief, S.H. van

der Burg, R. Arens Administrative, technical, or material support (i.e., reporting or organizing data, constructing databases): S. van Duikeren, H. Yagita

**Study supervision:** C.J.M. Melief, S.H. van der Burg, R. Arens

## Acknowledgments

The authors acknowledge Suzanne Welten, Marjolein Sluiter, Thorbald van Hall, and Margreet de Vries for providing transgenic and knockout mice. The authors would like to thank Willemien Benckhuijsen, Jan Wouter Drijfhout, and Kees Franken for constructing peptides and tetramers. The authors greatly appreciate the help from Els van Beelen for cytokine multiplex assays.

## Grant Support

This work was supported by a grant from the Dutch Cancer Society (KWF 2009-4400 to C.J.M. Melief and S.H. van der Burg), a grant from Leiden University Medical Center (LUMC; E. Beyranvand Nejad), a Gisela Thier grant from LUMC (R. Arens), and a grant from the Macropa Foundation (R. Arens).

The costs of publication of this article were defrayed in part by the payment of page charges. This article must therefore be hereby marked advertisement in accordance with 18 U.S.C. Section 1734 solely to indicate this fact.

Received March 25, 2016; revised July 25, 2016; accepted August 1, 2016;  
published OnlineFirst August 28, 2016.



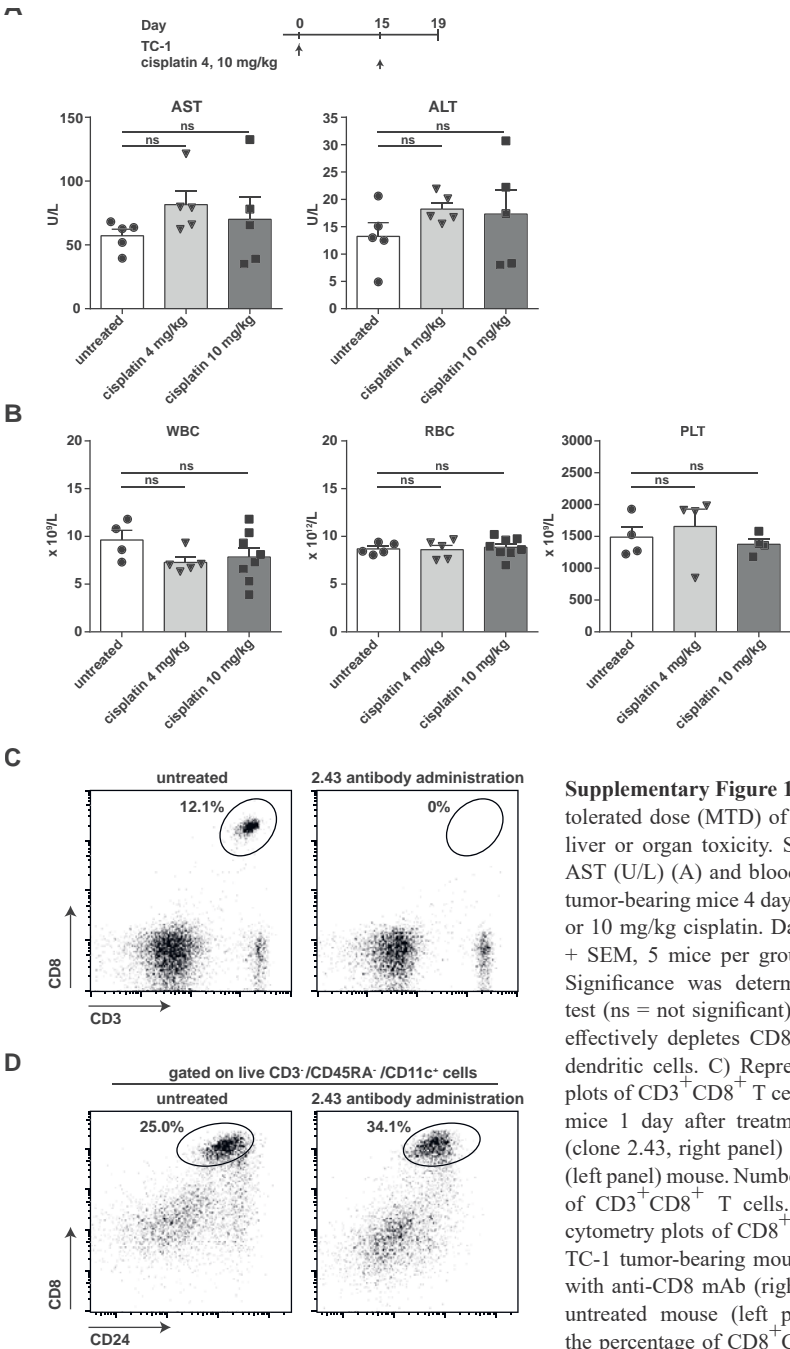
## References

1. Schreiber RD, Old LJ, Smyth MJ. Cancer immunoediting: integrating immunity's roles in cancer suppression and promotion. *Science* 2011;331: 1565–70.
2. Arens R. Rational design of vaccines: learning from immune evasion mechanisms of persistent viruses and tumors. *Adv Immunol* 2012;114: 217–43.
3. Gajewski TF, Woo SR, Zha Y, Spaapen R, Zheng Y, Corrales L, et al. Cancer immunotherapy strategies based on overcoming barriers within the tumor microenvironment. *Curr Opin Immunol* 2013;25:268–76.
4. van der Burg SH, Arens R, Ossendorp F, van Hall T, Melief CJ. Vaccines for established cancer: overcoming the challenges posed by immune evasion. *Nat Rev Cancer* 2016;16:219–33.
5. Mihich E. Combined effects of chemotherapy and immunity against leukemia L1210 in DBA-2 mice. *Cancer Res* 1969;29:848–54.
6. Mihich E. Modification of tumor regression by immunologic means. *Cancer Res* 1969;29:2345–50.
7. Schwartz HS, Grindey GB. Adriamycin and daunorubicin: a comparison of antitumor activities and tissue uptake in mice following immunosuppression. *Cancer Res* 1973;33:1837–44.
8. Galluzzi L, Senovilla L, Zitvogel L, Kroemer G. The secret ally: immunostimulation by anticancer drugs. *Nat Rev Drug Discov* 2012;11:215–33.
9. Zitvogel L, Kepp O, Kroemer G. Immune parameters affecting the efficacy of chemotherapeutic regimens. *Nat Rev Clin Oncol* 2011;8:151–60.
10. Kroemer G, Galluzzi L, Kepp O, Zitvogel L. Immunogenic cell death in cancer therapy. *Annu Rev Immunol* 2013;31:51–72.
11. Kepp O, Senovilla L, Vitale I, Vacchelli E, Adjemian S, Agostinis P, et al. Consensus guidelines for the detection of immunogenic cell death. *Oncoimmunology* 2014;3:e955691.
12. Obeid M, Tesniere A, Ghiringhelli F, Fimia GM, Apetoh L, Perfettini JL, et al. Calreticulin exposure dictates the immunogenicity of cancer cell death. *Nat Med* 2007;13:54–61.
13. Tesniere A, Schlemmer F, Boige V, Kepp O, Martins I, Ghiringhelli F, et al. Immunogenic death of colon cancer cells treated with oxaliplatin. *Oncogene* 2010;29:482–91.
14. Martins I, Kepp O, Schlemmer F, Adjemian S, Tailler M, Shen S, et al. Restoration of the immunogenicity of cisplatin-induced cancer cell death by endoplasmic reticulum stress. *Oncogene* 2011;30:1147–58.
15. Sodhi A, Singh SM. Increased capacity of lymphocytes to lyse tumor cells in vitro and production of lymphotoxins after cisplatin treatment. *Int J Immunopharmacol* 1988;10:753–61.
16. Ramakrishnan R, Assudani D, Nagaraj S, Hunter T, Cho HI, Antonia S, et al. Chemotherapy enhances tumor cell susceptibility to CTL-mediated killing during cancer immunotherapy in mice. *J Clin Invest* 2010;120:1111–24.
17. van der Sluis TC, van Duikeren S, Huppelschoten S, Jordanova ES, Beyranvand NE, Sloots A, et al. Vaccine-induced tumor necrosis factor-producing T cells synergize with cisplatin to promote tumor cell death. *Clin Cancer Res* 2015;21:781–94.
18. Cook AM, Lesterhuis WJ, Nowak AK, Lake RA. Chemotherapy and immunotherapy: mapping the road ahead. *Curr Opin Immunol* 2016; 39:23–9.
19. Borriello F, Sethna MP, Boyd SD, Schweitzer AN, Tivol EA, Jacoby D, et al. B7-1 and B7-2 have overlapping, critical roles in immunoglobulin class switching and germinal center formation. *Immunity* 1997;6:303–13.
20. Welten SP, Redeker A, Franken KL, Oduro JD, Ossendorp F, Cicin-Sain L, et al. The viral context instructs the redundancy of costimulatory pathways in driving CD8 T cell expansion. *Elife* 2015;4:e07486.

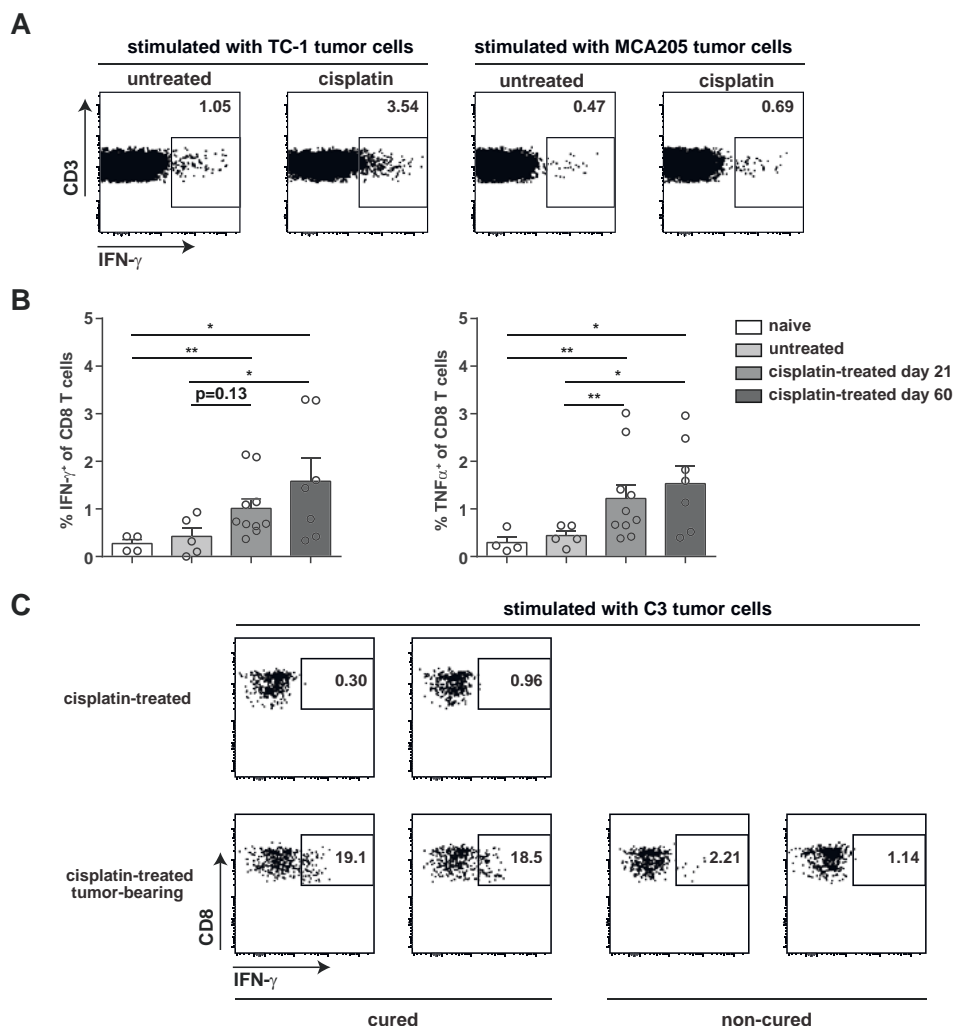


21. Overwijk WW, Theoret MR, Finkelstein SE, Surman DR, de Jong LA, Vyth-Dreese FA, et al. Tumor regression and autoimmunity after reversal of a functionally tolerant state of self-reactive CD8 $\beta$  T cells. *J Exp Med* 2003; 198:569–80.
22. Lin KY, Guarnieri FG, Staveley-O'Carroll KF, Levitsky HI, August JT, Pardoll DM, et al. Treatment of established tumors with a novel vaccine that enhances major histocompatibility class II presentation of tumor antigen. *Cancer Res* 1996;56:21–6.
23. van Duikeren S, Fransen MF, Redeker A, Wieles B, Platenburg G, Krebber WJ, et al. Vaccine-induced effector-memory CD8 T cell responses predict therapeutic efficacy against tumors. *J Immunol* 2012;189: 3397–403.
24. Feltkamp MC, Smits HL, Vierboom MP, Minnaar RP, de Jongh BM, Drijfhout JW, et al. Vaccination with cytotoxic T lymphocyte epitopecontaining peptide protects against a tumor induced by human papillomavirus type 16-transformed cells. *Eur J Immunol* 1993;23:2242–9.
25. Arens R, Schoenberger SP. Plasticity in programming of effector and memory CD8 T-cell formation. *Immunol Rev* 2010;235:190–205.
26. Scaffidi P, Misteli T, Bianchi ME. Release of chromatin protein HMGB1 by necrotic cells triggers inflammation. *Nature* 2002;418:191–5.
27. Apetoh L, Ghiringhelli F, Tesniere A, Criollo A, Ortiz C, Lidereau R, et al. The interaction between HMGB1 and TLR4 dictates the outcome of anticancer chemotherapy and radiotherapy. *Immunol Rev* 2007;220: 47–59.
28. van der Sluis TC, Sluijter M, van Duikeren S, West BL, Melief CJ, Arens R, et al. Therapeutic peptide vaccine-induced CD8 T cells strongly modulate intratumoral macrophages required for tumor regression. *Cancer Immunol Res* 2015;3:1042–51.
29. Welters MJ, van der Sluis TC, van Meir H, Loof NM, van Ham VJ, van Duikeren S, et al. Vaccination during myeloid cell depletion by cancer chemotherapy fosters robust T cell responses. *Sci Transl Med* 2016;8: 334ra52.
30. Tanaka H, Matsushima H, Mizumoto N, Takashima A. Classification of chemotherapeutic agents based on their differential invitro effects on dendritic cells. *Cancer Res* 2009;69:6978–86.
31. Apetoh L, Ghiringhelli F, Tesniere A, Obeid M, Ortiz C, Criollo A, et al. Tolllike receptor 4-dependent contribution of the immune system to anticancer chemotherapy and radiotherapy. *Nat Med* 2007;13:1050–9.
32. Han J, Zhong J, Wei W, Wang Y, Huang Y, Yang P, et al. Extracellular high-mobility group box 1 acts as an innate immune mediator to enhance autoimmune progression and diabetes onset in NOD mice. *Diabetes* 2008;57:2118–27.
33. Kang TH, Mao CP, Lee SY, Chen A, Lee JH, Kim TW, et al. Chemotherapy acts as an adjuvant to convert the tumor microenvironment into a highly permissive state for vaccination-induced antitumor immunity. *Cancer Res* 2013;73:2493–504.
34. Oizumi S, Strbo N, Pahwa S, Deyev V, Podack ER. Molecular and cellular requirements for enhanced antigen cross-presentation to CD8 cytotoxic T lymphocytes. *J Immunol* 2007;179:2310–7.
35. Hu W, Jain A, Gao Y, Dozmorov IM, Mandraju R, Wakeland EK, et al. Differential outcome of TRIF-mediated signaling in TLR4 and TLR3 induced DC maturation. *Proc Natl Acad Sci U S A* 2015;112:13994–9.
36. Tabachnyk M, Distel LV, Buttner M, Grabenbauer GG, Nkenke E, Fietkau R, et al. Radiochemotherapy induces a favourable tumour infiltrating inflammatory cell profile in head and neck cancer. *Oral Oncol* 2012;48:594–601.
37. Ma Y, Adjemian S, Mattarollo SR, Yamazaki T, Aymeric L, Yang H, et al. Anticancer chemotherapy-induced intratumoral recruitment and differentiation of antigen-presenting cells. *Immunity* 2013;38:729–41.

# Supplementary Figure legends:

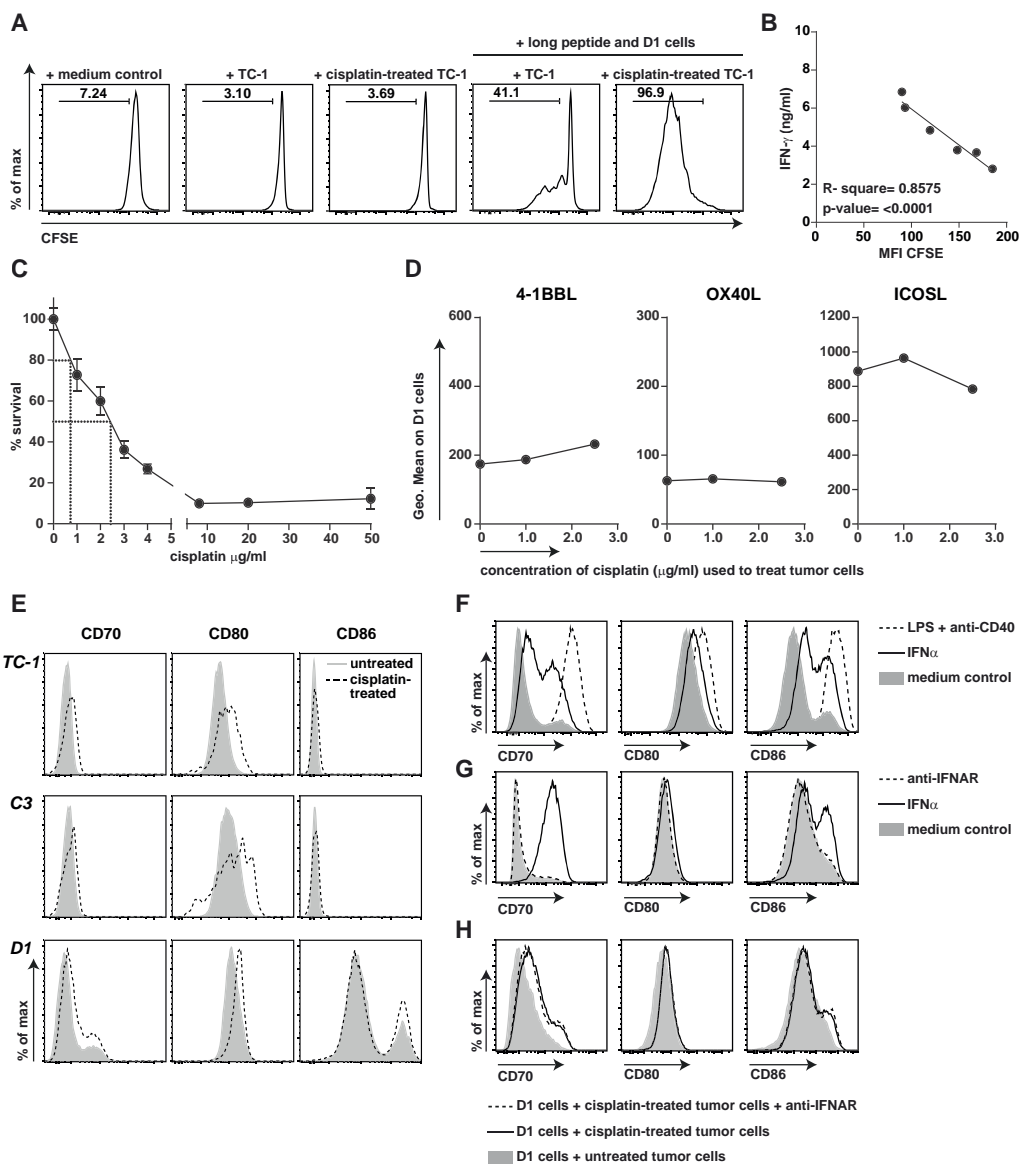


**Supplementary Figure 1.** A and B) The maximum tolerated dose (MTD) of cisplatin does not induce liver or organ toxicity. Serum levels of ALT and AST (U/L) (A) and blood cell counts (B) in TC-1 tumor-bearing mice 4 days after administration of 4 or 10 mg/kg cisplatin. Data are displayed as mean + SEM, 5 mice per group from one experiment. Significance was determined by Mann-Whitney test (ns = not significant). CD8 depleting antibody effectively depletes CD8<sup>+</sup> T cells but not CD8<sup>+</sup> dendritic cells. C) Representative flow cytometry plots of CD3<sup>+</sup>CD8<sup>+</sup> T cells in TC-1 tumor-bearing mice 1 day after treatment with anti-CD8 mAb (clone 2.43, right panel) compared to an untreated (left panel) mouse. Numbers indicate the percentage of CD3<sup>+</sup>CD8<sup>+</sup> T cells. D) Representative flow cytometry plots of CD8<sup>+</sup> splenic dendritic cells in TC-1 tumor-bearing mouse 4 days after treatment with anti-CD8 mAb (right panel) compared to an untreated mouse (left panel). Numbers indicate the percentage of CD8<sup>+</sup>CD24<sup>+</sup> cells gated on live singlet CD3<sup>+</sup>B220<sup>-</sup>CD11c<sup>+</sup> cells.



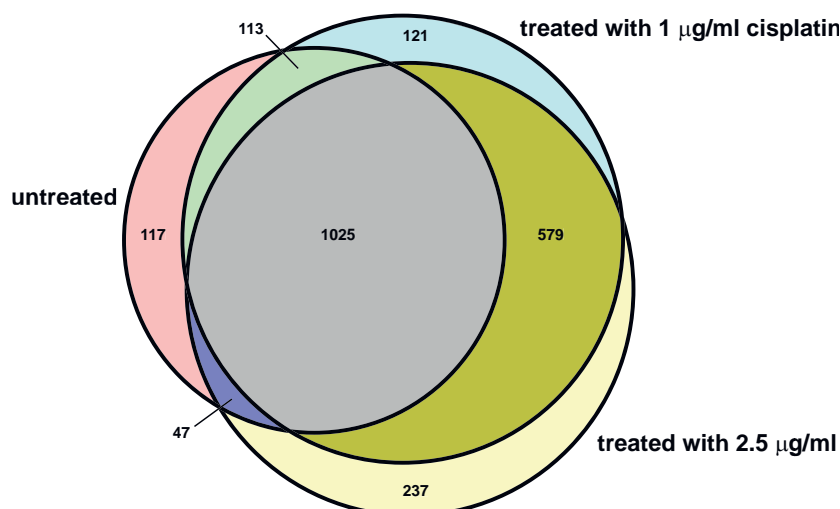
**Supplemental Figure 2.** Induction of tumor-specific T-cell responses are dependent on cisplatin treated tumor cells. C57BL/6 mice were injected s.c with  $1 \times 10^5$  TC-1 tumor cells in the flank and treated on day 8 with 10 mg/kg cisplatin or left untreated. A) Flow cytometry plots of IFN- $\gamma$  producing splenic CD8<sup>+</sup> T cells of naive (non tumor-bearing) and cisplatin-treated TC-1 or MCA205 tumor-bearing mice (day 60 post tumor challenge). IFN- $\gamma$  production in splenic CD8<sup>+</sup> T cells was determined after 4 days *in vitro* stimulation with irradiated tumor cells or left unstimulated as described in Supplementary Materials and Methods. B) On day 21 post tumor challenge, naive, untreated and cisplatin-treated mice (cisplatin-treated day 21) were sacrificed. At the same day, cisplatin-treated mice that survived tumor challenge and remained tumor free until day 60 post tumor challenge (cisplatin-treated day 60) were also sacrificed. IFN- $\gamma$  and TNF production in splenic CD8<sup>+</sup> T cells was determined after 4 days *in vitro* stimulation with irradiated TC-1 tumor cells or left unstimulated. The percentage of IFN- $\gamma$ <sup>+</sup> cells within the CD3<sup>+</sup>CD8<sup>+</sup> T cells are normalized to non-stimulated conditions. C) Flow cytometry plots of IFN- $\gamma$  producing CD8<sup>+</sup> splenic T cells of cisplatin-treated non-tumor-bearing mice (upper two plots) and cisplatin-treated C3 tumor-bearing mice (lower four plots). Wild-type C57BL/6 mice were injected s.c with  $5 \times 10^5$  C3 tumor cells in the flank or kept unchallenged. Mice were treated on day 14 with 10 mg/kg cisplatin. On day 60 post tumor challenge, all mice were sacrificed. On that day, 50% of the cisplatin-treated C3 tumor-bearing mice were cured. Spleens were dissected and single cell suspensions were stimulated overnight with irradiated C3 tumor cells in presence of brefeldin A. Next, cells were stained intracellular for IFN- $\gamma$ . Numbers indicate the percentage of IFN- $\gamma$ <sup>+</sup> cells within CD3<sup>+</sup>CD8<sup>+</sup> cells.



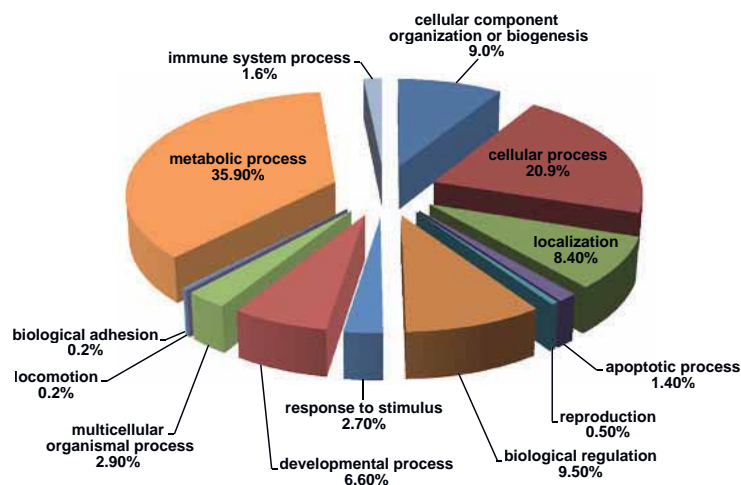


◀ **Supplementary Figure 3.** Cisplatin-induced cell death enhances T-cell activation by upregulating CD70, CD80 and CD86 costimulatory molecules. A) Representative flow cytometry plots for CD8<sup>+</sup> T-cell proliferation. Shown is the CFSE level in isolated CD8<sup>+</sup> pmel-1 cells incubated with medium control or TC-1 tumor cells without any treatment or treated with 1.0 µg/ml cisplatin in the presence of D1 dendritic cells and long peptide as described in Supplementary Materials and Methods. The numbers show the percentage of proliferated cells. Data shown is representative of three independent experiments. B) Shown is the correlation of IFN-γ production (ng/ml) and CFSE level of pmel-1 CD8<sup>+</sup> cells in the presence of D1 cells and TC-1 tumor cells treated with different dosages of cisplatin with the geometric mean of CFSE at each concentration. Data shown is representative of three independent experiments. C) Percentage of survival of TC-1 tumor cells upon exposure to cisplatin (µg/ml) as measured by an MTT assay. Percentages of viable cells were calculated based on the OD of each condition compared to untreated sample and expressed as percentage. Dotted lines show the concentrations that inhibited the proliferation of cells for 50% and 20%. Data shown is representative of three independent experiments. D) Expression of the costimulatory molecules 4-1BBL, OX40L and ICOSL on D1 cells in the presence of cisplatin-treated tumor cells. TC-1 tumor cells (7,000 cells/well) were incubated overnight with the indicated doses of cisplatin. Tumor cells were washed and D1 cells were added. Expression of the costimulatory molecules was measured after 72 hours incubation. Data shown is representative of three independent experiments. E) Representative flow cytometry plots for CD70, CD80 and CD86 on TC-1 and C3 tumor cells and D1 cells upon direct exposure to cisplatin. In brief, tumor cells (7,000 cells/well) and D1 cells (50,000 cells/well) were cultured in a 96-well culture flat-bottom plate. After 3 hours, cells were treated with 1 µg/ml cisplatin and incubated overnight. Then, cells were thoroughly washed and expression of CD70, CD80 and CD86 was measured on these cells by flow cytometry. F and G) Expression of CD70, CD80 and CD86 on D1 cells in the presence of IFNα with and without IFNAR blocking antibody. D1 cells were incubated for 24 hours with 1.3 µg/ml of IFNα (F) or for 72 hrs with 1.3 µg/ml IFNα and 20 µg/ml anti-IFNAR blocking antibody (G), after which the costimulatory molecule expression was determined by flow cytometry. LPS + anti-CD40 was used as a positive control and medium alone as a negative control. H) Expression of CD70, CD80 and CD86 on D1 cells with and without anti-IFNAR blocking antibody. D1 cells were incubated for 72 hours in the presence of cisplatin-treated (2.5 µg/ml) or untreated TC-1 tumor cells with and without 20 µg/ml anti-IFNAR blocking antibody, after which the costimulatory molecule expression was determined by flow cytometry.

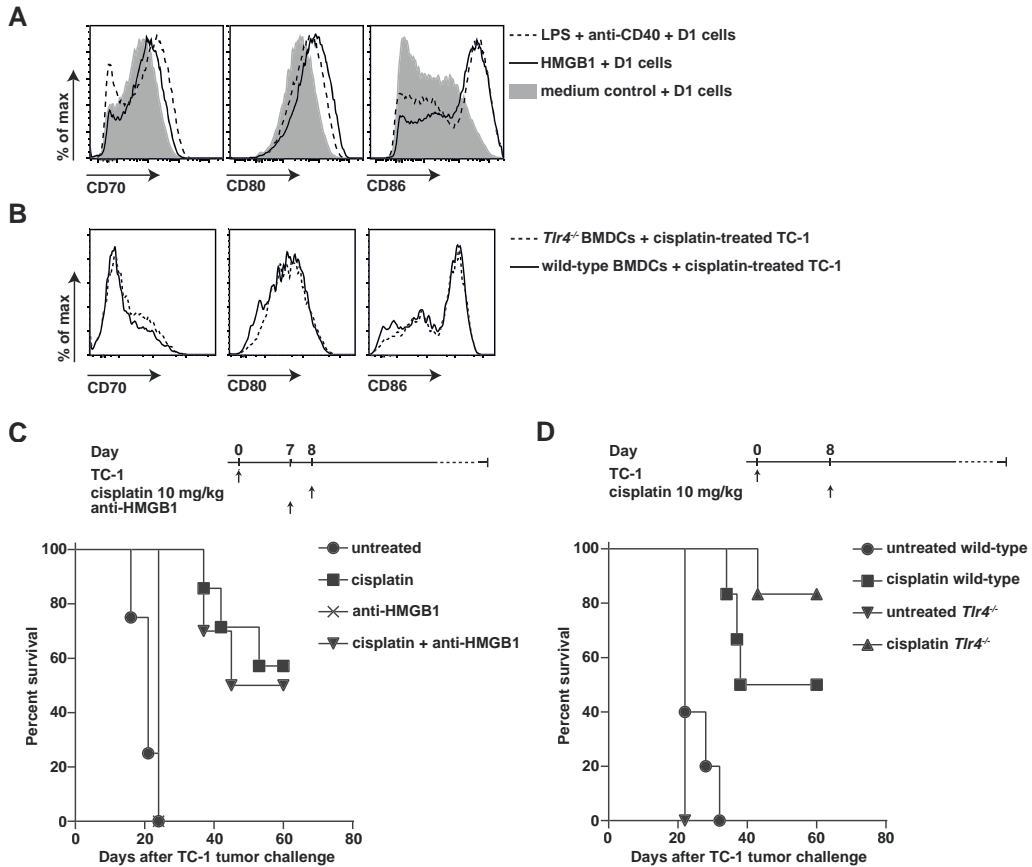
A



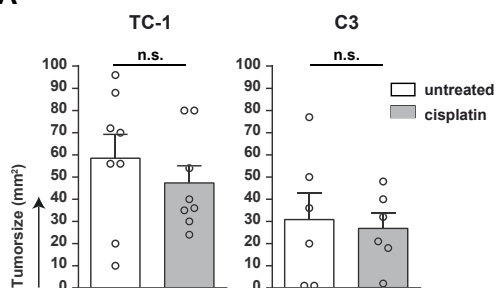
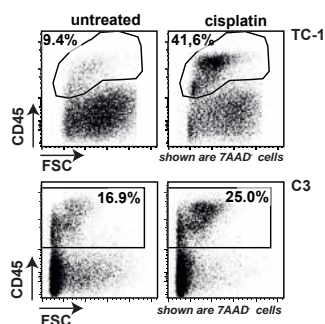
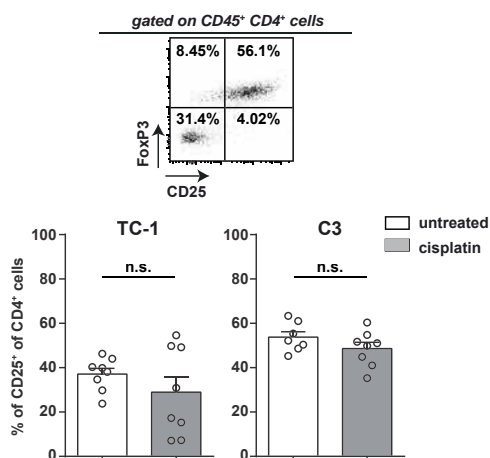
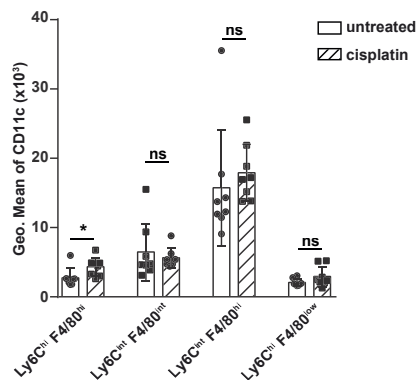
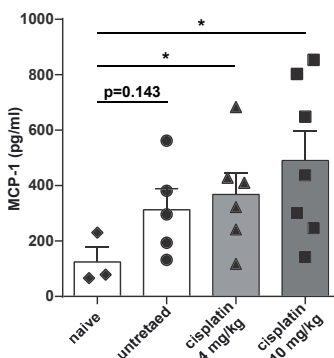
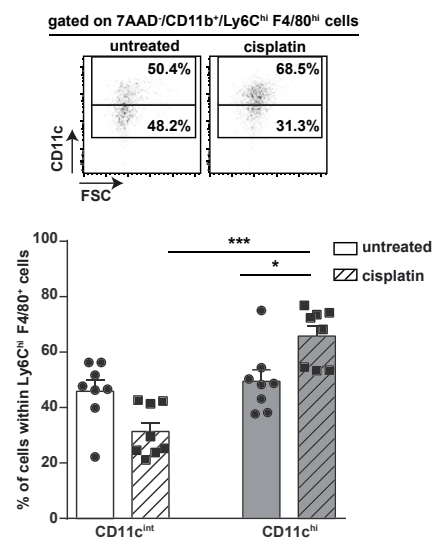
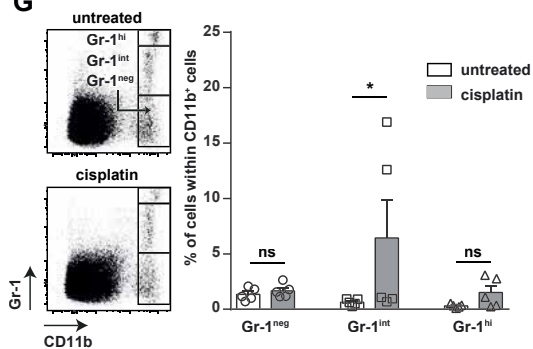
B



**Supplemental Figure 4.** Categorizations of proteins released upon cisplatin treatment of tumor cells. Venn diagram of protein profile overlap between cisplatin-treated and untreated tumor cells. Supernatants of untreated TC-1 tumor cells or treated with 1 or 2.5 µg/ml cisplatin were measured by mass spectrometry. Numbers indicate the number of proteins in each area. B) Categorizations of cisplatin-treated TC-1 tumor cells protein profile. Supernatant of untreated and treated TC-1 tumor cells with 1 µg/ml cisplatin were measured by mass spectrometry as described in Supplemental materials and methods. Proteins with ratio of 3 or higher compared to untreated control were categorized based on their biological process according to PANTHER (Protein Analysis Through Evolutionary Relationships) database classification system.

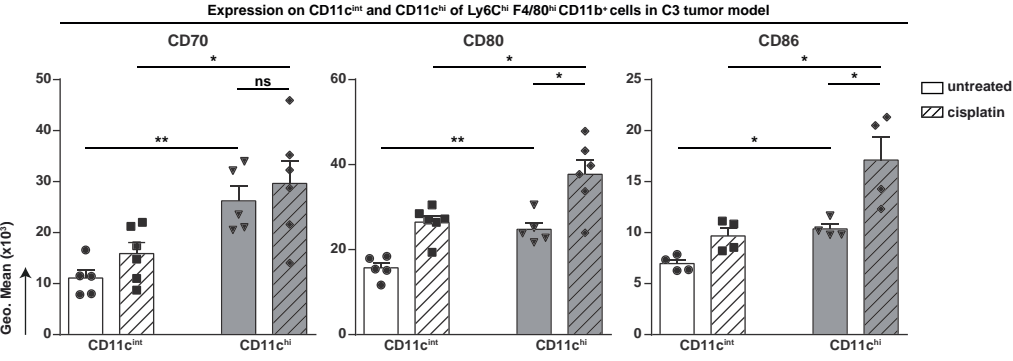


**Supplemental Figure 5.** Modulation of costimulatory molecule expression by HMGB1. A) Expression of CD70, CD80 and CD86 on D1 cells in the presence of HMGB1. D1 cells were incubated for 4 days with 20 ng/ml of HMGB1, after which the expression of CD70, CD80 and CD86 was determined by flow cytometry. LPS + anti-CD40 was used as a positive control and medium alone as a negative control. B) Expression of CD70, CD80 and CD86 on wild-type or *Tlr4*<sup>-/-</sup> BMDCs in the presence of TC-1 tumor cells treated with 2.5 µg/ml cisplatin. The cells were incubated for 72 hours, after which the expression of CD70, CD80 and CD86 was determined by flow cytometry. C) Survival of TC-1 tumor-bearing wild-type mice following treatment with cisplatin and HMGB1 neutralizing antibody (anti-HMGB1). A schematic diagram of the therapy regimen is displayed at the top. Experiment is performed once with 4 mice in the untreated and anti-HMGB1 groups and 7-9 mice in the cisplatin treated groups with and without treatment with anti-HMGB1. D) Survival of TC-1 tumor-bearing wild-type and *Tlr4*<sup>-/-</sup> mice following treatment with cisplatin. A schematic diagram of the therapy regimen is displayed at the top. Experiment is performed once with 4-5 mice in the untreated groups and 6-7 mice in the cisplatin treated.

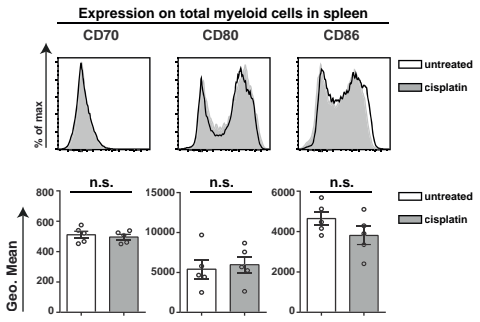
**A****B****C****D****F****E****G**

◀ **Supplemental Figure 6.** Effects of cisplatin on the tumor microenvironment. Wild-type C57BL/6 mice were injected s.c with  $1 \times 10^5$  TC-1 or  $5 \times 10^5$  C3 tumor cells in the flank (day 0). On day 14 (TC-1 model) or day 20 (C3 model), mice were treated systemically with 10 mg/kg cisplatin. Four days later, tumors were dissected and analysed by flow cytometry. A) Tumor sizes of cisplatin treated and untreated mice on day 4 after cisplatin in TC-1 and C3 tumor models. Data is expressed as the mean with SEM. Significance was determined by a Mann-Whitney test. B) Representative flow cytometry plots of leukocytes (CD45<sup>+</sup>) within the live gate on day 18 for the TC-1 (upper panels) and day 24 for C3 (lower panels) tumors of untreated and cisplatin-treated animals. C) Representative flow cytometry plot of intratumoral CD25 and FoxP3 cells gated on CD45<sup>+</sup>CD4<sup>+</sup>classII<sup>-</sup> cells. Percentage of intratumoral CD25<sup>+</sup> of CD4<sup>+</sup> cells in TC-1 and C3 tumor model analysed 4 days after cisplatin treatment. D) The expression of CD11c on the four myeloid subsets isolated from TC-1 tumor. Each dot represents data from an individual mouse. Data is expressed as the mean with SEM. Significance was determined by a Mann-Whitney test. \*,  $P < 0.05$ , \*\*,  $P < 0.01$ , \*\*\*,  $P < 0.001$ . E) The percentage of CD11c<sup>int</sup> and CD11c<sup>hi</sup> of Ly6C<sup>hi</sup> F4/80<sup>hi</sup> CD11b<sup>+</sup> myeloid cells isolated from TC-1 tumor. Each dot represents data from an individual mouse. Data is expressed as the mean with SEM. Significance was determined by a Mann-Whitney test. \*,  $P < 0.05$ , \*\*,  $P < 0.01$ , \*\*\*,  $P < 0.001$ . F) Wild-type C57BL/6 mice were injected s.c with  $1 \times 10^5$  TC-1 tumor cells in the flank and treated on day 8 with 4 or 10 mg/kg cisplatin or left untreated. After 4 days, MCP-1 levels were measured in serum of mice by cytokine multiplex assays. G) Representative flow cytometry plot of MDSCs, based on gating on CD11b and Gr-1 expression, in untreated and cisplatin-treated mice. Graphs indicate the percentage of intratumoral CD11b<sup>+</sup>Gr-1<sup>hi</sup>, CD11b<sup>+</sup>Gr-1<sup>int</sup> and CD11b<sup>+</sup>Gr-1<sup>lo</sup> analysed 4 days after cisplatin treatment in TC-1 tumor model.

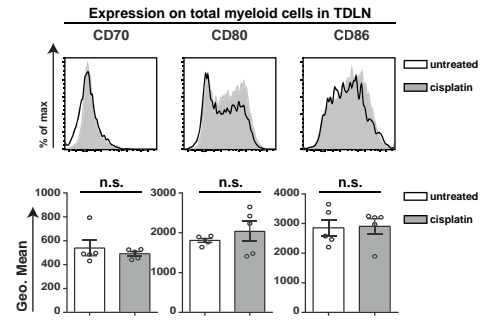
**A**



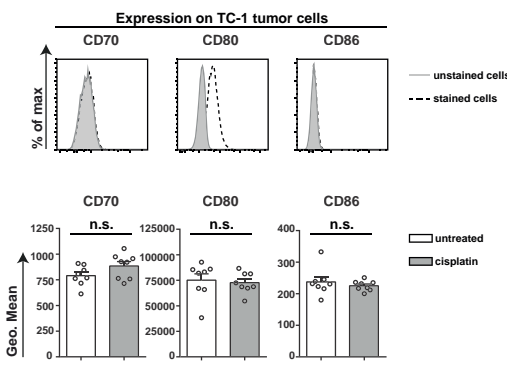
**B**



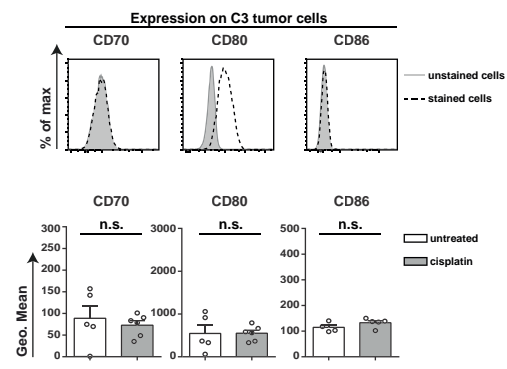
**C**



**D**



**E**



◀ **Supplemental Figure 7.** Cisplatin treatment does not affect the expression of costimulatory molecules on tumor cells, total myeloid cells of spleen and TDLN *in vivo*. C57BL/6 mice were injected s.c with  $1 \times 10^5$  TC-1 or  $5 \times 10^5$  C3 tumor cells in the flank. On day 14 (TC-1 model) or day 20 (C3 model), mice were treated systemically with 10 mg/kg cisplatin. Four days later, tumors were dissected and analysed by flow cytometry. A) The expression of CD70, CD80 and CD86 on CD11c<sup>int</sup> and CD11c<sup>hi</sup> cells of Ly6C<sup>hi</sup> F4/80<sup>hi</sup> CD11b<sup>+</sup> myeloid cells isolated from C3 tumor. Each dot represents data from an individual mouse. Data is expressed as the mean with SEM. Significance was determined by a Mann-Whitney test. \*,  $P < 0.05$ ; \*\*,  $P < 0.01$ ; \*\*\*,  $P < 0.001$ . B and C) Expression of CD70, CD80 and CD86 on total myeloid cells in spleens (B) and tumor draining lymph nodes (TDLN) (C) of TC-1 tumor-bearing mice. The expression of CD70, CD80 and CD86 was determined on total myeloid cells gated on 7AAD<sup>-</sup> CD45<sup>+</sup> CD3<sup>-</sup> CD11b<sup>+</sup> cells in spleens and TDLN of TC-1 tumor-bearing mice. Upper panels show the representative flow cytometry plots (samples closest to median value) for CD70, CD80 and CD86 on total myeloid cells in spleens and TDLNs of untreated mice (solid black lines), cisplatin-treated mice (grey histograms). Lower panels show the expression of CD70, CD80 and CD86 on the total myeloid cells in spleens (B) and TDLN (C) of untreated and cisplatin-treated TC-1 tumor-bearing mice in bar graphs. Data shown is representative for two individual experiments. Each dot represents data from an individual mouse. Data is expressed as the mean with SEM. Significance was determined by a Mann-Whitney test. \*,  $P < 0.05$ , \*\*,  $P < 0.01$ , \*\*\*,  $P < 0.001$ . D and E) Expression of CD70, CD80 and CD86 on TC-1 and C3 tumor cells. Upper panels: Representative flow cytometry plots for CD70, CD80 and CD86 on TC-1 and C3 tumor cells *in vitro*. TC-1 or C3 tumor cells (7000 cells/well) were cultured in a 96-well culture flat-bottom plate and after 48 hours incubation, cells were stained for CD70, CD80 and CD86 (solid grey line) or kept unstained (black dashed line). The expression of CD70, CD80 and CD86 was measured by flow cytometry. Lower panels: Expression of CD70, CD80 and CD86 on TC-1 and C3 from tumor-bearing mice. C57BL/6 mice were injected s.c with  $1 \times 10^5$  TC-1 or  $5 \times 10^5$  C3 tumor cells in the flank. On day 14 (TC-1 model) or day 20 (C3 model), mice were treated systemically with 10 mg/kg cisplatin. Four days later, tumors were dissected and analysed by flow cytometry. Shown is the expression of CD70 (left), CD80 (middle) and CD86 (right) on TC-1 and C3 tumor cells (7AAD<sup>-</sup> CD45<sup>+</sup>). Each circle represents data from an individual mouse. Mean with SEM is indicated. Significance was determined by a Mann-Whitney test. \*,  $P < 0.05$ , \*\*,  $P < 0.01$ .



## Supplementary Materials and Methods

### Cell line culture conditions

Iscove's Modified Dulbecco's Media (IMDM) (BioWhittaker) supplemented with 8% fetal calf serum (FCS) (Greiner), 2 mM L-glutamine (Life Technologies), 50 IU/ml penicillin (Life Technologies) and 50 µg/ml streptomycin (Life Technologies) was used to culture tumor cell lines. Cells were cultured in a humidified incubator at 37°C and 5% CO<sub>2</sub>. D1 cells are long-term growth factor-dependent immature splenic DCs derived from C57BL/6 mice cells (1). *Mycoplasma* tests that were frequently performed for all cell lines by PCR were negative.

### Flow cytometric analysis of splenic and intratumoral immune cells

For analysis of (tumor-infiltrating) immune populations, wild-type C57BL/6 mice were injected s.c with  $1 \times 10^5$  TC-1 or  $5 \times 10^5$  C3 tumor cells in the flank. On day 14 (TC-1 model) or day 20 (C3 model), mice were treated systemically with 10 mg/kg cisplatin. Four days later, lymphoid organs and tumors were collected after transcardial perfusion. Tumors were disrupted in small pieces and incubated with Liberase (Roche) in IMDM for 15 minutes at 37°C. Spleen and lymph nodes were digested by incubating with 0.02 mg/ml DNase and 1 mg/ml collagenase for 10 min at room temperature. Single-cell suspensions were prepared by mincing spleen and tumor pieces through a 70 µm cell strainer (BD Biosciences). Cells were resuspended in staining buffer (PBS + 2% FCS + 0.05% sodium azide) and incubated with various fluorescently labelled antibodies against: CD11b (clone M1/70), CD11c (clone N418), CD45.2 (clone 104), CD70 (clone FR70), CD80 (clone 16-10A1), CD86 (clone GL-1), 4-1BBL (clone TKS-1), OX40L (clone RM134L), ICOSL (clone HK5.3), F4/80 (clone BM8), Ly6C (clone HK1.4), Ly6G (clone 1A8), and CD90.2/Thy1.2 (clone 53-2.1). Antibodies were obtained from eBioscience and Biolegend. For dead cell exclusion, 7-aminoactinomycin D (7-AAD; Invitrogen) was used. Samples were analysed with a BD LSRII or LSRFortessa flow cytometer, and results were analysed using FlowJo software (Tree Star).

For intracellular cytokine staining, single cell suspensions of spleens isolated from naive and cisplatin treated mice were plated at concentrations of  $8 \times 10^5$  cells in 96-well cell culture flat-bottom plates in the presence or absence of irradiated tumor cells and brefeldin A. After overnight incubation, cell surface markers were stained, and cells were fixed in 1% paraformaldehyde for 30 minutes. Thereafter, cells were washed, stained for cytokines and subsequently analysed by flow cytometry.

### Blood counts

Complete blood counts were measured by the Sysmex XP-300 hematology analyser.

## Generation of bone marrow derived dendritic cells (BMDCs)

Bone marrow derived dendritic cells (BMDCs) were generated from bone marrow of mice as follows. The femurs and tibias were collected and flushed. After red blood cell lysis, the bone marrow cells were cultured in a humidified incubator at 37°C and 5 % CO<sub>2</sub> at a density of  $40 \times 10^6$  cells/ml in IMDM medium containing FCS and 200 ng/ml murine recombinant Flt3L (generated in-house). After 8-10 days, cells were harvested from the cultures and live cells were enriched by high-density solution of Ficoll and centrifugation.

## *In vivo* antibody usage and immune cell depletion

The CD8 T-cell depleting monoclonal antibody clone 2.43 was purified from hybridoma cultures and 50 µg per mouse was administrated one day before cisplatin treatment. CD8 T-cell depletion was repeated every week and checked by staining for CD3 and CD8 followed by flow cytometric analysis. Depletion with 2.43 did not lead to depletion of CD8<sup>+</sup> DCs (Supplementary Fig. 1C and 1D). CD4 and NK cell depletion was accomplished through injection of 50 µg per mouse GK1.5 (anti-CD4) and 100µg per mouse PK136 (anti-NK1.1), respectively. CD4 and NK depletion was initiated one day before cisplatin treatment and repeated every 4-6 days. Agonistic CD27 antibody (clone: RM27-3E5) (25) was provided 4 times at 100 µg per mouse every 3 days. CTLA-4 blocking antibody (clone 9H10) was given 3 times at 200 µg per mouse every 3 days. All antibodies were administrated by intraperitoneal (i.p.) injection. Macrophage and dendritic cell depletion was achieved by i.p. administration of 1.5 mg/mouse clodronate liposomes 1 day before cisplatin treatment and repeated every 4-5 days (26).

## *In vivo* HMGB1 neutralization

To neutralize HMGB1, chicken anti-HMGB1 polyclonal antibody was purchased from IBL International GmbH (Manufactured and sold by SHINO-TEST Corporation, Japan) and was used at the concentration of 2 mg/kg to neutralize HMGB1 in mice as suggested by the manufacturer.

## Toxicity measurements

To measure toxicity induced by cisplatin, serum samples of mice were taken 4 days after cisplatin treatment, and the levels of aspartate transaminase (AST) and alanine transaminase (ALT) were measured according to standard protocols of the Department of Clinical Chemistry of LUMC.

## Anti-tumor vaccination

Concurrent with the first administration of cisplatin on day 8, mice were vaccinated in the contralateral flank with synthetic long HPV16 E7<sub>43-77</sub> peptide (GQAEPDRAHYNIVTFCKCDSTLRLCVQSTHVDIR) dissolved in 200 µl PBS and

emulsified with Montanide ISA51 (2). Cisplatin was obtained from Pharmachemie B.V. (Haarlem, The Netherlands) and Accord Healthcare LTD (Middlesex, England).

### **T-cell activation measurement**

For T-cell proliferation determination, TCR transgenic pmel-1 CD8<sup>+</sup> T cells were isolated from spleens and lymph nodes by using the mouse CD8<sup>+</sup> T lymphocyte enrichment set (BD Biosciences). CD8<sup>+</sup> T cells were labelled with CFSE by incubation in PBS containing 1 mM CFSE and 0.1% BSA at 37°C for 10 minutes. Cells were then washed three times with PBS containing 0.1% BSA. TC-1 cells (7000 cells/well) were cultured in a 96-well culture flat-bottom plate (Corning Costar) in the presence of 1.0 µg/ml cisplatin. After overnight incubation, cells were washed and further cultured with fresh medium. After another overnight incubation, D1 cells or BMDCs ( $5 \times 10^4$  cells/well) were co-cultured with the CFSE-labelled pmel-1 cells ( $0.5 \times 10^6$ /well) in the presence of long mgp100 EGP<sub>20-49</sub> for 72 hours at 37°C, 5% CO<sub>2</sub>. Then, cells were harvested and stained for Thy 1.1 (CD90.1). After washing, the amount of CFSE dilution was measured by flow cytometry. To measure the functionality of T cells, IFN-γ was measured in the supernatant of cells by ELISA. To determine the functionality of T cells in the presence of cisplatin-treated tumor cells and different BMDCs, TC-1 tumor cells were treated with 1.0 µg/ml cisplatin overnight or left untreated, and BMDCs derived from wild-type, *Cd70*<sup>-/-</sup>, *Cd80/86*<sup>-/-</sup> and *Cd70/80/86*<sup>-/-</sup> mice were added and co-cultured with CD8<sup>+</sup> pmel-1 T cells in the presence of gp100<sub>25-33</sub> peptide. After 72 hours incubation, supernatant was collected and IFN-γ was measured by ELISA. IFN-γ production is normalized compared to stimulation with untreated tumor cells

### **Analysis of costimulatory molecule expression *in vitro***

To dissect the effect of cisplatin-treated tumors on maturation of dendritic cells, TC-1 tumor cells were harvested and seeded at 7000 cells per well in a 96-well cell culture flat-bottom plate. Six hours later, cisplatin was added and the cells were incubated overnight. The next day, cells were washed and  $5 \times 10^4$  D1 cells were added to the cells. To analyse the effect of HMGB1 and type I IFN on DCs,  $1 \times 10^4$  wild-type BMDCs or  $5 \times 10^4$  D1 cells were incubated with 20 ng/ml HMGB1 protein (IBL international) or 1.3 µg/ml type I IFN (produced as described ((3))). To block IFNAR, InVivoMAb anti-mouse IFNAR-1 (Clone: MAR1-5A3, BioXcell) was used. LPS (1 µg/ml) (Sigma-Aldrich) and anti-CD40 antibody (1 µg/ml) (clone HM40-3, BD Biosciences) were used as positive control. All samples were incubated for 72 hours at 37°C. Cells were then harvested and stained with fluorescently labelled antibodies against costimulatory molecules (CD70, CD80, CD86, 4-1BBL, OX40L, ICOSL) after which the samples were analysed by flow cytometry.



### **Intracellular cytokine staining after 4 days *in vitro* stimulation**

Spleens were dissected and single cell suspensions seeded at about  $6 \times 10^6$  cells per well in a 24-well cell culture flat-bottom plate and stimulated for 4 days with irradiated TC-1 or MCA-205 tumor cells or left unstimulated. After four days, cells were harvested and live cells were enriched by high-density solution of Ficoll and centrifugation. Cells were rested for 2-3 days in the presence of 10 IU IL-2 per ml. After resting, harvested cells were transferred to 96-well culture round-bottom plate and stimulated overnight as described above in presence of Brefeldin A. Next, cells were stained for intracellular IFN- $\gamma$  and TNF production.

### **MTT assay**

TC-1 tumor cells (7000 cells per well) were cultured in a 96-well culture flat-bottom plate for 24 hours. Following overnight treatment with escalating dosages of cisplatin, cells were extensively washed and grown for an additional 24 hours in fresh medium. Cell viability assay was determined using a standard colorimetric MTT (3-(4,5-dimethylthiazol-2-yl)-2,5-diphenyl-tetrazolium bromide) reduction assay. Absorbance was measured with at a test wavelength of 570 nm, and a reference wavelength of 655 nm.

### **Multiplex assay**

TC-1 tumor cells were incubated with indicated amounts of cisplatin. After overnight incubation, cells were washed and incubated overnight. Then, supernatant was collected and stored at  $-80^{\circ}\text{C}$  until further use. Cytokines were measured using a mouse Bio-Plex Pro Mouse Cytokine 23-plex immunoassay (Bio-Rad, Hercules, CA, United States) according to manufacturer's protocol. This multiplex assay detects: Eotaxin, G-CSF, GM-CSF, IFN- $\gamma$ , IL-1 $\alpha$ , IL-1 $\beta$ , IL-2, IL-3 IL-4, IL-5, IL-6, IL-9, IL-10, IL-12 (p40), IL-12 (p70), IL-13, IL-17a, KC, MCP-1 (CCL2), MIP-1 $\alpha$ , MIP-1 $\beta$ , RANTES, TNF $\alpha$ . IFN $\alpha$  was measured with a mouse ProcartaPlex multiplex immunoassay (eBioscience).

### **HMGB1 ELISA**

To measure HMGB1 produced by cisplatin-treated tumor cells, TC-1 tumor cells were incubated with indicated amounts of cisplatin. After overnight incubation, cells were washed and incubated overnight, and HMGB1 levels in the supernatant were determined by ELISA (IBL international) according to the manufacture's protocol.

### **Proteome analysis of chemotherapy-treated tumor cells by mass spectrometry**

To determine the proteins released after chemotherapy treatment, TC-1 tumor cells were cultured at concentration of  $4 \times 10^6$  in T175 CELLSTAR® Tissue Cell Culture Flasks (Corning). Six hours later, cells were treated with 1 or 2.5  $\mu\text{g}/\text{ml}$  cisplatin or kept untreated for overnight. Next, the cells were extensively washed and the medium is replaced with fresh medium without FCS. After overnight incubation, the supernatants were collected and

centrifuged in two steps; first at 1500 rpm for 15 min and then at 2,500 rpm for 15 min both at 4°C to remove cells and cell debris. Cell-free supernatants were acidified to 1% formic acid, concentrated 20× by lyophilization and filter fractionated using 10 kDa Microcon filters (Millipore). The >10 kDa fraction was subjected to a modified filter aided sample preparation procedure (4). After two 25 mM NH<sub>4</sub>HCO<sub>3</sub> washes, the proteins were reduced for 30 min at 37°C on the filter with 200 µl 5 mM DTT and thereafter alkylated for 30 min at room temperature by the addition of 200 µl of 30 mM iodoacetamide. Next, proteins were washed twice with 25 mM NH<sub>4</sub>HCO<sub>3</sub> and digested overnight at 37 °C with 5 µg of trypsin. Tryptic peptides were recovered from the filtrate and analysed by mass spectrometry without further purification. Samples were analysed by online nano high-performance liquid chromatography MS/MS.

Tryptic peptides were analysed using an Easy nLC1000 (Thermo, Bremen, Germany) coupled to a Q-Exactive mass spectrometer (Thermo). Injection was done onto a homemade precolumn (100 µm × 15 mm; Reprosil-Pur C18-AQ 3 µm, Dr. Maisch, Ammerbuch, Germany) and elution via a homemade analytical column (15 cm × 50 µm; Reprosil-Pur C18-AQ 3µm). The gradient was 0% to 30% solvent B (90% ACN/0.1% FA) in 120 min. The analytical column was drawn to a tip of ~5 µm and acted as the electrospray needle of the MS source. The Q-Exactive mass spectrometer was operated in top10-mode. Parameters were as follows: full scan, 70,000 resolution, 3,000,000 AGC target, max fill time 20 ms; MS/MS, 35,000 resolution, 100,000 AGC target, 60 ms max fill time, 17,400 intensity threshold. Apex trigger was set to 1–5 s, and allowed charges were 2–5. Proteome Discoverer version 2.1 was used for peptide and protein identification, using the mascot node for identification, using mascot version 2.2.04 with the Uniprot/SwissProt database (June 2015; 548,586 entries). Up to two missed cleavages were allowed, and methionine oxidation was set as a variable modification; carbamidomethyl on Cys was set as a fixed modification. Peptide assignments were made with a tolerance of 10 ppm. MS/MS fragment tolerance was 20 mmu. Protein identifications were assigned on the basis of a minimum of two confident peptides at 1% false discovery rate (FDR) using the Proteome Discoverer target decoy PSM validator at a strict FDR of 1%. For protein quantitation emPAI values were calculated on the basis of the top 3 intense peptides of each protein (5).

## References

- Winzler C, Rovere P, Rescigno M, Granucci F, Penna G, Adorini L, et al. Maturation stages of mouse dendritic cells in growth factor-dependent long-term cultures. *J Exp Med* 1997;185:317-28.
- van Duikeren S, Fransen MF, Redeker A, Wieles B, Platenburg G, Krebber WJ, et al. Vaccine-induced effector-memory CD8<sup>+</sup> T cell responses predict therapeutic efficacy against tumors. *J Immunol* 2012;189:3397-403.
- Welten SP, Redeker A, Franken KL, Oduro JD, Ossendorp F, Cicin-Sain L, et al. The viral context instructs the redundancy of costimulatory pathways in driving CD8(+) T cell expansion. *Elife* 2015;4:e07486.
- Wisniewski JR, Zougman A, Nagaraj N, Mann M. Universal sample preparation method for proteome analysis. *Nat Methods* 2009;6:359-62.
- Ishihama Y, Oda Y, Tabata T, Sato T, Nagasu T, Rappsilber J, et al. Exponentially modified protein abundance index (emPAI) for estimation of absolute protein amount in proteomics by the number of sequenced peptides per protein. *Mol Cell Proteomics* 2005;4:1265-72.





# Chapter 3

## The microenvironment of tumor cells resisting non-curative immunotherapy determines the type of immune escape

*Elham Beyranvand Nejad<sup>1</sup>, Camilla Labrie<sup>1</sup>, Eva Rademaker<sup>2</sup>, Jan Willem Kleinovink<sup>1</sup>, Tetje C. van der Sluis<sup>3</sup>, Amina FAS Teunisse<sup>4</sup>, Aart G Jochemsen<sup>4</sup>, Jan Oosting<sup>2</sup>, Noel F. de Miranda<sup>2</sup>, Thorbald van Hall<sup>1</sup>, Ramon Arens<sup>3</sup>, Sjoerd H. van der Burg<sup>1</sup>*

Manuscript in preparation

Departments of

1. Medical Oncology, Leiden University Medical Center, Leiden, the Netherlands
2. Pathology, Leiden University Medical Center, Leiden, the Netherlands
3. Immunohematology and Blood Transfusion, Leiden University Medical Center, Leiden, the Netherlands
4. Molecular Cell Biology, Leiden University Medical Center, Leiden, the Netherlands



## Abstract

Several types of tumor-specific T-cell based immunotherapeutic approaches have clinical success. Although complete tumor regressions have been observed oftentimes tumors partially regress followed by tumor recurrence. To study the mechanisms of refractory tumors a mouse model was used where tumor-specific therapeutic vaccination results in tumor regression followed by local recurrence and resistance to vaccination. Recurrent tumors displayed therapy-induced downregulation of the p53- and TNF-signaling pathways as well as upregulation of the epithelial–mesenchymal transition pathway, reflected by a ring of TGF $\beta$ <sup>+</sup> fibroblasts surrounding the escaped tumors. This led to a strong reduction in the numbers of inflammatory immune cells, in particular CD8<sup>+</sup> T cells, infiltrating the tumor. Escape was intrinsic to the tumor cells as ex-vivo cell-sorted recurrent tumor cells, directly reinjected in naïve hosts retained their resistance to vaccination. Remarkably, these reinjected tumor cells contained tumor-specific CD8<sup>+</sup> T cells after vaccination but displayed a strongly impaired influx of inflammatory myeloid cells, shown to be required for tumor regression. These data demonstrate that the same tumor cells may employ different escape mechanisms when grown up in a therapy-experienced or a therapy-naïve microenvironment, indicating that the tissue microenvironment hosting the tumor cells co-selects the type of immune escape after non-curative immunotherapy.

## Introduction

Immunotherapy has become clinically effective in multiple cancers. Blockade of the immune inhibitory checkpoints CTLA-4 and PD-1 as well as adoptive transfer of (genetically modified) T cells are the great examples (1). In addition, therapeutic vaccines targeting tumor-specific antigens start to show clinical benefit, specifically when used in combination with other therapies (2, 3). Despite the many patients with complete responses, the majority of clinically responding patients, however, show partial regressions after immunotherapy (4-6). Furthermore, several primary and acquired resistance mechanisms, including low tumor-specific antigen load, antigen processing defects, loss of HLA cell surface expression, T-cell exclusion, and local immune suppression by suppressive myeloid cell populations, regulatory T cells and co-inhibitory molecule expression, allow the tumors to become therapy resistant, limiting the clinical efficacy of the immunotherapeutic approaches used (7).

The concept of immune editing dictates that a non-curative immune response eventually drives immune escape (8). Unfortunately, most of the tumor models in which systemic immunotherapy is tested show tumor growth delay but not actual tumor regression and by this deviate from what is observed in the clinic. We have shown that under optimal conditions, therapeutic vaccination with the HPV16 E7<sub>43-77</sub> synthetic long peptide (SLP) and the TLR9 agonist CpG results in full tumor regression and cure of all mice with an established TC-1 tumor. However, under suboptimal vaccine conditions TC-1 tumors do show regressions but after a period regrow (9, 10), hereby mimicking non-curative partial clinical responses.

To understand the consequences of non-curative immunotherapy, we made a detailed analysis of extrinsic and intrinsic mechanisms fostering the development of these recurrent tumors. Non-curative, suboptimal therapeutic vaccination led to the regrowth of tumors, which had rewired their oncogenic signaling pathways. Remarkably, the immune escape mechanism employed by these vaccine-resistant tumor cells was completely different when growing in a therapy-experienced or therapy-naïve setting.

## Results

### Non-curative immunotherapy drives the development of immune resistant tumors

Vaccination with the HPV16 E7<sub>43-77</sub> SLP, containing both a CTL epitope and a Th epitope, and CpG results in the full eradication of almost all established TC-1 tumors in mice under optimal vaccine conditions (**Figure 1A and Supplementary Fig 1A**), whereas under suboptimal conditions – resulting in a lower E7-specific T-cell response – vaccination still induced tumor regression in all mice between days 16-22 but from day 28 onwards the tumors recurred (**Figure 1B and Supplementary Fig 1B**). Amplification of the tumor-specific T-cell response by booster vaccination at day 22 could not prevent tumor recurrence (**Figure 1A-B**



**and Supplementary Fig 1C).** This was not due to the incapacity of tumor-bearing animals to respond to this booster vaccination as the magnitude of circulating E7-specific CD8<sup>+</sup>CD127<sup>-</sup>KLRG-1<sup>+</sup> short-lived effector T cells (SLEC) and CD8<sup>+</sup>CD127<sup>+</sup>KLRG-1<sup>+</sup> double-positive effector T cells (DPEC) increased in blood (**Figure 1C and D, Supplementary Fig 1D**). In addition, splenic and lymph node-derived T cells were fully capable to produce IFN $\gamma$ , TNF and IL-2 after E7 stimulation and were cytotoxic to TC-1 cells (**Figure 1E-F, Supplementary Fig 1E-F**). Moreover, the numbers of splenic CD4<sup>+</sup> IFN $\gamma$ , TNF and IL-2 producing T cells were increased (**Figure 1G**). There was no significant difference in tumor sizes, excluding potential influence of this on vaccine-induced T cells (**Supplementary figure 1G**). These data suggested that the recurrent TC-1 tumors had acquired to escape from the tumor-specific T-cell response. To investigate if the failure to control tumor recurrences was due to mechanisms related to the changes in the tumor-microenvironment or to host immunity, we tested if TC-1 cells isolated at the time of the relapse can respond to the same vaccination protocol when injected in a naïve host. TC-1 tumors were harvested from untreated mice at day 18 or from treated mice at day 36 when tumors had recurred. Flow cytometry sorted live TC-1 tumor cells were reinjected in two groups of naïve mice, one of which received the vaccine on day 8 and 22 while the other was left untreated (**Figure 2A**). Reinjected tumor cells from untreated mice fully regressed upon SLP vaccination whereas reinjected recurrent tumor cells did not respond at all (**Figure 2B**). Tumor growth of untreated tumors was similar. Together, these data indicate that therapeutic vaccination can mediate cure of established tumors, however, as soon as the induced T-cell response is only transiently effective it will foster the outgrowth of tumor cells that have acquired an immune resistant profile.

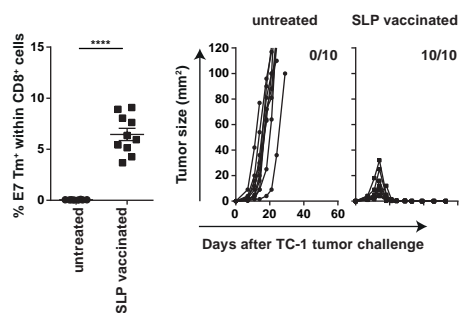
### **Classical immune escape mechanisms do not play a role in tumor recurrence**

Loss of tumor antigen or MHC I expression can mediate immune resistance (11, 12). However, all the relapsed tumors retained E7 expression at comparable levels to the TC-1 tumor cell line (**Supplementary Figure 2A**). Also, the expression of H2-Db, which presents the E7<sub>49-57</sub> T-cell epitope, was retained on recurrent tumors at levels not lower than untreated

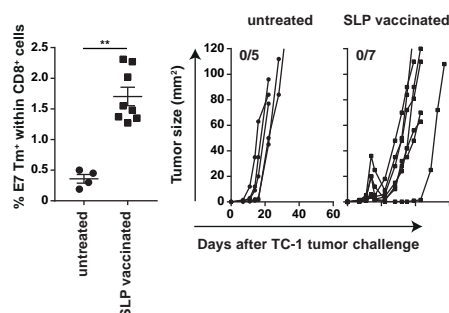
#### **Figure 1. Booster vaccination amplifies the magnitude of circulating E7-specific T cells but is not capable of preventing relapse ►**

Mice were injected with TC-1 tumor cells on day 0 and vaccinated with prime and boost vaccine subcutaneously in flank (A) (suboptimal) or tail base (B) (optimal) on day 8 and 22, respectively. Percentage of E7 Tm<sup>+</sup> cells within CD8<sup>+</sup> cells and tumor outgrowth of untreated mice and SLP vaccinated mice that received the vaccination in flank (A) or tail base (B). C-G) The scheme of the experiment is shown in Supplementary figure 1C. C) The percentage of E7 Tm<sup>+</sup>, CD62L<sup>+</sup>CD44<sup>+</sup> (activated cells), CD127<sup>+</sup>KLRG-1<sup>+</sup> (SLEC), CD127<sup>+</sup>KLRG-1<sup>+</sup> (DPEC) in blood at day 16 (prime) and day 36 (boost). D) The percentage of CD62L<sup>+</sup>CD44<sup>+</sup> (activated cells), CD127<sup>+</sup>KLRG-1<sup>+</sup> (SLEC), CD127<sup>+</sup>KLRG-1<sup>+</sup> (DPEC) within E7 Tm<sup>+</sup> in blood at day 16 (prime) and day 36 (boost). E-G) Percentage of IFN $\gamma$ <sup>+</sup>, TNF $\alpha$ <sup>+</sup> and IL-2<sup>+</sup> cells within CD8<sup>+</sup> T cells in spleen (E) and tumor draining lymph node (TDLN) (F) and CD4<sup>+</sup> T cells in spleen (G) at day 18 (prime) and day 39 (boost). Data represents mean values  $\pm$  SEM (n = 5-9 mice per group). Data are representative of two independent experiments. \*P<0.05, \*\*P<0.01, \*\*\*P<0.001.

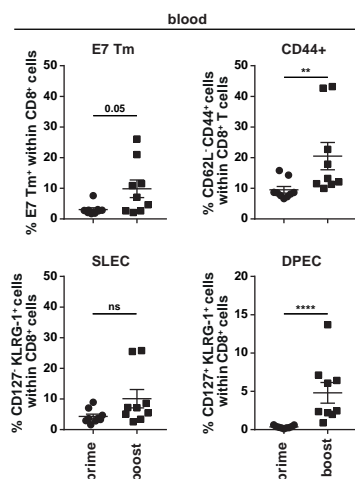
**A**



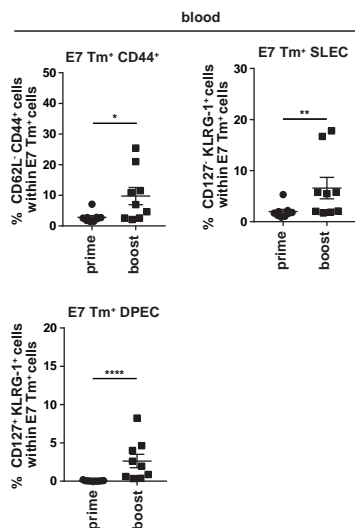
**B**



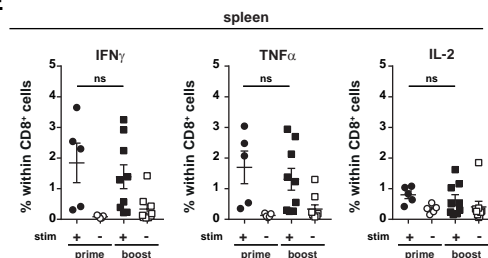
**C**



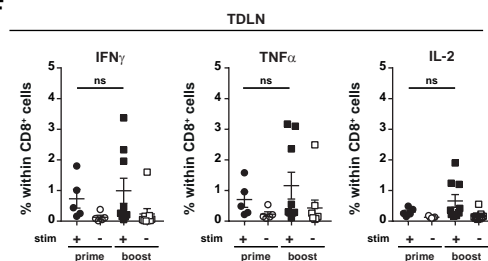
**D**



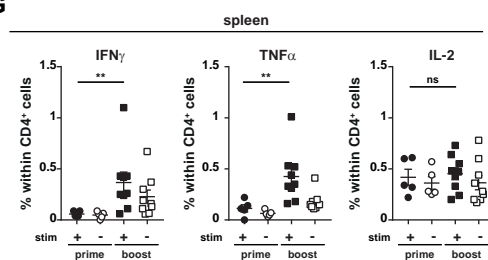
**E**



**F**



**G**



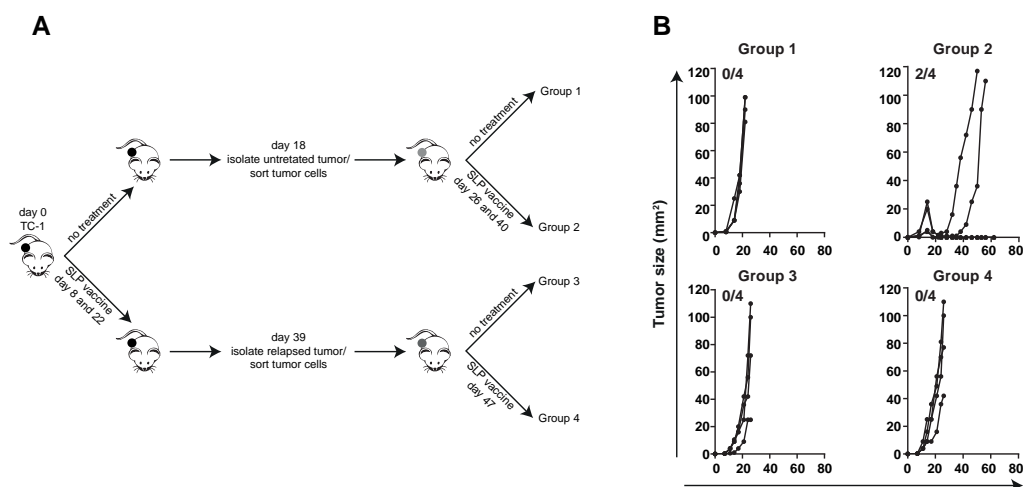


**Figure 2. Non-curative immunotherapy drives the development of immune resistant tumors**

A) Scheme of the experimental procedure. In brief, mice were injected with TC-1 tumor cells on day 0. Then, mice were vaccinated with SLP vaccine on day 8 and 22 or kept untreated. Untreated mice were sacrificed on day 18. Tumor cells were sorted and injected back to the naïve mice. These mice were vaccinated further on day 26 and 40 or kept untreated. Vaccinated mice were sacrificed on day 39 and tumor cells were sorted and injected back to naïve mice, which were vaccinated further on day 47 or left untreated. B) Tumor outgrowth of the mice shown in (A).

and regressing tumors (**Supplementary Figure 2B**). Furthermore, tumor cells isolated from both untreated and recurrent tumors were efficiently killed by CD8<sup>+</sup> T cells isolated from vaccinated mice but not when isolated from non-vaccinated mice (**Supplementary Figure 2C**).

Another obvious immune escape mechanism is formed by the PDL1/PD1 inhibitory pathway (13) (14). Vaccination of TC-1 tumor-bearing mice resulted in a strong increase in the number of intratumoral leukocytes including CD8 T cells and myeloid cells (15). Among these leukocytes, the number of highly activated, type 1 cytokine producing CD8<sup>+</sup> T cells expressing several co-inhibitory molecules increased while the percentage of intratumoral inflammatory myeloid cells were decreased (**Supplementary Figure 2D-F**). This coincided with a lower percentage of TC-1 tumor cells expressing Ki-67 (**Supplementary Figure 2G**). Comparison of PD-1, TIM-3 and LAG-3 expression on T cells revealed that almost all intratumoral and splenic E7-specific T cells (~90-100%) expressed PD-1 both at the time of recurrence and at start of regression (**Supplementary Figure 3A and B**). In addition, the expression of PDL-1 and PDL-2 was significantly increased on recurrent tumor cells at the time of relapse when compared to regressing tumors but PD-L1 was not increased on different subsets of tumor-infiltrating myeloid cells (**Supplementary Figure 3C and D**). However, immunotherapy-driven recurrence of immune resistance tumors could not be prevented by using immune checkpoint blockade of the PD-1/PD-L1 pathway and booster

vaccination. Administration of PD-1 or PD-L1 blocking antibodies both before or at the time of regression did not prevent tumor recurrence (**Supplementary Figure 3E and F**).

### **Vaccine resistant local recurrences display an immunologically “cold” phenotype**

Thus, the tumor cells had found other means to escape the immune response and, therefore, we focused on the immune infiltration of the tumors by quantifying the different subsets of immune cells in the tumor microenvironment. Overall leukocyte infiltration was strongly reduced and altered in composition in the relapsed tumor (**Figure 3A**) leading to the almost absence of CD8<sup>+</sup> T cells, including E7-specific CD8<sup>+</sup> T cells (**Figure 3A and B**). The percentage of CD4<sup>+</sup> T cells and Tregs, both present in low quantities among the tumor infiltrating immune cells, was not altered (**Figure 3B**). In contrast to the CD8<sup>+</sup> T cells, the percentage of intratumoral CD11b<sup>+</sup> myeloid cells strongly increased among intratumoral leukocytes at the time of the relapse (**Figure 3B**). In addition, the composition of the intratumoral myeloid cells, comprising inflammatory (Ly6C<sup>high</sup>) myeloid cells, tumor associated macrophages (Ly6C<sup>low</sup> cells) and neutrophils (Ly6G<sup>+</sup>), was changed in favor of the Ly6C<sup>low</sup>F4/80<sup>hi/low</sup> cells (**Figure 3C**). Thus, tumor recurrence was associated with an impaired tumor infiltration by inflammatory immune cells.

Interestingly, the cytokine production of the intratumoral CD8<sup>+</sup> T cells in the recurrent tumors, albeit present at much lower numbers, was similar to that of the CD8<sup>+</sup> T cells in regressing tumors while the percentage of type 1 cytokine producing CD4<sup>+</sup> T cells was increased (**Supplementary Figure 4A and B**). The significantly lower presence of CD8<sup>+</sup> T cells in recurrent tumors could reflect a lower capacity of tumors to attract these T cells, a failure of the T cells to proliferate and expand locally, or both. To explore potential defects in the attraction of T cells to the tumor, the mRNA expression of 84 chemokines and chemokines receptors from all cells present in the tumors from non-treated, regressed and recurrent tumors was measured (**Supplementary table 2**). This showed that CXCL9 – known to be required for T-cell trafficking to tumors – was amongst the many strongly expressed cytokines in regressing tumors but absent in recurrent tumors. In addition, the expression of its receptor CXCR3 was lower on the relapsed tumor-infiltrating CD8<sup>+</sup> T cells, albeit not significant (**Supplementary figure 4C**). Antibody mediated blocking of CXCR3 delayed the onset of tumor regression but did not prevent recurrence and influence overall survival of the mice (**Supplementary figure 4D and E**), indicating that CXCL9 was not absolutely required in this process. As we previously have shown that tumor cells can produce several chemokines after activation by IFN $\gamma$ -producing tumor-infiltrating T cells (15, 16), the lower expression of chemokines in recurrent tumors most likely is a reflection of reduced T-cell numbers and not the cause for immune escape. The capacity of the intratumoral T cells to locally expand was assessed by their expression of Ki67 and showed that the percentage of CD8<sup>+</sup> T cells



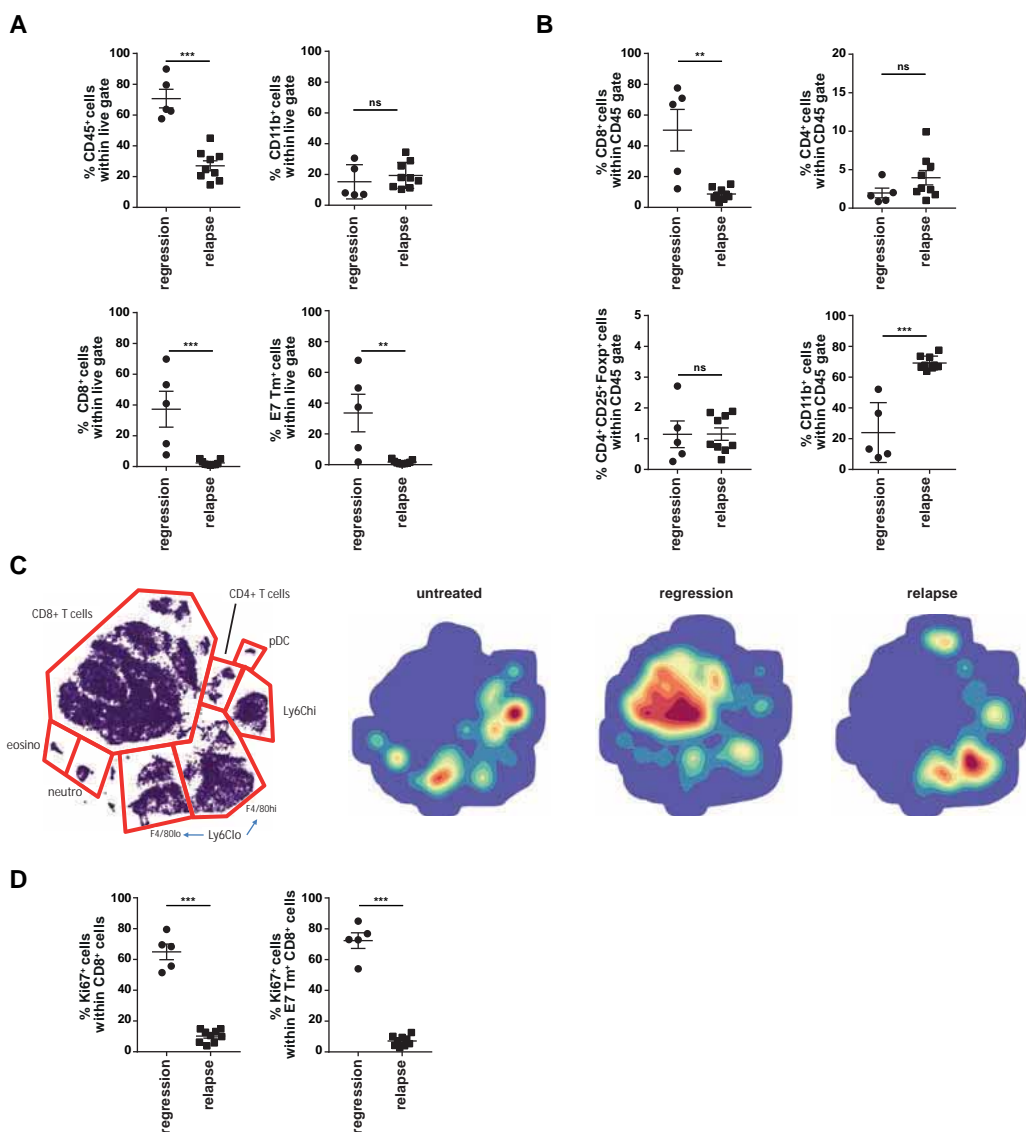


**Figure 3. Vaccine resistant local recurrences display an immunologically “cold” phenotype**

A) Percentage of CD45<sup>+</sup>, CD11b<sup>+</sup>, CD8<sup>+</sup> and E7 Tm<sup>+</sup> cells within live gate at day 18 (regression) and day 39 (relapse). B) percentage of CD8<sup>+</sup>, CD4<sup>+</sup>, Tregs and CD11b<sup>+</sup> within CD45<sup>+</sup> cells at day 18 (regression) and day 39 (relapse). C) H-SNE plots of total CD45<sup>+</sup> immune infiltrates of TC-1 tumors of untreated, regressed or relapsed tumors. Tumors were analyzed by mass cytometry followed by non-supervised clustering using Cytosplore as described in materials and methods. Major myeloid and lymphoid cell types could be distinguished in the H-SNE plot, as indicated. D) Percentage of Ki67<sup>+</sup> cells within CD8<sup>+</sup> T cells and E7 Tm<sup>+</sup> CD8<sup>+</sup> T cells.

expressing Ki67 is lower in recurrent than in regressing tumors (**Figure 3D**). Amplification of the T-cell stimulatory signals OX40 or 4-1BB to overcome this problem (17-19) by administration of agonistic antibodies against these co-stimulatory molecules at the time of regression, did not prevent tumor recurrence or improve the survival of vaccinated mice, nor in combination with PD-1 blockade (**Supplementary Figure 5A-C**).

Next, we hypothesized that the relative increase in the Ly6C<sup>low</sup> myeloid cell population may have suppressed T-cell infiltration and expansion. Therefore, mice were continuously fed with the CSF1R inhibitor PLX3397 (PLX), starting 4 days after the start of regression (day 20). This depleted intratumoral but not splenic macrophages and had no effect on the vaccine-induced CD8<sup>+</sup> T-cell response (**Supplementary figure 5D and E**), confirming our earlier report (15). Moreover, depleting these intratumoral Ly6C<sup>low</sup> myeloid cells had no effect on tumor recurrence (**Supplementary figure 5F**). These data excluded a lack of co-stimulation or suppression by tumor-associated macrophages as extrinsic factors for a lack of dense T-cell infiltration.

### Local recurrences are associated with rewiring of oncogenic pathways

After ruling out several extrinsic factors, we reasoned that the lack of T cell infiltration in relapsed samples could be explained by cancer cell features. This hypothesis was strongly supported by the observation that relapsed tumors remained resistant to therapeutic vaccination after their injection in naïve mice. To investigate this, RNA sequencing was performed in flow cytometry sorted fractions of cancer cells derived from untreated and relapsed tumors. Gene Set Enrichment Analysis of the Hallmark gene set collection (20) showed differential expression of 160 of the 2086 genes composing that set between untreated and relapsed samples. In the latter, strong upregulation of epithelial-mesenchymal transition (EMT) genes and downregulation in the TNF $\alpha$  and TP53 pathways was observed. Of note, most genes that were differentially expressed in the EMT gene set are transforming growth factor-beta (TGF $\beta$ ) transcriptional targets. (**Figure 4A and B and Supplementary Table 3 and 4**). It has been extensively shown that several signaling pathways, including TGF $\beta$  and Wnt/ $\beta$ -catenin, play a role in EMT (21, 22). Therefore, we confirmed the transcriptome data at the protein level for these molecules by immunohistochemistry. While the expression of cytoplasmic and nuclear  $\beta$ -catenin was somewhat increased in the stroma of recurrent tumors (**Supplementary Figure 6A**), the expression of TGF $\beta$  was strongly increased in a layer of cells – presumably fibroblasts – that completely surrounded the tumor (**Figure 4C**). In addition, increased quantities of TGF $\beta$  were measured in the supernatant of ex-vivo recurrent tumors (**Figure 4D**). In accordance with the down regulation of the genes involved in P53 pathway, the expression levels of *mdm2*, *ccng1*, *ei24* and *pidd* were lower in recurrent tumors (**Figure 4E**). Together, these data show that tumor cells had become differently wired as a consequence of a non-curative T-cell attack. Recently, TGF $\beta$ -signaling in fibroblasts was



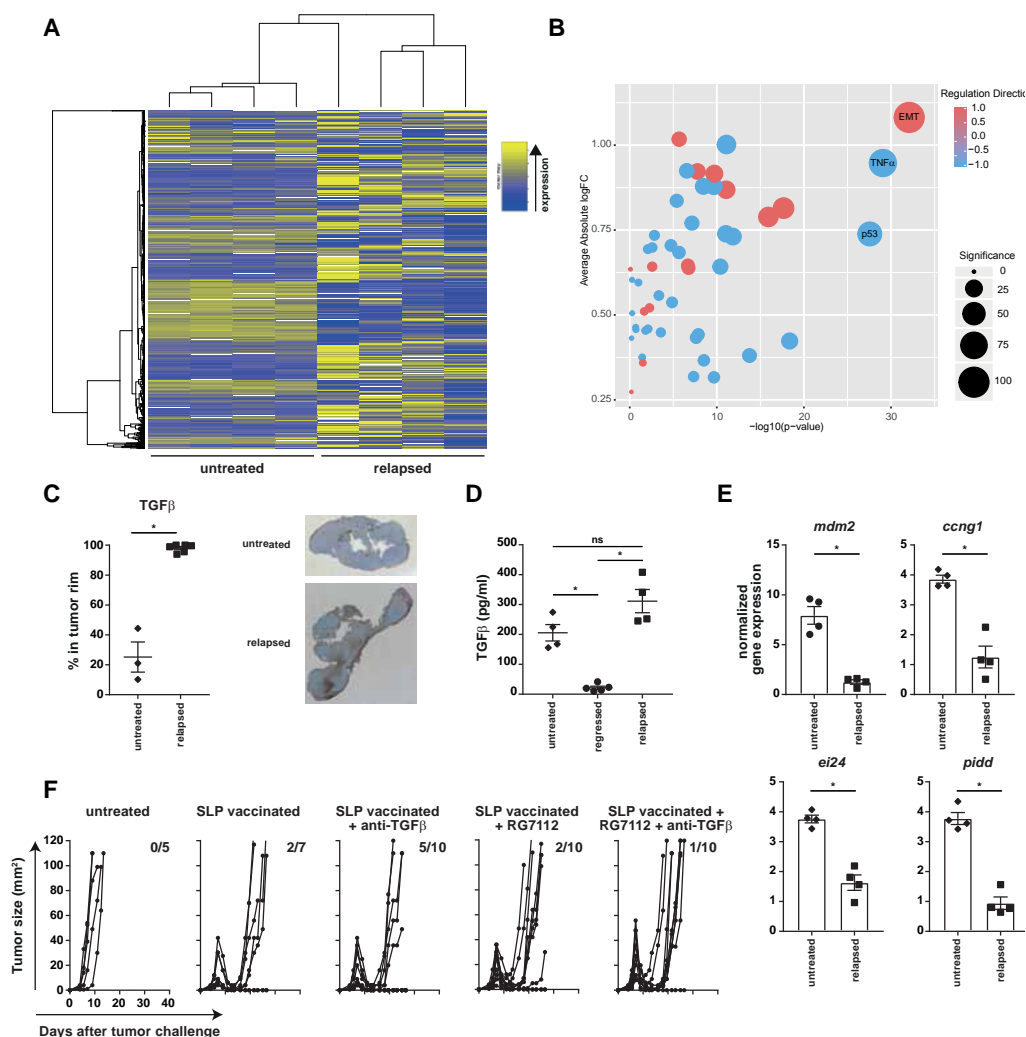


**Figure 4. Local recurrences are associated with rewiring of oncogenic pathways**

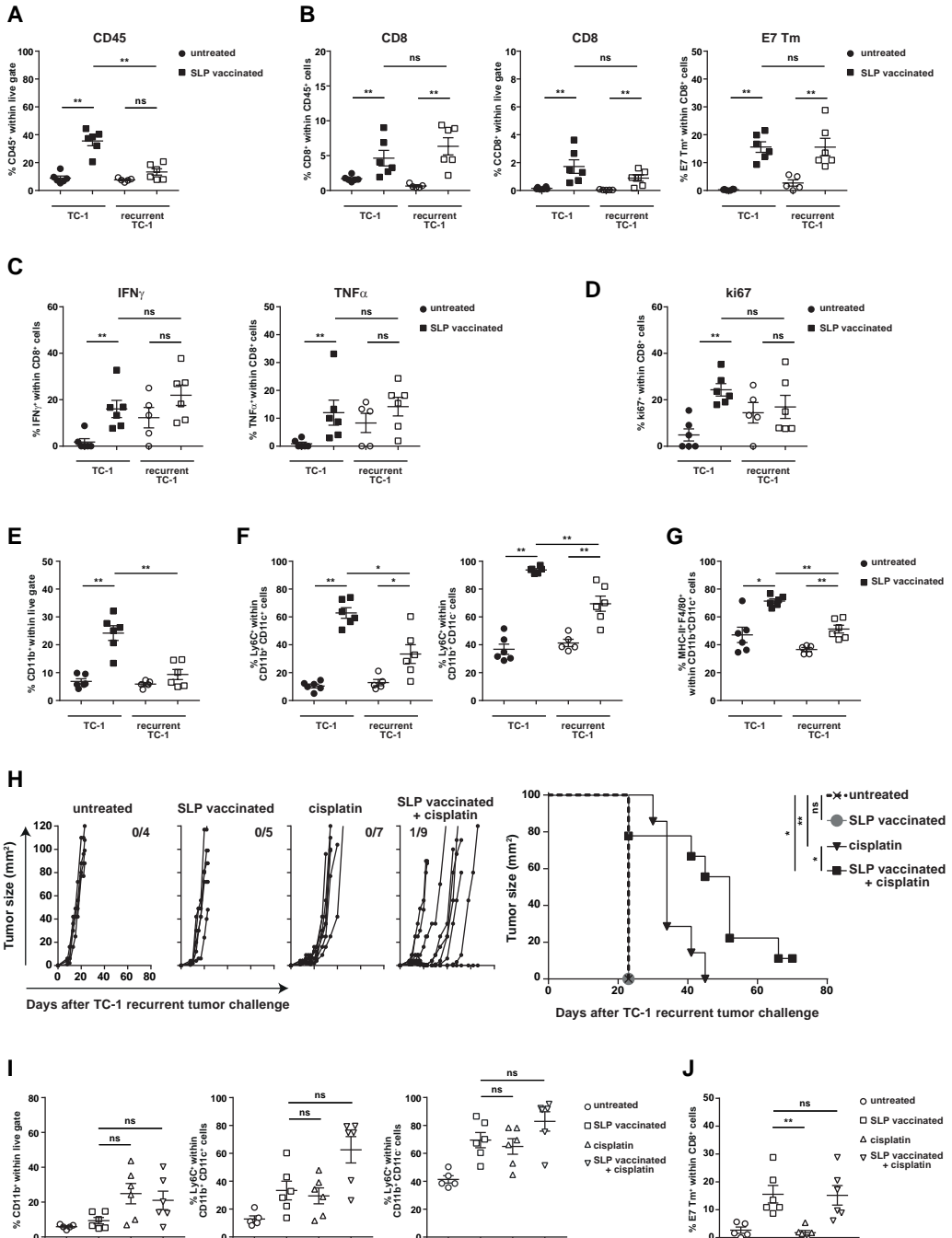
A-B) RNA seq and gene set enrichment analysis of tumor cells sorted from untreated tumor bearing mice (day 18) or mice with relapsed tumors (day 39). C) TGF- $\beta$  score of the rim of the tumor microenvironment from untreated and relapsed tumor bearing mice. D) Measurement of TGF- $\beta$  production by ELISA from the cells present in the tumor microenvironment of the untreated mice or SLP vaccinated mice at the time of the regression (day 18) or relapse (day 39). E) RNA expression of *mdm2*, *ccng1*, *ei24* and *pidd* genes by qPCR from tumor cells sorted from untreated mice or SLP vaccinated mice at the time of the relapse (day 39). F) Tumor outgrowth of the mice treated with SLP vaccine alone or in combination with TGF $\beta$  blocking antibody and/or RG7112. Tumor outgrowth was followed for 40 days. The number of tumor-free mice from the total mice is indicated above each tumor out growth graph. Data are representative of one experiment. \* $P < 0.05$ , \*\* $P < 0.01$ , \*\*\* $P < 0.001$ .

shown to restrict T-cell infiltration of tumors (23, 24), suggesting that this particular immune-driven difference in recurrent tumors would be responsible for a lack of T-cell infiltration. Indeed, when we used TGF $\beta$ -blocking antibodies from the regression phase onwards, the number of mice developing recurrences was significantly decreased (**Figure 4F**). However, activation of P53 signaling by using MDM2 small-molecule antagonist RG7112, did not affect the recurrences following SLP vaccine (**Figure 4F**).

### **Recurrent tumor cells employ a completely different immune escape mechanism when reinjected in a therapy-naïve microenvironment**

Having shown that recurrent tumors displayed a completely altered immune microenvironment, we wondered if the vaccine-resistant tumors would be phenocopied in a naïve host. Mice were challenged with TC-1 tumor cells (TC-1) or flow cytometry sorted tumor cells from the mice with recurrent tumors (TC-1 recurrent), vaccinated at day 8 and then their tumor microenvironment was analyzed at day 15. Similar to what was observed before, the tumors originating from reinjected recurrent tumor cells displayed a strong reduction in the number of CD45<sup>+</sup> tumor-infiltrating immune cells (**Figure 5A**). Remarkably, this was not due to a lack of CD8<sup>+</sup> T-cell infiltration as their numbers, including the HPV-specific CD8<sup>+</sup> T cells, type 1 cytokine production and Ki67 expression, were similar to what is seen in the vaccine-responsive tumors originating from TC-1 tumor cells (**Figure 5B-D**). Instead, the numbers of tumor-infiltrating CD11b<sup>+</sup> myeloid cells, inflammatory (Ly6C<sup>high</sup>) myeloid cells and DC-like MHC class II<sup>+</sup> macrophages were decreased (**Figure 5E-G**). Interestingly, TGF $\beta$  blockade as well as MDM2 inhibitor, RG7112 did not reinstall tumor sensitivity to vaccination (**Supplementary Figure 6B**). To show that a lack of tumor-infiltrating inflammatory myeloid cells facilitated vaccine resistance in this setting, we made use of the fact that treatment of tumors with cisplatin chemotherapy induces an influx of inflammatory Ly6C<sup>high</sup> myeloid cells expressing higher level of T cell costimulatory molecules (15, 25). Indeed, combined treatment of reinjected recurrent tumors with vaccine and cisplatin chemotherapy restored the sensitivity of the tumors to vaccine therapy (**Figure 5H and Supplementary Figure 6C**) and this coincided with a restoration of the myeloid cell composition in these tumors (**Figure 5I**). No changes in the numbers of intratumoral HPV-specific T cells were observed (**Figure 5J**). These data clearly show that immune escaped tumor cells reinjected in a therapy-naïve environment employ a different mechanism to resist immunotherapy than the same tumor cells growing in a microenvironment that has been altered as a consequence of vaccine-mediated tumor regression.

Of note, cisplatin can also directly kill tumor cells and its effect is enhanced by T-cell produced TNF (15, 16). This may have helped to restore the sensitivity of reinjected recurrent tumors to vaccine therapy. In addition, administration of cisplatin during the regression phase of TC-1 tumors perfectly prevents the outgrowth of recurrences (**Supplementary Figure**



7A). However, this is not due to changes in the numbers or composition of the myeloid cell population or the numbers of intratumoral CD8<sup>+</sup> Tm<sup>+</sup> or CD8<sup>+</sup>Ki67<sup>+</sup> T cells, as they remained unaltered (**Supplementary Figure 7B**). In this situation, the effect of cisplatin most likely resides in its capacity to kill the few tumor cells that remained after the first T-cell mediated tumor regression, stressing the notion that strong curative approaches are required to prevent immunotherapy-driven immune escape.

## Discussion and conclusions

In our model, the induction of a less strong T-cell response makes the difference between cure and recurrence of tumors, probably reflecting the spectrum of vaccine-induced immune responses which can be obtained in the clinic. Adding cytotoxic compounds, such as cisplatin, which are known to synergize with tumor-specific T cell responses (9) at the time that immunotherapy induces tumor regression, overcomes the negative result of a less strong immunotherapy-induced anti-tumor response.

Direct tumor escape was associated with changes in 3 major pathways, well known to influence tumor immunity. Down regulation of the p53 and TNF signaling pathways may have dampened tumor immunity as it is known that activation of p53 in tumor cells induces immunogenic cell death and attraction of CD11c<sup>+</sup> APCs into the tumor (26) while TNF-signaling also induces immunogenic tumor cell death. Furthermore, the observed upregulation of an EMT signature, and more specifically increased  $\beta$ -catenin expression and a remarkable strong expression of TGF $\beta$  in a ring of fibroblasts surrounding the tumors, are all associated with T cell exclusion (23, 24, 27-29). These changes have resulted in a tumor cell population with the intrinsic property to modulate its tumor microenvironment in such way that it can resist vaccine therapy, as demonstrated by the experiments in which locally regrowth of

### ◀ Figure 5. Recurrent tumor cells reinjected in a therapy-naïve environment employ a different mechanism to resist immunotherapy

A-G) Mice were injected with TC-1 tumor cells on day 0. Then, mice were vaccinated on day 8 and 22 with SLP vaccine. When the tumors relapsed (day 39), mice were sacrificed. Tumor cells were isolated and sorted and injected back to the naïve (TC-1 recurrent). The other group of mice were injected with TC-1 tumor cells. Both groups were vaccinated with SLP vaccine on day 8 or kept untreated. Tumor microenvironment of all the groups was analyzed on day 15 post tumor challenge. A) Percentage of CD45<sup>+</sup> cells within live gate in the tumor microenvironment. B) Percentage of CD8<sup>+</sup> T cells within CD45<sup>+</sup> cells, live gate and percentage of E7 Tm<sup>+</sup> within CD8<sup>+</sup> intratumoral T cells. C) IFN $\gamma$  and TNF $\alpha$  production of intratumoral CD8<sup>+</sup> T cells. D) Percentage of ki67<sup>+</sup> intratumoral CD8<sup>+</sup> T cells. E) Percentage of intratumoral CD11b<sup>+</sup> cells within live gate. F) Percentage of intratumoral Ly6C<sup>+</sup> cells within CD11b<sup>+</sup> CD11c<sup>+</sup> or CD11b<sup>+</sup>CD11c<sup>-</sup> cells. G) Percentage of intratumoral MHCII<sup>+</sup> F4/80<sup>+</sup> cells within CD11b<sup>+</sup>CD11c<sup>+</sup> cells. H) Tumor outgrowth of the mice treated with SLP vaccine, cisplatin or combination. The scheme of the experiment has been shown in supplementary figure 6C. I-J) Percentage of intratumoral CD11b<sup>+</sup> cells within live gate, Ly6C<sup>+</sup> cells within CD11b<sup>+</sup>CD11c<sup>+</sup> or CD11b<sup>+</sup> CD11c<sup>-</sup> cells (I) and percentage of E7 Tm<sup>+</sup> CD8<sup>+</sup> intratumoral T cells (J) in mice described in H and were analyzed on day 15 post second tumor challenge. Data are representative of one experiment. \*P<0.05, \*\*P<0.01, \*\*\*P<0.001.

tumor cells, that are cell sorted and reinjected as a pure tumor cell population in naïve hosts, retained the capacity to develop into vaccine-resistant tumors.

To our great surprise, the tumor microenvironment of the reinjected recurrent tumor cells strongly differed from the original therapy-resistant tumor. While in the latter there was a strong T cell exclusion, the reinjected tumor cells developed into tumors readily infiltrated with T cells but which lacked infiltration with inflammatory myeloid cells, required for tumor regression (15). A major difference between these two tumors is that local recurrences develop in a milieu where the therapy has resulted in massive but not complete tumor cell eradication as well as attracted many inflammatory macrophages. This mixture of tumor cell-debris, some remaining living tumor cells and macrophages was recently shown to facilitate the growth of otherwise nontumorigenic numbers of tumor cells due to proinflammatory cytokines produced by tumor-debris stimulated macrophages (30). In contrast, the reinjected recurrent tumor cells grew out in a therapy-naïve microenvironment and, as a consequence, exploited a completely different immune escape mechanism to resist therapeutic vaccination. The impact of the microenvironment on the immune resistance mechanism employed by tumor cells not only contributes to our understanding on how tissue microenvironments determine the immune composition of primary tumors (31), their metastases (32) and as shown here, therapy-driven immune resistant tumors that develop locally or in another location but also points out that the treatment of relapses and metastases which develop during or after partly successful immunotherapy may require different immunotherapeutic approaches.

## Materials and methods

### Mice

C57BL/6 mice were purchased from Charles River Laboratories (L'Arbresle, France). All mice were 6-8 weeks old at the beginning of the experiment. Mice were housed in individually-ventilated cages under specific pathogen-free conditions in the animal facility of Leiden University Medical Center (LUMC, The Netherlands). All animal experiments were approved by the Animal Experiments Committee of LUMC and were executed according to the animal experimentation guidelines of LUMC in compliance with the guidelines of Dutch and European committees.

### Tumor challenge and treatments

The tumor cell line TC-1 was generated by retroviral transduction of C57BL/6 lung epithelial cells with the HPV16 E6/E7 and c-H-ras oncogenes (33) and cultured as previously described. Mice were inoculated subcutaneously with  $1 \times 10^5$  TC-1 tumor cells in 200  $\mu$ l PBS containing 0.2% BSA on day 0. Tumor size (horizontal dimension  $\times$  vertical dimension) was measured two times a week using a calliper. When tumor was palpable on day 7 post tumor injection,

mice were divided into groups with comparable tumor sizes. On day 8 and 22 post tumor challenge, mice were vaccinated with synthetic long peptide (SLP) vaccine subcutaneously in the contralateral flank (all figures) or tail base (only in figure 1). SLP vaccine contains 100 µg HPV16 E7<sub>43-63</sub> (GQAEPDRAHYNIVTFCKCDS) covering both Th epitope and the CTL epitope with 20 µg CPG (ODN1826, InvivoGen) dissolved in 200 µl (flank) or 50 µl (tail base) PBS and emulsified with IFA. Cisplatin is administered 10 mg/kg in NaCl in 300µl intraperitoneally (i.p.). Mice were routinely weighed 2-3 times per week. After cisplatin administration, mice were weighed 3-4 times per week until mice recovered. To deplete the myeloid cells, CSF1R inhibitor PLX3397 or control chow was incorporated into chow at 290 mg/kg chow which results in a daily delivery of approximately 45 mg/kg. Mice were euthanized when tumor size reached >2000 mm<sup>3</sup> in volume or when mice lost over >20% of their total body weight (relative to initial body mass).

For antibodies treatments, anti-PD-1 blocking antibody clone: RMP1-14 (150-200µg/mouse, BioXcell or purified in-house from hybridoma cultures), Anti-PD-L1 clone: MIH-5 (150 µg/mouse, purified in-house from hybridoma cultures), OX-40 agonistic monoclonal antibody clone: OX86 (150µg/mouse, Bioceros) and 4-1BB agonistic antibodies clone: 3H3 (150 µg/mouse, purified in-house from hybridoma cultures) were used. To block CXCR3, anti-mouse CXCR3 blocking antibody clone: CXCR3-173 were obtained from BioXcell and was used 200µg/mouse i.p every three days. TGFβ neutralizing antibody clone: 1D11.16.8 was obtained from BioXcell and was administered 200µg/mouse. Antibodies were administered on days as mentioned in the legend of each figure. RG7112 was purchased from Chemgood (USA) and was given daily 100mg/kg by oral suspension in 200µl of 0.5 w/v% methyl cellulose 400 (Wako Pure Chemical Industries; Osaka, Osaka, Japan).

#### *Flow cytometric analysis of splenic and intratumoral immune cells*

For analysis of immune populations, tumors were collected after transcardial perfusion and were disrupted in small pieces by incubating with Liberase (Roche) in IMDM for 15 minutes at 37°C. Spleen and lymph nodes were digested by incubating with 0.02 mg/ml DNase and 1 mg/ml collagenase for 10 min at room temperature. Single-cell suspensions were prepared by mincing spleen and tumor pieces through a 70 µm cell strainer (BD Biosciences). Cells were resuspended in staining buffer (PBS + 2% FCS + 0.05% sodium azide) and incubated with various fluorescently labelled antibodies against: CD11b (clone M1/70), CD11c (clone N418), CD45.2 (clone 104), F4/80 (clone BM8), Ly6C (clone HK1.4), Ly6G (clone 1A8). Antibodies were obtained from eBioscience and Biolegend. APC labelled- H-2D<sup>b</sup> tetramers containing HPV16 E7<sub>49-57</sub> peptide (RAHYNIVTF) were used as E7 tetramer (E7 Tm). For dead cell exclusion, 7-aminoactinomycin D (7-AAD; Invitrogen) was used. For intracellular cytokine staining, single cell suspensions of spleens or tumors were plated in 96-well cell culture flat-bottom plates in the presence of dendritic cells preloaded with SLP and brefeldin

A (4µg/ml). After 5 hours incubation, cells were stained for surface markers and were fixed in 0.5% paraformaldehyde for overnight. Thereafter, cells were washed, stained for cytokines and subsequently analysed by flow cytometry. Samples were measured with a BD LSRII flow cytometer, and results were analysed using FlowJo software (Tree Star).

### Mass cytometry and data analysis

Mass cytometry (CyTOF) staining and acquisition was performed as generally described (31). In short, single-cell suspensions of TC-1 tumors were purified by Percoll gradient to remove aggregates and debris, stained with 37 mouse immune markers, and acquired on a Helios mass cytometer (Fluidigm Sciences). The metal-conjugated antibodies are listed in supplementary table 1. After manual gating of alive singlet CD45<sup>+</sup> cells using FlowJo, non-supervised clustering was performed by H-SNE analysis with default parameters using the Cytosplore software (34). After clustering was performed based on all markers, cell types were manually assigned to clusters using the following criteria: CD8<sup>+</sup> T cells (CD3<sup>+</sup>CD8a<sup>+</sup>), CD4<sup>+</sup> T cells (CD3<sup>+</sup>CD8a<sup>-</sup>), inflammatory myeloid cells (CD11b<sup>+</sup>Ly6C<sup>hi</sup>F4/80<sup>low</sup>), tumor-associated macrophages (CD11b<sup>+</sup>F4/80<sup>hi</sup>Ly6C<sup>low</sup>), neutrophils (CD11b<sup>+</sup>Ly6G<sup>+</sup>), eosinophils (CD11b<sup>+</sup>Siglec-F<sup>+</sup>) and pDCs (Siglec-H<sup>+</sup>BST2<sup>+</sup> B220<sup>+</sup>).

### qPCR analysis

Single cells isolated from the digested tumors or sorted from the digested tumor for CD45<sup>+</sup> (immune cells) and CD45<sup>-</sup> (tumor cells) were used. To sort tumor cells, live CD45<sup>-</sup>CD31<sup>-</sup>CD90.2<sup>+</sup>CD44<sup>+</sup> cells were sorted. RNA were isolated from the cells with RNeasy kit (Qiagen) according to manufacturer's protocol. CDNA was synthesized using High capacity RNA-to-cDNA kit (Applied Biosystems) according to the kit's protocol. Analysis of qPCR analyses were performed using the SybrGreen supermix (Bio-Rad).

To measure the chemokine and chemokine receptors, mouse chemokines and receptors RT2 Profiler PCR Array was purchased from Qiagen.

### CTL assay

Naïve C57BL/6 mice were vaccinated with SLP vaccines as described above on day 0 and 14. Splenocytes were isolated 8 days after the last vaccination and restimulated *in vitro* with DCs loaded with SLP and irradiated TC-1 tumor cells. After restimulation, splenocytes were harvested by using EDTA and CD8 T cells were isolated by using the mouse CD8<sup>+</sup> T lymphocyte enrichment set (BD Biosciences) and used as effector cells. Tumor cells isolated from the untreated or relapsed tumor bearing mice were exposed to IFNγ (10 IU, Prospeg) one day before CTL assay and were use as target cells. Target cells were labelled with 100µl <sup>51</sup>Cr for 1 h, washed and plated into a 96-well round-bottom plate at a density of 2.000 tumor cells/well with different ratios of effector cells. After 4 h incubation, supernatant of the cells were harvested and the percentage of <sup>51</sup>Cr release was measured by a gamma counter.

## Statistical analysis

Statistical analyses were performed using Prism (GraphPad). Survival data were analysed by Kaplan-Meier and the log-rank (Mantel-Cox) test. Statistical significance was determined using the Mann Whitney test. *P* values of  $\leq 0.05$  were considered statistically significant.





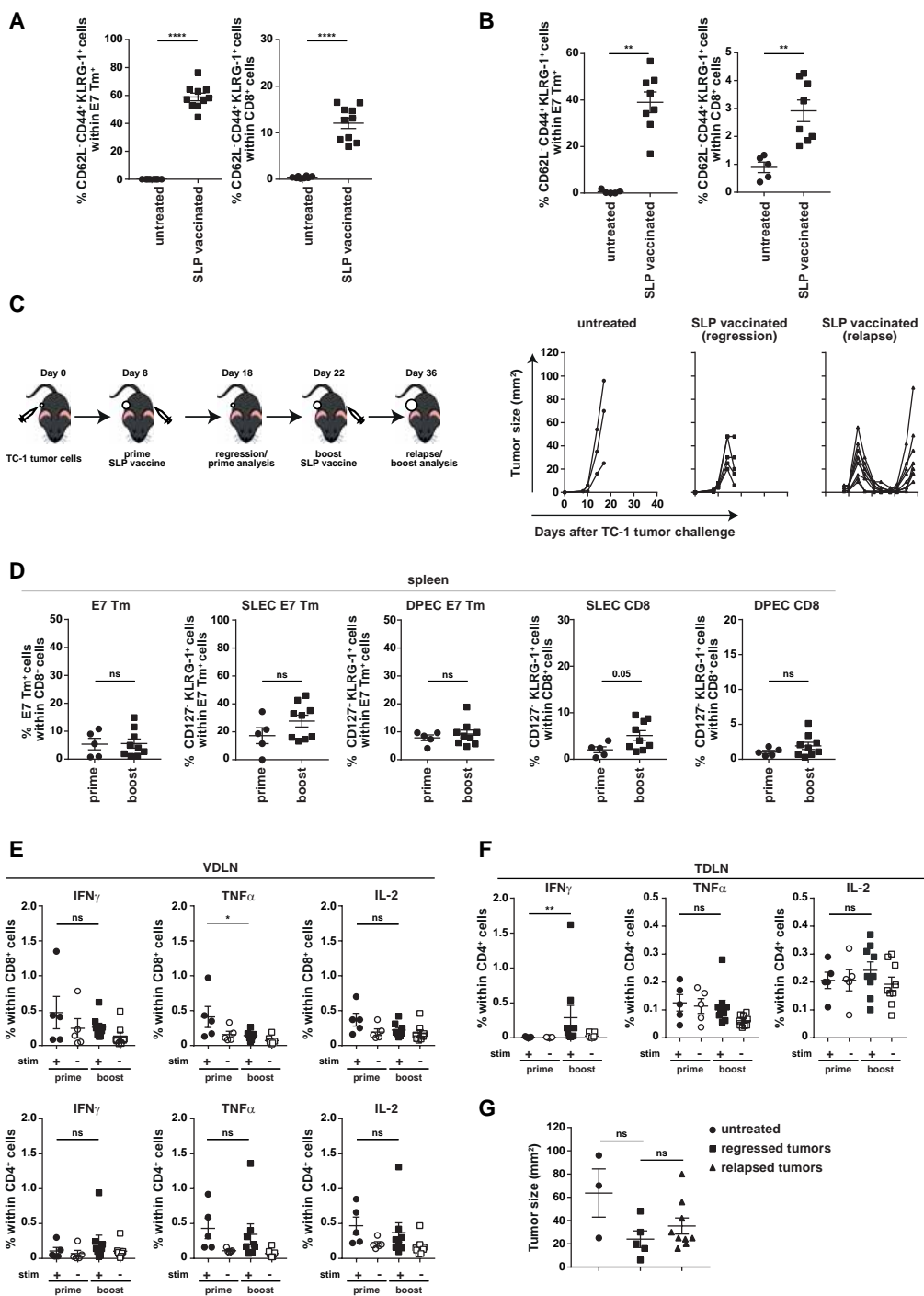
## References

1. Mellman I, Coukos G, Dranoff G. Cancer immunotherapy comes of age. *Nature*. 2011;480(7378):480-9.
2. Massarelli E, William W, Johnson F, Kies M, Ferrarotto R, Guo M, et al. Combining Immune Checkpoint Blockade and Tumor-Specific Vaccine for Patients With Incurable Human Papillomavirus 16-Related Cancer: A Phase 2 Clinical Trial. *JAMA Oncol*. 2018.
3. van der Burg SH, Arens R, Ossendorp F, van Hall T, Melief CJ. Vaccines for established cancer: overcoming the challenges posed by immune evasion. *Nat Rev Cancer*. 2016;16(4):219-33.
4. Ascierto PA, Del Vecchio M, Robert C, Mackiewicz A, Chiarion-Sileni V, Arance A, et al. Ipilimumab 10 mg/kg versus ipilimumab 3 mg/kg in patients with unresectable or metastatic melanoma: a randomised, double-blind, multicentre, phase 3 trial. *Lancet Oncol*. 2017;18(5):611-22.
5. Hodi FS, Chiarion-Sileni V, Gonzalez R, Grob JJ, Rutkowski P, Cowey CL, et al. Nivolumab plus ipilimumab or nivolumab alone versus ipilimumab alone in advanced melanoma (CheckMate 067): 4-year outcomes of a multicentre, randomised, phase 3 trial. *Lancet Oncol*. 2018;19(11):1480-92.
6. Weber JS, D'Angelo SP, Minor D, Hodi FS, Gutzmer R, Neyns B, et al. Nivolumab versus chemotherapy in patients with advanced melanoma who progressed after anti-CTLA-4 treatment (CheckMate 037): a randomised, controlled, open-label, phase 3 trial. *Lancet Oncol*. 2015;16(4):375-84.
7. Sharma P, Hu-Lieskovan S, Wargo JA, Ribas A. Primary, Adaptive, and Acquired Resistance to Cancer Immunotherapy. *Cell*. 2017;168(4):707-23.
8. Schreiber RD, Old LJ, Smyth MJ. Cancer immunoediting: integrating immunity's roles in cancer suppression and promotion. *Science*. 2011;331(6024):1565-70.
9. van der Sluis TC, van Duikeren S, Huppelschoten S, Jordanova ES, Beyranvand Nejad E, Sloots A, et al. Vaccine-induced tumor necrosis factor-producing T cells synergize with cisplatin to promote tumor cell death. *Clin Cancer Res*. 2015;21(4):781-94.
10. Zwaveling S, Ferreira Mota SC, Nouta J, Johnson M, Lipford GB, Offringa R, et al. Established human papillomavirus type 16-expressing tumors are effectively eradicated following vaccination with long peptides. *J Immunol*. 2002;169(1):350-8.
11. DuPage M, Cheung AF, Mazumdar C, Winslow MM, Bronson R, Schmidt LM, et al. Endogenous T cell responses to antigens expressed in lung adenocarcinomas delay malignant tumor progression. *Cancer Cell*. 2011;19(1):72-85.
12. Matsushita H, Vesely MD, Koboldt DC, Rickert CG, Uppaluri R, Magrini VJ, et al. Cancer exome analysis reveals a T-cell-dependent mechanism of cancer immunoediting. *Nature*. 2012;482(7385):400-4.
13. Iwai Y, Ishida M, Tanaka Y, Okazaki T, Honjo T, Minato N. Involvement of PD-L1 on tumor cells in the escape from host immune system and tumor immunotherapy by PD-L1 blockade. *Proc Natl Acad Sci U S A*. 2002;99(19):12293-7.
14. Latchman Y, Wood CR, Chernova T, Chaudhary D, Borde M, Chernova I, et al. PD-L2 is a second ligand for PD-1 and inhibits T cell activation. *Nat Immunol*. 2001;2(3):261-8.
15. van der Sluis TC, Sluijter M, van Duikeren S, West BL, Melief CJ, Arens R, et al. Therapeutic Peptide Vaccine-Induced CD8 T Cells Strongly Modulate Intratumoral Macrophages Required for Tumor Regression. *Cancer Immunol Res*. 2015;3(9):1042-51.
16. Doorduijn EM, Sluijter M, Salvatori DC, Silvestri S, Maas S, Arens R, et al. CD4(+) T Cell and NK Cell Interplay Key to Regression of MHC Class I(low) Tumors upon TLR7/8 Agonist Therapy. *Cancer Immunol Res*. 2017;5(8):642-53.
17. Croft M. Control of immunity by the TNFR-related molecule OX40 (CD134). *Annu Rev Immunol*. 2010;28:57-78.



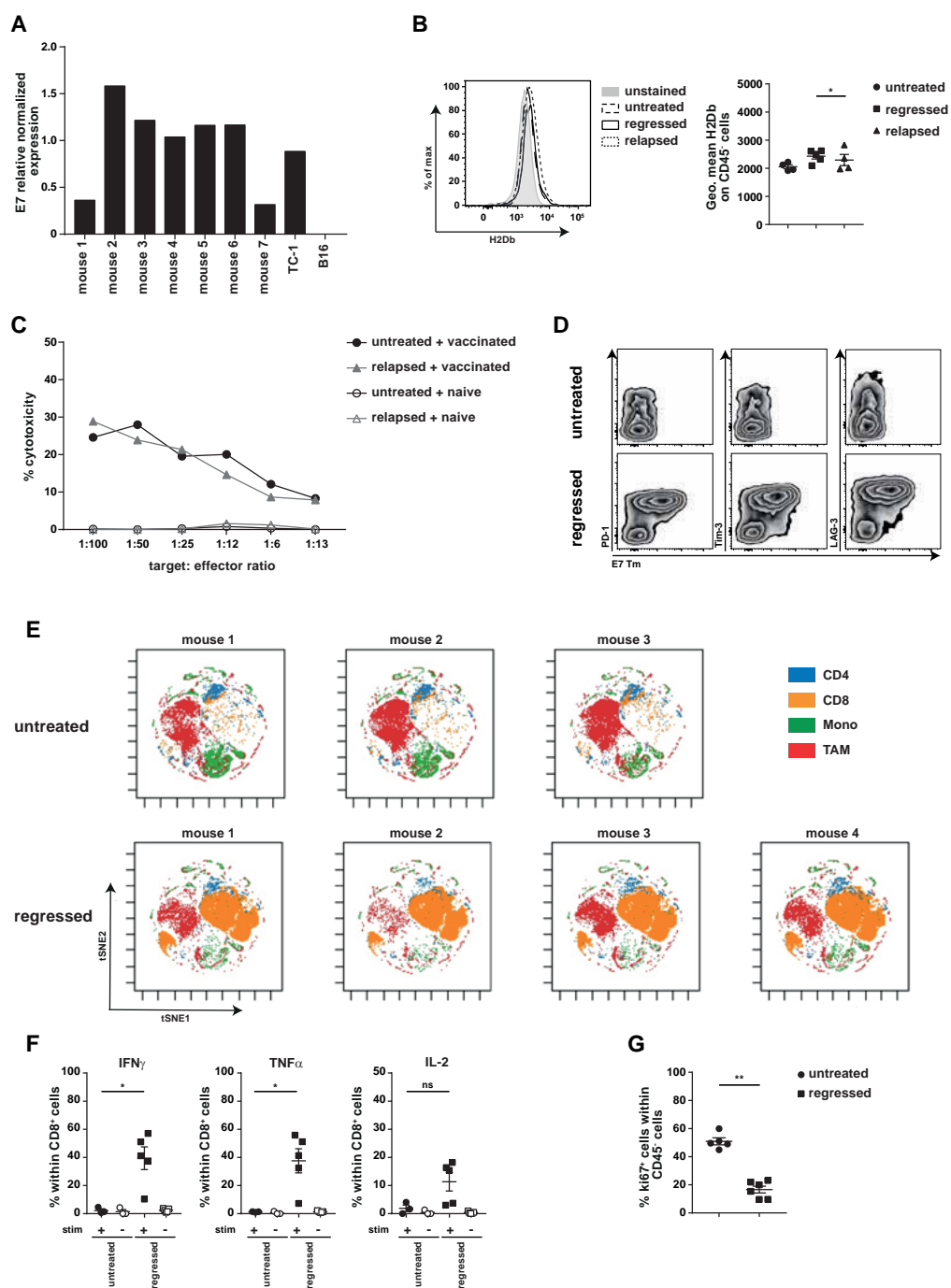
18. Oh HS, Choi BK, Kim YH, Lee DG, Hwang S, Lee MJ, et al. 4-1BB Signaling Enhances Primary and Secondary Population Expansion of CD8<sup>+</sup> T Cells by Maximizing Autocrine IL-2/IL-2 Receptor Signaling. *PLoS One*. 2015;10(5):e0126765.
19. Othman AS, Franke-Fayard BM, Imai T, van der Gracht ETI, Redeker A, Salman AM, et al. OX40 Stimulation Enhances Protective Immune Responses Induced After Vaccination With Attenuated Malaria Parasites. *Front Cell Infect Microbiol*. 2018;8:247.
20. Liberzon A, Birger C, Thorvaldsdottir H, Ghandi M, Mesirov JP, Tamayo P. The Molecular Signatures Database (MSigDB) hallmark gene set collection. *Cell Syst*. 2015;1(6):417-25.
21. Gonzalez DM, Medici D. Signaling mechanisms of the epithelial-mesenchymal transition. *Sci Signal*. 2014;7(344):re8.
22. Lamouille S, Xu J, Derynck R. Molecular mechanisms of epithelial-mesenchymal transition. *Nat Rev Mol Cell Biol*. 2014;15(3):178-96.
23. Mariathasan S, Turley SJ, Nickles D, Castiglioni A, Yuen K, Wang Y, et al. TGFbeta attenuates tumour response to PD-L1 blockade by contributing to exclusion of T cells. *Nature*. 2018;554(7693):544-8.
24. Tauriello DVF, Palomo-Ponce S, Stork D, Berenguer-Llgero A, Badia-Ramentol J, Iglesias M, et al. TGFbeta drives immune evasion in genetically reconstituted colon cancer metastasis. *Nature*. 2018;554(7693):538-43.
25. Beyranvand Nejad E, van der Sluis TC, van Duikeren S, Yagita H, Janssen GM, van Veelen PA, et al. Tumor Eradication by Cisplatin Is Sustained by CD80/86-Mediated Costimulation of CD8<sup>+</sup> T Cells. *Cancer Res*. 2016;76(20):6017-29.
26. Guo G, Yu M, Xiao W, Celis E, Cui Y. Local Activation of p53 in the Tumor Microenvironment Overcomes Immune Suppression and Enhances Antitumor Immunity. *Cancer Res*. 2017;77(9):2292-305.
27. Luke JJ, Bao R, Sweis RF, Spranger S, Gajewski TF. WNT/beta-catenin pathway activation correlates with immune exclusion across human cancers. *Clin Cancer Res*. 2019.
28. Spranger S, Bao R, Gajewski TF. Melanoma-intrinsic beta-catenin signalling prevents anti-tumour immunity. *Nature*. 2015;523(7559):231-5.
29. Chae YK, Chang S, Ko T, Anker J, Agte S, Iams W, et al. Epithelial-mesenchymal transition (EMT) signature is inversely associated with T-cell infiltration in non-small cell lung cancer (NSCLC). *Sci Rep*. 2018;8(1):2918.
30. Sulciner ML, Serhan CN, Gilligan MM, Mudge DK, Chang J, Gartung A, et al. Resolvins suppress tumor growth and enhance cancer therapy. *J Exp Med*. 2018;215(1):115-40.
31. Santeogoets SJ, van Ham VJ, Ehsan I, Charoentong P, Duurland CL, van Unen V, et al. The Anatomical Location Shapes the Immune Infiltrate in Tumors of Same Etiology and Affects Survival. *Clin Cancer Res*. 2019;25(1):240-52.
32. Remark R, Alifano M, Cremer I, Lupo A, Dieu-Nosjean MC, Riquet M, et al. Characteristics and clinical impacts of the immune environments in colorectal and renal cell carcinoma lung metastases: influence of tumor origin. *Clin Cancer Res*. 2013;19(15):4079-91.
33. Lin KY, Guarnieri FG, Staveley-O'Carroll KF, Levitsky HI, August JT, Pardoll DM, et al. Treatment of established tumors with a novel vaccine that enhances major histocompatibility class II presentation of tumor antigen. *Cancer Res*. 1996;56(1):21-6.
34. van Unen V, Holtt T, Pezzotti N, Li N, Reinders MJT, Eisemann E, et al. Visual analysis of mass cytometry data by hierarchical stochastic neighbour embedding reveals rare cell types. *Nat Commun*. 2017;8(1):1740.

# Supplementary Figures



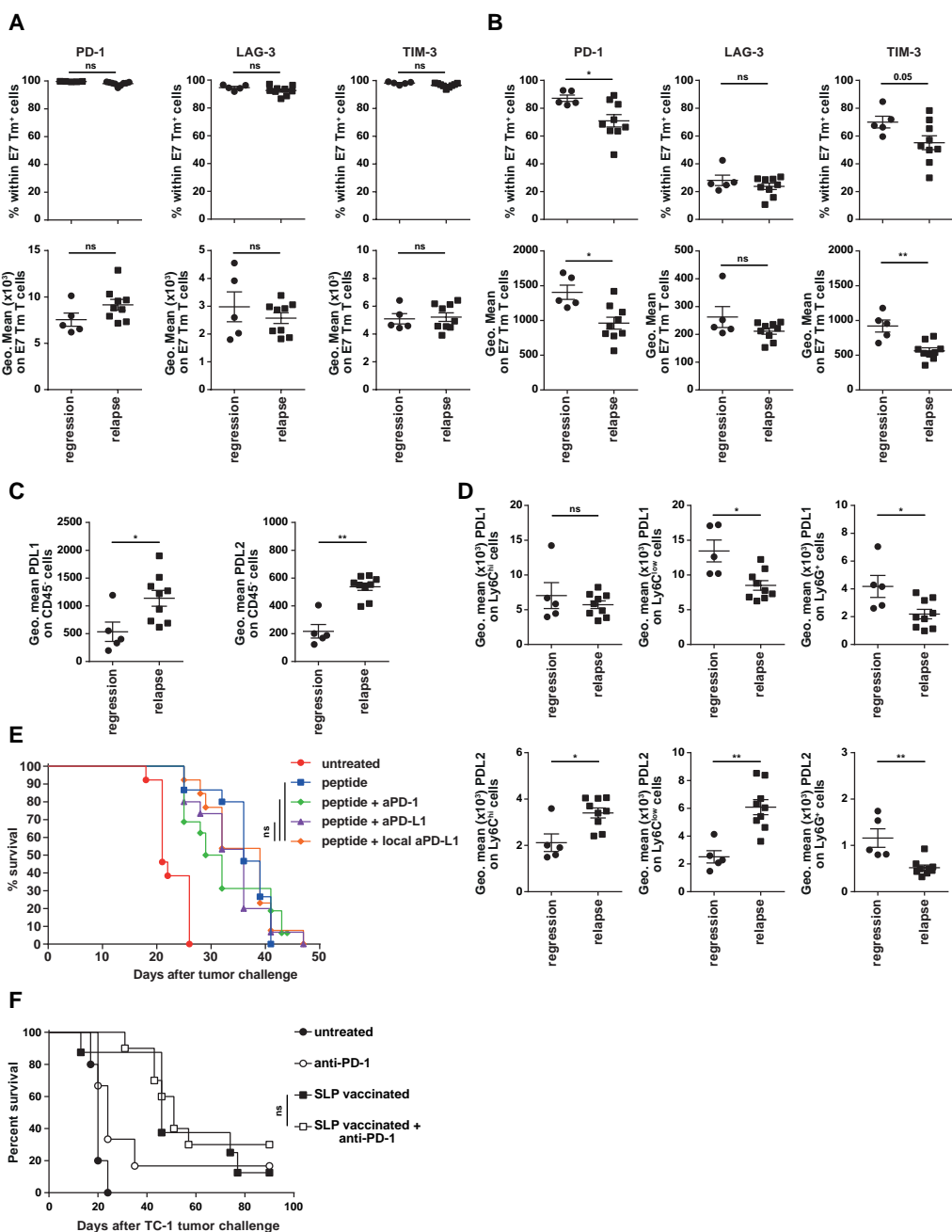
### ◀ **Supplementary figure 1. Booster vaccination amplifies the magnitude of systemic E7-specific T cells**

Mice were injected with TC-1 tumor cells on day 0 and vaccinated with prime and boost vaccine subcutaneously in flank (A) (suboptimal) or tail base (B) (optimal) on day 8 and 22, respectively. Percentage of CD62L<sup>+</sup> CD44<sup>+</sup> KLRG-1<sup>+</sup> cells with E7 Tm<sup>+</sup> and CD62L<sup>+</sup> CD44<sup>+</sup> KLRG-1<sup>+</sup> within CD8<sup>+</sup> T cells of untreated mice and SLP vaccinated mice that received the vaccination in flank (A) or tail base (B). C) (Left panel) Scheme of the experiment shown in Figure 1 and the rest of the figures. In brief, mice were injected with TC-1 tumor cells on day 0 and vaccinated with prime vaccine on day 8. A group of mice were sacrificed on day 18 at the time of regression (regression/prime analysis). The other group received boost vaccine on day 22 and sacrificed at the time of relapse on day 39 (relapse/boost analysis). (Right panel) Tumor outgrowth of untreated mice, SLP vaccinated mice sacrificed on day 18 (regression/prime analysis) and 39 (relapse/boost analysis). D) The percentage of E7 Tm<sup>+</sup>, SLEC and DPEC within E7 Tm<sup>+</sup> or CD8<sup>+</sup> in spleen at day 18 (prime) and day 39 (boost). E and F) Percentage of IFN $\gamma$ <sup>+</sup>, TNF $\alpha$ <sup>+</sup> and IL-2<sup>+</sup> cells within CD8<sup>+</sup> T cells and CD4<sup>+</sup> T cells in VDLN (E) and TDLN (F) at day 18 (prime) and day 39 (boost). Data represents mean values  $\pm$  SEM (n = 5-9 mice per group). G) Tumor size of the mice at the day that they were sacrificed (untreated and regressed tumors at the day 18 and relapsed tumors at the day 39). Data are representative of one experiment. \*P< 0.05, \*\*P<0.01, \*\*\*P<0.001.



◀ **Supplementary figure 2. Classical immune escape mechanisms do not play a role in tumor recurrence**

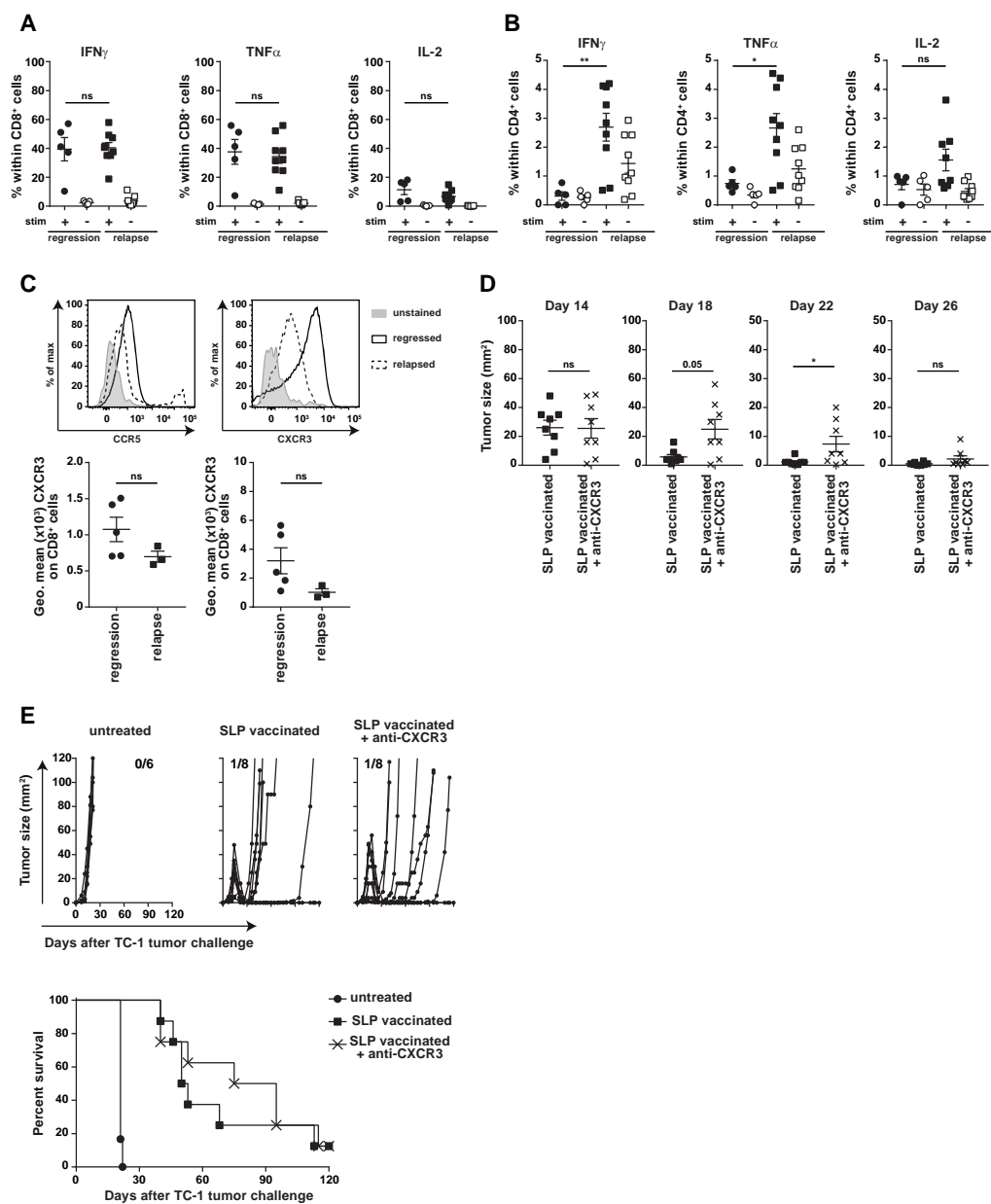
A) Expression level of E7 oncogene in relapsed TC-1 tumor cells. In brief, the relapsed tumors from the mice (mouse 1-7) were harvested and sorted for CD45<sup>+</sup> cells. In vitro TC-1 tumor cells and B16 tumor cells have been used as positive and negative controls, respectively. RNA expression level of E7 has been measured by qPCR. B) Expression levels H2Db on CD45<sup>+</sup> TC-1 tumor cells from untreated mice and SLP vaccinated mice at the time of regression (day 18) and relapse (day 39) measured by flow cytometry. C) The percentage of cytotoxicity <sup>51</sup>Cr-release CTL assay. Shown is the percentage of tumor cells from untreated or relapsed tumors (target cells) killed by splenocytes isolated from SLP vaccinated or naïve mice as control (effector cells) at different ratios as measured by CTL assay as described in materials and methods. D) Expression of PD-1, Tim-3 and LAG-3 on intratumoral CD8 T cells in untreated and regressed tumor at day 18 (E), tSNE (t-distributed stochastic neighbor embedding) plot of all intratumoral CD45<sup>+</sup> cells of the untreated and regressed tumors after SLP vaccine analyzed by mass cytometry followed by non-supervised clustering (viSNE) in Cytobank. Monocytes (Mono) and tumor associated macrophages (TAM) were gated based CD11b<sup>+</sup> Ly6C<sup>+</sup> CCR2<sup>+</sup> and CD11b<sup>+</sup> F4/80<sup>+</sup> Ly6C<sup>+</sup>. (F) Percentage of IFN $\gamma$ <sup>+</sup>, TNF $\alpha$ <sup>+</sup> and IL-2<sup>+</sup> cells within CD8<sup>+</sup> T cells in tumor of untreated and regressed tumors at day 18. (G) Percentage of ki67<sup>+</sup> cells within CD45<sup>+</sup> tumor cells in tumor of untreated and regressed tumors at day 18. Data are representative of two independent experiments. \*P< 0.05, \*\*P<0.01, \*\*\*P<0.001.



◀ **Supplementary figure 3 - Immunotherapy-driven recurrence of immune resistance tumors could not be prevented by using immune checkpoint blockade of the PD-1/PD-L1 pathway and booster vaccination**

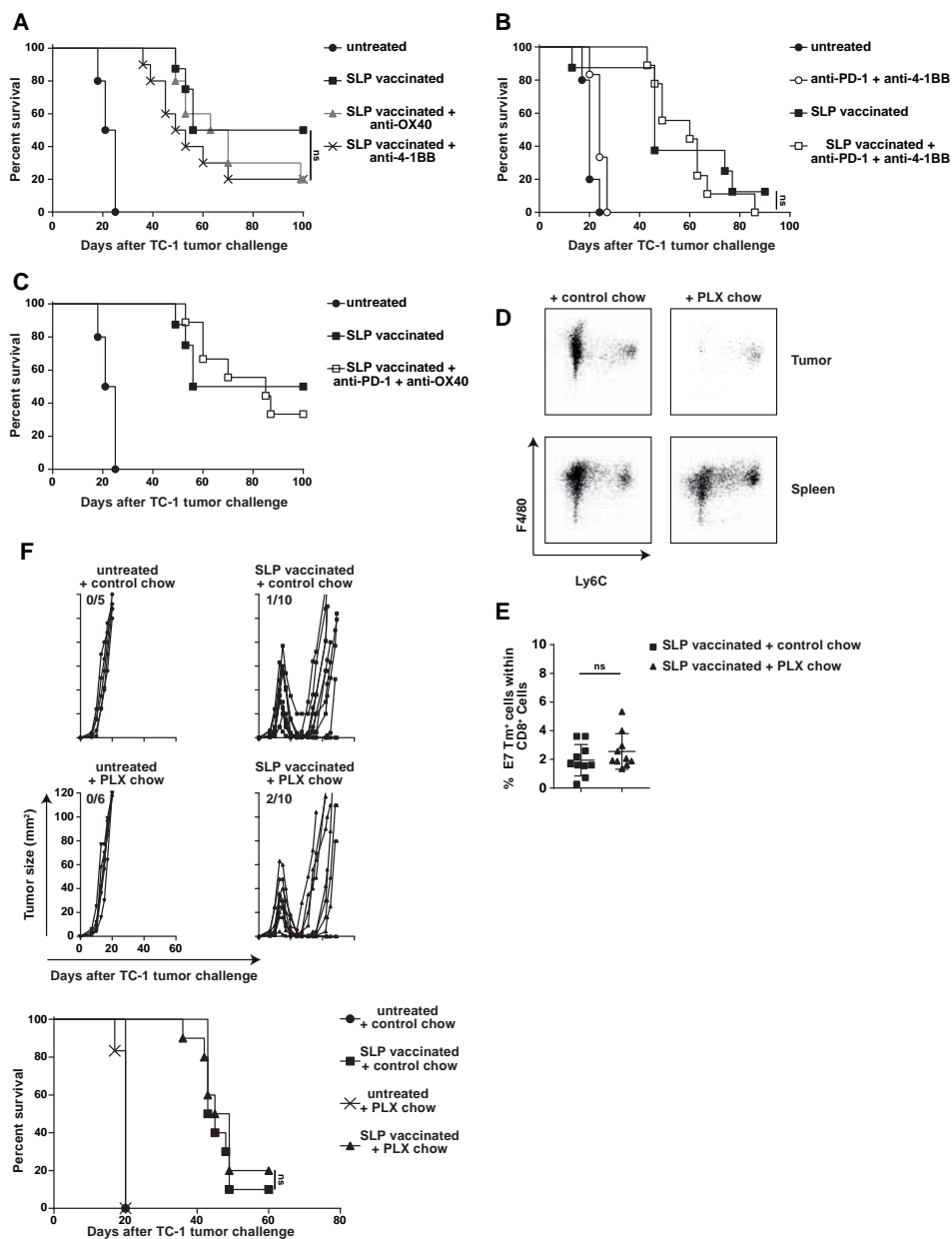
A-B) Percentage of PD-1<sup>+</sup>, LAG-3<sup>+</sup> and TIM-3<sup>+</sup> (upper panel) and geometric mean of PD-1, LAG-3, TIM-3 (lower panel) on intratumoral (A) or splenic (B) E7 Tm<sup>+</sup> CD8<sup>+</sup> cells. C) Expression of PDL1 and PDL2 on CD45<sup>+</sup> tumor cells. D) Expression level of PDL1 and PDL2 on intratumoral Ly6C<sup>hi</sup>, Ly6C<sup>low</sup> and Ly6G<sup>+</sup> CD11b<sup>+</sup> cells. E-G) Survival of the mice treated with only anti-PD-1 or SLP vaccine or the combination. In brief, Mice were injected with TC-1 tumor cells on day 0 and were vaccinated with prime and boost vaccine on day 8 and 22, respectively. Anti-PD-1 and anti-PD-L1 were administrated in (E) from day 14-29 (before regression) or (F) from day 20-35 (at the time of regression). Data are representative of two independent experiments. \*P< 0.05, \*\*P<0.01, \*\*\*P<0.001.





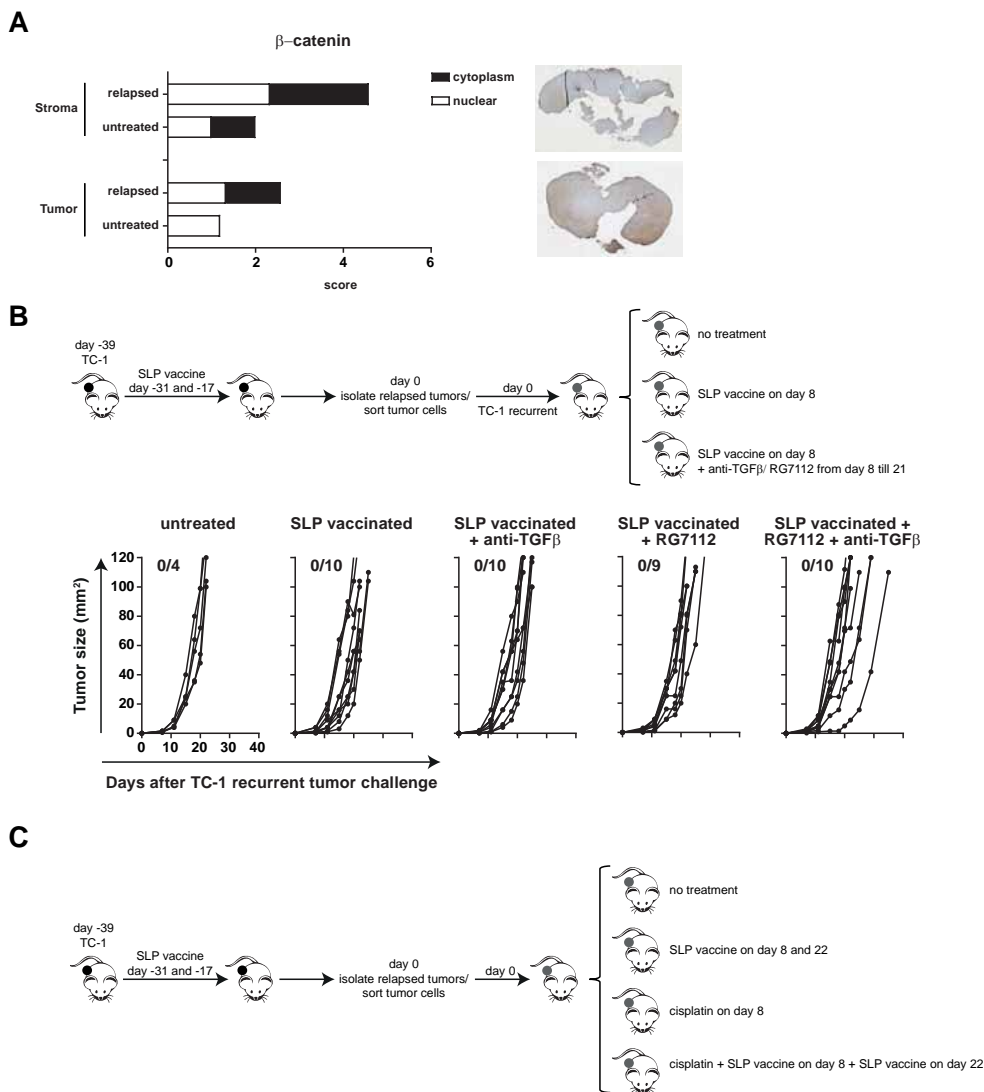
◀ **Supplementary figure 4. Antibody mediated blocking of CXCR3 delayed the onset of tumor regression but did not prevent recurrence**

A-B) Percentage of IFN $\gamma$ <sup>+</sup>, TNF $\alpha$ <sup>+</sup> and IL-2<sup>+</sup> cells within intratumoral CD8<sup>+</sup> T cells (A) and CD4<sup>+</sup> T cells (B). C) Expression level of CCR5 and CXCR3 on intratumoral CD8<sup>+</sup> T cells from regressed or relapsed tumors. D-E) Mice were injected with TC-1 tumor cells on day 0. Mice were vaccinated with SLP vaccine on day 8 and 22 or kept untreated. A group of mice were received anit-CXCR3 at day 8 and onwards until day 24 every 3 days. D) Tumor size (mm<sup>2</sup>) of the mice on day 14,18, 22 and 26. E) Tumor outgrowth and survival of the mice shown in (D). The number above the each graph shows the number of alive mice from the total. Data represents mean values  $\pm$  SEM (n = 5-9 mice per group). Data is representative of one experiment. \*P< 0.05, \*\*P<0.01, \*\*\*P<0.001.



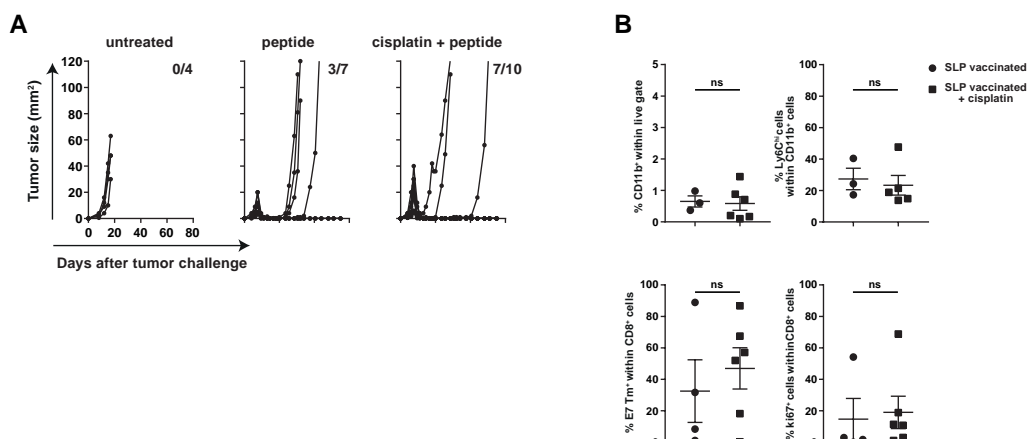
◀ **Supplementary figure 5. Amplification of the T-cell stimulatory signals or depleting tumor-associated macrophages could not prevent tumor recurrence**

A-C) Survival of mice treated with SLP vaccine in combination with anti-OX40 or anti-4-1BB (A) or anti-PD-1 and anti-4-1BB alone or in combination with SLP vaccine (B) or in combination with anti-PD-1 and anti-OX-40 (C). Anti-OX40, Anti-4-1BB and Anti PD-1 were administered on day 22 in (A) and (C) and from day 20-35 in (B). Data are representative of two independent experiments. D-F) Mice were injected with TC-1 tumor cells on day 0 and were vaccinated with prime and boost vaccine on day 8 and 22, respectively. Control chow or PLX chow was provided from day 20. D) Upper panel: Representative flow cytometry plots of Ly6C and F4/80 myeloid cells in tumor and spleen of mice fed with PLX or control chow. Cells were gated from 7AAD<sup>-</sup>/CD45<sup>+</sup>/CD11b<sup>+</sup> cells. Lower panel: Percentage of CD11c<sup>hi</sup> cells within Ly6C<sup>+</sup> F4/80<sup>+</sup> cells in tumor. E) Percentage of E7 Tm<sup>+</sup> CD8<sup>+</sup> T cells on day 29 in blood. F) Tumor outgrowth and survival of untreated and SLP vaccinated mice with control chow or PLX chow. Tumor outgrowth was followed for 60 days. The number of tumor-free mice from the total mice is indicated above each tumor out growth graph. Data represents mean values  $\pm$  SEM (n = 5-10 mice per group). Data are representative of one experiment. \*P<0.05, \*\*P<0.0, \*\*\*P<0.001.



**Supplementary figure 6. Targeting the TGF $\beta$  and P53 pathways in immune escaped tumor cells reinjected in naïve mice could not restore their sensitivity to immunotherapy**

$\beta$ -catenin (cytoplasm and nuclear) score of tumor microenvironment of untreated and relapsed tumors at day 18 and 39, respectively. B) Tumor outgrowth of the mice treated with SLP vaccine alone or in combination with anti-TGF $\beta$  and RG7112. Scheme of the experiment is shown on top. The number of tumor-free mice from the total mice is indicated above each tumor out growth graph. C) Scheme of the experiment shown in figure 5H-J. In brief, mice were injected with TC-1 tumor cells on day 0 and vaccinated with SLP vaccine on day 8 and 22. When the tumor relapsed on day 39, mice were sacrificed and tumors were harvested and tumor cells were isolated. Sorted tumor cells (TC-1 recurrent) were injected into naïve mice and treated on day with SLP vaccine or cisplatin or the combination or kept untreated.



**Supplementary figure 7. Administration of cisplatin during the regression phase of TC-1 tumors prevented tumor recurrences**

Tumor outgrowth of the mice treated with SLP vaccine alone or in combination with cisplatin. In brief, mice were injected with TC-1 tumor cells on day 0 and vaccinated with prime and boost vaccine subcutaneously in flank on day 8 and 22, respectively. In combination treatment group, mice received cisplatin on day 20. B) Shown is the percentage of the intratumoral CD11b<sup>+</sup> within live gate, Ly6C<sup>hi</sup> cells with CD11b<sup>+</sup> cells, E7 Tm<sup>+</sup> cells within CD8<sup>+</sup> T cells and ki67<sup>+</sup> cells within CD8<sup>+</sup> T cells.



Supplementary table 1.

	Marker	Metal	Host	Isotype	Clone	Company	Cat.no
1	<b>CD3e</b>	172 Yb	Hamster	IgG	145-2C11	BioLegend (MaxPar-Ready)	100345
2	<b>CD8a</b>	168 Er	Rat	IgG2a	53-6.7	Fluidigm	3168003B
3	<b>CD11b</b>	154 Sm	Rat	IgG2b	M1/70	Fluidigm	3154006B
4	<b>CD19</b>	166 Er	Rat	IgG2a	6D5	Fluidigm	3166015B
5	<b>CD45</b>	89 Y	Rat	IgG2b	30-F11	Fluidigm	3089005B
6	<b>CD11c</b>	167 Er	Hamster	IgG	N418	BioLegend (MaxPar-Ready)	117341
7	<b>CD115</b>	144 Nd	Rat	IgG2a	AFS98	Fluidigm	3144012B
8	<b>F4/80</b>	174 Yb	Rat	IgG2a, k	BM8	BioLegend (MaxPar-Ready)	123143
9	<b>Ly6G</b>	141 Pr	Rat	IgG2a	1A8	Fluidigm	3141008B
10	<b>PDL1</b>	160 Gd	Rat	IgG2b, κ	10F.9G2	BioLegend	124301
11	<b>Ly6C</b>	165 Ho	Rat	IgG2c	HK1.4	BioLegend (MaxPar-Ready)	128039
12	<b>CD86</b>	171 Yb	Rat	IgG2a, κ	GL-1	BioLegend	105001
13	<b>CD14</b>	156 Gd	Rat	IgG2a, κ	Sa14-2	Fluidigm	3156009B
14	<b>CD38</b>	163 Dy	Rat	IgG2a, κ	90	BioLegend (MaxPar-Ready)	102723
15	<b>PD-1</b>	159 Tb	Rat	IgG2a	29F.1A12	Fluidigm	3159024B
16	<b>MHC-II</b>	115 In	Rat	IgG2b	M5/114.15.2	BioLegend (MaxPar-Ready)	107637
17	<b>CD103</b>	173 Yb	Hamster	IgG	2E7	BioLegend	121401
18	<b>CD40</b>	147 Sm	Rat	IgG2a, κ	3/23	BioLegend	124601
19	<b>Clec9A</b>	150 Nd	Rat	IgG1, κ	7H11	BioLegend	143502
20	<b>CD205</b>	169 Tm	Rat	IgG2a, κ	NLDC-145	BioLegend	138202
21	<b>Gr-1</b>	152 Sm	Rat	IgG2b, κ	RB6-8C5	BioLegend (MaxPar-Ready)	108449
22	<b>BST2</b>	151 Eu	Rat	IgG2b, κ	129C1	BioLegend	127102
23	<b>SiglecH</b>	153 Eu	Rat	IgG1, κ	551	BioLegend	129606
24	<b>B220</b>	176 Yb	Rat	IgG2a, k	RA3-6B2	Fluidigm	3176002B
25	<b>CD24</b>	161 Dy	Rat	IgG2b, κ	M1/69	BioLegend (MaxPar-Ready)	101829
26	<b>CD48</b>	162 Dy	Hamster	IgG	HM48-1	BioLegend (MaxPar-Ready)	103433
27	<b>CD169</b>	170 Er	Rat	IgG2a, κ	3D6.112	Fluidigm	3170018B
28	<b>CD64</b>	158 Gd	Mouse	IgG1, κ	X54-5/7.1	BioLegend	139301
29	<b>PD-L2</b>	148 Nd	Rat	IgG2a, k	Ty25	eBioscience	14-5986-82
30	<b>CD70</b>	142 Nd	Rat	IgG2b, k	FR70	eBioscience	14-0701-82
31	<b>ICOSL</b>	143 Nd	Rat	IgG2a, κ	HK5.3	BioLegend	107407
32	<b>OX40L</b>	149 Sm	Rat	IgG2b, k	RM134L	BioLegend	108802
33	<b>SiglecF</b>	175 Lu	Rat	IgG2a, κ	E50-2440	BD	552125
34	<b>CD90.2</b>	145 Nd	Rat	IgG2b, κ	30-H12	BioLegend (MaxPar-Ready)	105333
35	<b>CD31</b>	155 Gd	Rat	IgG2a, κ	390	BioLegend (MaxPar-Ready)	102425
36	<b>CX3CR1</b>	164 Dy	Mouse	IgG2a, κ	SA011F11	Fluidigm	3164023B
37	<b>CCR2</b>	209 Bi	Rat	IgG2b	475301	R&D	MAB55381

Supplementary table 2

gene name	description	fold change regression/ untreated		fold change relapse/ ntreated	
		p value		p value	
C5ar1	Complement component 5a receptor 1	17,87525694	0,004208	0,982441352	0,725113
Ackr2	Chemokine binding protein 2	0,608785315	0,442566	1,060656209	0,708967
Ccl1	Chemokine (C-C motif) ligand 1	4,229398127	0,08472	1,268828253	0,53271
Ccl11	Chemokine (C-C motif) ligand 11	4,373548889	0,16125	1,617402015	0,107111
Ccl12	Chemokine (C-C motif) ligand 12	9,27603028	0,000637	0,884087385	0,954444
Ccl17	Chemokine (C-C motif) ligand 17	0,787139645	0,345695	0,608059886	0,103785
Ccl19	Chemokine (C-C motif) ligand 19	0,855103821	0,758313	1,07834766	0,800192
Ccl2	Chemokine (C-C motif) ligand 2	0,563161527	0,124889	0,466810294	0,066825
Ccl20	Chemokine (C-C motif) ligand 20	0,387635479	0,012272	0,66849897	0,547662
Ccl22	Chemokine (C-C motif) ligand 22	7,325784855	0,024787	0,808525324	0,530408
Ccl24	Chemokine (C-C motif) ligand 24	0,705396962	0,302565	1,094596506	0,806953
Ccl25	Chemokine (C-C motif) ligand 25	0,912920543	0,728113	1,182349798	0,555346
Ccl26	Chemokine (C-C motif) ligand 26	0,950144292	0,973325	1,33847376	0,256822
Ccl28	Chemokine (C-C motif) ligand 28	0,705396962	0,302565	1,094596506	0,806953
Ccl3	Chemokine (C-C motif) ligand 3	21,2886318	0,000777	1,50527732	0,178541
Ccl4	Chemokine (C-C motif) ligand 4	21,23212725	0,001401	1,500487947	0,193625
Ccl5	Chemokine (C-C motif) ligand 5	4,254038927	0,000161	0,976073302	0,806272
Ccl6	Chemokine (C-C motif) ligand 6	11,70809172	0,071621	0,985190056	0,92653
Ccl7	Chemokine (C-C motif) ligand 7	1,475048862	0,4377	0,7041009	0,380961
Ccl8	Chemokine (C-C motif) ligand 8	81,43163761	0,005846	6,172465122	0,004655
Ccl9	Chemokine (C-C motif) ligand 9	4,691307029	0,066598	0,634109055	0,225121
Ccr1	Chemokine (C-C motif) receptor 1	10,04406749	0,000416	1,065271209	0,867925
Ccr10	Chemokine (C-C motif) receptor 10	0,822126589	0,309464	0,877167895	0,95592
Ccr11	Chemokine (C-C motif) receptor 1-like 1	2,52922517	0,056908	0,649812201	0,225672
Ccr2	Chemokine (C-C motif) receptor 2	34,32568787	0,001513	2,622866472	0,03688
Ccr3	Chemokine (C-C motif) receptor 3	25,79500383	0,007104	1,752956199	0,134365
Ccr4	Chemokine (C-C motif) receptor 4	0,864980577	0,498912	0,647028857	0,442187
Ccr5	Chemokine (C-C motif) receptor 5	40,23859548	0,002987	2,510203097	0,041316
Ccr6	Chemokine (C-C motif) receptor 6	0,592468134	0,344867	0,313167331	0,073446
Ccr7	Chemokine (C-C motif) receptor 7	25,24363202	0,004668	2,705265822	0,066635
Ccr8	Chemokine (C-C motif) receptor 8	2,162001968	0,163512	0,786531892	0,421406
Ccr9	Chemokine (C-C motif) receptor 9	1,313966255	0,320392	0,584118016	0,130119
Ackr4	Chemokine (C-C motif) receptor-like 1	0,410082042	0,228031	0,942500459	0,613231
Ccr12	Chemokine (C-C motif) receptor-like 2	12,24183139	0,003131	0,877731085	0,813914
Cmk1r1	Chemokine-like receptor 1	9,916362609	0,005733	0,923697322	0,628306
Cmtm2a	CKLF-like MARVEL transmembrane domain containing 2A	0,356232599	0,034966	0,401625111	0,048085
Cmtm3	CKLF-like MARVEL transmembrane domain containing 3	0,805048608	0,049392	0,937969192	0,430961
Cmtm4	CKLF-like MARVEL transmembrane domain containing 4	0,408956607	0,005219	0,592763057	0,015828
Cmtm5	CKLF-like MARVEL transmembrane domain containing 5	0,862560148	0,676229	1,33847376	0,256822
Cmtm6	CKLF-like MARVEL transmembrane domain containing 6	2,168588305	0,021061	0,856134363	0,426053





**Supplementary table 2.** Continued

gene name	description	fold change regression/ untreated	p value	fold change relapse/ untreated	p value
Cx3cl1	Chemokine (C-X3-C motif) ligand 1	0,299300329	0,079107	1,029477468	0,904802
Cx3cr1	Chemokine (C-X3-C) receptor 1	1,189555845	0,316826	0,704801715	0,102914
Cxcl1	Chemokine (C-X-C motif) ligand 1	6,465850148	0,119109	1,149216083	0,670383
Cxcl10	Chemokine (C-X-C motif) ligand 10	1,088985357	0,512536	0,550645207	0,005693
Cxcl11	Chemokine (C-X-C motif) ligand 11	3,006716926	0,034127	0,72781668	0,181257
Cxcl12	Chemokine (C-X-C motif) ligand 12	1,987482499	0,273726	0,924034699	0,616615
Cxcl13	Chemokine (C-X-C motif) ligand 13	4,100120236	0,179369	1,182647406	0,763718
Cxcl14	Chemokine (C-X-C motif) ligand 14	0,885011066	0,889469	2,152499104	0,113201
Cxcl15	Chemokine (C-X-C motif) ligand 15	0,685672138	0,262889	1,137844516	0,702475
Cxcl16	Chemokine (C-X-C motif) ligand 16	16,43403287	0,000577	1,216129294	0,374965
Cxcl2	Chemokine (C-X-C motif) ligand 2	6,655004077	0,011969	1,037507271	0,64995
Cxcl3	Chemokine (C-X-C motif) ligand 3	20,77712308	0,058455	1,256843014	0,292237
Cxcl5	Chemokine (C-X-C motif) ligand 5	39,22538672	0,143602	2,69407315	0,02469
Cxcl9	Chemokine (C-X-C motif) ligand 9	13,71398524	0,010808	1,370677999	0,471735
Cxcr1	Chemokine (C-X-C motif) receptor 1	0,740722221	0,33692	1,094596506	0,806953
Cxcr2	Chemokine (C-X-C motif) receptor 2	1,797994038	0,298779	0,553722249	0,17406
Cxcr3	Chemokine (C-X-C motif) receptor 3	17,15299476	0,049697	1,103967857	0,909282
Cxcr4	Chemokine (C-X-C motif) receptor 4	7,080733372	0,002538	1,101904653	0,913501
Cxcr5	Chemokine (C-X-C motif) receptor 5	1,014609527	0,812845	0,987944691	0,997114
Cxcr6	Chemokine (C-X-C motif) receptor 6	17,56636894	0,033306	1,519151037	0,078171
Ackr3	Chemokine (C-X-C motif) receptor 7	1,57386911	0,294366	3,672457441	0,002172
Ackr1	Duffy blood group, chemokine receptor	3,462712198	0,296126	1,09966329	0,800123
Fpr1	Formyl peptide receptor 1	2,911893405	0,022954	0,553683337	0,121135
Gpr17	G protein-coupled receptor 17	0,311014702	0,021067	0,609614689	0,145748
Hif1a	Hypoxia inducible factor 1, alpha subunit	1,196682224	0,108426	1,204137089	0,044228
Ifng	Interferon gamma	326,2800057	0,001759	4,003714598	0,05303
Il16	Interleukin 16	5,538931203	0,019677	1,468474649	0,089628
Il1b	Interleukin 1 beta	45,69539329	0,002144	2,597600794	0,059957
Il4	Interleukin 4	0,666323691	0,302848	0,384850823	0,191457
Il6	Interleukin 6	1,257471541	0,493576	0,726472299	0,517054
Itgam	Integrin alpha M	13,82210739	0,003043	1,429789469	0,136439
Itgb2	Integrin beta 2	32,24508713	0,000697	1,88383208	0,045447
Mapk1	Mitogen-activated protein kinase 1	0,639151526	0,017424	0,917905505	0,39941
Mapk14	Mitogen-activated protein kinase 14	0,774245669	0,022775	0,820527944	0,083837
Pf4	Platelet factor 4	3,19387565	0,057528	0,979257497	0,802073
Ppbp	Pro-platelet basic protein	1,977195952	0,134338	0,82067808	0,754255
Slit2	Slit homolog 2 (Drosophila)	0,324933904	0,013101	0,556167746	0,052311
Tgfb1	Transforming growth factor, beta 1	1,421728627	0,020014	1,385992116	0,000597
Tlr2	Toll-like receptor 2	4,053260603	0,02681	0,724302748	0,193246
Tlr4	Toll-like receptor 4	1,762306223	0,080841	1,02385581	0,960932
Tnf	Tumor necrosis factor	25,48292393	0,010211	1,569880155	0,287651
Tymp	Thymidine phosphorylase	0,312398405	0,074898	0,489865903	0,129243
Xcl1	Chemokine (C motif) ligand 1	27,68376645	0,002788	3,307990098	0,293397
Xcr1	Chemokine (C motif) receptor 1	6,11007679	0,007499	0,839353152	0,458806

Supplementary table 3

	symbol	logFC relapsed/untreated	AveExpr	P.Value	adj.P.Val
1	Aspn	3,750034	6,304115	1,71721E-07	0,000169043
2	Ackr3	3,118817	4,571009	1,04738E-05	0,00231637
3	Igsf10	2,854812	7,185085	9,761E-07	0,000496509
4	Pmepal	2,747946	6,197001	7,21885E-10	1,1016E-05
5	Crifl	2,605471	6,16468	3,09695E-06	0,001114898
6	Itgb11	2,48235	4,761967	5,6401E-06	0,001536926
7	Mgat3	2,459198	3,307252	1,98474E-05	0,003481281
8	Fam101b	2,440107	6,361934	3,07272E-08	6,69852E-05
9	Rbms3	2,414338	3,719754	3,32617E-06	0,00112794
10	Itgb8	2,219571	5,190866	4,20076E-06	0,001359629
11	Irak2	2,209289	4,611382	5,06766E-06	0,00145439
12	Bpgm	2,168682	5,584404	2,2006E-05	0,003773159
13	Nrp1	2,098738	7,509337	2,65885E-08	6,69852E-05
14	Nt5e	2,0808	4,569089	3,19929E-05	0,004931426
15	Unc5b	2,051906	6,82899	1,5905E-07	0,000169043
16	Bmf	2,026076	5,037071	8,69838E-06	0,002106941
17	Bmper	2,016264	3,809976	3,02723E-05	0,004762425
18	Stra6	1,946453	5,514035	8,88866E-07	0,000467728
19	Ak4	1,913096	3,86141	9,4351E-06	0,002173504
20	Gpr153	1,886252	7,741594	7,54674E-07	0,000460653
21	<NA>	1,846802	4,835161	9,23513E-06	0,002168124
22	Nrp2	1,809106	7,273531	3,0236E-08	6,69852E-05
23	Irs1	1,770067	5,503942	8,56364E-07	0,000466718
24	Sertad4	1,766263	5,813917	6,66676E-06	0,001784819
25	Tnfaip2	1,749275	7,60261	8,42256E-07	0,000466718
26	Rab31l1	1,731383	5,930902	4,41125E-05	0,005997945
27	Chst15	1,691084	5,977654	3,29106E-06	0,00112794
28	Fgf2	1,660112	5,647116	5,1466E-06	0,00145439
29	Plod1	1,603239	6,802378	1,80856E-05	0,003285541
30	Nupr1	1,535792	5,165646	2,73908E-06	0,001043268
31	Igfbp4	1,530846	9,991975	5,5457E-07	0,00038467
32	Sema5a	1,522959	7,953553	4,27668E-06	0,001359629
33	Il17rd	1,454735	3,889588	1,38639E-05	0,002820849
34	Slc27a3	1,454627	6,542826	3,88999E-05	0,005547784
35	Tenm3	1,410217	7,416774	1,55211E-05	0,003036557
36	Mex3b	1,358996	4,498014	4,8674E-06	0,00145439
37	Lox	1,338137	8,505828	3,32673E-05	0,004977054
38	Dhrs3	1,327491	5,480791	1,65543E-05	0,003118756
39	Slc6a6	1,313049	8,267823	6,55481E-08	9,09331E-05
40	Olfml3	1,272772	5,58427	1,60326E-05	0,003096937
41	Abca1	1,256574	7,459632	1,71169E-05	0,003147027
42	Plod2	1,249523	7,330136	5,46751E-06	0,001516984
43	Tgfb1	1,241185	8,826932	3,32266E-05	0,004977054
44	Rhoj	1,227147	5,325021	3,23637E-05	0,004938698
45	Sorcs2	1,203791	6,853354	1,64541E-05	0,003118756
46	Eid1	1,203525	7,104477	9,02521E-06	0,002151949
47	Pdgfrb	1,192477	7,954187	3,63488E-05	0,005385268
48	Vat1	1,167668	6,724629	3,25558E-07	0,000261474
49	Wls	1,164261	8,620713	0,000001296	0,000599302
50	Nr2f1	1,083876	6,263735	3,17255E-05	0,004931426
51	Mical2	1,083089	5,67514	1,92744E-05	0,003460313



Supplementary table 3. Continued

	symbol	logFC relapsed/untreated	AveExpr	P.Value	adj.P.Val
52	Ajuba	1,052258	5,767902	8,36503E-06	0,002058878
53	Thbd	1,041433	10,09541	2,46829E-05	0,004139134
54	Mxra8	1,041414	9,103924	3,75942E-05	0,005516222
55	Ptgfrn	1,017703	6,776935	5,02986E-06	0,00145439
56	Exoc4	-1,006164	6,611974	2,29321E-06	0,000920904
57	Fbxo45	-1,041587	5,451765	1,69233E-05	0,003147027
58	Tbx3	-1,055207	7,679557	2,42215E-05	0,004106886
59	Clnn	-1,103652	4,760423	4,28935E-05	0,005912697
60	Slc43a3	-1,114708	6,665306	2,61723E-06	0,001024074
61	Sardh	-1,143073	5,881424	3,14159E-06	0,001114898
62	Pitpnm2	-1,192685	5,605535	1,44587E-05	0,002865449
63	Hspa5	-1,200144	10,40625	1,16137E-05	0,002427734
64	Sesn2	-1,206409	6,098972	4,06672E-05	0,005746124
65	Isoc1	-1,227162	4,94684	1,11922E-05	0,002407806
66	Glpr1	-1,242656	6,342803	1,28976E-06	0,000599302
67	Kife5b	-1,317252	4,804769	3,67117E-07	0,000266772
68	Tbx5	-1,347193	5,099484	2,15523E-05	0,003737365
69	Btg3	-1,358979	4,511982	7,3685E-06	0,001905818
70	Slc20a1	-1,368591	7,33547	2,64359E-05	0,000429352
71	Gtse1	-1,429648	5,631688	9,7329E-06	0,002184176
72	Trp53inp1	-1,499037	6,123713	1,80983E-06	0,000812293
73	Ptp4a3	-1,597982	5,26031	2,10641E-06	0,000892885
74	Aen	-1,618191	5,420355	1,12191E-05	0,002407806
75	Mdm2	-1,673177	7,172028	9,54291E-06	0,002173504
76	Ccne1	-1,677149	4,496256	3,86669E-05	0,005547784
77	Pidd1	-1,742963	4,804291	6,47123E-07	0,000429352
78	Zmat3	-1,744009	6,954821	8,12638E-09	4,13362E-05
79	Rcan1	-1,75224	6,560429	1,13606E-05	0,002407806
80	Slc19a2	-1,766079	4,866409	5,1509E-08	8,73363E-05
81	Ddias	-1,787181	4,012196	2,80302E-06	0,001043268
82	Akl	-1,798054	6,478878	6,51348E-08	9,09331E-05
83	Phlda3	-1,853761	6,529234	1,67484E-07	0,000169043
84	Ccng1	-1,883349	7,155701	8,2639E-08	0,000105089
85	Eda2r	-1,917078	5,174444	1,44426E-05	0,002865449
86	Ccrn4l	-1,922017	6,516289	1,29033E-05	0,002660865
87	Lacc1	-1,964999	4,166464	2,00018E-06	0,000872077
88	Il1rl1	-2,030472	10,14847	1,7724E-07	0,000169043
89	Ramp3	-2,077386	5,500887	1,05274E-06	0,000518222
90	Sulf2	-2,200703	7,966733	1,80732E-08	6,69852E-05
91	Nphp4	-2,205145	4,091887	8,03235E-07	0,000466718
92	Ephx1	-2,244453	5,786785	2,66837E-07	0,000226219
93	Pscl	-2,269099	6,055767	3,176E-09	2,42329E-05
94	Cd80	-2,41664	4,751497	6,89049E-07	0,00043812
95	Atg9b	-2,427535	5,956978	3,66195E-07	0,000266772
96	Cdkn1a	-2,517809	7,918332	4,06519E-08	7,75435E-05
97	Fam212b	-2,615146	3,420543	7,94638E-06	0,001988547
98	9030617O03Rik	-2,644776	5,230556	2,48178E-07	0,000222776
99	Fbn2	-3,013478	8,662419	7,07921E-06	0,001862565
100	Nutm1	-5,881215	3,539851	3,58628E-06	0,001189711

Supplementary table 4

Gene symbol	pathway	logFC	AveExpr	P.Value	adj.P.Val
CRLF1	EPITHELIAL_MESENCHYMAL_TRANSITION	2,604143	6,16468	0,0000071	0,0009901
DDIT4	P53 PATHWAY	1,777519	6,598344	0,0000893	0,0048791
FGF2	EPITHELIAL MESENCHYMAL TRANSITION	1,659642	5,647116	0,0000108	0,0014056
BGN	EPITHELIAL MESENCHYMAL TRANSITION	1,64031	10,46155	0,0002181	0,0085842
IGFBP4	EPITHELIAL MESENCHYMAL TRANSITION	1,530938	9,991975	0,0000013	0,000312
FBN1	EPITHELIAL MESENCHYMAL TRANSITION	1,349583	7,073461	0,0003704	0,0121104
FBLN5	EPITHELIAL MESENCHYMAL TRANSITION	1,3444	8,047009	0,0001128	0,0053164
LOX	EPITHELIAL MESENCHYMAL TRANSITION	1,338801	8,505828	0,0000655	0,004143
PDGFRB	EPITHELIAL MESENCHYMAL TRANSITION	1,193092	7,954187	0,0000545	0,0037926
CALD1	EPITHELIAL MESENCHYMAL TRANSITION	1,144069	7,345882	0,0007802	0,0206024
DPYSL3	EPITHELIAL MESENCHYMAL TRANSITION	1,108945	7,552066	0,0003774	0,0121104
MMP14	EPITHELIAL MESENCHYMAL TRANSITION	1,061553	9,781442	0,0001138	0,0053164
COL5A2	EPITHELIAL MESENCHYMAL TRANSITION	0,979661	9,541117	0,0009188	0,022378
P3H1	EPITHELIAL MESENCHYMAL TRANSITION	0,917877	5,640759	0,0000706	0,0043305
XPC	P53 PATHWAY	0,877725	4,436618	0,0005915	0,0169009
LOXL1	EPITHELIAL MESENCHYMAL TRANSITION	0,589168	8,053686	0,0010931	0,0250576
EPHA2	P53 PATHWAY	-0,69734	7,414886	0,0004505	0,0138206
EI24	P53 PATHWAY	-0,80909	6,259984	0,0000622	0,0040561
CSF1	TNFA SIGNALING VIA NFKB	-0,89604	7,914468	0,0004129	0,0130515
BAX	P53 PATHWAY	-0,94477	5,281182	0,0000754	0,004493
PLAUR	TNF $\alpha$ SIGNALING VIA NFKB, EPITHELIAL MESENCHYMAL TRANSITION	-1,02754	6,307811	0,0003765	0,0121104
PLK2	TNF $\alpha$ SIGNALING VIA NFKB, P53 PATHWAY	-1,11842	7,884715	0,0009621	0,0230688
DUSP5	TNF $\alpha$ SIGNALING VIA NFKB	-1,52796	6,707215	0,0009226	0,022378
IER5	TNF $\alpha$ SIGNALING VIA NFKB, P53 PATHWAY	-1,54798	8,63411	0,001235	0,0263184
EGR2	TNF $\alpha$ SIGNALING VIA NFKB	-1,55261	5,81364	0,0008068	0,02073
AEN	P53 PATHWAY	-1,61427	5,420355	0,0000239	0,0021916
MDM2	P53 PATHWAY	-1,67238	7,172028	0,000019	0,0020873
AK1	P53 PATHWAY	-1,79755	6,478878	0,0000002	0,0000905
PHLDA3	P53 PATHWAY	-1,85377	6,529234	0,0000004	0,0001433

**Supplementary table 4.** Continued

Gene symbol	pathway	logFC	AveExpr	P.Value	adj.P.Val
AREG	TNF $\alpha$ SIGNALING VIA NFKB, EPITHE- LIAL MESENCHYMAL TRANSITION	-1,87297	7,139056	0,0002588	0,0098145
CCNG1	P53 PATHWAY	-1,88407	7,155701	0,0000002	0,0000927
PLK3	P53 PATHWAY	-2,10807	7,275334	0,0008007	0,02073
LIF	TNF $\alpha$ SIGNALING VIA NFKB, P53 PATHWAY	-2,20338	6,382069	0,0008943	0,0222075
FOSB	TNF $\alpha$ SIGNALING VIA NFKB	-2,21502	11,26722	0,0012042	0,0263184
EPHX1	P53 PATHWAY	-2,24637	5,786786	0,0000007	0,0001776
CD80	TNF $\alpha$ SIGNALING VIA NFKB	-2,40368	4,751497	0,0000027	0,0005026
SGK1	TNF $\alpha$ SIGNALING VIA NFKB	-2,41643	9,621731	0,0000912	0,0048791
ATF3	TNF $\alpha$ SIGNALING VIA NFKB, P53 PATHWAY	-2,5753	7,838792	0,0008149	0,02073
ZNF365	P53 PATHWAY	-4,09016	3,044299	0,000163	0,0065384





# Chapter 4

## Counteracting interleukin-6 associated resistance to immunotherapy and chemotherapy

*Elham Beyranvand Nejad, Camilla Labrie, Hans-Willi Mittrücker, Kees L. M. C. Franken, Sylvia Heink, Thomas Korn, Rueshandra Shanty Roosenhoff, Ramon Arens, Thorbald van Hall, Sjoerd H. van der Burg*

Work in progress



## Abstract

IL-6 is a pleiotropic cytokine that induces pro- and anti-inflammatory responses. Overexpression of IL-6 has been detected in several types of cancer and correlates with poor prognosis and chemotherapy resistance. Blockade of the tumor-promoting effects of IL-6 has so far been proven to be unsuccessful. Here, we created a mouse tumor model expressing IL-6 at levels that reflected the range found in human cancers, and used it to investigate the impact of tumor-expressed IL-6 on chemotherapy and immunotherapy. Overexpression of IL-6 shifted the systemic and intratumoral populations of myeloid cells towards a MHC class II<sup>low</sup> non-stimulatory phenotype and led to impaired regression and cure of tumors following cisplatin chemotherapy or therapeutic vaccination. IL-6 blockade before or during treatment partly restored the myeloid cell phenotype, yet did not reinstall sensitivity to immunotherapy and chemotherapy. In depth studies revealed that IL-6 signaling was required for the expansion of vaccine-induced T cells and the optimal function of tumor-infiltrating macrophages, both required for full regression of the treated tumors. However, IL-6 blockade after initial vaccine-driven tumor regression partly prevented subsequent tumor recurrence and led to a higher survival rate of mice with IL-6 overexpressing tumors. Interestingly, while the high-level IL-6 mediated changes provided resistance to the two different single therapies, their combination still successfully mediated tumor control. Altogether, our study shows that the effects of IL-6 in tumors is context dependent and that blockade of the negative effects requires appropriate timing in order to successfully treat otherwise resistant tumors.

## Introduction

The composition of the tumor microenvironment plays a critical role in the progression of cancer and the response to chemo-, radio- and immune-therapy (1, 2). In general, the presence of type 1 tumor-specific T cells, DCs and M1 macrophages have been positively correlated with outcome, whereas immunosuppressive cells such as Tregs, MDSCs and M2 macrophages in the tumor microenvironment can dampen tumor immunity and are related to a worse prognosis (1). Their composition as well as the dynamic interaction between these immune cells, and with tumor cells, affect the anti-tumor response that is induced or modulated by the different cancer therapeutic modalities currently used (3).

Well-known interactions are those between the different co-stimulatory and co-inhibitory molecules and their ligands expressed by these immune cells and tumor cells (4). Other interactions are governed by the chemokines and cytokines in the tumor microenvironment thereby influencing the attraction, proliferation and function of receptive cells locally but also at distant sites (5, 6). One example is IL-6, a pleiotropic cytokine that plays an important role in infection, inflammation and hematopoiesis. Signaling via IL-6 is transferred via three routes. Classical signaling occurs when IL-6 bind to membrane expressed IL-6R (mIL-6R), which is present only on a limited number of cells. In addition, IL-6 can bind to the soluble IL-6R allowing it to induce trans-signaling in cells expressing gp130 (7). Binding of IL-6 to membrane or soluble IL-6R leads to dimerization of signal transducing component gp130 and activation of downstream pathways that control cell survival and proliferation, both of tumor cells and immune cells (8). It is known that classical signaling and trans-signaling induces anti-inflammatory and pro-inflammatory responses, respectively in many diseases and cancer. Finally, DCs can present IL-6 via their surface IL-6R to gp130 on T cells, a process called IL-6 trans-presentation or cluster-signaling (9). IL-6 is produced by various immune and non-immune cells and has a wide range of effects on several types of cells (10). Normal physiological serum concentrations of IL-6 are low and in the picogram range whereas in disease settings it may go up to micrograms per ml (11).

In many independent types of cancer increased serum concentrations of IL-6 are reported and this positively correlates with bigger tumors, higher disease stage and worse performance status (12). IL-6 influences the recruitment, functional activation, differentiation and survival of leukocytes as well as is important for the sustainment of adaptive immunity (8). The pro-tumorigenic effects of IL-6 include the generation of MDSC, decreased expression of MHC class II, CD80/86 and IL-12 in DC, lowered activity of CD8<sup>+</sup> T cells and phenotype switching from M1 to M2 macrophages (8, 13). However, IL-6 is also required for the expansion, that is proliferation and survival, of T cells (8, 14, 15), as well as the local proliferation of Ly6C inflammatory monocytes (16). Targeting of IL-6 in a mouse multiple myeloma model and in



patients showed anti-tumor activity (17, 18) but subsequent trials in several types of cancer have shown poor clinical responses, indicating that there is still a large gap in our knowledge preventing appropriate exploitation of anti-IL-6 therapy in cancer (8).

Human papilloma virus (HPV) induced cancers of the anogenital region and oropharynx are highly representative for immunogenic tumors in which the tumor-specific T-cell response can be repressed by several immunological mechanisms (19). Increased serum IL-6 is found in HPV-related cervical and oropharyngeal cancers (20-22) and when produced by cervical cancer cells (23) or oropharyngeal cancer cells (24) it is related to a worse response to radiotherapy or chemotherapy, respectively. A number of reports suggest that cancer cell-derived IL-6 impairs the immune stimulatory population of tumor-infiltrating myeloid cells (25-29). To investigate the role of tumor-expressed IL-6 in immunotherapy and chemotherapy, we engineered TC-1 tumor cells to overexpress IL-6 in order to have one tumor model that reflected both extreme ends of the range of tumor-expressed IL-6 as observed *in vivo*. We showed that overexpression of IL-6 by tumor cells altered the composition of the myeloid cells and reduced the therapeutic effect induced by peptide vaccination and cisplatin treatment. Blockade of IL-6 signaling improved the sensitivity of IL-6 producing tumor cells to immunotherapy, but only when it is applied after initial therapy-induced tumor regression as both vaccine-induced T cells and tumoricidal inflammatory macrophages required intact IL-6 signaling for an optimal antitumor response.

## Materials and methods

### Mice

Six to eight week old wild-type female C57BL/6 mice were obtained from Charles River Laboratories. *Il6ra<sup>fl/fl</sup>×LysM<sup>cre</sup>* and *Il6ra<sup>fl/fl</sup>×LysM<sup>cre+</sup>* transgenic mice were obtained from University Medical Center Hamburg-Eppendorf, Germany and were generated as previously described (30, 31). Mice were housed in individually ventilated cages under specific pathogen-free conditions in the animal facility of Leiden University Medical Center (LUMC, Leiden, the Netherlands). All animal experiments were approved by the Animal Experiments Committee of LUMC and were executed according to the animal experimentation guidelines of LUMC in compliance with the guidelines of Dutch and European committees.

### Tumor cell line and culture conditions

The tumor cell line TC-1 was generated by retroviral transduction of C57BL/6 lung epithelial cells with the HPV16 E6/E7 and c-H-ras oncogenes (32) and cultured as described previously (33). TC-1 control and IL-6 tumor cell lines were made by transfection of TC-1 tumor line with pcDNA3.1 vector with hygromycin resistance gene. This vector is adapted by replacement of CMV promotor with a short elongation factor (EFS) promotor. A fragment was inserted with the IRES sequence and GFP. IL-6 gene was inserted between EFS

promotor and IRES sequence and GFP (TC-1 IL-6) (Supplementary figure 1A and B). For a control, no gene was inserted between EFS promotor and IRES sequence and GFP (TC-1 control). All the cell lines were cultured in Iscove's Modified Dulbecco's Media (IMDM) (BioWhittaker) supplemented with 8% fetal calf serum (FCS) (Greiner), 2 mM L-glutamine (Life Technologies), 50 IU/ml penicillin (Life Technologies) and 50 µg/ml streptomycin (Life Technologies). Cells were cultured in a humidified incubator at 37°C and 5% CO<sub>2</sub>. Mycoplasma tests that were frequently performed for all cell lines by PCR were negative.

### Tumor experiments and treatments

Mice were inoculated subcutaneously with  $1 \times 10^5$  tumor cells in 200 µL PBS containing 0.2% BSA on day 0. Tumor size (horizontal dimension  $\times$  vertical dimension) was measured two times a week using a caliper. When a palpable tumor was present (day 8), mice were divided into groups with comparable tumor sizes. On day 8 post tumor challenge, mice were treated with synthetic long peptide (SLP) (prime) vaccine or cisplatin. SLP vaccine containing 100 µg HPV16 E7<sub>43-77</sub> SLP (GQAEPDRAHYNIVTFCKCDSTLRCLCVQSTHVDIR) with 20 µg CPG (ODN1826, InvivoGen) dissolved in 50 µl PBS was administrated subcutaneously in tail base of mice. Boost vaccine was given on day 22 post tumor challenge. Low dose (LD) (4 mg/kg) and maximum tolerated dose (MTD) (10 mg/kg) of cisplatin was provided intraperitoneally in 300 µl in NaCl. Mice were routinely weighed 2–3 times per week. After cisplatin administration, mice were weighed 3–4 times per week until mice recovered. Exclusion criteria were ulceration of tumors and insusceptibility for cisplatin treatment as evidenced by complete lack of weight loss. Mice were euthanized when tumor size reached  $>2,000 \text{ mm}^3$  in volume or when mice lost  $>20\%$  of their total body weight (relative to initial body mass).

### Flow cytometric analysis of splenic and tumor-infiltrating immune cells

For analysis of (tumor-infiltrating) immune populations, tumors were disrupted in small pieces and incubated with Liberase (Roche) in IMDM for 15 minutes at 37°C. Spleens were digested by incubating with 0.02 mg/ml DNase and 1 mg/ml collagenase for 10 min at room temperature. Single-cell suspensions were prepared by mincing spleen and tumor pieces through a 70 µm cell strainer (BD Biosciences). Cells were resuspended in staining buffer (PBS + 2% FCS + 0.05% sodium azide) and incubated with various fluorescently labelled antibodies against: CD8a (clone 53-6.7), CD3 (clone 145-2C11), CD11b (clone M1/70), CD11c (clone N418), CD45.2 (clone 104), F4/80 (clone BM8), Ly6C (clone HK1.4), Ly6G (clone 1A8), class II (clone M5/114.15.2) and IL-6 (clone MP5-20F3). Antibodies were obtained from eBioscience and Biolegend. APC labelled- H-2D<sup>b</sup> tetramers containing HPV16 E7<sub>49-57</sub> peptide (RAHYNIVTF) were used as E7 tetramer (E7 Tm). For dead cell exclusion, 7-aminoactinomycin D (7-AAD; Invitrogen) was used. For intracellular cytokine staining, single cell suspensions of spleens or tumors were plated in 96-well cell culture flat-

bottom plates in the presence of dendritic cells preloaded with SLP and brefeldin A (4µg/ml). After 5 hours incubation, cells were stained for surface markers and were fixed in 0.5% paraformaldehyde for overnight. To measure the production of IL-6 by tumor cells, tumor cells were plated in 96-well cell culture flat-bottom plates in the presence brefeldin A (4 mg/ml). After overnight incubation, cells were fixed in 1% paraformaldehyde for 30 minutes. Thereafter, cells were washed, stained for cytokines. Samples were analyzed with a BD LSRII or LSRFortessa flow cytometer, and results were analyzed using FlowJo software (Tree Star).

### **In vivo antibody usage**

Rat anti-mouse IL-6R antibody (clone: MR16-1, a kind gift from Chugai Pharmaceutical Co., Tokyo, Japan) was used to block the IL-6R. To block IL-6, *InVivo*Mab anti-mouse IL-6 (clone: MP5-20F3, BioXcell) was used. Both antibodies were given at 200µg per mouse dissolved in PBS in 200 µl and administrated intravenously in the tail vein or retro-orbital every 3 days for total 7 injections. These antibodies were administered from 8 till 29 post tumor challenge unless stated differently in the legend of figures.

### **MTT assay**

Tumor cells (7000 cells per well) were plated in a 96-well culture flat-bottom plate. After 24 hours, cells were treated with escalating dosages of cisplatin. Cells were extensively washed after overnight incubation and grown for an additional 24 hours in fresh medium. Cell viability assay was determined using a standard colorimetric MTT (3-(4,5-dimethylthiazol-2-yl)-2, 5-diphenyl-tetrazolium bromide) reduction assay. Absorbance was measured with at a test wavelength of 570 nm, and a reference wavelength of 655 nm.

### **IL-6 ELISA**

Mouse IL-6 ELISA Ready-SET-Go! Kit (Invitrogen) was used to measure the amount of IL-6. Serum of the mice or supernatant of cultured cells were obtained and proceed as described in the protocol of the kit.

### **CTL assay**

Naïve C57BL/6 mice were vaccinated with SLP vaccine as described above on day 0 and 14. Splenocytes were isolated 8 days after the last vaccination and restimulated *in vitro* with DCs loaded with SLP. After 6 days restimulation, splenocytes were harvested by using EDTA. Next, live cells were enriched by high-density solution of Ficoll and centrifugation and used as effector cells in CTL assay. TC-1 control and TC-1 IL-6 tumor cells were exposed to IFNγ (10 IU, Prospec) one day before CTL assay and were use as target cells. Target cells were labelled with 100µl <sup>51</sup>Cr for 1 hour, washed and plated into a 96-well round-bottom plate at a density of 2.000 tumor cells/well with different ratios of effector cells. After 4 hours

incubation, supernatant of the cells were harvested and the percentage of  $^{51}\text{Cr}$  release was measured by a gamma counter.

### Statistical analysis

Survival for differentially treated mice was compared using the Kaplan–Meier method and the log-rank (Mantel–Cox) test. Additional statistical methods are stated in the legends. All  $P < 0.05$  were considered significant.

## Results

### IL-6 produced by tumor cells hampers the therapeutic effect induced by immunotherapy and chemotherapy

To investigate the importance of IL-6 produced by tumor cells in immunotherapy and chemotherapy, we used TC-1 tumor cells, expressing the HPV-16 oncoproteins E6 and E7, and engineered these cells to express IL-6 (TC-1 IL-6) (**Supplementary figure 1A and B**). This IL-6 was secreted in the supernatant of TC-1 IL-6 cells and at much higher levels in the serum of mice injected with these tumor cells when compared to control TC-1 (**Supplementary figure 1C–E**). To assess the impact of tumor-produced IL-6 on the efficacy of immunotherapy and chemotherapy, we injected TC-1 control and TC-1 IL-6 tumor cells into mice. When the tumor was palpable on day 8, the mice were treated either with a peptide vaccine (and boosted at day 22) or with cisplatin. The efficacy of these individual treatments was high with 100% survival for mice challenged with TC-1 control but a strong and significant reduction to 50% after vaccination and 75% survival after chemotherapy was observed in mice challenged with TC-1 IL-6 (**Figure 1A and 1B**). These data confirm that tumor expressed IL-6 hampers the therapeutic effect of chemotherapy and shows that the effect on immunotherapy is even more dramatic. We excluded that this difference in clinical reactivity was due to an intrinsic difference in the growth rate of IL-6 expressing tumor cells, as suggested in previous reports (34, 35), both *in vitro* (**Supplementary figure 1F**) and *in vivo* (**Supplementary figure 1G**). In addition, we excluded that IL-6 provided intrinsic resistance to immune mediated killing (**Supplementary figure 1H**). Similarly, there was no difference in cisplatin sensitivity between TC-1 control and TC-1 IL-6 tumor cells as the IC<sub>50</sub> for TC-1 control (3.36  $\mu\text{g}/\text{ml}$ ) and TC-1 IL-6 (3.36  $\mu\text{g}/\text{ml}$ ) are quite similar (**Supplementary figure 1I**). Taken together, these data showed that tumor-expressed IL-6 hampers the anti-tumor effect of peptide vaccination or cisplatin chemotherapy and this was not caused by intrinsic tumor cell differences.



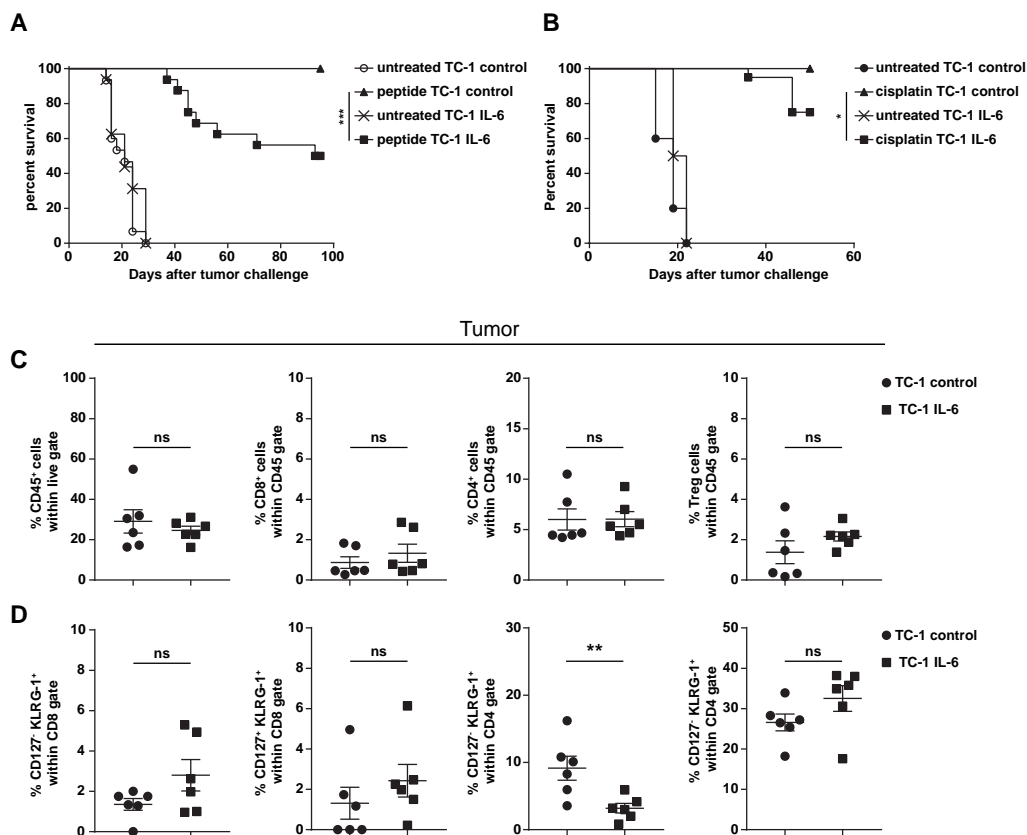


**Figure 1- IL-6 produced by tumor cells induce resistance to immunotherapy and chemotherapy**

Survival graph of the TC-1 control and TC-1 IL-6 tumor bearing mice that received SLP vaccine (A) or cisplatin (MTD) (B) as described in the material and methods. Data is pooled from two independent experiments, yielding similar results. Significance was determined by a log-rank (Mantel-Cox) test (\*,  $P < 0.05$ ; \*\*,  $P < 0.01$ ; \*\*\*,  $P < 0.001$ ). C) The percentage of intratumoral leukocytes (CD45<sup>+</sup>), CD8<sup>+</sup>, CD4<sup>+</sup> and Treg T cells in TC-1 control and IL-6 tumor bearing mice analyzed 18 days post tumor challenge. D) The percentage of CD127<sup>+</sup>KLRG-1<sup>+</sup> and CD127<sup>+</sup> KLRG-1<sup>+</sup> cells within intratumoral CD4<sup>+</sup> and CD8<sup>+</sup> T cells. Each dot represents data from an individual mouse. Graphs indicate mean values with SEM. Significance was determined by Mann-Whitney test. \*,  $P < 0.05$ ; \*\*,  $P < 0.01$ ; \*\*\*,  $P < 0.001$ . Experiments were performed twice with similar outcomes.

## Tumor-produced IL-6 alters the composition and phenotype of local and systemic immune cells

Our previous work showed that tumor-expressed IL-6 skews the phenotype of myeloid cells towards immune-supportive cells *in vitro* (25). Thus, we hypothesized that the observed resistance to immunotherapy and chemotherapy of IL-6 producing tumors was based on an altered tumor microenvironment. Hence, we examined its effect on the composition and phenotype of immune cells present in the tumor or in the system (spleen). Comparison of the T cell infiltrate in TC-1 control and TC-1 IL-6 tumors showed no significant differences



in the percentages of tumor-infiltrating CD45<sup>+</sup> immune cells, CD8<sup>+</sup> cells, CD4<sup>+</sup> cells and CD4<sup>+</sup>Tregs (**Figure 1C**). In addition, no alteration was found in the percentage of CD8<sup>+</sup>CD127<sup>-</sup>KLRG-1<sup>+</sup> short-lived effector cells (SLECs) and CD8<sup>+</sup>CD127<sup>+</sup>KLRG-1<sup>+</sup> double-positive effector cells (DPECs), although the population of CD4<sup>+</sup> SLECs was decreased (**Figure 1D**). The percentage of total CD11b<sup>+</sup> myeloid cells within intratumoral leukocytes was slightly increased in TC-1 IL-6 (**Figure 2A**). The myeloid cells were subdivided into three subsets based on CD11b and CD11c; CD11b<sup>+</sup>CD11c<sup>-</sup>, CD11b<sup>+</sup>CD11c<sup>+</sup> and CD11b<sup>-</sup>CD11c<sup>+</sup> myeloid cells. The gating strategy is shown in **supplementary figure 2A**. Strikingly, not only had half of the CD11b<sup>+</sup> cell population lost the expression of MHC class II, also the overall expression of MHC class II on intratumoral CD11b<sup>+</sup> myeloid cells was strongly reduced (**Figure 2A**). While the population of CD11b<sup>+</sup>CD11c<sup>+</sup> DC-like macrophages was increased, the CD11b<sup>-</sup>CD11c<sup>+</sup> cells (DC) was lowered and more than half of this population did not display MHC class II (**Figure 2B and C**). Further analysis based on the expression of MHC class II and F4/80 indicated that the percentage of F4/80<sup>+</sup> cells co-expressing MHC class II was decreased (**Figure 2D**) while their MHC class II-negative counterparts were strongly increased. Moreover, the percentage of Ly6C<sup>+</sup> inflammatory macrophages within the F4/80<sup>+</sup> CD11b<sup>+</sup>CD11c<sup>-</sup> population was slightly enhanced in TC-1 IL-6 (**Figure 2E**) but again the great majority of these cells did not express MHC class II (**Figure 2E and supplementary figure 2B**). Finally, the percentage of Ly6G<sup>+</sup> cells within the population of CD11b<sup>+</sup>CD11c<sup>-</sup> cells (MDSCs) was not altered by tumor-produced IL-6 (**Supplementary figure 2C**). Thus, the great majority of tumor-infiltrating myeloid cells known to stimulate tumor immunity had an immature phenotype based on the low expression of MHC class II.

To determine the systemic effect of tumor-produced IL-6, we measured the percentage of different types of T cells and myeloid cells in the spleen. The percentages of total CD8<sup>+</sup> and CD4<sup>+</sup> cells were decreased in the spleen, albeit that these cells displayed a more activated phenotype (**Supplementary figure 3A**). The percentage of total CD11b<sup>+</sup> myeloid cells slightly increased (**Supplementary figure 3B**), however, the percentage of MHC class II<sup>+</sup> CD11b<sup>+</sup> cells was lower and the MHC class II expression level was decreased on these cells (**Supplementary figure 3B**). Furthermore, the CD11b<sup>+</sup>CD11c<sup>-</sup> and Ly6G<sup>+</sup> cells increased while CD11b<sup>+</sup>CD11c<sup>+</sup> cells were decreased (**Supplementary figure 3C**). Importantly, the percentage of MHC class II<sup>+</sup>Ly6C<sup>hi</sup> cells was decreased (**Supplementary figure 3D**). Thus, these data show that tumor cell-produced IL-6 skews myeloid cells to a less mature phenotype, both locally and systemically. The fact that the systemic myeloid cell population is a phenocopy of those found in the tumor was also found by us in other studies (36). Blocking the IL-6 pathway during immunotherapy does not reinstall its therapeutic efficacy. To overcome, the negative effect of IL-6 on the intratumoral myeloid cells and on the therapeutic efficacy of peptide vaccination and cisplatin treatment, we blocked the IL-6 pathway using the MR16-I IL-6R blocking antibody in combination with peptide vaccine or chemotherapy.



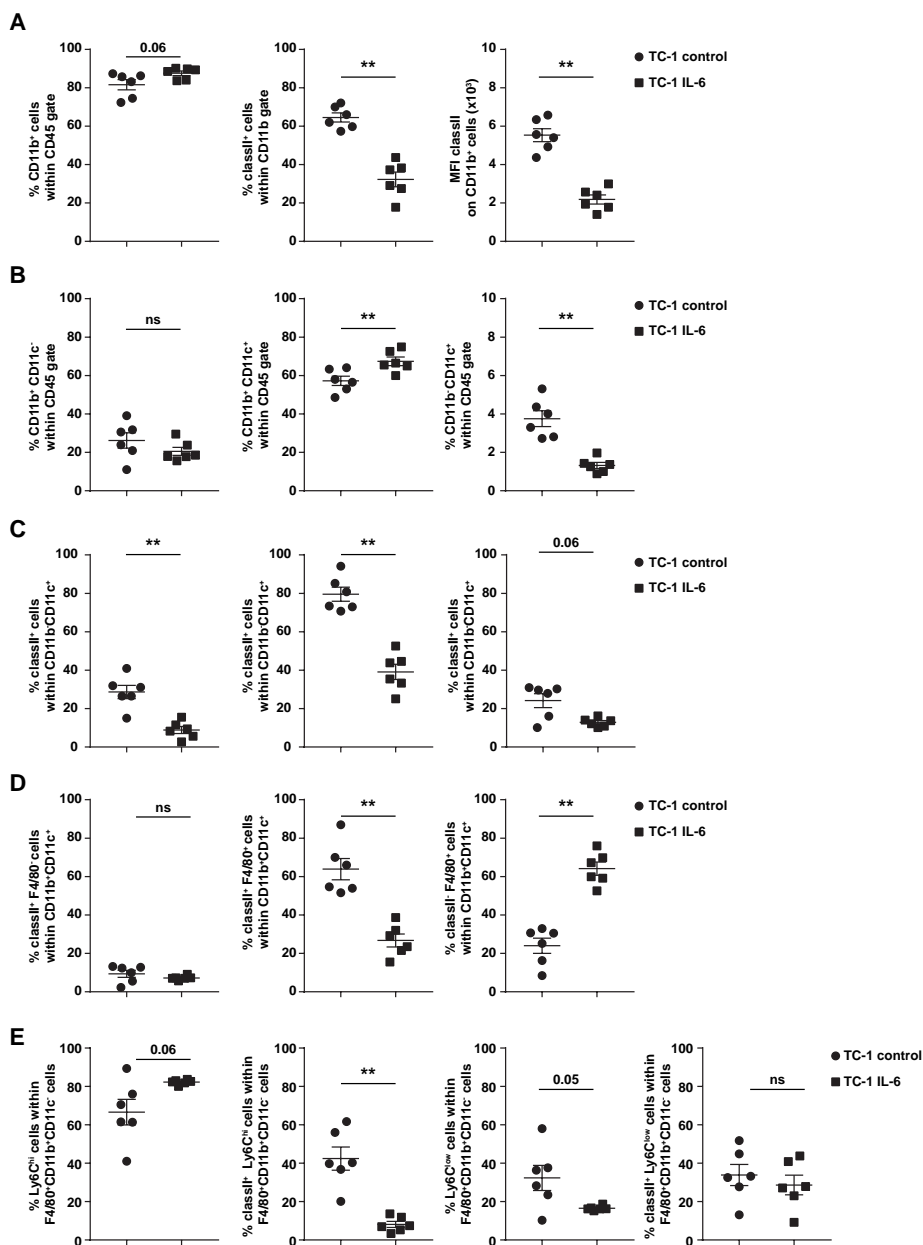
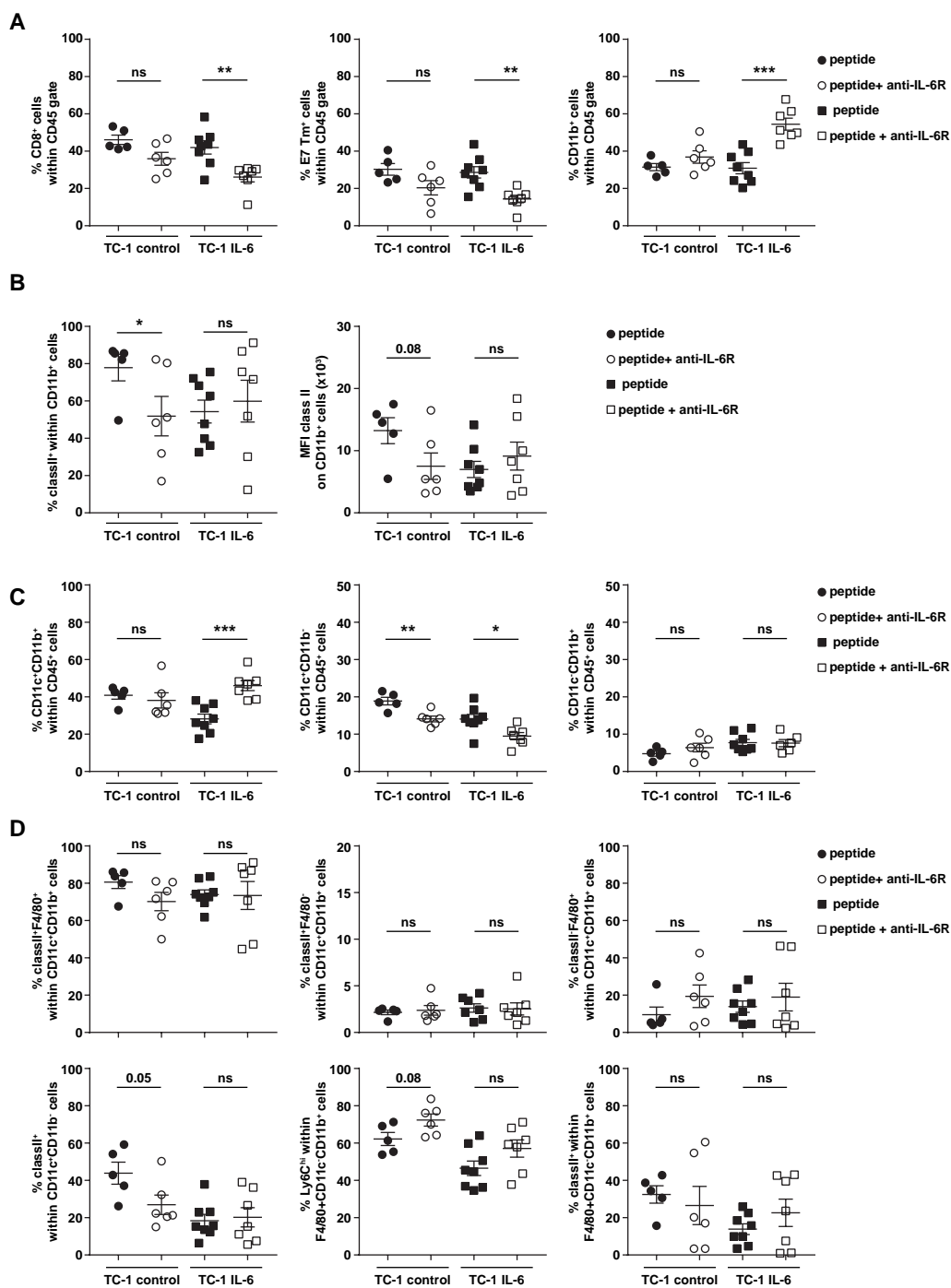


**Figure 2. IL-6 produced by tumor cells induce immature myeloid cells in the tumor**

A) The percentage of intratumoral CD11b<sup>+</sup>, classII<sup>+</sup> cells and MFI classII within intratumoral CD11b<sup>+</sup> cells. B) The percentage of CD11b<sup>+</sup>CD11c<sup>-</sup>, CD11b<sup>+</sup>CD11c<sup>+</sup> and CD11b<sup>+</sup>CD11c<sup>+</sup> intratumoral myeloid cells within CD45 gate. C) The percentage of classII<sup>+</sup> on CD11b<sup>+</sup>CD11c<sup>+</sup>, CD11b<sup>+</sup>CD11c<sup>+</sup> and CD11b<sup>+</sup>CD11c<sup>+</sup> intratumoral myeloid. D) The percentage of classII<sup>+</sup>F4/80<sup>-</sup>, classII<sup>+</sup>F4/80<sup>+</sup>, classII<sup>+</sup>F4/80<sup>+</sup> within CD11b<sup>+</sup>CD11c<sup>+</sup> and classII<sup>+</sup> cells within CD11b<sup>+</sup>CD11c<sup>+</sup>. E) The percentage of Ly6C<sup>hi</sup>, classII<sup>+</sup>Ly6C<sup>hi</sup>, Ly6C<sup>low</sup> and classII<sup>+</sup>Ly6C<sup>low</sup> within F4/80<sup>+</sup>CD11b<sup>+</sup>CD11c<sup>+</sup> cells. Each dot represents data from an individual mouse. Graphs indicate mean values with SEM. Significance was determined by Mann-Whitney test. \*, P < 0.05; \*\*, P < 0.01; \*\*\*, P < 0.001. Experiments were performed twice with similar outcomes.

Previously, we have shown that peptide vaccination increases the percentage of intratumoral CD8<sup>+</sup> and CD11b<sup>+</sup> in TC-1 tumor model, significantly (37). Detailed analysis of the intratumoral immune composition showed a strong increase in CD45<sup>+</sup> cells, CD8<sup>+</sup> (SLEC and DPEC) T cells and HPV-specific CD8<sup>+</sup> T cells, but not in CD4<sup>+</sup> T cells and Tregs were even lowered (**Supplementary figure 4A**). Also the percentage of CD11b<sup>+</sup> cells was strongly increased by peptide vaccination but there were no differences between TC-1 control and TC-1 IL-6 tumors (**Supplementary figure 4A**). IL-6R blockade slightly reduced the percentage of intratumoral CD8<sup>+</sup> T cells and HPV-specific T cells among the tumor infiltrating immune cells, while the number of CD11b<sup>+</sup> cell increased and this effect was most pronounced in TC-1 IL-6 tumors (**Figure 3A and Supplementary figure 4A**). The percentage of MHC class II<sup>+</sup>CD11b<sup>+</sup> myeloid cells increased after vaccination, however, both the percentage of MHCII<sup>+</sup> cells and the expression levels of MHC II were lower in TC-1 IL-6 (**Supplementary figure 4B**). IL-6R blockade decreased the expression levels of MHC II on CD11b<sup>+</sup> cells in TC-1 control to the same level as seen in TC-1 IL-6 (**Figure 3B**). Detailed analysis of myeloid composition demonstrated that the percentage of CD11b<sup>+</sup>CD11c<sup>-</sup> cells were reduced significantly by peptide vaccination and did not show any difference with IL-6R blockade (**Figure 3C and supplementary figure 4C**). Peptide vaccination did not affect the percentage of CD11b<sup>+</sup> CD11c<sup>+</sup> cells although this population is significantly less abundant in TC-1 IL-6 tumors (**Supplementary figure 4C**). However, IL-6 blockade increased this population in TC-1 IL-6 tumors (**Figure 3C**). The percentage of CD11b<sup>+</sup> CD11c<sup>+</sup> was significantly increased by peptide vaccination although is lower in TC-1 IL-6 tumors (**Supplementary figure 4C**). Importantly, especially the percentage of MHC class II<sup>+</sup> cells CD11b<sup>+</sup>CD11c<sup>+</sup> cells was lower in TC-1 IL-6 tumors after peptide vaccination (**Supplementary figure 4D**) and while IL-6 blockade did not have any further effect on these cells in TC-1 IL-6 tumors, it did decrease these MHC class II<sup>+</sup> cells in the TC-1 control tumors (**Figure 3CD**). Further analysis of the CD11b<sup>+</sup>CD11c<sup>+</sup> population showed three distinct population; classII<sup>+</sup>F4/80<sup>+</sup>, classII<sup>+</sup>F4/80<sup>-</sup> and classII<sup>-</sup>F4/80<sup>+</sup> which were a bit different in TC-1 IL-6 but after peptide vaccination no differences were found anymore (**Supplementary figure 4D**). Also IL-6R blockade did not affect the percentage of these vaccine-altered populations (**Figure 3D**). Systemically, TC-1 IL-6 tumor bearing mice showed a slightly different immune composition based on the percentage of CD11b<sup>+</sup>CD11c<sup>hi</sup> cells, CD11b<sup>+</sup>CD11c<sup>int</sup> and Ly6G<sup>+</sup> cells and IL-6R blockade almost normalized these changes (**Supplementary figure 5A-B**).

Thus, the effects of tumor-expressed IL-6, specifically on MHC class II expression of intratumoral myeloid cells, was also observed after therapeutic vaccination and this intratumoral effect could not be counteracted by simultaneous administration of IL-6R blocking antibodies. Rather IL-6R blockade had a negative effect on the intratumoral immune composition. This was seen both in TC-1 IL-6 as in TC-1 control, albeit that the effects in the latter tumor were less pronounced. The data fitted with the clinical outcome of the treated



mice. IL-6R blockade in peptide vaccinated TC-1 IL-6 tumor bearing mice not only failed to improve the therapeutic efficacy of vaccination, in fact it worsened the clinical response to vaccine therapy as none of the mice survived in this latter group (**Figure 4A and B**). Similarly, local administration of the IL-6R blocking antibody, to overcome the potential lower availability of the antibody in the tumor when provided systemically, also impaired the curative effect of therapeutic vaccination (**Figure 4A and B**). The tumors of treated mice showed less deep regressions and rapidly recurred. The negative impact of the IL-6R antibody was not limited to immunotherapy since blocking the IL-6R also did not improve the anti-tumor effect induced by cisplatin in TC-1 IL-6 tumor bearing mice (**Supplementary figure 6A and B**), fitting with the fact that the therapeutic effect of cisplatin is associated with the influx of Ly6C<sup>hi</sup>CD11c<sup>+</sup> macrophages (38). Although IL-6R blockade enhanced the influx of Ly6C<sup>hi</sup> cells, both the percentage of Ly6C<sup>hi</sup>CD11c<sup>+</sup> cells as well as the expression of CD11c and MHC class II on these cells was much lower in TC-1 IL-6 tumors and not restored upon IL-6R blocking (**Supplementary figure 6C and D**). Together, these data not only indicated that IL-6R blockade was unable to normalize the intratumoral myeloid cell composition but the detrimental effect of IL-6R blockade on tumor regression and recurrences also suggested that IL-6 signaling is required for a strong therapy-induced tumor regression.

### Simultaneous blocking of the IL-6 pathway during vaccination affects the tumor-specific T cell response

The relative reduction in tumor-infiltrating HPV-specific CD8<sup>+</sup> T cells amongst tumor infiltrating immune cells when IL-6R blocking antibody was provided may be due to a lower availability of HPV-specific T cells, their attraction or both. To gain more insight, we analyzed their availability by assessing the number of circulating HPV-specific T cells at time of regression (day 20) and recurrence (days 30). Following vaccination, the number of HPV-specific CD8<sup>+</sup> T cells in the blood ranged between 5.7-8.4% and 26.9-28.1% in TC-1 control and TC-1 IL-6 tumor bearing mice on day 20 and 30 post tumor challenge, respectively (**Figure 5A**). However, IL-6R blockade during vaccination resulted in a reduced number of circulating HPV-specific T cells in TC-1 IL-6 tumor bearing mice (**Figure 5A**).

#### ◀ Figure 3. IL-6R blocking antibody is incapable of normalizing the altered phenotype of myeloid cells induced by IL-6 produced by tumor in peptide vaccinated mice

A-D) Intratumoral analysis of TC-1 control and TC-1 IL-6 tumor-bearing mice following treatment with SLP vaccine and IL-6R blocking antibody on day 16. A) The percentage of CD8<sup>+</sup>, E7 Tm<sup>+</sup>, CD11b<sup>+</sup> cells within CD45<sup>+</sup> gate. B) The percentage of classII<sup>+</sup> cells within CD11b<sup>+</sup> cells and expression level of classII on CD11b<sup>+</sup> cells. C) The percentage of CD11c<sup>+</sup>CD11b<sup>+</sup>, CD11c<sup>+</sup>CD11b<sup>-</sup> and CD11c<sup>-</sup>CD11b<sup>+</sup> cells within CD45<sup>+</sup> cells. D) The percentage of classII<sup>+</sup>F4/80<sup>+</sup>, classII<sup>+</sup>F4/80<sup>-</sup> and classII<sup>-</sup>F4/80<sup>+</sup> cells within CD11c<sup>+</sup>CD11b<sup>+</sup> cells, classII<sup>+</sup> cells within CD11c<sup>+</sup>CD11b<sup>-</sup> and Ly6C<sup>hi</sup> and classII<sup>+</sup> within F4/80<sup>+</sup>CD11c<sup>+</sup>CD11b<sup>+</sup> cells. The data shown is representative of two independent experiments. Significance was determined by a Mann-Whitney test (\*, P < 0.05; \*\*, P < 0.01; \*\*\*, P < 0.001).

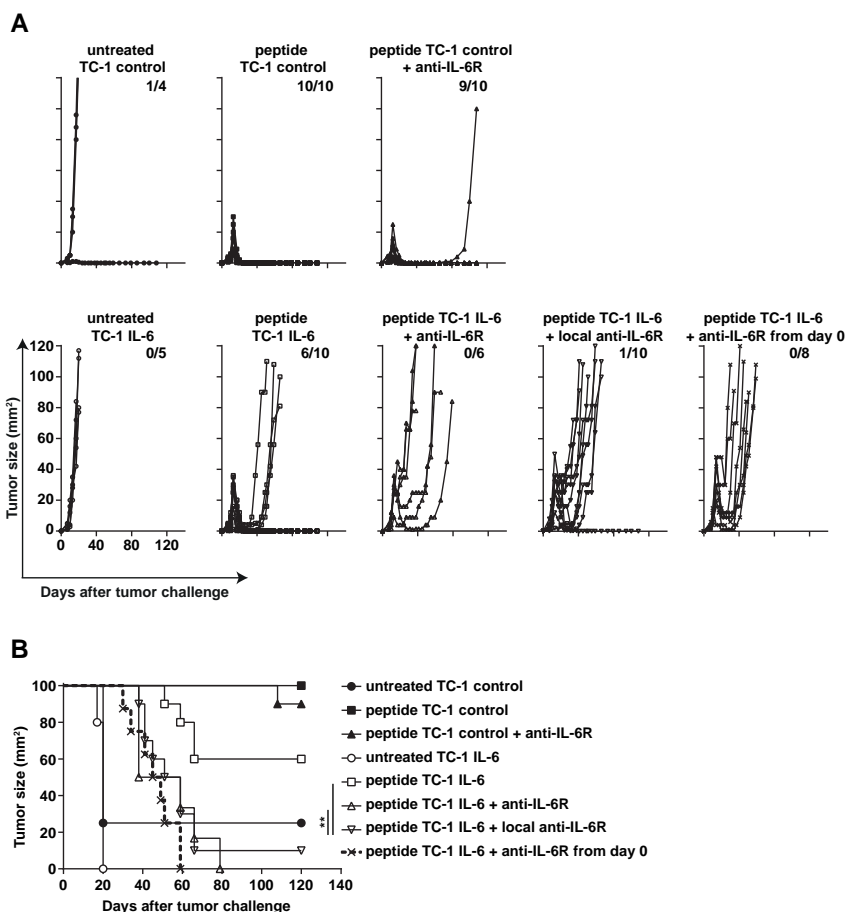


**Figure 4. IL-6 signaling is required for the vaccine-induced anti-tumor response**

A and B) Tumor growths (A) and survival (B) of TC-1 control and TC-1 IL-6 tumor-bearing mice following treatment SLP vaccine (day 8 and 22) with and without IL-6R blocking antibody (from day 8-29 or 0-29). The number of tumor-free mice from the total mice is indicated. The data is representative from two independent experiments, yielding similar results. Significance was determined by a log-rank (Mantel-Cox) test (\*,  $P < 0.05$ ; \*\*,  $P < 0.01$ ; \*\*\*,  $P < 0.001$ ).

Recent literature revealed that IL-6R blockade may not only prevent IL-6 classical- and trans- signaling but also may interfere with a recently discovered form of IL-6 signaling that is called cluster-signaling and shown to be important for priming of T cells by DC (9). To prevent this latter, we used the anti-mouse IL-6 blocking antibody as this would not interfere with cluster signaling. However, also IL-6 blockade of classical- and trans-signaling reduced the number of circulating HPV-specific CD8<sup>+</sup> T cells in tumor bearing mice (**Figure 5B**). Moreover, the TC-1 IL-6 tumors of mice receiving the combination of anti-IL-6 and vaccine showed less deep regressions and in all cases the tumor recurred (**Figure 5C**). Thus, blockade of IL-6 signaling during therapeutic vaccination not only failed to normalize the myeloid cell

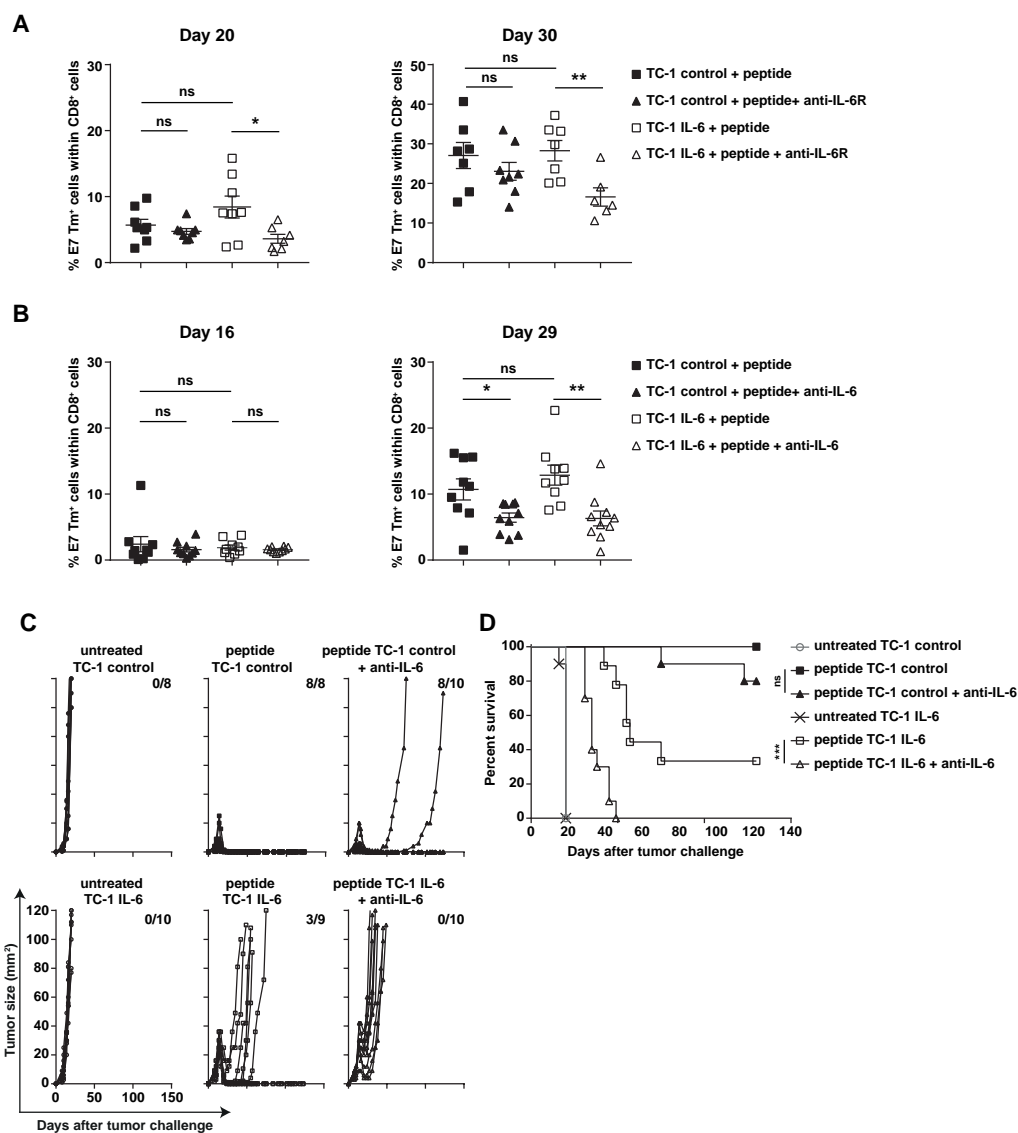


**Figure 5. IL-6 blocking antibody decrease the circulating tumor-specific CD8 T cells and reduce anti-tumor response induced by peptide vaccination**

A and B) The percentage of E7 Tm<sup>+</sup> cells within CD8<sup>+</sup> T cells in blood of TC-1 control and TC-1 IL-6 tumor-bearing mice following treatment with SLP vaccine and anti-IL-6R in (A) or anti-IL-6 in (B). C-D) Tumor outgrowths and survival of TC-1 control and TC-1 IL-6 tumor-bearing mice following treatment with SLP vaccine and IL-6 blocking antibody. The number of tumor-free mice from the total mice is indicated. Data is from one experiments. Significance was determined by a log-rank (Mantel-Cox) or Mann-Whitney test (\*,  $P < 0.05$ ; \*\*,  $P < 0.01$ ; \*\*\*,  $P < 0.001$ ).

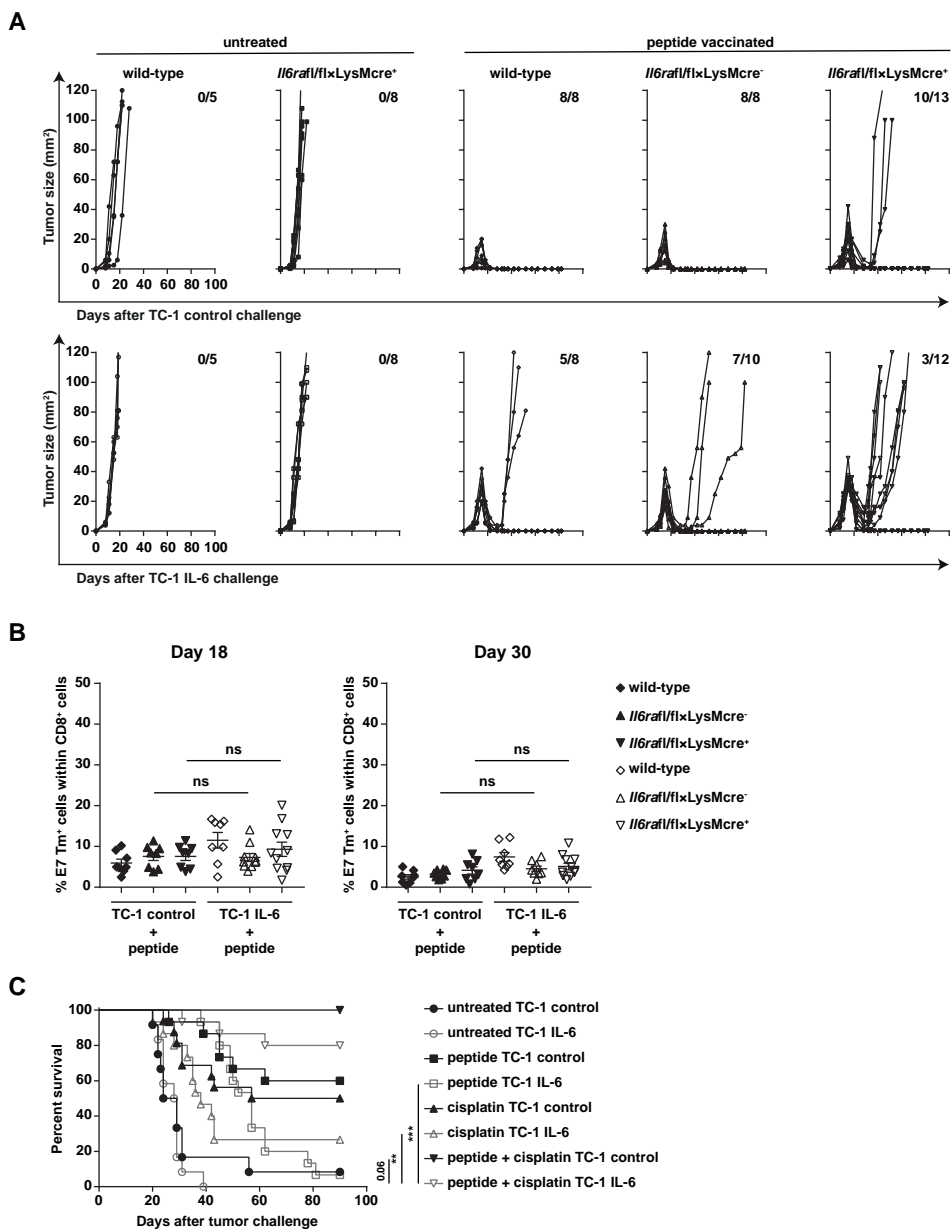


**Figure 6. IL-6 receptor on myeloid cells are required for the anti-tumor response induced by peptide vaccination**

A) Tumor outgrowths of TC-1 control and TC-1 IL-6 tumor-bearing wild-type, *Il6ra<sup>fl/fl</sup> × LysM<sup>cre</sup>-/-*, *Il6ra<sup>fl/fl</sup> × LysM<sup>cre</sup>+/-* mice following treatment with SLP vaccine. The number of tumor-free mice from the total mice is indicated. B) The percentage of E7 Tm<sup>+</sup> cells within CD8<sup>+</sup> T cells in blood of shown in (A). Data is from one experiments. C) Survival of TC-1 control and TC-1 IL-6 tumor-bearing mice following treatment with cisplatin (LD) or SLP vaccine or the combination. Data is pooled from two independent experiments. Significance was determined by a log-rank (Mantel–Cox) test or Mann–Whitney test (\*,  $P < 0.05$ ; \*\*,  $P < 0.01$ ; \*\*\*,  $P < 0.001$ ).

phenotype but also impaired the long-term vaccine-induced tumor-specific T cell response, fitting with an earlier report suggesting that IL-6 is required for T cell expansion (14).

### **IL-6 signaling in intratumoral macrophages is required for full vaccine-induced tumor regression but does not confer therapy resistance**

To dissect the specific role of the IL-6 triggered macrophages, we used *Il6ra*<sup>fl/fl</sup>×*LysM*<sup>cre+</sup> transgenic mice lacking the expression of the IL-6R on macrophages as well as the *Il6ra*<sup>fl/fl</sup>×*LysM*<sup>cre-</sup> mice as control mice. The mice were challenged with TC-1 control and TC-1 IL-6 tumor cells, vaccinated 8 days later and then followed in time. In the control mice both TC-1 control and TC-1 IL-6 tumors fully regressed (**Figure 6A**). However, the tumors in mice lacking the IL-6R on macrophages showed less deep regressions after vaccination, an observation that was most prominent in TC-1 IL-6 tumor bearing mice. Moreover, there was a rapid recurrence of tumors in these mice (**Figure 6A**). Vaccination lead to a strong circulating HPV-specific T cell response that was similar in both types of mice after vaccination (**Figure 6B**), suggesting that the observed effects of IL-6 blockade on tumor regression mainly was due to impaired IL-6 signaling in the intratumoral macrophages.

In conclusion, this experiment showed that IL-6 signaling in macrophages was required for optimal vaccine-induced tumor regression. In addition, since all tumors rapidly recurred in mice lacking the IL-6R on macrophages, the results also indicated that the effects of IL-6 on macrophages was not underlying IL-6 mediated resistance to vaccine therapy.

### **Increasing the strength of the initial tumoricidal response decreases the escape of IL-6 producing tumors**

Cumulatively, our studies suggested that a less optimal immune response of T cells and subsequent change in intratumoral myeloid cell composition in IL-6 producing tumors after therapeutic vaccination results in less deep TC-1 IL-6 tumor regression and underlies therapy resistance. Based on our previous studies showing improved vaccine efficacy through the synergistic effects of T-cell produced TNF $\alpha$  and cisplatin on tumor cell death (38, 39), we hypothesized that the use of cisplatin in combination with vaccination will result in enhanced tumor cell death and as such in more pronounced tumor regression. Indeed, while TC-1 IL-6 tumors showed resistance to each of the two therapies as single treatment, their combined use proved to be an effective treatment (**Figure 6C**). These data suggest that specifically the IL-6 producing tumor cells which remain after vaccine therapy are responsible for ultimate therapy resistance.

### **IL-6 blockade after tumor regression increases the sensitivity of TC-1 IL-6 tumors to therapeutic vaccination**

We, therefore, asked the question if IL-6 blockade at a later phase could counteract IL-6 mediated therapy resistance. Mice were challenged with TC-1 IL-6 tumor cells, divided in





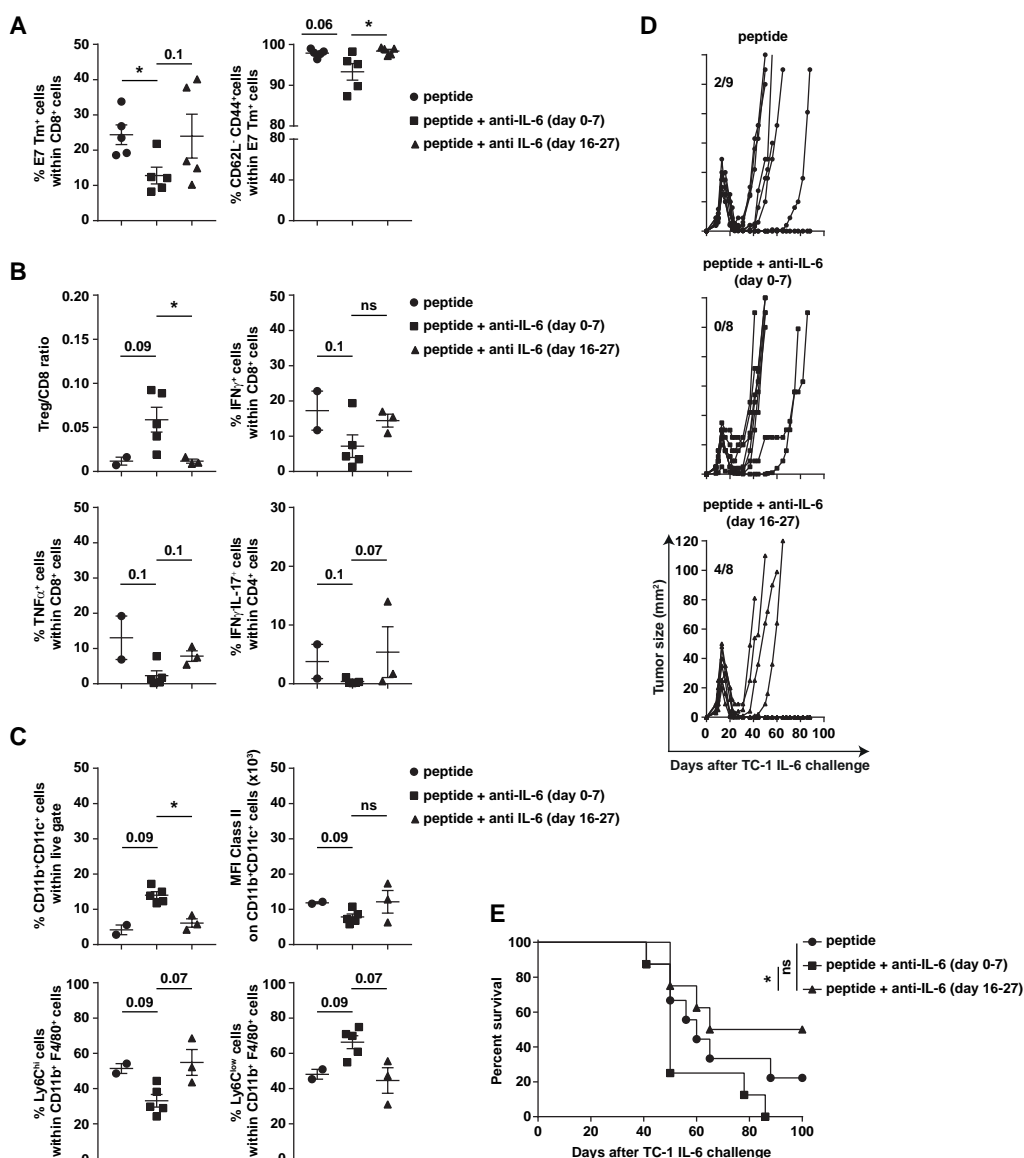


**Figure 7. IL-6 blockade after tumor regression increases the sensitivity of TC-1 IL-6 tumors to therapeutic vaccination**

Mice were injected with TC-1 IL-6 tumor cells and vaccinated with SLP vaccine on day 8. One group of mice received anti-IL-6 from day 0-7 (peptide + anti-IL-6 day 0-7). The other group received anti-IL-6 from day 16-27 (peptide + anti-IL-6 day 16-27). A) The percentage of E7 Tm<sup>+</sup> and CD62L<sup>+</sup>CD44<sup>+</sup> cells within CD8<sup>+</sup> and E7 Tm<sup>+</sup> T cells, respectively in blood on day 16. B) The ratio of Treg/CD8, the percentage of IFN $\gamma$ <sup>+</sup>, TNF $\alpha$ <sup>+</sup> cells within CD8<sup>+</sup> T cells and the percentage of IFN $\gamma$ /IL-17<sup>+</sup> cells within CD4<sup>+</sup> cells in tumor. C) The intratumoral percentage of CD11b<sup>+</sup>CD11c<sup>+</sup> within live gate, MFI of MHC II on CD11b<sup>+</sup>CD11c<sup>+</sup> cells, Ly6C<sup>hi</sup> and Ly6C<sup>low</sup> cells with CD11b<sup>+</sup>F4/80<sup>+</sup> cells. D-E) Tumor outgrowths (D) and survival (E) of TC-1 IL-6 tumor bearing mice treated with only peptide or in combination with anti-IL-6 from day 0-7 or 16-27. The number of tumor-free mice from the total mice is indicated. Data shown is from one experiment. Significance was determined by a log-rank (Mantel-Cox) or Mann-Whitney test (\*,  $P < 0.05$ ; \*\*,  $P < 0.01$ ; \*\*\*,  $P < 0.001$ ).

three groups which were vaccinated at day 8 and either received anti-IL6 antibody from the start until vaccination (days 0-7), after initial tumor regression (days 16-27) or not at all. Early IL-6 blockade was associated with a decreased number of circulating total and activated HPV-specific CD8<sup>+</sup> T cells (**Figure 7A**) as well as a lower percentage of tumor infiltrating IFN $\gamma$  and/or TNF $\alpha$  producing CD8<sup>+</sup> T cells, and IFN $\gamma$ IL-17<sup>+</sup> producing CD4<sup>+</sup> T cells, as well as a higher Treg/CD8 T cell ratio when compared to late IL-6 blockade (**Figure 7B**). A profile which is phenocopied in the spleen (**Supplementary Figure 7**). In addition, early blockade results in stronger tumor- infiltration with CD11b<sup>+</sup>CD11c<sup>+</sup> cells expressing lower levels of MHC class II as well as more Ly6C<sup>low</sup> F4/80<sup>+</sup> and less Ly6C<sup>hi</sup> F4/80<sup>+</sup> macrophages when compared to late IL-6 blockade (**Figure 7C**).

In contrast to TC-1 IL-6 bearing mice with early IL-6 blockade, showing less deep tumor regressions and fast tumor recurrences, late IL-6 blockade allowed the immune system to induce full tumor regression and an improved overall survival not only compared to mice receiving early IL-6 blockade but also when compared to mice receiving vaccination only (**Figure 7D and E**). Thus, IL-6 blockade after full deployment of the vaccine-induced immune response and initial tumor regression improves the efficacy of immunotherapy in IL-6 producing tumors.

## Discussion

In this study, we have shown that IL-6 produced by tumor cells induces resistance to immunotherapy and chemotherapy in an HPV-induced tumor model. TC-1 tumor cells were engineered to express normal or high levels of IL-6, as can be found in certain disease settings (11), with the purpose to study the impact of tumor-produced IL-6 at the extreme ends of what can be found in the human setting and how to modulate this to reinstall effective tumor immunity. In the past, the tumor-intrinsic effects of IL-6 to stimulate tumor cell proliferation and survival pathways were suggested to mediate therapy resistance but in our tumor model we did not observe any difference in growth rate between these two cell lines *in vitro* or *in vivo*. Injection of the same numbers of TC-1 control or TC-1 IL-6 cells into naïve mice resulted in comparable tumor outgrowth curves and all the mice succumbed at day 30 after tumor challenge. Although it has been shown that both exogenous and endogenous IL-6 induce resistance to cisplatin and paclitaxel even in non-IL-6 expressing tumor cells by decreasing proteolytic activation of caspase-3 and increase expression of multidrug resistance-related genes and apoptotic inhibitory proteins (40), there was no difference in cisplatin sensitivity between TC-1 control and TC-1 IL-6 tumor cells. Moreover, both cell lines displayed a comparable sensitivity, at several effector-to-target ratio's, to the killing activity of E7-specific CD8 T cells present in the splenocytes of vaccinated mice. Furthermore, both TC-1 and TC-1 IL-6 tumors regressed following peptide vaccine and cisplatin treatment although

IL-6 producing tumors recurred quickly. Thus, despite the gross difference in IL-6 production of the two cell lines, there were no differences in IL-6 instigated properties that would explain the difference in clinical response when treated with therapeutic vaccination or cisplatin chemotherapy.

In depth analyses of systemic and local immunity revealed that tumor-produced IL-6 in particular affected the composition and phenotype of myeloid cells. There were no gross alterations in T cells except for the observation that spontaneously tumor-infiltrating CD4<sup>+</sup> SLECs were lower in TC-1 IL-6 tumors, corresponding with an earlier report that CD4<sup>+</sup> effector T cell differentiation is somewhat hampered by IL-6 in the tumor microenvironment (41). The percentage of myeloid cells, including the Ly6C<sup>+</sup> inflammatory cells, was slightly increased in TC-1 IL-6 which potentially is due to IL-6 mediated increased proliferation of these cells (16). However, the numbers of CD11b<sup>+</sup>CD11c<sup>+</sup> cells (DC) were decreased in TC-1 IL-6. There was no difference in Ly6G<sup>+</sup> MDSCs. The most important observation, however, was the strong decrease in the percentage of MHC class II<sup>+</sup> cells as well as the expression levels of MHC class II on the remaining positive cells among macrophages, DCs and Ly6C<sup>+</sup> inflammatory cells in TC-1 IL-6 tumors. This fits with earlier data showing that the IL-6-STAT3 pathway reduces intracellular MHC II  $\alpha\beta$ -dimers through enhanced cathepsin S activity (42). The IL-6 associated reduced influx with CD11b<sup>+</sup>CD11c<sup>+</sup> MHC class II<sup>low</sup> DCs is likely to explain why IL-6 producing tumors are refractory to cisplatin treatment, as it was shown earlier that cisplatin-induced cure of TC-1 tumor-bearing mice required the influx of both tumor-specific CD8<sup>+</sup> T cells and phagocytic Ly6C<sup>hi</sup> CD11c<sup>hi</sup> DCs (38), similar to what was observed after anthracycline chemotherapy (43).

While therapeutic vaccination led to a strong influx of both TC-1 and TC-1 IL-6 tumors with IFN $\gamma$ -producing tumor-specific T cells, the levels of MHC class II on the different types of antigen presenting cells and the numbers of MHC class II<sup>+</sup> myeloid cells remained lower in TC-1 IL-6 tumors. To overcome the negative effects of IL-6 on systemic and local immunity, we blocked the IL-6R as this would interfere with both classical- and trans-signaling by IL-6. Administration of IL-6R blocking antibodies at the time of therapy, before start of therapy or peritumorally resulted in an almost complete correction of the systemic myeloid cell alterations but could only partly restore the effects of IL-6 on the tumor-infiltrating myeloid cells. Importantly, IL-6 signaling blockade had a negative effect on treatment outcome, which was most pronounced in TC-1 IL-6. The tumors became more refractory to treatment, reflected by less deep regressions and quicker recurrences. Similar observations were made when IL-6 blocking antibodies were used. The regression phase of TC-1 tumors requires the influx of tumor-specific CD8<sup>+</sup> T cells but depends on the presence of macrophages attracted by these intratumoral T cells (37). Blockade of IL-6 signaling was shown to reduce the number of tumor-specific T cells after vaccination, partly explaining why blockade of IL-6

signaling could not restore the myeloid cell composition in tumors. Importantly, therapeutic vaccination mediated regression of tumors was also impaired in mice of which macrophages lacked the expression of the IL-6R, indicating that IL-6 signaling in macrophages was also required for optimal tumor regression. Recently, simultaneous IL-6R blockade was also shown to reduce the efficacy of oncolytic virus-based immunotherapy of B16 melanoma, and this also coincided with a reduced tumor-infiltration by CD8<sup>+</sup> T cells (44). The overexpression of IL-6 by tumor cells resulted in minor effects on therapy-mediated tumor regression but specifically impacted the recurrence of the IL-6 producing tumors. Therefore, IL-6 blockade was performed after initial regression with the aim to prevent recurrences. When compared to no blockade or to IL-6 blockade early during therapy, TC-1 IL-6 tumors still fully regressed and less of them recurred showing that late IL-6 blockade is more effective and suggesting that the higher doses of IL-6 produced by TC-1 IL-6 tumor cells played a major role in the secondary escape of the tumors. In another study, IL-6 blockade was performed relatively late at 13 days after the first vaccine dose, but still before the third and last dose of vaccine, and resulted in a delayed tumor outgrowth, albeit that no regressions or cure was observed (45).

The fact that all TC-1 IL-6 tumors recurred in mice of which the macrophages lacked the expression of the IL-6R indicates that therapy resistance of TC-1 IL-6 tumors was not mediated by IL-6 converted macrophages. We and others observed a suppressive effect of IL-6 on CD4<sup>+</sup> effector T cells (46, 47) which in fact may reflect the suppressive effect of IL-6 on MHC class II, co-stimulatory molecules and IL-12 production (48) by professional APC, resulting in dysfunctional DCs. The absence of functional DC in tumors may lead to T cell exclusion (49) and, therefore, escape of the recurrent tumors. Clearly IL-6 reduced the number of functional DCs already in the primary IL-6 producing tumors, and we recently showed that TC-1 recurrence after therapeutic vaccination is related to CD8 T cell exclusion in the relapsed tumors (Beyranvand Nejad E et al., chapter 3). Since these DCs also play an important role in cisplatin chemotherapy, it is highly likely that part of the IL-6 induced therapy resistance is due to its effect on the number and functional capacity of intratumoral DCs. An alternative or additional mechanisms which may play a role and would explain why late IL-6 blockade works, is the reduction in cancer-associate fibroblasts (46), which in escaped TC-1 tumors express TFG $\beta$  and are associated with T cell exclusion (Beyranvand Nejad E et al., chapter 3).

Finally, our data extend prior observations on some unexpected outcomes of IL-6 blockade for the treatment of cancer and reveal the underlying mechanisms. The pleiotropic effects of IL-6 on different immune cells makes it important to understand where in the cancer immune cycle, and under which conditions, IL-6 blockade is detrimental or effective. Inappropriate timing, for instance during the expansion phase of tumor-specific T cells or the effector

phase of tumoricidal macrophages, may have negative consequences, while at later stages when tumor-immunity is fully developed and the tumor-promoting effects of IL-6 are more dominant, its blockade can be beneficial.

## References

1. Galon J, Bruni D. Approaches to treat immune hot, altered and cold tumours with combination immunotherapies. *Nat Rev Drug Discov*. 2019.
2. Hui L, Chen Y. Tumor microenvironment: Sanctuary of the devil. *Cancer Lett*. 2015;368(1):7-13.
3. van der Burg SH, Arens R, Ossendorp F, van Hall T, Melief CJ. Vaccines for established cancer: overcoming the challenges posed by immune evasion. *Nat Rev Cancer*. 2016;16(4):219-33.
4. Driessens G, Kline J, Gajewski TF. Costimulatory and coinhibitory receptors in anti-tumor immunity. *Immunol Rev*. 2009;229(1):126-44.
5. Chow MT, Luster AD. Chemokines in cancer. *Cancer Immunol Res*. 2014;2(12):1125-31.
6. Dranoff G. Cytokines in cancer pathogenesis and cancer therapy. *Nat Rev Cancer*. 2004;4(1):11-22.
7. Wolf J, Rose-John S, Garbers C. Interleukin-6 and its receptors: a highly regulated and dynamic system. *Cytokine*. 2014;70(1):11-20.
8. Jones SA, Jenkins BJ. Recent insights into targeting the IL-6 cytokine family in inflammatory diseases and cancer. *Nat Rev Immunol*. 2018;18(12):773-89.
9. Heink S, Yogev N, Garbers C, Herwerth M, Aly L, Gasperi C, et al. Trans-presentation of IL-6 by dendritic cells is required for the priming of pathogenic TH17 cells. *Nat Immunol*. 2017;18(1):74-85.
10. Kishimoto T, Akira S, Narazaki M, Taga T. Interleukin-6 family of cytokines and gp130. *Blood*. 1995;86(4):1243-54.
11. Waage A, Brandtzaeg P, Halstensen A, Kierulf P, Espevik T. The complex pattern of cytokines in serum from patients with meningococcal septic shock. Association between interleukin 6, interleukin 1, and fatal outcome. *J Exp Med*. 1989;169(1):333-8.
12. Lippitz BE. Cytokine patterns in patients with cancer: a systematic review. *Lancet Oncol*. 2013;14(6):e218-28.
13. Tsukamoto H, Fujieda K, Senju S, Ikeda T, Oshiumi H, Nishimura Y. Immune-suppressive effects of interleukin-6 on T-cell-mediated anti-tumor immunity. *Cancer Sci*. 2018;109(3):523-30.
14. Castellino F, Germain RN. Chemokine-guided CD4<sup>+</sup> T cell help enhances generation of IL-6RalphahighIL-7Ralphahigh prememory CD8<sup>+</sup> T cells. *J Immunol*. 2007;178(2):778-87.
15. Hunter CA, Jones SA. IL-6 as a keystone cytokine in health and disease. *Nat Immunol*. 2015;16(5):448-57.
16. Dixit A, Bottek J, Beerlage AL, Schuettpelz J, Thiebes S, Brenzel A, et al. Frontline Science: Proliferation of Ly6C(+) monocytes during urinary tract infections is regulated by IL-6 trans-signaling. *J Leukoc Biol*. 2018;103(1):13-22.
17. Bataille R, Barlogie B, Lu ZY, Rossi JF, Lavabre-Bertrand T, Beck T, et al. Biologic effects of anti-interleukin-6 murine monoclonal antibody in advanced multiple myeloma. *Blood*. 1995;86(2):685-91.
18. Vink A, Coulie P, Warnier G, Renauld JC, Stevens M, Donckers D, et al. Mouse plasmacytoma growth in vivo: enhancement by interleukin 6 (IL-6) and inhibition by antibodies directed against IL-6 or its receptor. *J Exp Med*. 1990;172(3):997-1000.
19. Stern PL, van der Burg SH, Hampson IN, Broker TR, Fiander A, Lacey CJ, et al. Therapy of human papillomavirus-related disease. *Vaccine*. 2012;30 Suppl 5:F71-82.
20. Kotowicz B, Fuksiewicz M, Kowalska M, Jonska-Gmyrek J, Bidzinski M, Kaminska J. The value of tumor marker and cytokine analysis for the assessment of regional lymph node status in cervical cancer patients. *Int J Gynecol Cancer*. 2008;18(6):1279-84.
21. St John MA, Li Y, Zhou X, Denny P, Ho CM, Montemagno C, et al. Interleukin 6 and interleukin 8 as potential biomarkers for oral cavity and oropharyngeal squamous cell carcinoma. *Arch Otolaryngol Head Neck Surg*. 2004;130(8):929-35.



22. Tjong MY, van der Vange N, ten Kate FJ, Tjong AHSP, ter Schegget J, Burger MP, et al. Increased IL-6 and IL-8 levels in cervicovaginal secretions of patients with cervical cancer. *Gynecol Oncol.* 1999;73(2):285-91.
23. Srivani R, Nagarajan B. A prognostic insight on in vivo expression of interleukin-6 in uterine cervical cancer. *Int J Gynecol Cancer.* 2003;13(3):331-9.
24. Jinno T, Kawano S, Maruse Y, Matsubara R, Goto Y, Sakamoto T, et al. Increased expression of interleukin-6 predicts poor response to chemoradiotherapy and unfavorable prognosis in oral squamous cell carcinoma. *Oncol Rep.* 2015;33(5):2161-8.
25. Dijkgraaf EM, Heusinkveld M, Tummers B, Vogelpoel LT, Goedemans R, Jha V, et al. Chemotherapy alters monocyte differentiation to favor generation of cancer-supporting M2 macrophages in the tumor microenvironment. *Cancer Res.* 2013;73(8):2480-92.
26. Hess S, Smola H, Sandaradura De Silva U, Hadaschik D, Kube D, Baldus SE, et al. Loss of IL-6 receptor expression in cervical carcinoma cells inhibits autocrine IL-6 stimulation: abrogation of constitutive monocyte chemoattractant protein-1 production. *J Immunol.* 2000;165(4):1939-48.
27. Heusinkveld M, de Vos van Steenwijk PJ, Goedemans R, Ramwadhoebe TH, Gorter A, Welters MJ, et al. M2 macrophages induced by prostaglandin E2 and IL-6 from cervical carcinoma are switched to activated M1 macrophages by CD4+ Th1 cells. *J Immunol.* 2011;187(3):1157-65.
28. Pahne-Zeppenfeld J, Schroer N, Walch-Ruckheim B, Oldak M, Gorter A, Hegde S, et al. Cervical cancer cell-derived interleukin-6 impairs CCR7-dependent migration of MMP-9-expressing dendritic cells. *Int J Cancer.* 2014;134(9):2061-73.
29. Walch-Ruckheim B, Stroder R, Theobald L, Pahne-Zeppenfeld J, Hegde S, Kim YJ, et al. Cervical cancer-instructed stromal fibroblasts enhance IL-23 expression in dendritic cells to support expansion of Th17 cells. *Cancer Res.* 2019.
30. Clausen BE, Burkhardt C, Reith W, Renkawitz R, Forster I. Conditional gene targeting in macrophages and granulocytes using LysMcre mice. *Transgenic Res.* 1999;8(4):265-77.
31. Sommer J, Engelowski E, Baran P, Garbers C, Floss DM, Scheller J. Interleukin-6, but not the interleukin-6 receptor plays a role in recovery from dextran sodium sulfate-induced colitis. *Int J Mol Med.* 2014;34(3):651-60.
32. Lin KY, Guarnieri FG, Staveley-O'Carroll KF, Levitsky HI, August JT, Pardoll DM, et al. Treatment of established tumors with a novel vaccine that enhances major histocompatibility class II presentation of tumor antigen. *Cancer Res.* 1996;56(1):21-6.
33. van Duikeren S, Fransen MF, Redeker A, Wieles B, Platenburg G, Krebber WJ, et al. Vaccine-induced effector-memory CD8+ T cell responses predict therapeutic efficacy against tumors. *J Immunol.* 2012;189(7):3397-403.
34. Bollrath J, Phesse TJ, von Burstin VA, Putoczki T, Bennecke M, Bateman T, et al. gp130-mediated Stat3 activation in enterocytes regulates cell survival and cell-cycle progression during colitis-associated tumorigenesis. *Cancer Cell.* 2009;15(2):91-102.
35. Grivennikov S, Karin E, Terzic J, Mucida D, Yu GY, Vallabhapurapu S, et al. IL-6 and Stat3 are required for survival of intestinal epithelial cells and development of colitis-associated cancer. *Cancer Cell.* 2009;15(2):103-13.
36. Welters MJ, van der Sluis TC, van Meir H, Loof NM, van Ham VJ, van Duikeren S, et al. Vaccination during myeloid cell depletion by cancer chemotherapy fosters robust T cell responses. *Sci Transl Med.* 2016;8(334):334ra52.
37. van der Sluis TC, Sluijter M, van Duikeren S, West BL, Melief CJ, Arens R, et al. Therapeutic Peptide Vaccine-Induced CD8 T Cells Strongly Modulate Intratumoral Macrophages Required for Tumor Regression. *Cancer Immunol Res.* 2015;3(9):1042-51.
38. Beyranvand Nejad E, van der Sluis TC, van Duikeren S, Yagita H, Janssen GM, van Veelen PA, et al. Tumor Eradication by Cisplatin Is Sustained by CD80/86-Mediated Costimulation of CD8+ T Cells. *Cancer Res.* 2016;76(20):6017-29.

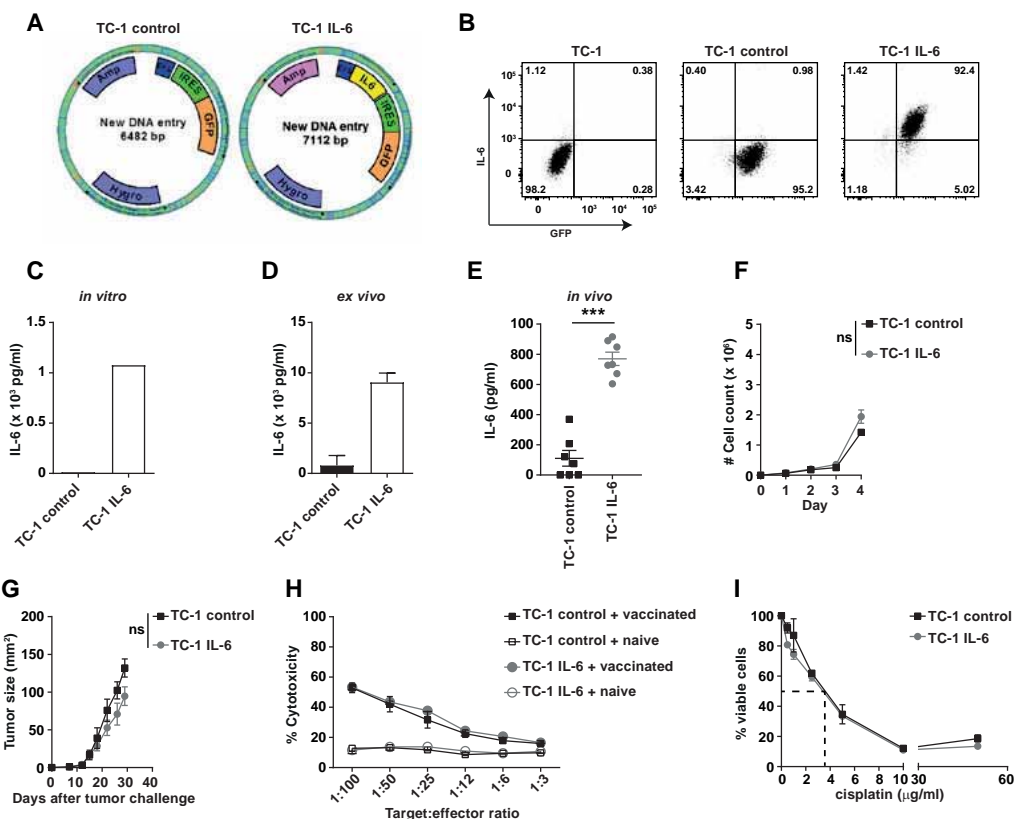




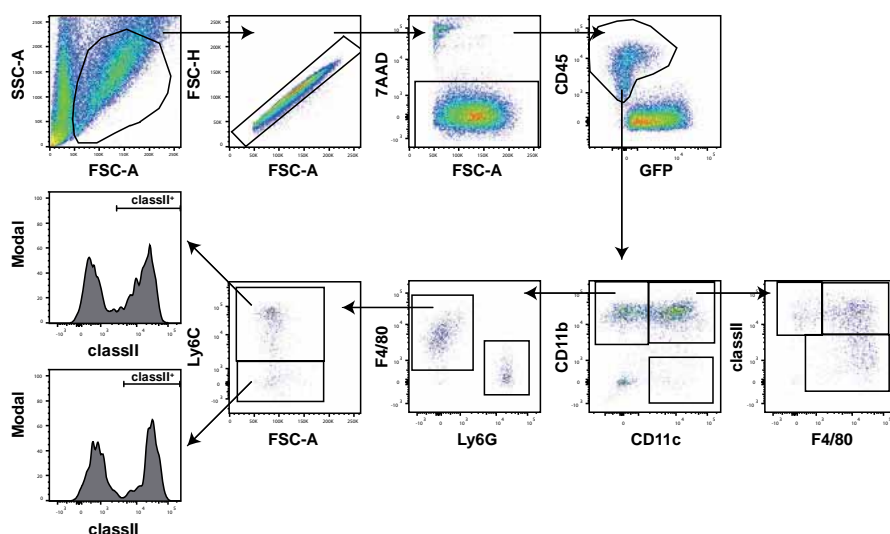
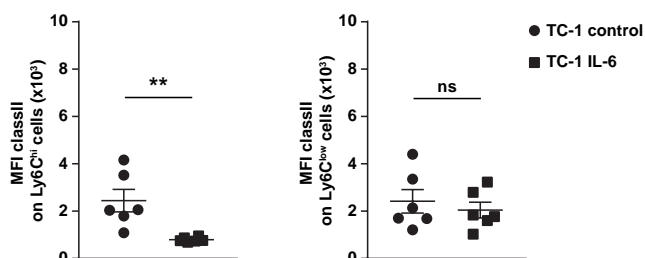
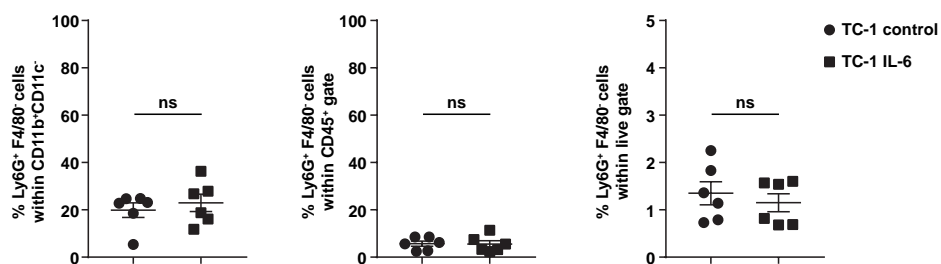
39. van der Sluis TC, van Duikeren S, Huppelschoten S, Jordanova ES, Beyranvand Nejad E, Sloots A, et al. Vaccine-induced tumor necrosis factor-producing T cells synergize with cisplatin to promote tumor cell death. *Clin Cancer Res.* 2015;21(4):781-94.
40. Wang Y, Niu XL, Qu Y, Wu J, Zhu YQ, Sun WJ, et al. Autocrine production of interleukin-6 confers cisplatin and paclitaxel resistance in ovarian cancer cells. *Cancer Lett.* 2010;295(1):110-23.
41. Tsukamoto H, Nishikata R, Senju S, Nishimura Y. Myeloid-derived suppressor cells attenuate TH1 development through IL-6 production to promote tumor progression. *Cancer Immunol Res.* 2013;1(1):64-76.
42. Kitamura H, Kamon H, Sawa S, Park SJ, Katunuma N, Ishihara K, et al. IL-6-STAT3 controls intracellular MHC class II alphabeta dimer level through cathepsin S activity in dendritic cells. *Immunity.* 2005;23(5):491-502.
43. Ma Y, Adjemian S, Mattarollo SR, Yamazaki T, Aymeric L, Yang H, et al. Anticancer chemotherapy-induced intratumoral recruitment and differentiation of antigen-presenting cells. *Immunity.* 2013;38(4):729-41.
44. Eriksson E, Milenova I, Wenthe J, Moreno R, Alemany R, Loskog A. IL-6 Signaling Blockade during CD40-Mediated Immune Activation Favors Antitumor Factors by Reducing TGF-beta, Collagen Type I, and PD-L1/PD-1. *J Immunol.* 2019;202(3):787-98.
45. Bialkowski L, Van der Jeught K, Bevers S, Tjok Joe P, Renmans D, Heirman C, et al. Immune checkpoint blockade combined with IL-6 and TGF-beta inhibition improves the therapeutic outcome of mRNA-based immunotherapy. *Int J Cancer.* 2018;143(3):686-98.
46. Mace TA, Shakya R, Pitarresi JR, Swanson B, McQuinn CW, Loftus S, et al. IL-6 and PD-L1 antibody blockade combination therapy reduces tumour progression in murine models of pancreatic cancer. *Gut.* 2018;67(2):320-32.
47. Tsukamoto H, Fujieda K, Miyashita A, Fukushima S, Ikeda T, Kubo Y, et al. Combined Blockade of IL6 and PD-1/PD-L1 Signaling Abrogates Mutual Regulation of Their Immunosuppressive Effects in the Tumor Microenvironment. *Cancer Res.* 2018;78(17):5011-22.
48. Ohno Y, Kitamura H, Takahashi N, Ohtake J, Kaneumi S, Sumida K, et al. IL-6 down-regulates HLA class II expression and IL-12 production of human dendritic cells to impair activation of antigen-specific CD4(+) T cells. *Cancer Immunol Immunother.* 2016;65(2):193-204.
49. Spranger S, Dai D, Horton B, Gajewski TF. Tumor-Residing Batf3 Dendritic Cells Are Required for Effector T Cell Trafficking and Adoptive T Cell Therapy. *Cancer Cell.* 2017;31(5):711-23 e4.



# Supplementary figures

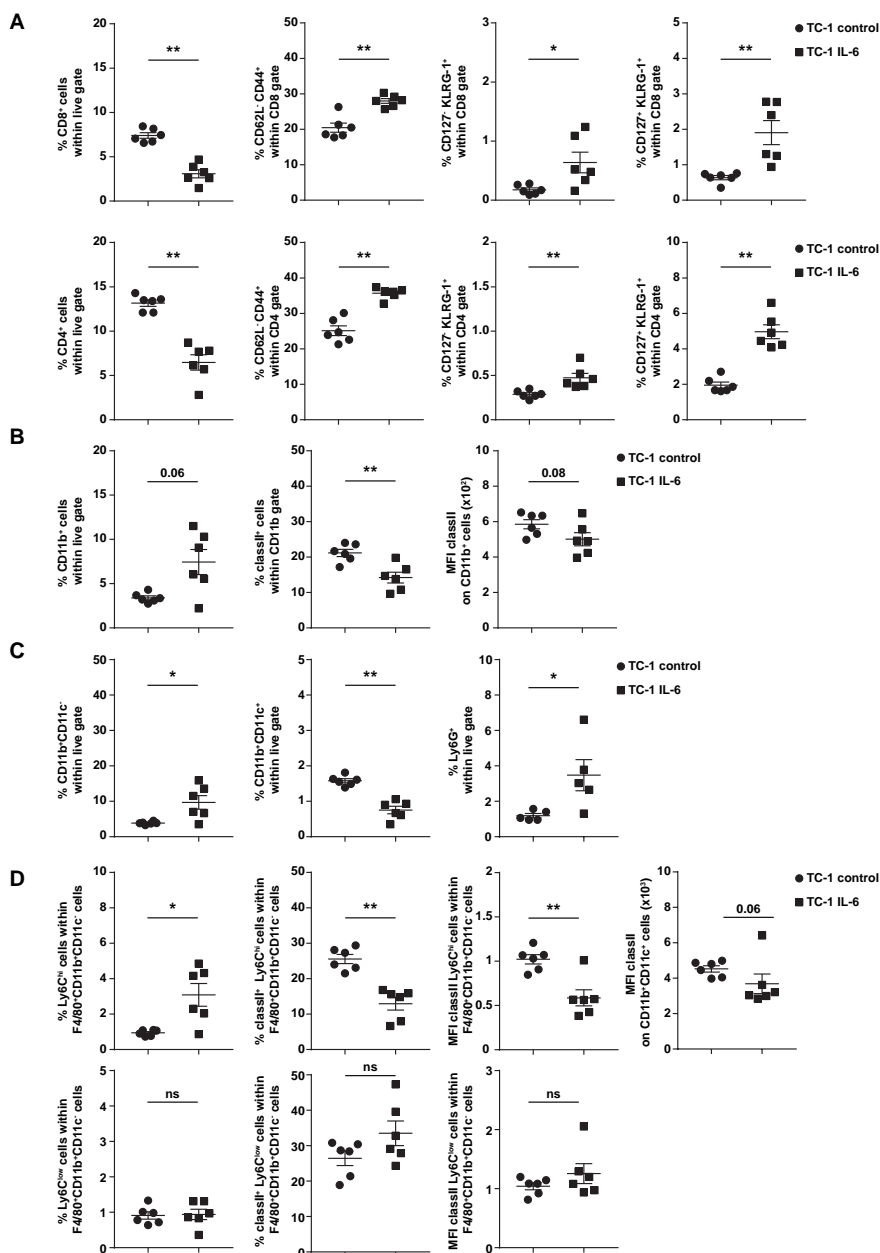


**Supplementary figure 1. TC-1 control and TC-1 IL-6 constructs, IL-6 production and growth rate**  
A) Schematic figure of pcDNA3.1 vector that used for TC-1 transfection as described in the materials and methods. This vectors express only GFP (TC-1 control) or GFP and IL-6 under EFS promoter (TC-1 IL-6). B) representative FACS plots of GFP and IL-6 production in TC-1 control and TC-1 IL-6 tumor as measured by intracellular staining. C-E) IL-6 measurement in the supernatant of TC-1 control and TC-1 IL-6 cultured *in vitro* cell lines (C), Supernatant of TC-1 control and TC-1 IL-6 tumor microenvironment isolated from TC-1 control and TC-1 IL-6 tumor bearing mice (D) and serum of the TC-1 control and TC-1 IL-6 tumor bearing mice at different time points after tumor inoculation. F) Cell count of cultured TC-1 control and TC-1 IL-6 tumor cells at the initial time point and 1, 2, 3 and 4 days after culturing. G) Tumor outgrowth of TC-1 control and TC-1 IL-6 tumor bearing mice. H) The percentage of TC-1 control and TC-1 IL-6 tumor cells (target cells) killed by splenocytes isolated from SLP vaccinated or naïve mice as control (effector cells) at different ratios as measured by CTL assay as described in materials and methods. I) the percentage of viable TC-1 control and IL-6 tumor cells in the presence of the different concentrations of cisplatin as measured by MTT assay.

**A****B****C**

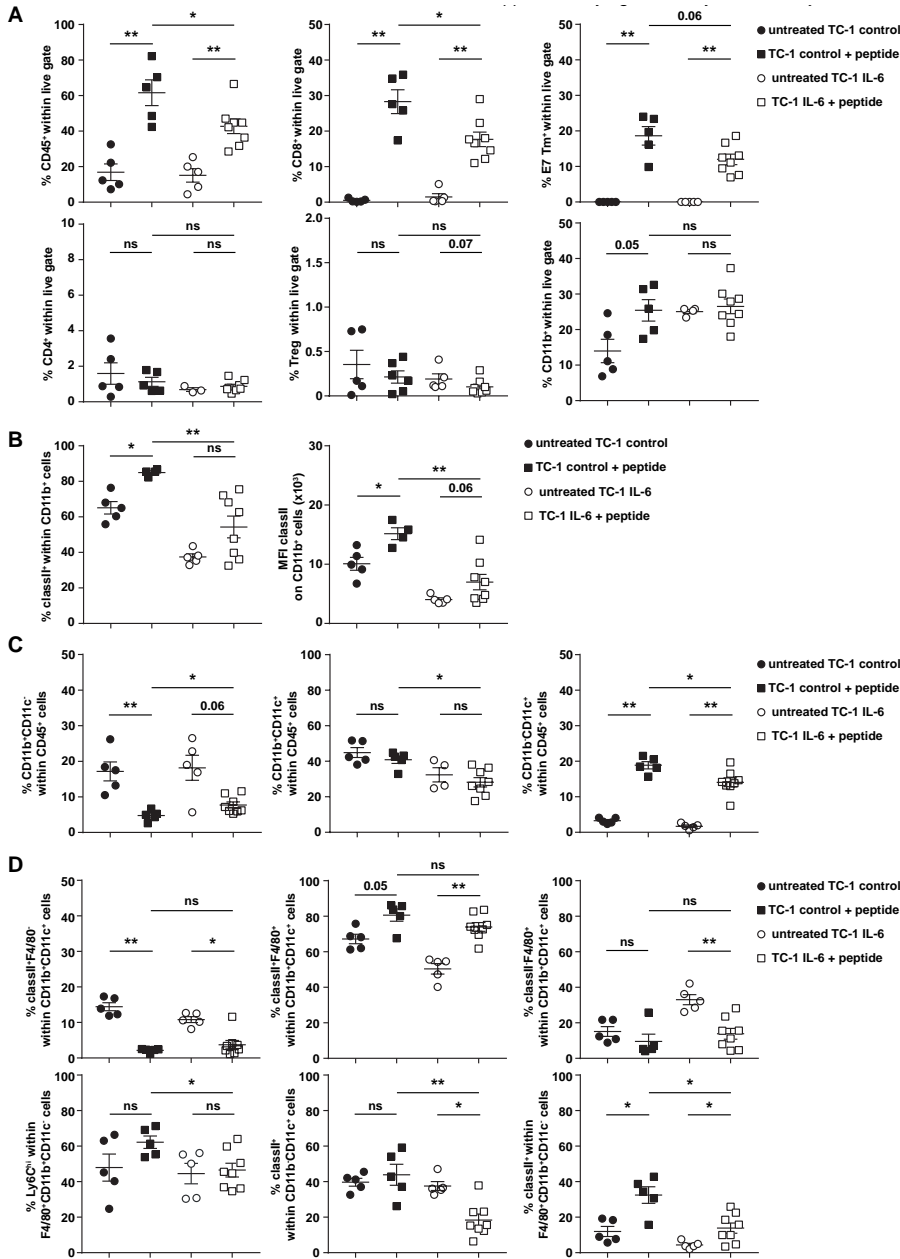
**Supplementary figure 2. IL-6 produced by tumor cells does not affect the percentage of intratumoral granulocytes**

A) Shown is the intratumoral myeloid gating strategy in untreated tumor-bearing mice. B) MFI of classII on intratumoral Ly6C<sup>hi</sup> and Ly6C<sup>low</sup> F4/80<sup>+</sup>CD11b<sup>+</sup>CD11c<sup>-</sup> myeloid cells. C) The percentage of the Ly6G<sup>+</sup>F4/80<sup>+</sup> cells within CD11b<sup>+</sup>CD11c<sup>-</sup>, CD45 and live gate.



**Supplementary figure 3. IL-6 produced by tumor cells induce immature myeloid cells in the spleen**

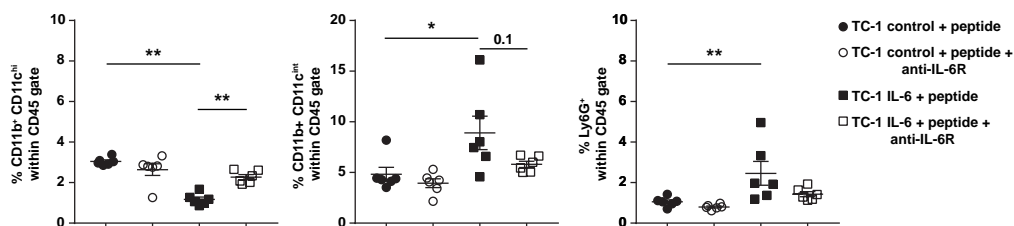
A) The percentage of CD8<sup>+</sup>, CD4<sup>+</sup>, CD62L<sup>+</sup>CD44<sup>+</sup>, CD127<sup>+</sup>KLRG-1<sup>+</sup> and CD127<sup>+</sup>KLRG-1<sup>+</sup> CD8<sup>+</sup> and CD4<sup>+</sup> T cells in spleen. B) The percentage of CD11b<sup>+</sup>, classII<sup>+</sup> cells and MFI of classII within CD11b<sup>+</sup> cells in spleen. C) The percentage of CD11b<sup>+</sup>CD11c<sup>+</sup>, CD11b<sup>+</sup>CD11c<sup>+</sup> and Ly6G<sup>+</sup> myeloid cells within live gate in spleen. D) The percentage of Ly6C<sup>hi</sup>, classII<sup>+</sup>Ly6C<sup>hi</sup>, MFI of classII on Ly6C<sup>hi</sup> F4/80<sup>+</sup>CD11b<sup>+</sup>CD11c<sup>+</sup> and the expression level of classII on CD11b<sup>+</sup>CD11c<sup>+</sup> (upper panel) and the percentage of Ly6C<sup>low</sup> and classII<sup>+</sup>Ly6C<sup>low</sup> within F4/80<sup>+</sup>CD11b<sup>+</sup>CD11c<sup>+</sup> cells and MFI of classII on Ly6C<sup>low</sup>F4/80<sup>+</sup>CD11b<sup>+</sup>CD11c<sup>+</sup> cells in spleen. Each dot represents data from an individual mouse. Graphs indicate mean values with SEM. Significance was determined by Mann-Whitney test. \*, P < 0.05; \*\*, P < 0.01; \*\*\*, P < 0.001. Experiments were performed twice with similar outcomes.



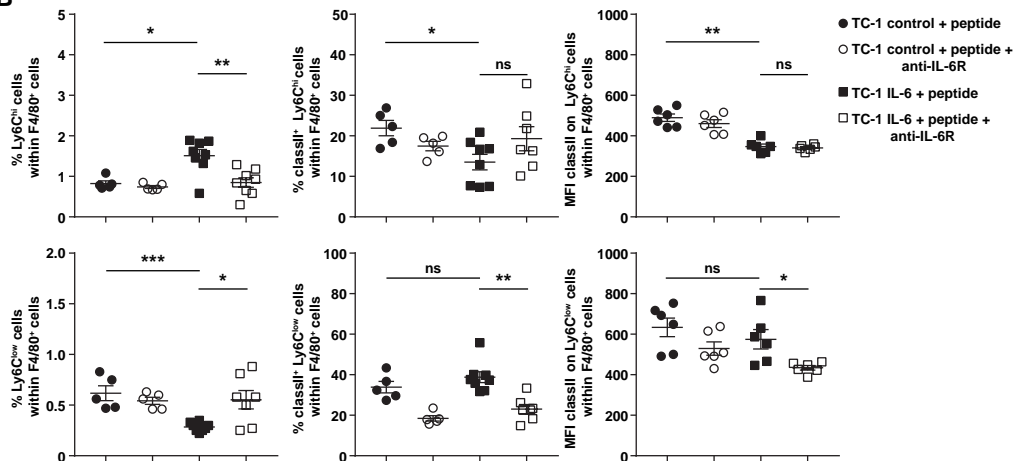
**Supplementary figure 4. Peptide vaccination affect the composition of intratumoral immune cells differently in IL-6 producing tumor**

A-D) Intratumoral analysis of TC-1 control and TC-1 IL-6 tumor-bearing mice following treatment with SLP vaccine on day 16. A) The percentage of CD45<sup>+</sup>, CD8<sup>+</sup>, E7 Tm<sup>+</sup>, CD4<sup>+</sup>, Treg and CD11b<sup>+</sup> cells within live gate. B) The percentage of classII<sup>+</sup> cells within CD11b<sup>+</sup> cells and expression level of classII on CD11b<sup>+</sup> cells. C) The percentage of CD11c<sup>+</sup>CD11b<sup>+</sup>, CD11c<sup>+</sup>CD11b<sup>-</sup> and CD11c<sup>+</sup>CD11b<sup>+</sup> cells within CD45<sup>+</sup> cells. D) The percentage of classII<sup>+</sup>F4/80<sup>+</sup>, classII<sup>+</sup>F4/80<sup>-</sup> and classII<sup>+</sup>F4/80<sup>+</sup> cells within CD11c<sup>+</sup>CD11b<sup>+</sup> cells, classII<sup>+</sup> cells within CD11c<sup>+</sup>CD11b<sup>-</sup> and Ly6C<sup>hi</sup> and classII<sup>+</sup> within F4/80<sup>+</sup>CD11c<sup>+</sup>CD11b<sup>+</sup> cells. The data shown in representative of two independent experiments. Significance was determined by a Mann-Whitney test (\*,  $P < 0.05$ ; \*\*,  $P < 0.01$ ; \*\*\*,  $P < 0.001$ ).

**A**



**B**

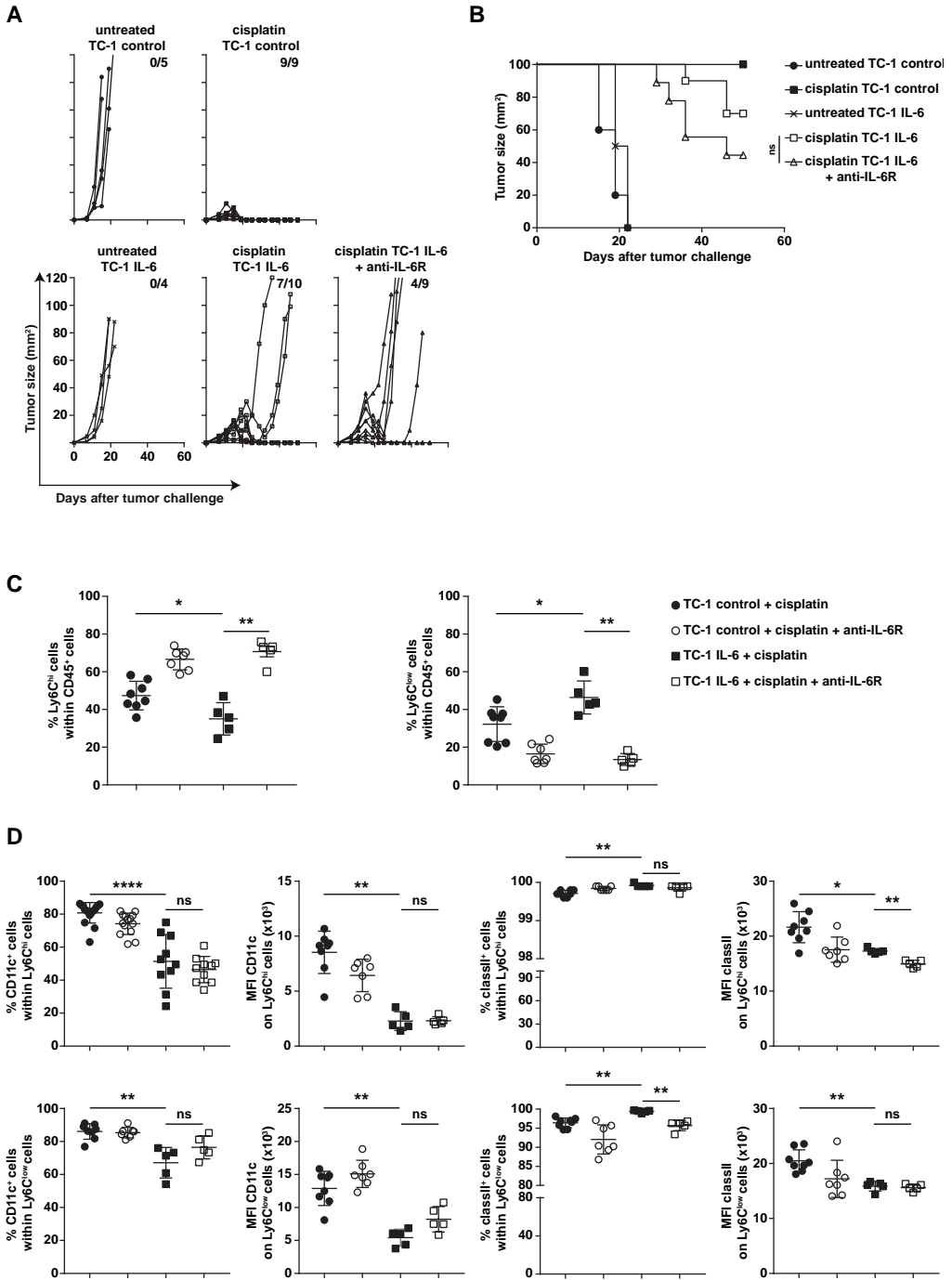


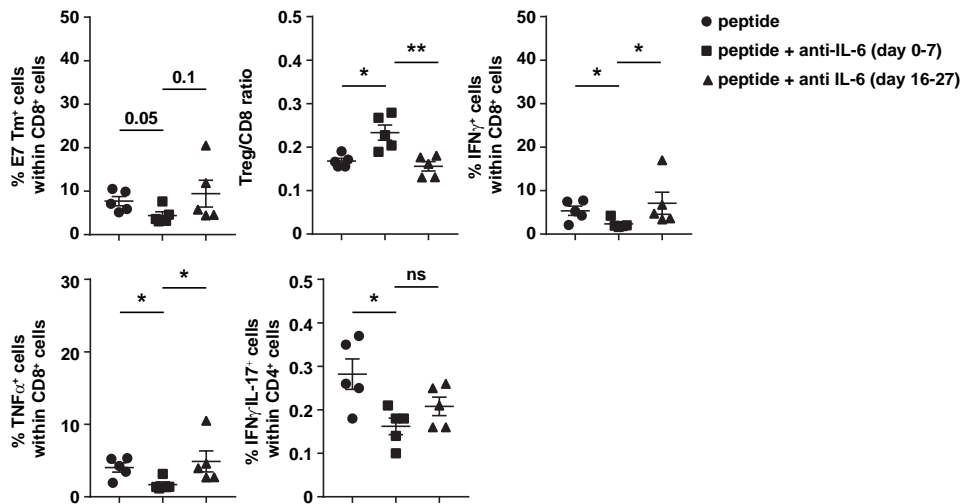
### Supplementary figure 5. IL-6R blocking antibody partially normalize the altered phenotype of myeloid cells in spleen induced by IL-6 produced by tumor in peptide vaccinated mice

Spleen analysis of TC-1 control and TC-1 IL-6 tumor-bearing mice following treatment with SLP vaccine and IL-6R blocking antibody on day 16. A) The percentage of CD11b<sup>+</sup>CD11c<sup>hi</sup>, CD11b<sup>+</sup>CD11c<sup>int</sup> and Ly6G<sup>+</sup> with CD45 gate in spleen. B) The percentage of Ly6C<sup>hi</sup> and classII<sup>+</sup> Ly6C<sup>hi</sup> cells within F4/80<sup>+</sup> cells and MFI of classII on ly6C<sup>hi</sup> cells (upper panel) and the percentage of ly6C<sup>low</sup> and classII<sup>+</sup>Ly6C<sup>low</sup> and MFI of classII on ly6C<sup>low</sup> cells (lower panel) in spleen. Data is representative of two independent experiments, yielding similar results. Each dot represents data from an individual mouse. Graphs indicate mean values with SEM. Significance was determined by Mann–Whitney test. \*, P < 0.05; \*\*, P < 0.01; \*\*\*, P < 0.001.

### Supplementary figure 6. IL-6R blocking antibody cannot change the phenotype of myeloid cells induced by chemotherapy in IL-6 producing tumor

A and B) Tumor growths (A) and survival (B) of TC-1 control and TC-1 IL-6 tumor-bearing mice following treatment cisplatin with and without IL-6R blocking antibody. The number of tumor-free mice from the total mice is indicated. C) The percentage of Ly6C<sup>hi</sup> and Ly6<sup>low</sup> with CD45 gate in TC-1 control and TC-1 IL-6 tumor bearing mice treated with cisplatin. D) The percentage and MFI of CD11c and class II on intratumoral Ly6C<sup>hi</sup> and Ly6C<sup>low</sup> myeloid cells. Each dot represents data from an individual mouse. Graphs indicate mean values with SEM. The data is from one experiment. Significance was determined by a log-rank (Mantel–Cox) or Mann–Whitney test (\*, P < 0.05; \*\*, P < 0.01; \*\*\*, P < 0.001).





**Supplementary figure 7. IL-6 blockade before prime vaccine decrease the systemic T-cell response induced by vaccine**

Mice were injected with TC-1 IL-6 tumor cells and vaccinated with SLP vaccine on day 8. One group of mice received anti-IL-6 from day 0-7 (peptide + anti-IL-6 day 0-7). The other group received anti-IL-6 from day 16-27 (peptide + anti-IL-6 day 16-27). The percentage of E7 Tm<sup>+</sup> within CD8<sup>+</sup>, the ratio of Treg/CD8, the percentage of IFN $\gamma$ <sup>+</sup>, TNF $\alpha$ <sup>+</sup> cells within CD8<sup>+</sup> T cells and the percentage of IFN $\gamma$ /IL-17<sup>+</sup> cells within CD4<sup>+</sup> cells in spleen. Significance was determined by Mann-Whitney test (\*,  $P < 0.05$ ; \*\*,  $P < 0.01$ ; \*\*\*,  $P < 0.001$ ).







# Chapter 5

## Demarcated thresholds of tumor-specific CD8 T cells elicited by MCMV-based vaccine vectors provide robust correlates of protection

*Elham Beyranvand Nejad<sup>1,2†</sup>, Robert B. Ratts<sup>3†</sup>, Eleni Panagioti<sup>1,2</sup>, Christine Meyer<sup>3</sup>, Jennifer D. Oduro<sup>4</sup>, Luka Cicin-Sain<sup>4,5,6</sup>, Klaus Früh<sup>3</sup>, Sjoerd H. van der Burg<sup>2</sup> and Ramon Arens<sup>1\*</sup>*

J Immunother Cancer. 2019 Jan 31;7(1):25. doi: 10.1186/s40425-019-0500-9.

1. Department of Immunohematology and Blood Transfusion, Leiden University Medical Center, Leiden, The Netherlands
2. Department of Medical Oncology, Leiden University Medical Center, Leiden, The Netherlands
3. Vir Biotechnology, Portland, OR, USA
4. Department of Vaccinology and Applied Microbiology, Helmholtz Centre for Infection Research, Braunschweig, Germany
5. Institute for Virology, Hannover Medical School, Hannover, Germany
6. German Centre for Infection Research (DZIF), Partner site, Hannover/Braunschweig, Germany

# Abstract

## Background

The capacity of cytomegalovirus (CMV) to elicit long-lasting strong T cell responses, and the ability to engineer the genome of this DNA virus positions CMV-based vaccine vectors highly suitable as a cancer vaccine platform. Defined immune thresholds for tumor protection and the factors affecting such thresholds have not well been investigated in cancer immunotherapy. We here determined using CMV as a vaccine platform whether critical thresholds of vaccine-specific T cell responses can be established that relate to tumor protection, and which factors control such thresholds.

## Methods

We generated CMV-based vaccine vectors expressing the E7 epitope and tested these in preclinical models of HPV16-induced cancer. Vaccination was applied via different doses and routes (intraperitoneal (IP), subcutaneous (SC) and intranasal (IN)). The magnitude, kinetics and phenotype of the circulating tumor-specific CD8<sup>+</sup> T cell response were determined. Mice were subsequently challenged with tumor cells, and the tumor protection was monitored.

## Results

Immunization with CMV-based vaccines via the IP or SC route eliciting vaccine-induced CD8<sup>+</sup> T cell responses of > 0.3% of the total circulating CD8 T cell population fully protects mice against lethal tumor challenge. However, low dose inoculations via the IP or SC route or IN vaccination elicited vaccine-induced CD8<sup>+</sup> T cell responses that did not reach protective thresholds for tumor protection. In addition, whereas weak pre-existing immunity did not alter the protective thresholds of the vaccine-specific T cell response following subsequent immunization with CMV-based vaccine vectors, strong pre-existing immunity inhibited the development of vaccine-induced T cells and their control on tumor progression.

## Conclusions

This study highlight the effectiveness of CMV-based vaccine vectors, and shows that demarcated thresholds of vaccine-specific T cells could be defined that correlate to tumor protection. Together, these results may hold importance for cancer vaccine development to achieve high efficacy in vaccine recipients.

## Keywords

T cells, Cancer, CMV-based vaccine vector, Pre-existing immunity

## Background

The role of the immune system in cancer eradication has been firmly established. Immunotherapy of cancer has set itself as a mainstream therapy among the conventional therapies comprising chemotherapy, radiotherapy and surgery. Adoptive cell therapy (ACT) with tumor-specific T cells and immunotherapeutic approaches in which the inhibitory pathways are blocked or the costimulatory pathways are triggered to invigorate tumor-specific T cells have shown efficacy in a significant number of patients [1, 2]. Vaccination is another promising form of cancer immunotherapy that has been extensively explored, yet few therapeutic vaccines have shown clinical benefit. The latter has been attributed to the lack of inducing substantial long-lasting functional T cell responses that are able to overcome the immunosuppressive environment [3].

Immune thresholds are instrumental to determine vaccine efficacy and effectiveness against pathogens [4]. In cancer immunotherapy, however, tumor protection thresholds and the factors affecting such thresholds have not well been investigated although as such they are instrumental for both practical reasons and mechanistic insights. To elicit and maintain high immune responses, cytomegalovirus (CMV) is considered as a promising vaccine vector. CMV is unique among viruses as chronic infection by this common betaherpesvirus is characterized by high frequencies of virus-specific T cells and antibodies that do not decline after primary infection but remain high or even increase over time in a process termed memory inflation [5–8]. Inflationary T cells are mostly effector-memory (EM)-like in phenotype, remain polyfunctional for life, and are found in both lymphoid organs and tissues [9]. Despite the induction of host immune responses, CMVs are still able to re-infect [10–12]. Based on these properties, together with the ability to engineer the genome of CMV to attenuate the pathogenicity and to express foreign antigens [13], CMV-based vaccines are currently being explored. In mice and non-human primates, CMV-based vaccines have demonstrated significant protection against pathogens including simian immunodeficiency virus (SIV), mycobacterium tuberculosis and Ebola virus [14–18]. Moreover, CMV-based vaccines comprising tumor antigens, including melanoma antigens gp100 and TRP2 [19–22], human prostate-specific antigen (PSA) [23], or model antigens like ovalbumin [22, 24], have shown anti-tumor efficacy in prophylactic and therapeutic mouse models.

Here we studied whether thresholds of vaccine-elicited T cell responses could be determined that relate to the efficacy of such vaccines to protect against tumor progression, and which factors influence these thresholds. Specifically, we investigated the vaccine thresholds of CMV-based vaccine vectors and the impact of inoculum dosages and routes of infection to achieve tumor protection. Given the high worldwide CMV prevalence, and the fact that pre-existing immunity varies, as evidenced by large variations in the magnitude of CMV-specific



T cell responses in the population, ranging from barely detectable to 40% of the memory compartment, we also addressed the impact of pre-existing immunity on the protective thresholds [7]. Defining protection thresholds could be highly relevant in determining correlates of protection, considered as a crucial element in vaccine development as it provides the level of vaccine efficacy in vaccine recipients.

We found that CMV-based vaccines eliciting clearly discernible CD8<sup>+</sup> T cell responses in the blood (> 0.3% of the total CD8 T cell population) fully protected mice against lethal tumor challenge while relatively low responses do not provide protection. Previous exposure to CMV resulting in a weak immune response did not impact vaccine efficacy, however, strong pre-existing immunity hampered the induction of vaccine-induced T cells consequently resulting in loss of tumor protection. The results highlight the premise of CMV-based vaccines, and put forward the potential of such vaccines in halting tumor development based on correlates of protection that are established on careful determination of vaccine-induced immune responses.

## Methods

### Mice

C57BL/6 mice were obtained from Charles River Laboratories (L'Arbresle, France) or Jackson Laboratory (Sacramento, CA, USA). At the start of the experiments, mice were 6 to 8 weeks old. Mice were housed in individually ventilated cages (IVC) under specific pathogen-free (SPF) conditions in the animal facility of Leiden University Medical Centre (LUMC, The Netherlands) or Oregon Health and Science University (OHSU, Oregon, USA). All animal experiments were approved by the institutional Animal Experiments Committee and were executed according to the institutional animal experimentation guidelines and were in compliance with the guidelines of the Institutional, European and Federal USA animal care and usage committees.

### Virus preparation

Viral titers of virus stocks or infected tissues were determined by plaque assays as previously described [25]. MCMV-IE2-E7 (RAHYNIVTF) and MCMV-IE2-OVA (SIINFEKL) were generated as described [26]. MCMV-IE2-E6/E7 full length fusion, MCMV-IE2-E6/E7 full length replace, MCMV-M79-FKBP-E7 (E7 epitope RAHYNIVTF, IE2 fusion), MCMV-M79-FKBP-gB (gB epitope SSIE-FARL, IE2 fusion) were constructed as follows. MCMV BACs were maintained in SW105 *E. coli* and modified by metabolic galactokinase (*galK*) selection [27], essentially as described [28]. In brief, bacteria containing the MCMV backbone were first transformed with a PCR product of *galK*/kanamycin (*kan*) and flanking homology to target a specific region in the MCMV BAC. Transformed bacteria were selected for *kan*

resistance, grown and subjected to a second transformation to replace the galK/kan cassette with the final insert. These included annealed oligos used for IE2 peptide fusion or the PCR product for M79-FKBP [29] and HPVE6/E7 insertions containing the desired modification with the same MCMV flanking homology to insert the galK/kan cassette. Recombinant bacteria were counter-selected on chloramphenicol 2-deoxy-galactose (DOG) minimal media plates with glycerol as the carbon source. MCMV BAC constructs were characterized by restriction digest, PCR screening, and Sanger and NGS sequencing. Virus was reconstituted by either Lipofectamine 3000 (Thermo-Fisher Scientific) transfection or electroporation (250 V and 950 uF) of NIH 3T3s.

Tissue culture-derived stocks of the MCMV vectors were amplified and titered in NIH 3 T3 cells grown in complete growth media (DMEM, FBS, PSG). FKBP-tagged viruses were grown in complete growth media supplemented with Shield-1 at a final concentration of 1 uM and added every 48 h [29]. Cell free virus was obtained from supernatant of infected cells, clarified at 3,000 rpm for 20 min and virus was pelleted at 24,000 rpm for 1 h through a sorbitol cushion (10% D-sorbitol, 0.05 M Tris pH 7.4, 1 mM MgCl<sub>2</sub>). Virus pellet was resuspended in PBS. For virus quantification, plaque assays were performed in 24-well plates by infection with appropriate serial virus dilution in 0.2 mL of media and then incubated at 37 °C for 2 h rocking. Following incubation, the infected cells were overlaid with 1 mL complete media supplemented with carboxymethylcellulose. After 5 to 6 days, the cells were fixed in 3.7% formaldehyde in PBS and stained with 0.001% aqueous methylene blue. The plaques were counted by light microscopy. Multi-step virus replication curves were performed in NIH 3 T3 cells at MOI 0.1 in 6 well plates, 3 replicates per virus per time-point. Virus was incubated at 37 °C for 2 h, washed 3 times with PBS and then 2 mL of media was added. Supernatant was harvested at 1, 3, 5, and 7 days post-infection, stored at – 80 °C and titered by plaque assay. FKBP-tagged viruses were grown in complete growth media supplemented with Shield-1 at a final concentration of 1 uM and added every 48 h.

**Tumor challenge models and anti-tumor vaccination** The tumor cell line TC-1 (a kind gift from T.C. Wu, John Hopkins University, Baltimore, MD) was generated by retroviral transduction of C57BL/6 lung epithelial cells with the HPV16 E6/E7 and c-H-ras oncogenes [30] and cultured as previously described [31]. The tumor cell line C3 was developed by transfection of mouse embryonic cells with the HPV16 genome and an activated ras oncogene and maintained as previously described [32]. The MC38-OVA tumor cell line is generated by a retroviral infection of the MC38 parental cell line with PMIG/MSCV-IRES-GFP plasmid encoding cytoplasmic bound OVA [33]. Iscove's Modified Dulbecco's Media (IMDM)(Lonza, Basel, Switzerland) supplemented with 8% fetal calf serum (FCS) (Greiner), 2 mM L-glutamine (Life Technologies, Carlsbad, CA, Unites States), 50 IU/ml Penicillin (Life Technologies) and 50 µg/ml Streptomycin (Life Technologies) was used to

culture tumor cell lines. Cells were cultured in a humidified incubator at 37 °C and 5%CO<sub>2</sub>. Mycoplasma tests that were frequently performed for all cell lines by PCR were negative.

Treatment schedule of experiments are indicated in the respective figures and legends. Mice were vaccinated with MCMV vectors via the intraperitoneal (IP), intranasal (IN) or subcutaneous (SC) route with the indicated inoculum size. In tumor experiments, mice were inoculated subcutaneously in the flank with 0.25–1×10<sup>5</sup> TC-1 tumor cells, 5×10<sup>5</sup> C3 tumor cells or with 2.5 × 10<sup>5</sup> MC38-OVA in 200 µl PBS containing 0.2% BSA on day 0. Tumor size was measured two times a week using a caliper. Mice were euthanized when tumor size reached > 1000 mm<sup>3</sup> in volume or when mice lost over > 20% of their total body weight (relative to initial body mass).

### **In vivo antibody usage**

CD8 T cell depleting monoclonal antibodies (clone 2.43) were purchased from Bio-X-Cell (West Lebanon, NH, United States) and administered IP twice weekly (200 µg/mouse) for 2–3 weeks. CD8 T cell depletion was started 4 days before tumor challenge. Depletion was checked by staining for CD3 and CD8 marker expression followed by flow cytometric analysis.

### **Flow cytometry**

Blood collection and processing was performed as described [34]. Cells were resuspended in staining buffer (PBS + 2% FCS + 0.05% sodium azide) and incubated with various fluorescently labelled antibodies detecting CD8 (clone 53–6.7), CD62L (clone MEL-14), CD44 (clone IM7), KLRG1 (clone 2F1), CD3 (clone 500A2), CD127 (clone A7R34). Antibodies were obtained from eBioscience (San Diego, CA, United States), BD Biosciences (San Jose, CA, United States) and Biolegend (San Diego, CA, United States). For dead cell exclusion, 7-Aminoactinomycin D (Invitrogen, Carlsbad, CA, United States) was used. To measure the MCMV-specific and tumor antigen-specific T cell responses, PE and APC-labelled class I-restricted multimers (tetramers or dextramers) with the peptide epitopes OVA257–264 (SIINFEKL), HPV E749–57 (RAHYNIVTF), MCMV M45985–993 (HGIRNASFI), MCMV M38316–323 (SSPPMFRV) were used. Tetramers were produced as described [35] and dextramers were obtained from Immudex. Samples were analyzed with a BD LSRII or LSR Fortessa flow cytometer, and results were analyzed using FlowJo software (Tree Star, Ashland, OR, United States).

### **In vivo cytotoxicity assay**

Splenocytes of naïve CD45.1 (Ly5.1) mice were isolated and loaded with MHC class I restricted-E7<sub>49–57</sub> or OVA2<sub>57–264</sub> peptides for 1 h at 37 °C at the final concentration of 1 µg/ml. After extensive washing, cells which were pulsed with specific peptide or irrelevant peptide

were labelled with high and low concentrations of CFSE (Invitrogen), respectively. Next,  $5 \times 10^6$  peptide pulsed cells were pooled and injected intravenous (IV) via the retro-orbital route into the mice that have been vaccinated 70 days earlier with MCMV-based vaccines. After 24 h, spleens of the recipient mice were isolated, stained for CD45.1, and subjected to flow cytometry. The cytotoxic capacity was calculated relative to naïve mice by using the following formula:  $[100 - ((\text{percentage of pulsed peptide in infected mice} / \text{percentage of unpulsed peptide in infected mice}) / (\text{percentage of pulsed peptide in naive mice} / \text{percentage of unpulsed peptide in naive mice}))] \times 100$ .

### Enzyme-linked ImmunoSpot (ELISpot) assay

Splenocytes of individual vaccinated mice were isolated and cultured on ELISpot plates (R&D systems, Minneapolis MN) pre-coated with anti-IFN- $\gamma$  antibodies. The indicated peptides (E7<sub>49-57</sub>, RAHYNIVTF; or a pool of peptides spanning the E7 sequence, 15-mers overlapping by 11) were added at 1  $\mu\text{g/ml}$ . 36 h later cells were removed and secondary antibodies added. Plates were developed according to the manufactures instructions. Spots were counted using an AID ELISpot reader.

### Statistical analysis

Statistical analyses were performed using GraphPad Prism (La Jolla, CA, United States). Survival data were analyzed by Kaplan-Meier and the log-rank (Mantel-Cox) test. Statistical significance was determined by Mann Whitney. P-values of  $\leq 0.05$  were considered statistically significant.

## Results

### Location and size of foreign sequences in CMV-based vaccine vectors impact vaccine-elicited T cell responses and associated tumor protection

To determine effective regions to insert foreign sequences, we generated recombinant MCMV-based vaccine vectors containing the entire E6 and E7 antigens of human papilloma virus type 16 (HPV16). In these vectors the E6/E7 genes replaced exon 3 of IE2 (MCMV-IE2-E6/E7 full length replace) or E6/E7 was placed in the end part of the IE2 region (MCMV-IE2 E6/E7 full length fusion)(Fig. 1a). To analyze the T cell responsiveness to the inserted foreign sequences induced by these vaccine vectors, we IP vaccinated mice and measured the E7-specific T cell responses by IFN- $\gamma$  ELISPOT, following restimulation with the immunodominant peptide epitope E7<sub>49-57</sub> or with a pool of overlapping peptides covering the whole E7 protein, and by staining with MHC class I multimers. Immunization with MCMV-IE2-E6/E7 full length fusion induced significantly higher E7-specific T cell responses ( $\sim 0.5$ –2% of the total CD8<sup>+</sup> T cell population) than MCMV-IE2-E6/E7 full length replace ( $< 0.3\%$ ) at 10 and 21 weeks after vaccination (Fig. 1b and c). To assess the anti-tumor



immunity induced by these recombinant viruses we challenged the vaccinated mice with TC-1 tumor cells, which are transformed by expression of the HPV16 E6 and E7 oncoproteins [30]. Vaccination with MCMV-IE2-E6/E7 full length fusion prevented tumor progression in most tumor-challenged mice, while the majority of the mice vaccinated with MCMV-IE2-E6/E7 full length replace developed tumors (Fig. 1d). Thus, consistent with our previous report we found that fusion of foreign sequences to the C-terminus of the IE2 protein works superior in eliciting T cell responses, and this event relates to higher amounts of the peptide epitope presented in peptide-MHC complexes [26].

Next, we analyzed the impact of the size of the E6/E7 antigens, and therefore generated a recombinant MCMV expressing only a single immunodominant CD8 T cell epitope, i.e. RAHYNIVTF (E7<sub>49-57</sub>), fused to the carboxyl terminus of the MCMV IE2 gene (MCMV-IE2-E7). Clearly, mice immunized with MCMV-IE2-E7 resulted in the highest E7-specific T cell response (~2–8%), and vaccination with MCMV-IE2-E7 fully protected mice against otherwise lethal TC-1 tumor challenge (Fig. 1c and d). In conclusion, both the location and size of inserted foreign sequences impact the vaccine-elicited T cell response of MCMV vaccine vectors and this corresponds to protection against tumor outgrowth.

### **The magnitude of inflationary T cell responses elicited by recombinant MCMV-based vaccine vectors is influenced by the inoculation route and dose and determines vaccine efficacy**

To investigate the impact of the route of inoculation on the application of MCMV-based vaccine vectors for vaccine-elicited immunity against cancer, we compared the magnitude and kinetics of the antigen-specific CD8<sup>+</sup> T cell response in the blood upon IP, IN and SC inoculation. The E7-specific CD8<sup>+</sup> T cell responses elicited with MCMV-IE2-E7 increased gradually to ~5% after IP immunization, while the responses were steadily ~0.6% after SC inoculation. Upon IN inoculation however, the E7-specific CD8<sup>+</sup> T cell responses were minute throughout infection (<0.3%) (Fig. 2a and b). The M38<sub>316-323</sub> epitope-specific CD8<sup>+</sup> T cell response after IP and SC inoculation showed similar magnitude and kinetics as the response to the E7 epitope in the same vector (Fig. 2a and b). Upon IN immunization, the M38-specific CD8<sup>+</sup> T cell response was barely detectable and did not show signs of inflation. Upon immunizations via the IP and SC routes, the non-inflationary response to the M45<sub>985-993</sub> epitope showed the typical response pattern of rapid expansion followed by swift contraction and stable memory formation (Fig. 2a and b). IN vaccination induced only ~0.1% M45-specific CD8<sup>+</sup> T cells, and during the memory phase this response was close to the detection limit (Fig. 2a and b).

Characteristic for inflationary T cells is their effector-memory (EM) like (CD44<sup>+</sup>CD62L<sup>low</sup>,CD127<sup>+/-</sup>,KLRG1<sup>+</sup>) appearance [6]. Early after IP and SC immunization,

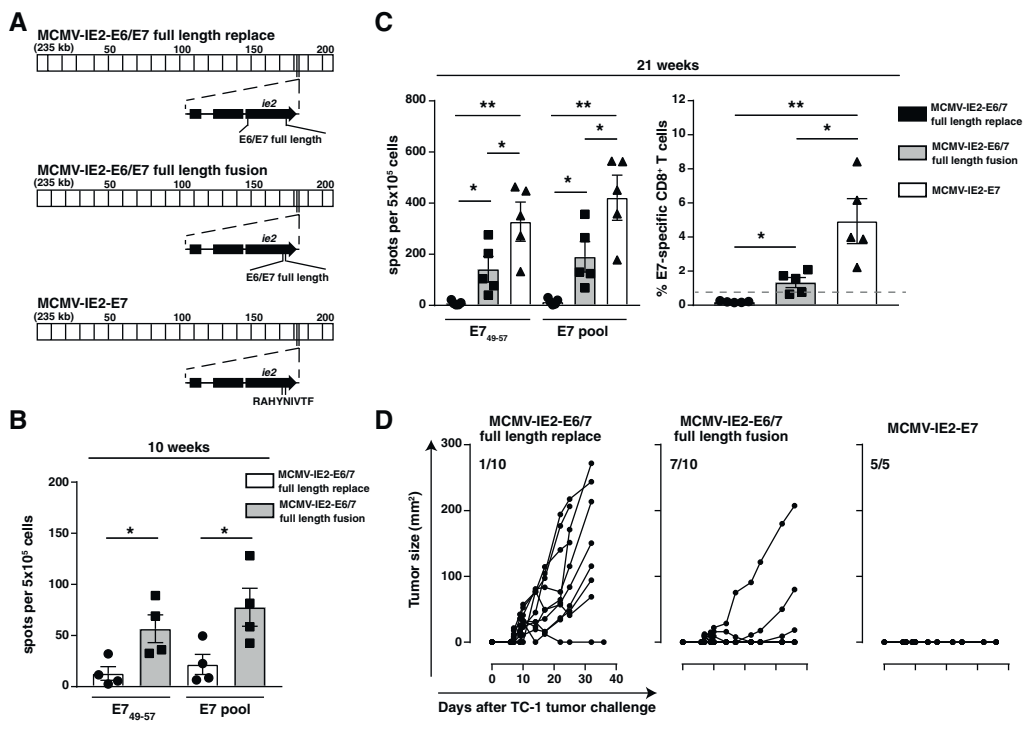


**Figure 1.** Position and epitope context of heterologous antigens in MCMV-vectored vaccines impact vaccine-elicited T cell responses and associated tumor protection. **a** Schematic of MCMV-IE2-E6/E7 full length replace/fusion and MCV-IE2-E7. The MCMV genome region at ~kb 186–187 corresponds to the MCMV gene *ie2* (enlarged). Constructs encoding the E6/E7 fusion protein or the E7 epitope were generated by BAC recombineering. DNA sequences encoding the full-length E6/E7 fusion protein were inserted either to replace the *ie2* gene (full length replace) or in frame at the very end of the *ie2* gene (full length fusion). The E7<sub>49–57</sub> epitope RAHYNIVTF was fused to the end of *ie2*. **b**, **c** C57BL/6 mice were vaccinated IP with  $1 \times 10^5$  PFU MCMV-IE2-E6/7 full length fusion, MCMV-IE2-E6/7 full length replace or MCMV-IE2-E7. Splenocytes were harvested 10 (**b**) or 21 (**c**) weeks after vaccination and stimulated with the immunodominant E7<sub>49–57</sub> peptide or with a pool of 15-mer peptides covering the entire E7 protein for 36 h. IFN- $\gamma$  production was measured by ELISpot assay. Shown is the number of spots per  $5 \times 10^5$  cells  $\pm$  SEM. **c** Frequency of E7<sub>49–57</sub>-specific T cells identified by MHC class I multimers within the total CD8 $^{+}$  cell population at 21 weeks post vaccination. Data represents mean values  $\pm$  SEM ( $n = 4–5$  mice per group). \*,  $P < 0.05$ ; \*\*,  $P < 0.01$ . **d** Tumor outgrowth of TC-1 tumor cells in mice challenged with TC-1 tumor cells 21 weeks after vaccination with  $1 \times 10^5$  PFU MCMV-IE2-E6/7 full length replace, MCMV-IE2-E6/7 full length fusion or MCMV-IE2-E7 (5–10 mice per group). The number of tumor-free/total mice is indicated in each tumor out growth graph.

the E7-specific CD8 $^{+}$  T cell population acquired an EM-like phenotypic profile, which remained high throughout the memory phase (Fig. 2c). The M38-specific CD8 $^{+}$  T cells displayed a gradual increase of the EM phenotype to 70–80% of the total Ag-specific T cell population. In contrast, only 40% of the M45-specific CD8 $^{+}$  T cells showed an EM phenotype throughout the memory phase. Upon IN immunization, the formation of the EM phenotype by the E7, M38 and M45-specific CD8 $^{+}$  T cells was much less pronounced (Fig.



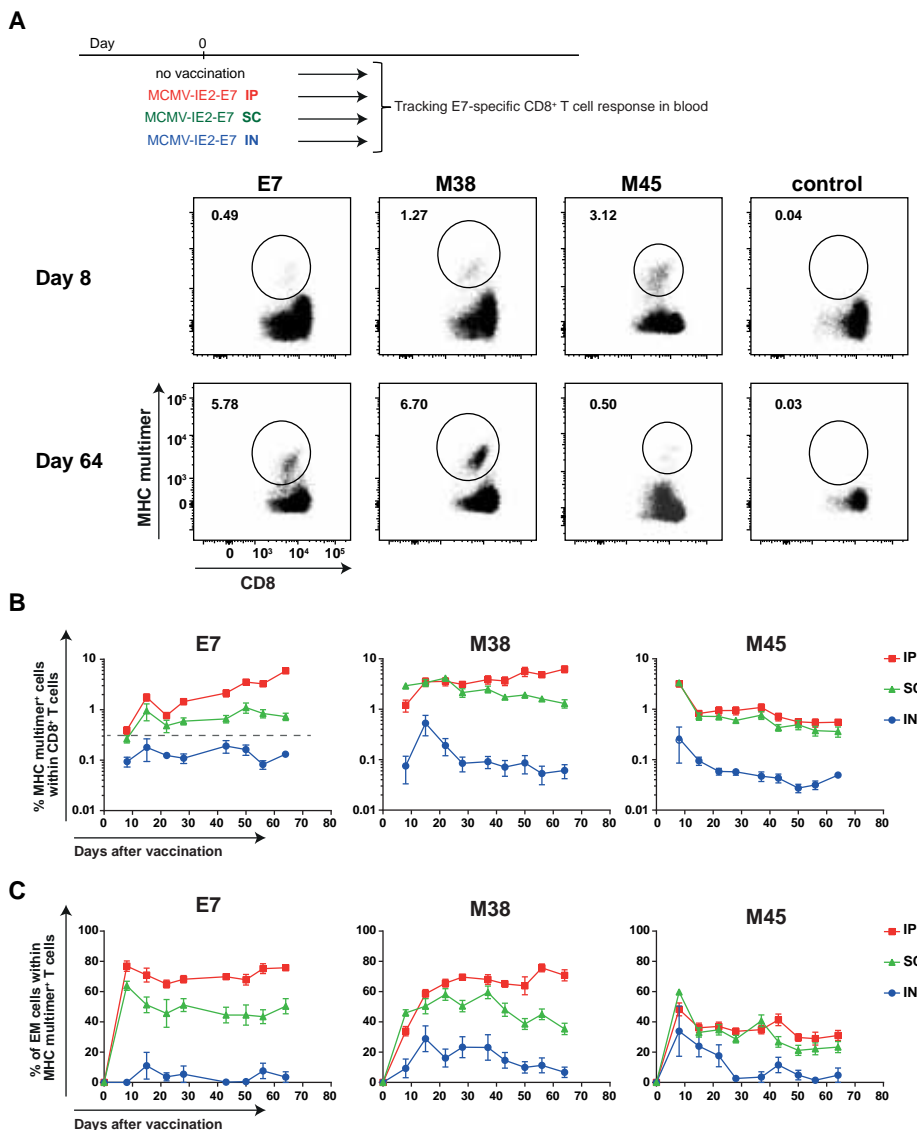


**Figure 2.** Vaccination with recombinant MCMV vectors via the IP and SC route induces potent specific T cell responses. Mice were vaccinated with MCMV-IE2-E7 via IP, SC or IN route or kept unvaccinated (control), and the CD8 T cell responses were examined in blood. **a** Representative flow cytometry plots for MHC class I multimer staining to E7, M38 and M45 epitopes in blood of MCMV-IE2-E7 infected mice via IP during acute phase (day 8 post vaccination) and memory phase (day 64 post vaccination). Numbers represent the percentage of Ag-specific CD8<sup>+</sup> T cells within the total CD8<sup>+</sup> T cell population. Control flow cytometry plots show the staining for E7 multimer in unvaccinated mice. Flow cytometry plots show similar numbers of total cells in each plot except for control. **b** Frequency of Ag-specific CD8<sup>+</sup> T cells to E7, M38 and M45 epitopes over time. **c** Frequency of effector-memory (EM) cells (KLRG1<sup>+</sup>, CD62L<sup>-</sup>) within E7, M38 and M45 MHC multimer<sup>+</sup> CD8<sup>+</sup> T cells over time. Data represents mean values  $\pm$  SEM ( $n = 7-8$  mice per group) and are representative of two independent experiments with similar results.

2c). Taken together, these data show that immunization with recombinant MCMV vectors via the IP and SC route induces prominent EM-like CD8<sup>+</sup> T cell responses, albeit with different kinetics, while IN infection resulted in weak responses at best.

Next, we investigated the influence of the route of immunization and the resulting vaccine-specific T cell response elicited by the MCMV vectors on efficacy in tumor challenge experiments. We vaccinated mice with MCMV-IE2-E7 via the IP, IN or SC routes and challenged these mice with TC-1 tumor cells. While TC-1 tumors grew out progressively in all naïve mice, immunization with MCMV-IE2-E7 via the IP and SC route induced complete protection against TC-1 tumor challenge (Fig. 3a). Conversely, IN immunization with MCMV-IE2-E7 protected only 50% of the mice (Fig. 3a). Notably, the IN immunized mice that were protected had stronger E7-specific CD8<sup>+</sup> T cell responses as compared to the unprotected group (Fig. 3b). Thus, MCMV vectors inducing circulating tumor-specific CD8<sup>+</sup> T cell responses > 0.3% provides full protection while responses below this threshold results in loss of protection. Immunizations with MCMV-based vaccine vectors via routes of vaccination that induce large tumor-specific T cell responses are thus superior in controlling tumor outgrowth. In addition, all the mice which remained tumor free until day 60, including the subset of the IN vaccinated mice, were protected against challenge with C3 tumor cells expressing HPV antigens including the E7 oncoprotein (Fig. 3c). Protection against MC38 tumor cells, which do not express E7, was however not established (data not shown). These results also indicate the induction of immunological memory including in those mice vaccinated via the IN route.

To assess the capacity of CMV-based vaccines to elicit responses to other inserted foreign epitopes, we tested MCMV expressing the H-2Kb-restricted OVA<sub>257–264</sub> (SIINFEKL) epitope from ovalbumin (OVA). Immunization with MCMV-IE2-OVA induced OVA-specific CD8<sup>+</sup> T cell responses against OVA<sub>257–264</sub> that were slightly higher than the response against E7 after MCMV-IE2-E7 immunization. The responses against the epitopes in M38 and M45 were similar (Additional file 1: Figure S1A). Moreover, vaccination with MCMV-IE2-OVA induced complete protection against OVA-expressing MC38 tumor cells (Additional file 1: Figure S1B).

Next, we examined whether tumor protection was solely due to the induction of tumor-specific T cell responses or whether possible bystander effects of virus infection were implicated. First, we established the requirement of CD8<sup>+</sup> T cells in the tumor protective role of MCMV-based vaccine vectors. CD8<sup>+</sup> T cell depletion 4 days before TC-1 tumor challenge in mice immunized earlier with MCMV-IE2-E7 via the IP route resulted in tumor progression, which underscores the importance of CD8<sup>+</sup> T cells (Fig. 4a). Second, mice inoculated with MCMV-IE2-OVA and challenged with TC-1 tumor cells, which do not express OVA antigen, were

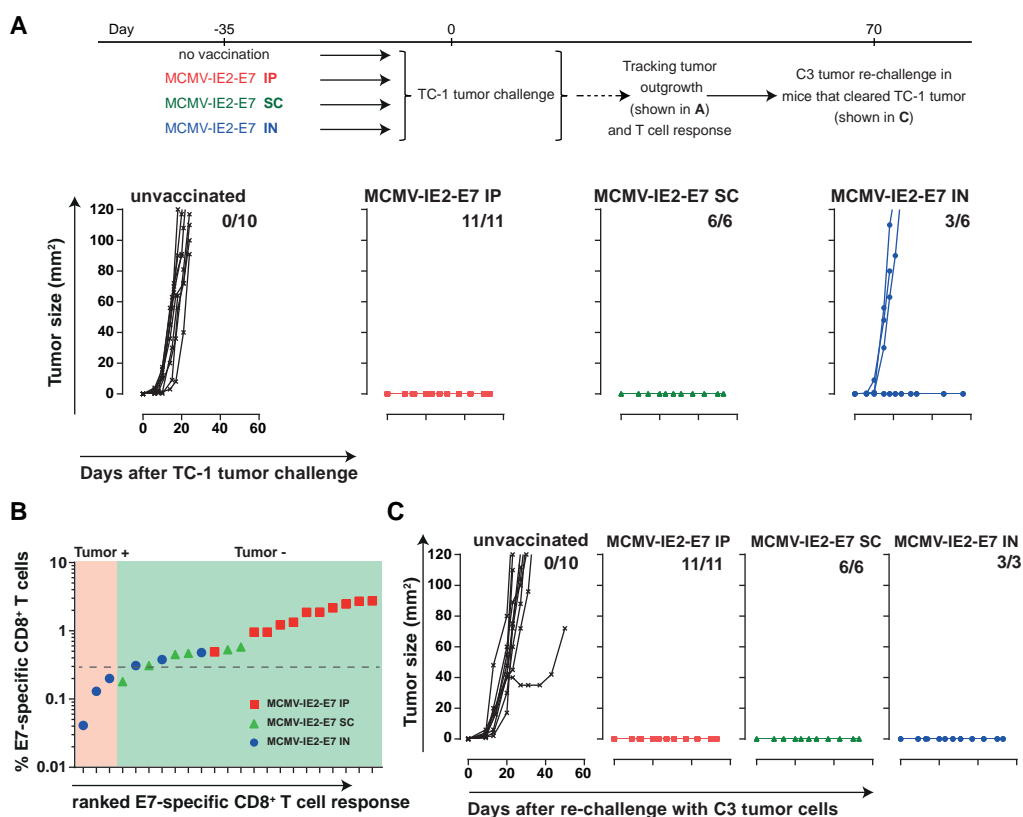


**Figure 3.** Immunization with MCMV-based vaccine vectors that induce substantial tumor-specific T cell responses via different routes of infection control tumor outgrowth. **a** TC-1 tumor outgrowth of unvaccinated mice and of mice previously vaccinated with MCMV-IE2-E7 via the IP, SC or IN route. The number of tumor-free/total mice is indicated in each graph. **b** The percentage of E7-specific CD8<sup>+</sup> T cells within the total CD8<sup>+</sup> T cell population in the blood (y-axis) plotted against the E7-specific CD8<sup>+</sup> T cell response ranked from low to high (x-axis) of the mice that were either tumor-free (tumor-) or tumor positive (tumor+). **c** The mice that cleared the TC-1 tumor in A were re-challenged with  $1 \times 10^5$  C3 tumor cells. The number of tumor-free/total mice is indicated in each graph. Data are representative of two independent experiments with similar results.

not protected whereas MCMV-IE2-OVA immunization protects against MC38-OVA (Fig. 4a and b). Vice versa MCMV-IE2-E7 immunization does not provide protection against MC38-OVA (Fig. 4b), while this vaccine vector provides protection against E7-expressing TC-1 tumor cells (Figs. 3a, 4a). To further demonstrate specific target-mediated killing induced by the MCMV-based vaccine vectors, we performed *in vivo* cytotoxicity assays. Target cells pulsed with vaccine-specific antigen or control antigen were injected into mice previously vaccinated with MCMV-IE2-E7 (Fig. 4c) or MCMV-IE2-OVA (Fig. 4d).

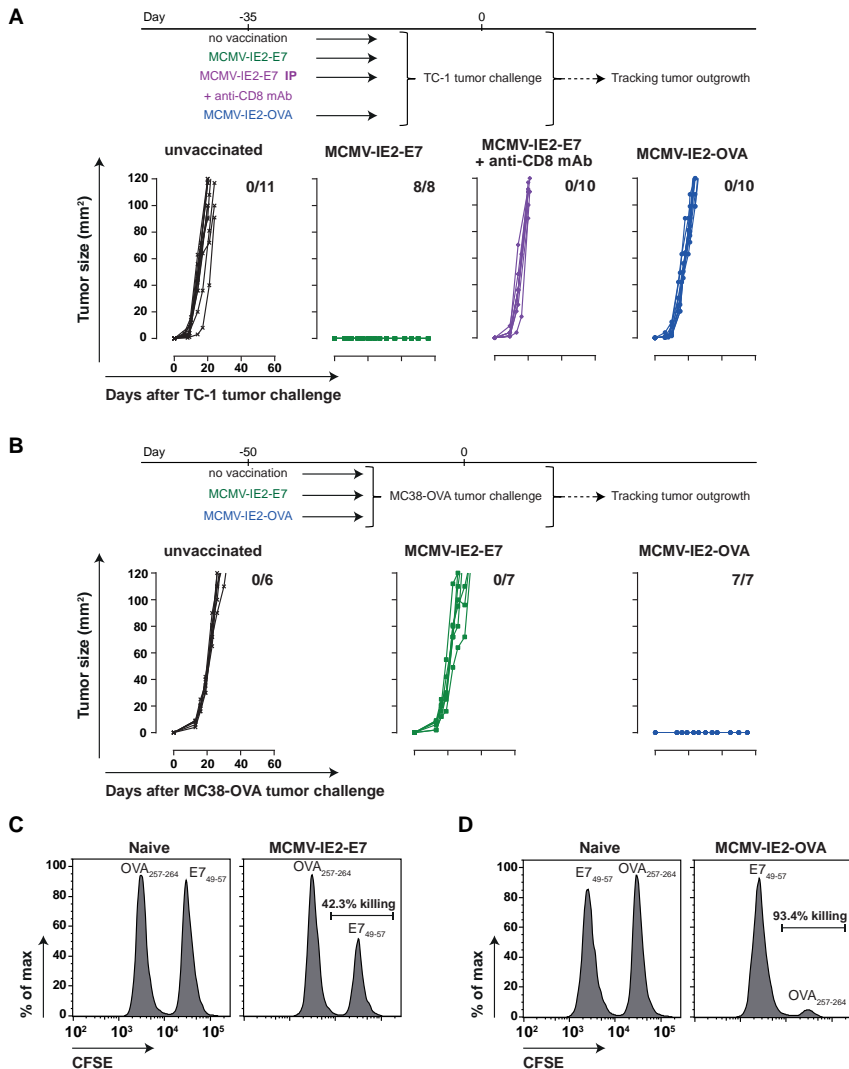


**Figure 4.** Specific anti-tumor immunity elicited by MCMV-based vaccine vectors is essential for protection. **a** TC-1 tumor outgrowth of unvaccinated mice and of mice previously vaccinated with MCMV-IE2-E7 or MCMV-IE2-OVA via the IP route. CD8 depleting antibody was given in the group of mice vaccinated with MCMV-IE2-E7 via IP starting 4 days before tumor challenge. The number of tumor-free/total mice is indicated in each graph. Data was pooled from two independent experiments. **b** MC38-OVA tumor outgrowth of unvaccinated mice and of mice previously vaccinated with MCMV-IE2-E7 or MCMV-IE2-OVA via the IP route. The number of tumor-free/total mice is indicated in each graph. Data are representative of two independent experiments with similar results. **c** and **d** Representative histograms of CTL-mediated killing responses induced by MCMV-IE2-E7 (**c**) or MCMV-IE2-OVA (**d**). Mice were vaccinated with  $5 \times 10^5$  PFU MCMV-IE2-E7 (**c**) or MCMV-IE2-OVA (**d**) via SC. After 69 days, splenocytes from naïve mouse were pulsed with specific peptide; E7<sub>49-57</sub> (**c**) or OVA<sub>257-264</sub> (**d**) or unspecific peptide and labelled with high and low concentrations of CFSE, respectively. Then, cells were adoptively transferred to the MCMV vaccinated mice or naïve mice as control. One day later, spleens of the mice were analyzed for the percentage of killing as described in materials and methods.

Both MCMV-based vaccine vectors induced exclusive killing of target cells presenting the vaccine-specific antigen. Thus, vaccine-induced specific CD8<sup>+</sup> T cell responses against antigens expressed by the tumor are required to induce protective immunity and responses against the vector alone do not provide protection.

To substantiate whether the magnitude of the circulating vaccine-specific CD8<sup>+</sup> T cell response relates to tumor protection, we IP and SC immunized mice with low inoculum dosages to achieve responses below the 0.3% threshold (Fig. 5a). Infection with a high dose of MCMV-IE2-E7 via the IP and SC route induced as expected stronger CD8<sup>+</sup> T cell responses (> 0.3%) against the E7 epitope compared to inoculum dosages with 1000 fold less virus, which resulted in responses < 0.3% in the blood (Fig. 5b). The higher response in magnitude correlated to a higher percentage of EM-like phenotype within the total Ag-specific CD8<sup>+</sup> T cell population (Fig. 5b). Importantly, immunization with high dose MCMV-IE2-E7 via the IP and SC route protected mice from tumor outgrowth (Fig. 5c and d, Group 2 and 3) while immunization with the low dose resulted in less protection (Fig. 5c and d, Group 5 and Group 6). In the SC but not in the IP low-dose immunized group some mice were protected despite circulating E7-specific CD8<sup>+</sup> T cells below the threshold. Furthermore, similar to the data shown in Fig. 3 IN immunization with  $1 \times 10^5$  PFU MCMV-IE2-E7 elicited a response of ~ 0.3%, and resulted in partial protection (40% survival) (Fig. 5 a-d, Group 4). Again, the IN immunized mice that were protected had E7-specific CD8<sup>+</sup> T cell responses >0.3% while the unprotected group had responses < 0.3% (data not shown). When a 200 fold lower vaccine dose (500 PFU) for the IN route was used, which elicited a lower response (~ 0.1%), all the mice succumbed to the tumor challenge (Fig. 5 a-d, Group 7). Taken together, these data indicate that the magnitude and EM phenotype of the vaccine-induced CD8<sup>+</sup> T cells are controlled by the route of vaccination and inoculum dosage, and are principal determinants for the efficacy of MCMV-based vaccine vectors against tumors.

### **Immunity to re-infection can hamper the formation of vaccine-induced CD8<sup>+</sup> T cell responses**

Although CMV has the capacity to re-infect the host despite the presence of CMV-specific T and B cell responses elicited upon primary infection, CMV-specific immunity clearly controls viral pathogenesis of primary and secondary infections as shown by the fact that CMV mainly causes disease in immature or immunocompromised situations, and pre-existing immunity strongly limits viremia upon secondary infection [11, 12]. To address the impact of pre-existing MCMV immunity on vaccine-induced CD8<sup>+</sup> T cell responses and hence the induction of protective immunity, we examined the kinetics of the MCMV vaccine-specific T cell responses in different settings of pre-existing immunity. To mimic the condition of pre-existing immunity in the TC-1 tumor challenge setting, we infected mice first with MCMV-IE2-OVA, which provokes pre-existing immunity but does not elicit



tumor-specific T cell immunity. After the establishment of pre-existing immunity, mice were vaccinated with MCMV-IE2-E7. This experimental setup allowed us to follow the antigen-specific T cell response following the first infection and after the subsequent immunization, in which a) the OVA-specific T cell response is primary after the infection and not boosted, b) the M38-specific CD8<sup>+</sup> T cell response is primary after the infection and then boosted by the immunization, and c) the E7-specific T cell response (which is tumor-specific in case of TC-1 tumor challenge) is not induced during the first infection, hence is primary upon the immunization. Here, we confirmed that IP infection with MCMV-OVA induces higher OVA and M38-specific CD8<sup>+</sup> T cell responses (~ 5% OVA and ~ 1.5 M38) in blood (Fig. 6a) compared to infection via IN (~ 0.5% OVA and ~ 0.4% M38). Next, we investigated the E7 (tumor)-specific T cell response in these high (IP) and low levels (IN) of pre-existing immunity. Vaccination with MCMV-IE2-E7 via the IP and SC route boosted the M38-specific T cell response (~ 3% M38 compared to 1.5 and 0.5% after primary infection) and this increase was more pronounced in the mice with low pre-existing immunity compared to high pre-existing immunity. Importantly, a higher E7-specific T cell response was also determined in the mice with low pre-existing immunity (0.7–1% versus 0.3%) (Fig. 6a). The CD8<sup>+</sup> T cell response against the OVA<sub>257–264</sub> epitope did not change upon subsequent immunization with MCMV-IE2-E7. Together, these data suggest that super-infection occurs more readily upon primary inoculation via the IN route versus the IP route. Moreover, the level of pre-existing immunity affects the magnitude of the T cell responses elicited to MCMV vectored antigens.

To assess how various levels of pre-existing MCMV immunity influence the tumor protection, mice with low and high pre-existing immunity were challenged with TC-1 tumor cells (Fig. 6b and c). Mice with a high level of pre-existing immunity (infected previously with a high dose MCMV-IE2-OVA via the IP route) and vaccinated IP, SC or IN with MCMV-IE2-E7 were not protected (Fig. 6b and c, Group 4, 5 and 6). This correlated with the elicited E7-specific responses in the blood that were < 0.3%, except for one mouse in group 5 (SC vaccinated) which cleared the tumor and correspondingly had an E7-specific CD8<sup>+</sup> T cell responses > 0.3% (Fig. 6a and d). Moreover, infection with a 1000 fold lower inoculum dosage of MCMV-IE2-OVA via the IP route followed by IP vaccination with MCMV-IE2-E7 resulted in partial protection (Fig. 6b and c, Group 7). Remarkably, the unprotected mice in this group had E7-specific CD8<sup>+</sup> T cell responses < 0.3% while all protected mice had responses > 0.3% (Fig. 6d). Moreover, in mice infected with MCMV-IE2-OVA via the IN route and then vaccinated with MCMV-IE2-E7 via the IP and SC route, none of the tumors grew out and the mice remained tumor-free (Fig. 6b and c, Group 2 and 3). Importantly, these mice had E7-specific CD8<sup>+</sup> T cell responses in the blood > 0.3% (Fig. 6a and d). Taken together, these data indicate that the level of pre-existing immunity can set the protection threshold of vaccine-induced CD8<sup>+</sup> T cell responses by CMV-based vaccine vectors: a strong T cell response against the vaccine vector elicited during primary infection inversely correlates with the ability of an MCMV-vectored vaccine to elicit protective immunity upon super-infection.



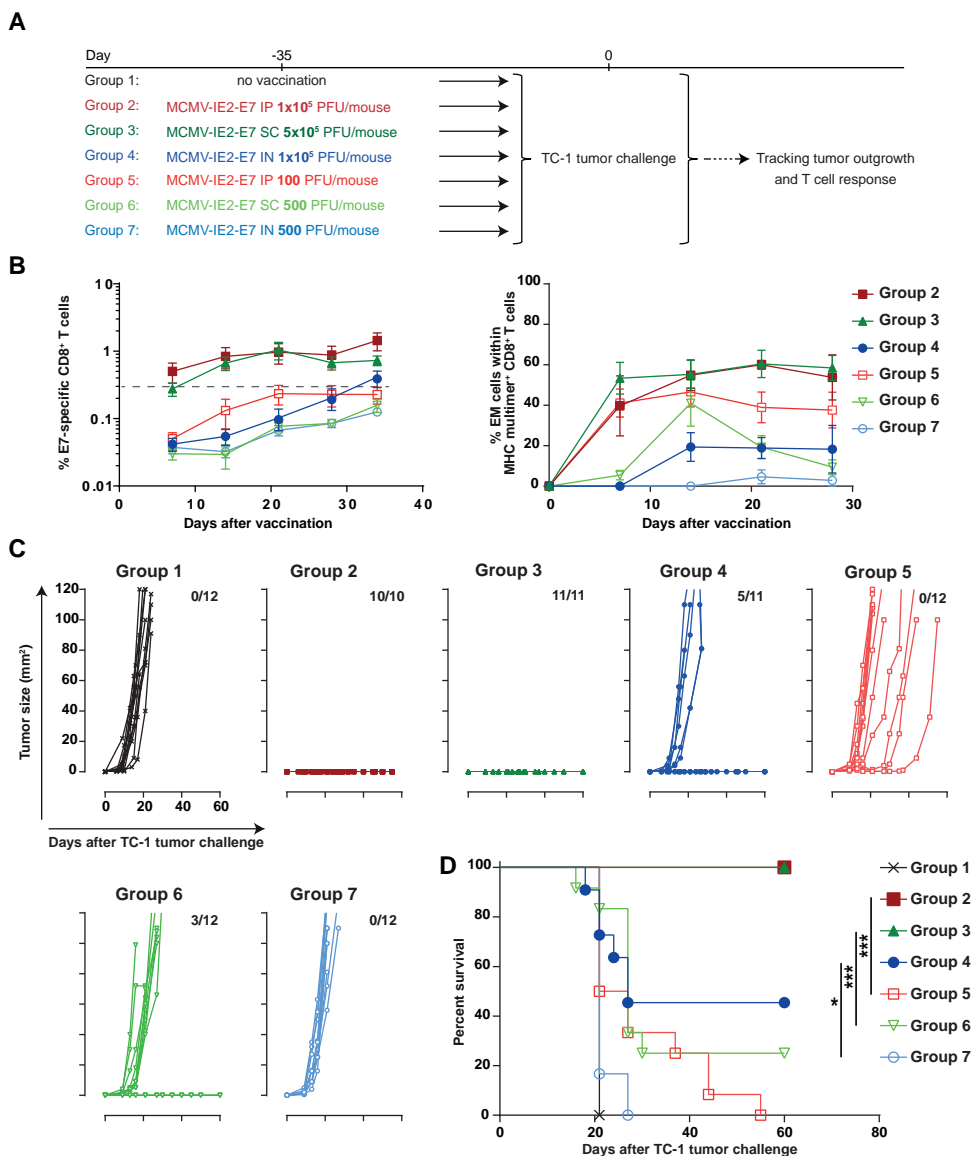


**Figure 5.** The inoculum dosage of recombinant MCMV-based vaccine vectors determines the magnitude of anti-tumor T cell response and protection efficacy. **a** Schematic of the experiment. Mice were infected with indicated doses and routes or kept unvaccinated. After 35 days, all the mice were challenged with TC-1 tumor cells. The tumor outgrowth and survival of the mice was followed for 60 days. **b** Percentage of E7-specific and the percentage of EM-like cells within the E7-specific CD8<sup>+</sup> T cells of the vaccinated mice. **c** and **d** TC-1 tumor outgrowth (**c**) and survival (**d**) graphs of mice immunized with MCMV-IE2-E7 (schematic shown in **a**). The number of tumor-free/total mice is indicated above each tumor outgrowth graph in (**c**). Tumor outgrowth was followed for 60 days. The number of tumor-free/total mice is indicated. \*,  $P < 0.05$ ; \*\*,  $P < 0.01$ ; \*\*\*,  $P < 0.001$ .

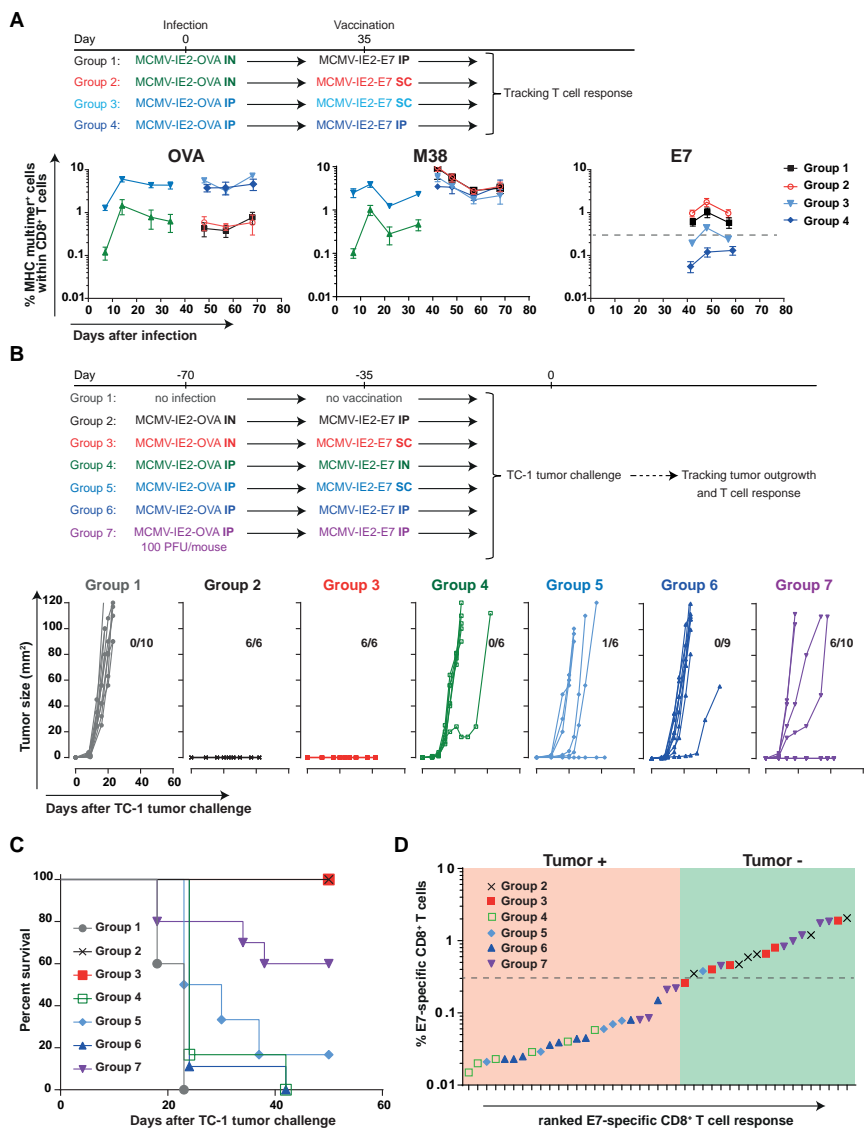


**Figure 6.** Pre-existing immunity against the MCMV vector affects the strength of T cell responses and anti-tumor efficacy. **a** Percentage of OVA, M38 and E7-specific CD8<sup>+</sup> T cells, identified using MHC class I multimers. Mice were infected with  $1 \times 10^5$  PFU via IP or IN MCMV-IE2-OVA at day 0. After 35 days, the mice were vaccinated with  $1 \times 10^5$  PFU MCMV-IE2-E7 via IP route or with  $5 \times 10^5$  MCMV-IE2-E7 via the SC route as shown in the schematic. T cell responses were followed for 70 days in blood. Data represent mean values  $\pm$  SEM. **b** and **c** Tumor outgrowth (**b**) and survival (**c**) of mice infected with  $1 \times 10^5$  PFU MCMV-IE2-OVA via IP or IN and vaccinated with  $1 \times 10^5$  PFU MCMV-IE2-E7 via IP or IN route or with  $5 \times 10^5$  MCMV-IE2-E7 via SC as shown in the schematic. After 70 days, all the vaccinated and control mice were challenged with  $1 \times 10^5$  TC-1 tumor cells. The number of tumor-free/total mice is indicated above each tumor outgrowth graph. **d** The percentage of E7-specific CD8<sup>+</sup> T cells within the total CD8<sup>+</sup> T cell population in the blood (y-axis) plotted against the E7-specific CD8<sup>+</sup> T cell response ranked from low to high (x-axis) of the mice that were either tumor-free (tumor-) or tumor positive (tumor+). Data are representative of two independent experiments with similar results.

## Single-cycle replication is sufficient for the anti-tumor efficacy of MCMV based vaccine vectors

Non-attenuated CMV may cause disease in immunosuppressed individuals. To facilitate the translation of CMV-based vaccine vectors into the clinic, we generated an attenuated E7-epitope-expressing MCMV vector by fusing the FKBP-degradation domain to the essential M79 protein (MCMV-M79-FKBP-E7), which restricts viral replication to a single-cycle in absence of the stabilizing ligand Shield-1 similar to corresponding HCMV FKBP constructs targeting the homologous UL79 gene (Additional file 2:FigureS2). Vaccination with the spread-deficient MCMV-M79-FKBP-E7 elicited E7-specific CD8<sup>+</sup> T cell responses that were > 0.5% of the total CD8<sup>+</sup> T cell population at 4 weeks and even up to 13 months after vaccination (Fig. 7a and b). In addition, the E7-specific CD8<sup>+</sup> T cells displayed an EM phenotype at late time-points post immunization (Fig. 7c). IP immunization with MCMV-M79-FKBP-E7, but not with a control single-cycle virus expressing the immuno-dominant HSV gB epitope (MCMV-M79-FKBP-gB), prevented TC-1 tumor progression at 4 weeks, 21 weeks and 13 months post-vaccination indicating long-lasting specific anti-tumor immunity (Fig. 7d). In a similar fashion, MCMV-M79-FKBP-E7 vaccination prevented outgrowth of C3 and TC-1 tumors in most mice (Fig. 7e, Additional file 3: Figure S3A and data not shown). Low level pre-existing immunity elicited via IN infection with MCMV-IE2-OVA did not impact the anti-tumor efficacy of MCMV-M79-FKBP-E7 (Fig. 7e). In mice that succumbed to the tumor challenge, the E7-specific CD8<sup>+</sup> T cell responses were all < 0.3%, while all (except one) of the protected mice had responses > 0.3% (Fig. 7f).

To investigate the efficacy of MCMV-based vaccine vectors in therapeutic settings, we challenged naïve mice with TC-1 tumor cells followed by vaccination when tumors were palpable. Tumor-bearing mice vaccinated with MCMV-IE2-E7 and with MCMV-M79-FKBP-E7 via the IP and SC route resulted in substantial suppression of tumor outgrowth (Fig. 7g and Additional file 3:Figure S3B). Together these data indicate that a single-cycle MCMV-based vector could offer a safe vaccine platform to induce effective anti-tumor CD8<sup>+</sup> T cell responses in prophylactic and therapeutic settings.

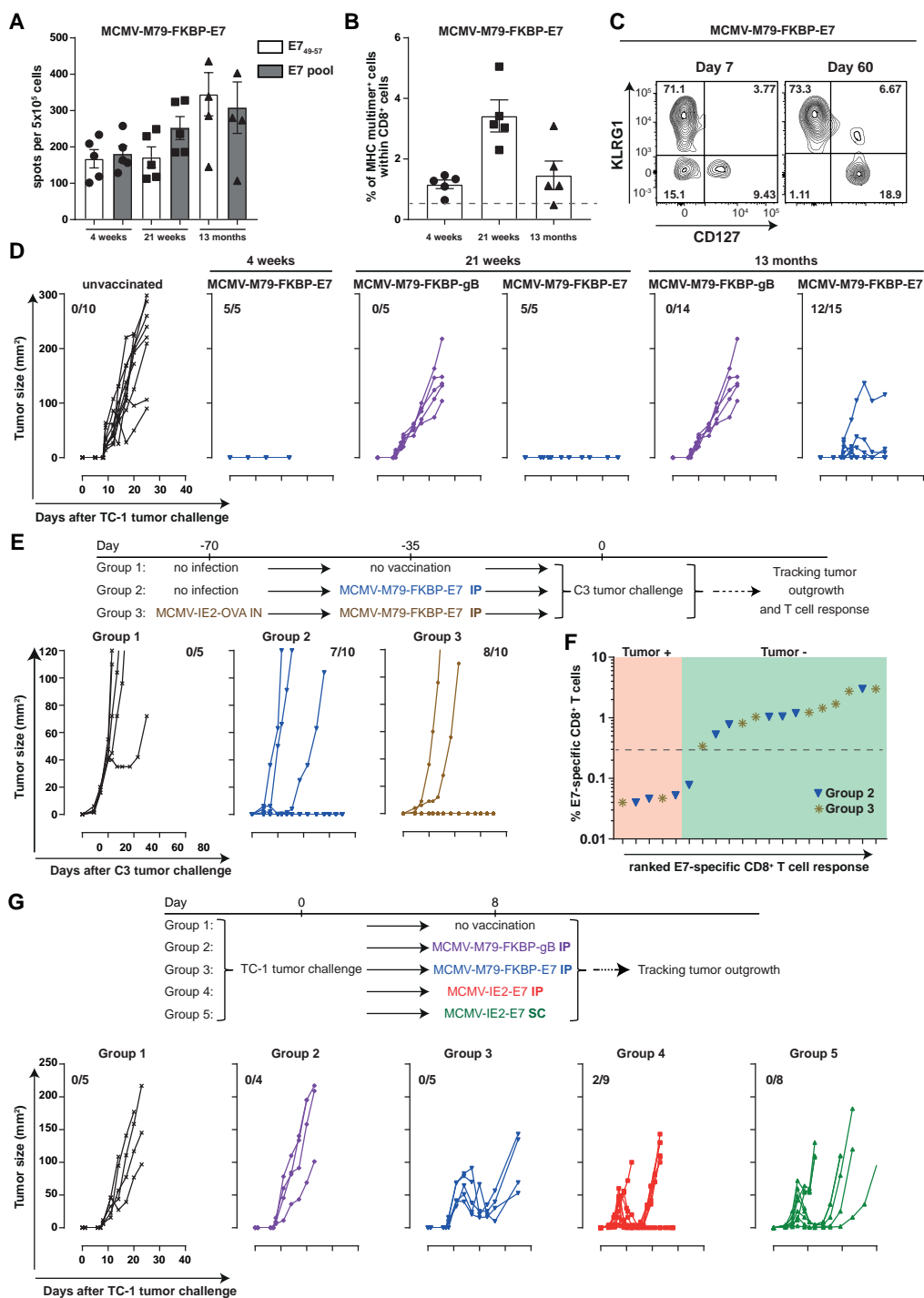
## Discussion

Here we interrogated whether vaccination thresholds based on the level of tumor-specific T cells elicited by CMV-based vaccines can be sharply defined in order to provide correlates of protection. In addition, we examined the critical factors impacting on the protection threshold and hence the efficacy of CMV-based vaccines against cancer. Fundamentally, we found that CMV-based vaccine vectors have the capacity to provide long-lasting tumor-specific T cell responses that protect against tumors, provided that such responses reach a defined threshold.

CMV-based vectors are thus able to generate defined thresholds of circulating vaccine-specific CD8 T cells that provide long-lasting tumor protection. The factors that determine this threshold such as virus dose, route of vaccination and pre-existing immunity have to be extensively studied to consider the development of effective CMV-based vaccines in cancer patients. CMVs are large viruses (> 230 Kb) encoding more than 170 proteins. Although large viral vaccine vectors eliciting strong T cell responses could possibly lead to competition for antigen-presentation and “space”, which may limit additional T cell responses, this seems not to hamper vaccine-specific T cell responses elicited by CMV. Both in mice and monkeys, CMVs have shown to be very potent inducers of T cell responses to antigens in SIV, *Mycobacterium tuberculosis*, Ebola [14–18] and several cancers including melanoma, prostate cancer and HPV+ cancer (unpublished data Klaus Früh). With respect to space limitation for effector-memory T cells. There is evidence in mice and human that superinfections are able to add more T cells to the memory pool [36, 37]. Although, the percentage of a given T cell population can decrease when more memory T cells are added to the memory pool the absolute numbers of a given T cell population generally does not reduce.

Defined thresholds for protection based on disease-specific T cells have been scarcely reported. Schmidt et al. reported that protection against malaria required a large threshold in memory CD8 T cell frequencies, i.e. > 1% specific T cells of the total CD8+ T cell population in blood [38]. Here we found that a threshold of > 0.3% specific blood CD8+ T cells links to full tumor protection. The sharp threshold we observed suggest that the elicited tumor-specific T cells have a controlled capacity to kill target cells, which is in line with studies showing that the *in vivo* killing capacity of CD8+ T cells is marked yet restricted [39]. This demarcated threshold is clearly reached upon vaccination with high dose inoculums of MCMV vectors delivered via the IP and SC route, and protects against the development of subcutaneous tumors. On the other hand, immunization via the IN route, considered as a natural route of infection [40], resulted in minor vaccine-specific responses and hence lower protection. However, IN immunization was superior in protection against respiratory pathogens compared to IP immunization due to enhanced induction of tissue-resident memory (TRM) T cells [41]. It is thus conceivable that lung tumors are better controlled following vaccination via the IN route. In line with this are the observations that upon SC immunization some mice (10–30%) are protected despite that the tumor-specific CD8+ T cell response in the blood is below the threshold. In these mice, the SC immunization may have led to induction of skin TRM cells, known to be able to provide tumor protection [42].

Besides the quantity it is expected that the phenotype of the elicited cells is of influence for the effectivity. Inflating or indefinitely maintained CMV-elicited T cell populations are characterized by their progressive EM-like phenotype [43, 44] and such responses seem to be



qualitatively different from CM T cells with respect to their immediate effector functions and tissue homing properties [45]. These features are important for protection against viruses at their sites of entry or reactivation, and may as well be crucial for clearance of tumors arising e.g. from epithelial or endothelial cells, or metastasis. Here and also reported elsewhere [46] a correlation between the magnitude and phenotype was observed. The combination of phenotype with magnitude provides a better predictor for protective thresholds than either parameter alone.

We found that high levels of pre-existing immunity elicited by SC or IP immunization hamper the development of vaccine-specific T cell responses due to anti-vector immunity thereby reducing the efficacy of MCMV-based vaccine vectors. In contrast, induction of pre-existing immunity by the natural IN route enables sufficient formation of vaccine-specific T cells upon re-inoculation leading to tumor protection. In support of the conclusion that CMVs can overcome natural immunity is also the observation that strains of HCMV have been reported to frequently re-infect seropositive individuals [47, 48]. Moreover, naturally infected seropositive rhesus macaques can be readily re-infected with rhesus CMV (RhCMV) even when given SC at very low dose [49]. Also, RhCMV/SIV vector-immunized monkeys can be repeatedly re-infected via the SC route [50]. In this animal model, the ability to re-infect has been shown to be in part due to the effective inhibition of MHC-I antigen presentation [49]. It may be possible to engineer recombinant HCMV vectors that are able to induce strong and protective immune responses despite pre-existing immunity. For rhesus macaques it was

◀ **Figure 7.** Single cycle replication of MCMV based vector vaccine is sufficient to induce anti-tumor effects in prophylactic and therapeutic settings.

**a.** Mice were vaccinated IP with  $1 \times 10^6$  PFU MCMV-M79-FKBP-E7 or control virus (MCMV-M79-FKBP-gB). Splenocytes were harvested 4, 21 weeks and 13 months after vaccination and stimulated with dominant peptide of E7 or pooled E7 peptides for 36 h (**a**). IFN- $\gamma$  production was measured by ELISPOT assay. Shown is the number of spots per  $5 \times 10^5$  cells  $\pm$  SEM. **b** Frequency of E7<sub>49-57</sub>-specific CD8+ T cells within total CD8+ T cell population at 4, 21 weeks and 13 months post vaccination. Data represents mean values  $\pm$  SEM ( $n = 5$  mice per group). **c** KLRG1 and CD127 marker expression on E7-specific CD8+ T cells at day 7 and 60 post vaccination with MCMV-M79-FKBP-E7. **d** TC-1 tumor outgrowth of the mice that were vaccinated with  $1 \times 10^6$  PFU MCMV-M79-FKBP-E7 or control virus MCMV-M79-FKBP-gB at 4, 21 weeks and 13 months before tumor challenge. Tumor out growth was followed for 23 or 40 days. **e** and **f** C3 tumor outgrowth of the mice were infected with  $1 \times 10^5$  PFU MCMV-IE2-OVA via IN route or kept uninfected. After 35 days, the mice were vaccinated with  $1 \times 10^6$  PFU MCMV-M79-FKBP IP or kept unvaccinated. Mice were challenged with C3 tumor cells after 35 days. Tumor outgrowth was followed for 60 days (**e**). The number of tumor-free mice from the total mice is indicated above each tumor out growth graph. **f** The percentage of E7-specific CD8+ T cells within the total CD8+ T cell population in the blood (y-axis) plotted against the E7-specific CD8+ T cell response ranked from low to high (x-axis) of the mice that were either tumor-free (tumor-) or tumor positive (tumor+) (**f**). **g** Mice were challenged with TC-1 tumor cells, and after 8 days when tumors were palpable mice were treated with  $1 \times 10^6$  PFU MCMV-m79-FKBP-E7 or control virus MCMV-m79-FKBP-gB via IP,  $1 \times 10^5$  PFU MCMV-IE2-E7 via IP or  $5 \times 10^5$  PFU MCMV-IE2-E7 via SC or kept unvaccinated. Tumor out growth was followed for 40 days. The number of tumor-free mice from the total mice is indicated. Data are representative of two independent experiments with similar results

already shown that RhCMV vectors containing SIV antigens provide strong vector-elicited T cell immunity and protection against highly virulent SIV challenge in CMV positive animals [50]. Interestingly, the specific vaccine vectors used in these challenge experiments were highly unusual in their T cell targeting phenotype since they elicited CD8<sup>+</sup> T cells recognizing epitopes presented by MHC class II and MHC-E molecules [51]. Unconventional T cell priming was in part due to conserved MHC class I evasion mechanisms and in part the result of spontaneous genetic changes that occurred in the vectors due to passaging in fibroblasts. However, fibroblast-adapted HCMV-based vaccines did neither elicit HCMV-typical strong effector memory T cell responses nor were the responses unconventional suggesting that unconventional T cell priming is the result of specific mutations that occurred in fibroblasts-adapted RhCMV, but not HCMV [52]. It remains thus to be determined whether HCMV vectors can be engineered both to overcome strong pre-existing immunity and to elicit the desired CD8 T cell response, be it conventional or unconventional, required for protection against specific infectious diseases or cancer. Alternatively, MCMV-based vectors might be used in the clinic as human cells can be abortively infected, still leading to expression and presentation of virally vectored genes [53, 54].

Synthetic vaccines and other viral vectors (than CMV-based such as recombinant vaccinia virus) eliciting T cell responses to the HPV-16 tumor antigens E6/E7 have also been extensively studied [31, 55–60], and some of these vaccines have also shown effectiveness in the clinic [61–63]. Although long-lasting responses with some of these vaccines were accomplished (especially after boosting), the percentage of circulating HPV-specific CD8<sup>+</sup> T cell responses seemed to be lesser as compared to the responses elicited by MCMV-IE2-E7 as reported here. Whether CMV-based vaccines are effective in patients still needs to be determined, and to accomplish this additional testing is required. A single high-dose vaccination may already be sufficient given the potential induction of large vaccine-specific CD8<sup>+</sup> T cell responses. Booster regimens with the same CMV-based vectors in therapeutic settings may not work because of high-levels of pre-existing immunity and/or acquired tumor cell resistance after the initial immunization [3]. Yet given their promising results in experimental models an endeavour to test CMV-vectors in the clinic is worth pursuing.

In conclusion, we show that protective thresholds upon immunization with MCMV vectors can be sharply defined via determination of tumor-specific CD8 T cells in blood, and that the inoculum dosage and route of infection are crucial elements determining the magnitude of these cells. In addition, our study shows the importance of determining the level of pre-existing immunity for CMV-based vaccines and suggests including stratification based on the magnitude of CMV-specific T cell responses in pre-vaccinated individuals. The route and dose of immunization may then even be adjusted to improve the vaccine efficacy. Further studies will be needed with the anticipation to improve the efficacy of CMV-based vaccines.

## Acknowledgements

The authors acknowledge Suzanne Welten and Anke Redeker for advice and practical help. The authors would like to thank Jan Wouter Drijfhout and Kees Franken for constructing tetramers.

## Funding

This work was supported by a grant from Leiden University Medical Center (LUMC; E. Beyranvand Nejad), and a Gisela Thier grant from LUMC (R. Arens).

## Availability of data and materials

All data generated or analyzed during this study are included in this published article [and its Additional files].

## Authors' contributions

EB, RB, KF, SB and RA contributed to the study concepts and study design. Data acquisition was performed by EB, RB, EP, CM, JO. All the authors contributed to the quality control data, analysis and interpretation of data. The manuscript preparation was performed by EB and RA and edited by all authors. All authors read and approved the final manuscript.

## Ethics approval and consent to participate

All animal experiments were approved by the institutional Animal Experiments Committee and were executed according to the institutional animal experimentation guidelines and were in compliance with the guidelines of the Institutional, European and Federal USA animal care and usage committees.

## Consent for publication

We confirm that the manuscript has been read and approved by all named authors and that there are no other persons who satisfied the criteria for authorship but are not listed. We further confirm that the order of authors listed in the manuscript has been approved by all of us.

We confirm that we have given due consideration to the protection of intellectual property associated with this work and that there are no impediments to publication, including the timing of publication, with respect to intellectual property. In so doing we confirm that we have followed the regulations of our institutions concerning intellectual property.

## Competing interests

The authors declare that they have no competing interests.





## **Publisher's Note**

Springer Nature remains neutral with regard to jurisdictional claims in published maps and institutional affiliations.

## **Author details**

1 Department of Immunohematology and Blood Transfusion, Leiden University Medical Center, Albinusdreef 2, 2333, ZA, Leiden, The Netherlands. 2Department of Medical Oncology, Leiden University Medical Center, Leiden, The Netherlands. 3Vir Biotechnology, Portland, OR, USA. 4Department of Vaccinology and Applied Microbiology, Helmholtz Centre for Infection Research, Braunschweig, Germany. 5Institute for Virology, Hannover Medical School, Hannover, Germany. 6German Centre for Infection Research (DZIF), Partner site, Hannover/Braunschweig, Germany.

Received: 18 September 2018 Accepted: 8 January 2019.

## References

1. Redeker A, Arens R. Improving Adoptive T Cell Therapy: The Particular Role of T Cell Costimulation, Cytokines, and Post-Transfer Vaccination. *Front Immunol.* 2016;7:345.
2. Sharma P, Allison JP. The future of immune checkpoint therapy. *Science.* 2015;348(6230):56–61.
3. van der Burg SH, Arens R, Ossendorp F, van Hall T, Melief CJ. Vaccines for established cancer: overcoming the challenges posed by immune evasion. *Nat Rev Cancer.* 2016;16(4):219–33.
4. Plotkin SA. Vaccines: correlates of vaccine-induced immunity. *Clin Infect Dis.* 2008;47(3):401–9.
5. Karrer U, Sierro S, Wagner M, Oxenius A, Hengel H, Koszinowski UH, et al. Memory inflation: continuous accumulation of antiviral CD8<sup>+</sup> T cells over time. *J Immunol.* 2003;170(4):2022–9.
6. O'Hara GA, Welten SP, Klenerman P, Arens R. Memory T cell inflation: understanding cause and effect. *Trends Immunol.* 2012;33(2):84–90.
7. Sylwester AW, Mitchell BL, Edgar JB, Taormina C, Pelte C, Ruchti F, et al. Broadly targeted human cytomegalovirus-specific CD4<sup>+</sup> and CD8<sup>+</sup> T cells dominate the memory compartments of exposed subjects. *J Exp Med.* 2005;202(5):673–85.
8. Welten SP, Redeker A, Toes RE, Arens R. Viral persistence induces antibody inflation without altering antibody avidity. *J Virol.* 2016;90(9):4402–11.
9. Klenerman P, Oxenius A. T cell responses to cytomegalovirus. *Nat Rev Immunol.* 2016;16(6):367–77.
10. Ross SA, Arora N, Novak Z, Fowler KB, Britt WJ, Boppana SB. Cytomegalovirus reinfections in healthy seroimmune women. *J Infect Dis.* 2010;201(3):386–9.
11. Trgovcich J, Kincaid M, Thomas A, Griessl M, Zimmerman P, Dwivedi V, et al. Cytomegalovirus Reinfections Stimulate CD8 T-Memory Inflation. *PLoS One.* 2016;11(11):e0167097.
12. Kenneson A, Cannon MJ. Review and meta-analysis of the epidemiology of congenital cytomegalovirus (CMV) infection. *Rev Med Virol.* 2007;17(4): 253–76.
13. Borst EM, Benkartek C, Messerle M. Use of bacterial artificial chromosomes in generating targeted mutations in human and mouse cytomegaloviruses. *Curr Protoc Immunol.* 2007; Chapter 10:Unit.
14. Hansen SG, Ford JC, Lewis MS, Ventura AB, Hughes CM, Coyne-Johnson L, et al. Profound early control of highly pathogenic SIV by an effector memory T-cell vaccine. *Nature.* 2011;473(7348):523–7.
15. Tsuda Y, Caposio P, Parkins CJ, Botto S, Messaoudi I, Cicin-Sain L, et al. A replicating cytomegalovirus-based vaccine encoding a single Ebola virus nucleoprotein CTL epitope confers protection against Ebola virus. *PLoS Negl Trop Dis.* 2011;5(8):e1275.
16. Beverley PC, Ruzsics Z, Hey A, Hutchings C, Boos S, Bolinger B, et al. A novel murine cytomegalovirus vaccine vector protects against *Mycobacterium tuberculosis*. *J Immunol.* 2014;193(5):2306–16.
17. Marzi A, Murphy AA, Feldmann F, Parkins CJ, Haddock E, Hanley PW, et al. Cytomegalovirus-based vaccine expressing Ebola virus glycoprotein protects nonhuman primates from Ebola virus infection. *Sci Rep.* 2016;6:21674.
18. Hansen SG, Zak DE, Xu G, Ford JC, Marshall EE, Malouli D, et al. Prevention of tuberculosis in rhesus macaques by a cytomegalovirus-based vaccine. *Nat Med.* 2018;24(2):130–43.
19. Erkes DA, Xu G, Daskalakis C, Zurbach KA, Wilski NA, Moghbeli T, et al. Intratumoral infection with murine cytomegalovirus synergizes with PD-L1 blockade to clear melanoma lesions and induce long-term immunity. *Mol Ther.* 2016;24(8):1444–55.
20. Xu G, Smith T, Grey F, Hill AB. Cytomegalovirus-based cancer vaccines expressing TRP2 induce rejection of melanoma in mice. *Biochem Biophys Res Commun.* 2013;437(2):287–91.
21. Benonisson H, Sow HS, Breukel C, Claassens JWC, Brouwers C, Linssen MM, et al. FcγRI expression on macrophages is required for antibody-mediated tumor protection by cytomegalovirus-based vaccines. *Oncotarget.* 2018;9(50):29392–402.



22. Qiu Z, Huang H, Grenier JM, Perez OA, Smilowitz HM, Adler B, et al. Cytomegalovirus-based vaccine expressing a modified tumor antigen induces potent tumor-specific CD8(+) T-cell response and protects mice from melanoma. *Cancer Immunol Res.* 2015;3(5):536–46.
23. Klyushnenkova EN, Kouivaskaia DV, Parkins CJ, Caposio P, Botto S, Alexander RB, et al. A cytomegalovirus-based vaccine expressing a single tumor-specific CD8+ T-cell epitope delays tumor growth in a murine model of prostate cancer. *J Immunother.* 2012;35(5):390–9.
24. Trsan T, Vukovic K, Filipovic P, Brizic AL, Lemmermann NAW, Schober K, et al. Cytomegalovirus vector expressing RAE-I $\gamma$  induces enhanced anti-tumor capacity of murine CD8(+) T cells. *Eur J Immunol.* 2017;47(8): 1354–67.
25. Welten SP, Redeker A, Franken KL, Benedict CA, Yagita H, Wensveen FM, et al. CD27-CD70 costimulation controls T cell immunity during acute and persistent cytomegalovirus infection. *J Virol.* 2013;87(12):6851–65.
26. Dekhtiarenko I, Ratts RB, Blatnik R, Lee LN, Fischer S, Borkner L, et al. Peptide processing is critical for T-cell memory inflation and may be optimized to improve immune protection by CMV-based vaccine vectors. *PLoS Pathog.* 2016;12(12):e1006072.
27. Warming S, Costantino N, Court DL, Jenkins NA, Copeland NG. Simple and highly efficient BAC recombineering using galK selection. *Nucleic Acids Res.* 2005;33(4):e36.
28. Dekhtiarenko I, Jarvis MA, Ruzsics Z, Cicin-Sain L. The context of gene expression defines the immunodominance hierarchy of cytomegalovirus antigens. *J Immunol.* 2013;190(7):3399–409.
29. Perng YC, Qian Z, Fehr AR, Xuan B, Yu D. The human cytomegalovirus gene UL79 is required for the accumulation of late viral transcripts. *J Virol.* 2011; 85(10):4841–52.
30. Lin KY, Guarnieri FG, Staveley-O'Carroll KF, Levitsky HI, August JT, Pardoll DM, et al. Treatment of established tumors with a novel vaccine that enhances major histocompatibility class II presentation of tumor antigen. *Cancer Res.* 1996;56(1):21–6.
31. van Duikeren S, Fransen MF, Redeker A, Wieles B, Platenburg G, Krebber W-J, et al. Vaccine-induced effector-memory CD8+ T cell responses predict therapeutic efficacy against tumors. *J Immunol.* 2012;189(7):3397–403.
32. Feltkamp MC, Smits HL, Vierboom MP, Minnaar RP, De Jongh BM, Drijfhout JW, et al. Vaccination with cytotoxic T lymphocyte epitope-containing peptide protects against a tumor induced by human papillomavirus type 16- transformed cells. *Eur J Immunol.* 1993;23(9):2242–9.
33. Redeker A, Welten SP, Baert MR, Vloemans SA, Tiemessen MM, Staal FJ, et al. The quantity of autocrine IL-2 governs the expansion potential of CD8+ T cells. *J Immunol.* 2015;195(10):4792–801.
34. Arens R, Loewendorf A, Redeker A, Sierro S, Boon L, Klenerman P, et al. Differential B7-CD28 costimulatory requirements for stable and inflationary mouse cytomegalovirus-specific memory CD8 T cell populations. *J Immunol.* 2011;186(7):3874–81.
35. Altman JD, Moss PAH, Goulder PJR, Barouch DH, McHeyzer-Williams MG, Bell JI, et al. Phenotypic analysis of antigen-specific T lymphocytes. *Science.* 1996;274(5284):94–6.
36. van Leeuwen EM, Koning JJ, Remmerswaal EB, van BD, van Lier RA, ten Berge IJ. Differential usage of cellular niches by cytomegalovirus versus EBV-and influenza virus-specific CD8+ T cells. *J Immunol* 2006;177(8):4998–5005.
37. Vezys V, Yates A, Casey KA, Lanier G, Ahmed R, Antia R, et al. Memory CD8 T- c e l l compartment grows in size with immunological experience. *Nature.* 2009;457(7226):196–9.
38. Schmidt NW, Podymnugin RL, Butler NS, Badovinac VP, Tucker BJ, Bahjat KS, et al. Memory CD8 T cell responses exceeding a large but definable threshold provide long-term immunity to malaria. *Proc Natl Acad Sci U S A.* 2008;105(37):14017–22.
39. Halle S, Keyser KA, Stahl FR, Busche A, Marquardt A, Zheng X, et al. In vivo killing capacity of cytotoxic T cells is limited and involves dynamic interactions and T cell cooperativity. *Immunity.* 2016;44(2):233–45.

40. Oduro JD, Redeker A, Lemmermann NA, Ebermann L, Marandu TF, Dekhtiarenko I, et al. Murine cytomegalovirus infection via the intranasal route offers a robust model of immunity upon mucosal CMV infection. *J Gen Virol*. 2016;97(1):185–95.
41. Morabito KM, Ruckwardt TR, Redwood AJ, Moin SM, Price DA, Graham BS. Intranasal administration of RSV antigen-expressing MCMV elicits robust tissue-resident effector and effector memory CD8<sup>+</sup> T cells in the lung. *Mucosal Immunol*. 2017;10(2):545–54.
42. Galvez-Cancino F, Lopez E, Menares E, Diaz X, Flores C, Caceres P, et al. Vaccination-induced skin-resident memory CD8<sup>+</sup> T cells mediate strong protection against cutaneous melanoma. *Oncoimmunology*. 2018;7(7): e1442163.
43. Redeker A, Remmerswaal EBM, van der Gracht ETI, Welten SPM, Holtt T, Koning F, et al. The contribution of cytomegalovirus infection to immune senescence is set by the infectious dose. *Front Immunol*. 2017;8:1953.
44. Pardieck IN, Beyrend G, Redeker A, Arens R. Cytomegalovirus infection and progressive differentiation of effector-memory T cells. *F1000Res*. 2018;7:1554.
45. Appay V, Dunbar PR, Callan M, Klenerman P, Gillespie GM, Papagno L, et al. Memory CD8<sup>+</sup> T cells vary in differentiation phenotype in different persistent virus infections. *Nat Med*. 2002;8(4):379–85.
46. Redeker A, Welten SP, Arens R. Viral inoculum dose impacts memory T-cell inflation. *Eur J Immunol*. 2014;44(4):1046–57.
47. Bale JF Jr, Petheram SJ, Souza IE, Murph JR. Cytomegalovirus reinfection in young children. *J Pediatr*. 1996;128(3):347–52.
48. Gorzer I, Kerschner H, Redlberger-Fritz M, Puchhammer-Stockl E. Human cytomegalovirus (HCMV) genotype populations in immunocompetent individuals during primary HCMV infection. *J Clin Virol*. 2010;48(2):100–3.
49. Hansen SG, Powers CJ, Richards R, Ventura AB, Ford JC, Siess D, et al. Evasion of CD8<sup>+</sup> T cells is critical for superinfection by cytomegalovirus. *Science*. 2010;328(5974):102–6.
50. Hansen SG, Vieville C, Whizin N, Coyne-Johnson L, Siess DC, Drummond DD, et al. Effector memory T cell responses are associated with protection of rhesus monkeys from mucosal simian immunodeficiency virus challenge. *Nat Med*. 2009;15(3):293–9.
51. Hansen SG, Wu HL, Burwitz BJ, Hughes CM, Hammond KB, Ventura AB, et al. Broadly targeted CD8<sup>+</sup> T cell responses restricted by major histocompatibility complex E. *Science*. 2016;351(6274):714–20.
52. Murray SE, Nesterenko PA, Vanarsdall AL, Munks MW, Smart SM, Veziroglu EM, et al. Fibroblast-adapted human CMV vaccines elicit predominantly conventional CD8 T cell responses in humans. *J Exp Med*. 2017; 31(20161988):20161988.
53. Wang X, Messerle M, Sapinoro R, Santos K, Hocknell PK, Jin X, et al. Murine cytomegalovirus abortively infects human dendritic cells, leading to expression and presentation of virally vectored genes. *J Virol*. 2003;77(13): 7182–92.
54. Tang Q, Maul GG. Mouse cytomegalovirus crosses the species barrier with help from a few human cytomegalovirus proteins. *J Virol*. 2006; 80(15):7510–21.
55. van der Burg SH, Kwappenberg KM, O'Neill T, Brandt RM, Melief CJ, Hickling JK, et al. Pre-clinical safety and efficacy of TA-CIN, a recombinant HPV16 L2E6E7 fusion protein vaccine, in homologous and heterologous prime-boost regimens. *Vaccine*. 2001;19(27):3652–60.
56. Baldwin PJ, van der Burg SH, Boswell CM, Offringa R, Hickling JK, Dobson J, et al. Vaccinia-expressed human papillomavirus 16 and 18 e6 and e7 as a therapeutic vaccination for vulval and vaginal intraepithelial neoplasia. *Clin Cancer Res*. 2003;9(14):5205–13.
57. Lee SY, Kang TH, Knoff J, Huang Z, Soong RS, Alvarez RD, et al. Intratumoral injection of therapeutic HPV vaccinia vaccine following cisplatin enhances HPV-specific antitumor effects. *Cancer Immunol Immunother*. 2013;62(7): 1175–85.

58. Galliverti G, Tichet M, Domingos-Pereira S, Hauert S, Nardelli-Haeffliger D, Swartz MA, et al. Nanoparticle conjugation of human papillomavirus 16 E7-long peptides enhances therapeutic vaccine efficacy against solid tumors in mice. *Cancer Immunol Res*. 2018;6(11):1301–13.
59. Peng S, Qiu J, Yang A, Yang B, Jeang J, Wang JW, et al. Optimization of heterologous DNA-prime, protein boost regimens and site of vaccination to enhance therapeutic immunity against human papillomavirus-associated disease. *Cell Bioscience*. 2016;6:16.
60. Domingos-Pereira S, Derre L, Warpelin-Decrausaz L, Haeffliger JA, Romero P, Jichlinski P, et al. Intravaginal and subcutaneous immunization induced vaccine specific CD8 T cells and tumor regression in the bladder. *J Urol*. 2014;191(3):814–22.
61. Andrews DM, Estcourt MJ, Andoniou CE, Wikstrom ME, Khong A, Voigt V, et al. Innate immunity defines the capacity of antiviral T cells to limit persistent infection. *J Exp Med*. 2010;207(6):1333–43.
62. Kenter GG, Welters MJ, Valentijn AR, Lowik MJ, Berends-van der Meer DM, Vloon AP, et al. vaccination against HPV-16 oncoproteins for vulvar intraepithelial neoplasia. *N Engl J Med*. 2009;361(19):1838–47.
63. van Poelgeest MI, Welters MJ, Vermeij R, Stynenbosch LF, Loof NM, Berends-van der Meer DM, et al. vaccination against Oncoproteins of HPV16 for noninvasive vulvar/vaginal lesions: lesion clearance is related to the strength of the T-cell response. *Clin Cancer Res*. 2016;22(10):2342–50.

Supplementary figures

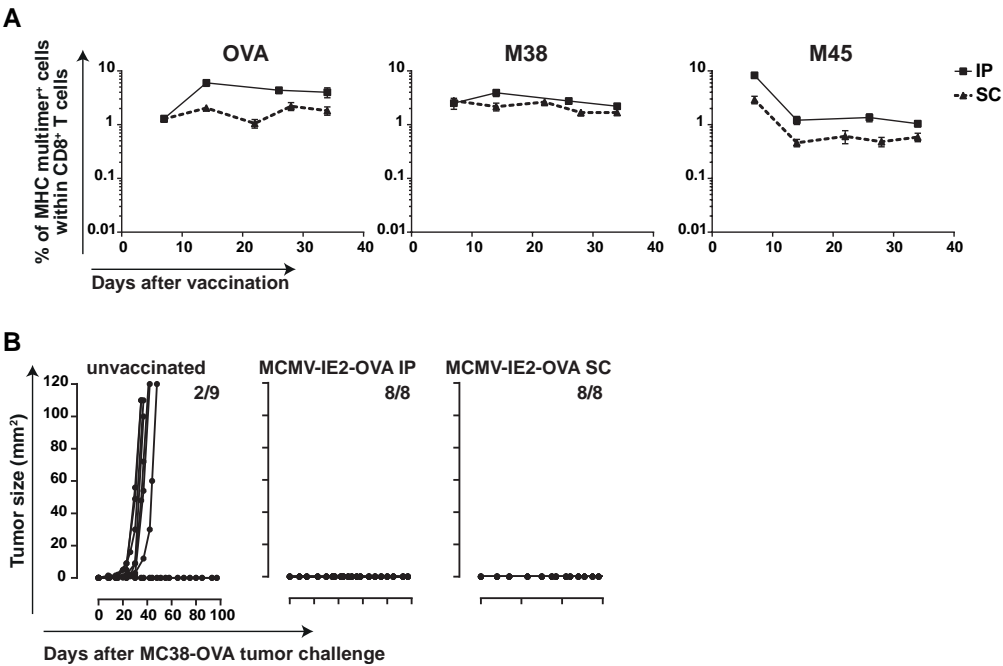


**Figure S1.** Immunization with MCMV-IE2-OVA induces vaccine-specific CD8+ T cell responses. (A) Mice were infected with  $1 \times 10^5$  PFU MCMV-IE2-OVA via IP or  $5 \times 10^5$  via SC. Frequency of antigen-specific CD8+ T cells for the M45 and M38 epitopes of MCMV and of the inserted OVA antigen were identified using MHC class I multimers. Data represents mean values  $\pm$  SEM ( $n = 6$  mice per group). Data are representative of two independent experiments. (B) MC38-OVA tumor outgrowth of unvaccinated mice and of mice previously vaccinated with MCMV-IE2-OVA via the IP or SC route. Mice were vaccinated with  $1 \times 10^5$  PFU MCMV-IE2-OVA via IP or  $5 \times 10^5$  via SC. After 35 days (MCMV-IE2-OVA IP) or 70 days (MCMV-IE2-OVA SC), mice were challenged with  $2.5 \times 10^5$  MC38-OVA tumor cells. The tumor outgrowth was followed for 100 days. The number of tumor-free/total mice is indicated in each graph. Data are representative of two independent with similar results. (EPS 1218 kb)

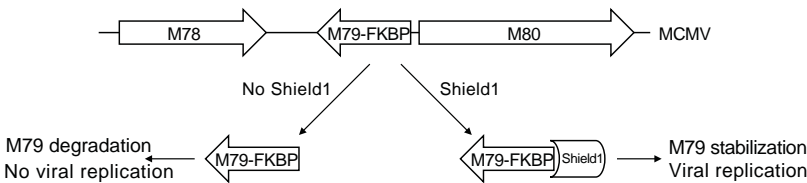
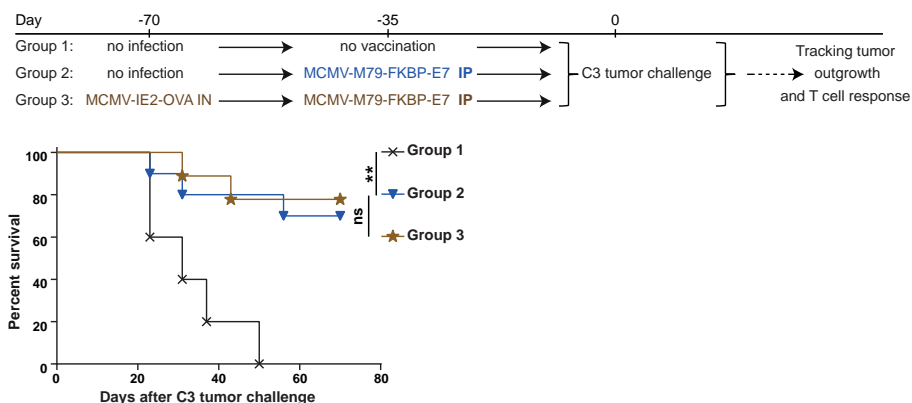


**Figure S2.** Fusion of the FKBP-degradation domain to the essential gene M79 results in a single cycle MCMV. Schematic diagram of the construct. The FKBP degradation domain was fused in frame to the N-terminus of M79 via BAC recombination (MCMV-M79-FKBP-E7). In the presence of the small molecule Shield1 the fusion protein is stabilized and virus production occurs. In the absence of Shield1 M79 is degraded and virus production is halted since M79 is essential for late gene expression. (EPS 1463 kb)



**A**



**B**

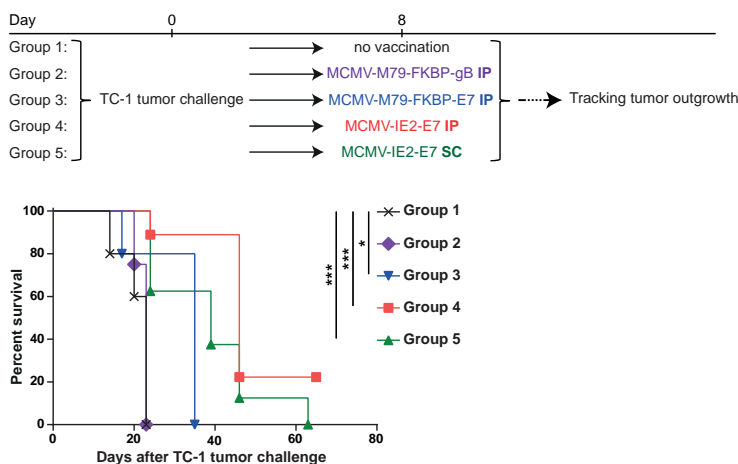


**Figure S3.** Single cycle replication of MCMV based vectors induces anti-tumor effects. **(A)** Survival of the mice which were infected with  $1 \times 10^5$  PFU MCMV-IE2-OVA IN or kept uninfected. After 35 days, the mice were vaccinated with  $1 \times 10^6$  PFU MCMV-M79-FKBP IP or kept unvaccinated. Mice were challenged with C3 tumor cells after 35 days. Survival was followed for 60 days. **(B)** Survival of the mice which were challenged with TC-1 tumor cells, and after 8 days when tumors were palpable mice were treated with  $1 \times 10^6$  PFU MCMV-M79-FKBP-E7 or control virus MCMV-M79-FKBP-gB via IP,  $1 \times 10^5$  PFU MCMV-IE2-E7 via IP or  $5 \times 10^5$  PFU MCMV-IE2-E7 via SC or kept unvaccinated. Survival growth was followed for 60 days. \*,  $P < 0.05$ ; \*\*,  $P < 0.01$ ; \*\*\*,  $P < 0.001$ . (EPS 1213 kb)







# Chapter 6

## The importance of correctly timing cancer immunotherapy

*Elham Beyranvand Nejad<sup>a,b\*</sup>, Marij J.P. Welters<sup>a\*</sup>, Ramon Arens<sup>b</sup> and Sjoerd H. van der Burg<sup>a</sup>*

Expert Opin Biol Ther. 2017 Jan;17(1):87-103. Epub 2016 Nov 16.

a. Department of Medical Oncology, Leiden University Medical Center, Leiden, The Netherlands

b. Department of Immunohematology and Blood Transfusion, Leiden University Medical Center, Leiden, The Netherlands

## **ABSTRACT**

### **Introduction**

The treatment options for cancer – surgery, radiotherapy and chemotherapy – are now supplemented with immunotherapy. Previously underappreciated but now gaining strong interest are the immune modulatory properties of the three conventional modalities. Moreover, there is a better understanding of the needs and potential of the different immune therapeutic platforms. Key to improved treatment will be the combinations of modalities that complete each other's shortcomings.

### **Area covered**

Tumor-specific T-cells are required for optimal immunotherapy. In this review, the authors focus on the correct timing of different types of chemotherapeutic agents or immune modulators and immunotherapeutic drugs, not only for the activation and expansion of tumor-specific T-cells but also to support and enhance their anti-tumor efficacy.

### **Expert opinion**

At an early phase of disease, clinical success can be obtained using single treatment modalities but at later disease stages, combinations of several modalities are required. The gain in success is determined by a thorough understanding of the direct and indirect immune effects of the modalities used. Profound knowledge of these effects requires optimal tuning of immunomonitoring. This will guide the appropriate combination of treatments and allow for correct sequencing the order and interval of the different therapeutic modalities.

### **Keywords**

Cancer; immunotherapy; timing; combination therapy; immunomonitoring.

## Introduction

The common treatment options for cancer patients so far were surgery, radiotherapy and/or chemotherapy. This is now supplemented with a fourth treatment modality that is called immunotherapy. The latter encompasses several strategies aiming to reinforce the immune system's attack of tumor cells by activation of tumor-specific lymphocytes, alleviation of immune suppressive mechanisms and stimulation of immune effector cell infiltration. Prime examples are vaccination strategies and the adoptive transfer of expanded tumor infiltrating (T-cell receptor engineered or re-educated) lymphocytes to increase the number of tumor-specific T-cells required to control tumor cell growth [1,2]. For instance, a synthetic long peptide (SLP) vaccination against human papillomavirus type 16 (HPV16) resulted in complete clearance of HPV16-induced high-grade premalignant lesions of the vulva in ~50% of the patients [3,4]. Importantly, prolonged survival was found in patients treated with the food and drug administration (FDA) approved autologous cellular vaccine sipuleucel-T for castration-resistant prostate cancer [5]. Furthermore, adoptive transfer of autologous T-cells resulted in clinical objective responses in half of the treated melanoma patients [6,7]. Moreover, cancer regression and improved survival has been achieved in melanoma and lung cancer patients using antibodies to coinhibitory molecules, including anticytotoxic T-lymphocyte-associated protein 4 (CTLA-4; ipilimumab, tremelimumab) antibodies [8,9], anti-programmed cell death protein 1 (anti-PD-1; nivolumab, pembrolizumab) antibodies [10–13] and anti-programmed death-ligand 1 (anti-PD-L1; avelumab, atezolizumab; durvalumab) antibodies [14–17]. Clinical success has also been achieved using targeted therapies aiming to inhibit molecular pathways that are important for tumor growth and maintenance, either as a single therapy or in combination with immunotherapeutic strategies [18]. In addition, epigenetic drugs to upregulate immune signaling combined with immunotherapy are currently under investigation [19,20], but this is beyond the scope of the current review.

In spite of all the mentioned immunotherapeutic strategies, there are still numerous cancer patients who do not benefit from these immunotherapeutic drugs. Monotherapy, although successful in a number of cases, is not expected to have a major impact as established tumors use diverse strategies to evade the immune system, a process that is called immunoediting [2,21,22]. Under the attack of the immune system, tumor cells may alter the processes involved in the presentation of antigens to T-cells (i.e. downregulation of major histocompatibility complex (MHC) class I, epigenetic silencing of the antigen processing machinery, loss of tumor associated antigens) or become more resistant to immune mediated effector mechanisms leading to growth arrest and cell death [2]. Furthermore, the tumor microenvironment may become more immunosuppressive by the attraction and/or induction of suppressive immune cells, i.e. regulatory T-cells (Tregs), myeloid-derived suppressor cells (MDSCs), type 2 macrophages (M2) [2,23]. This process leads to a less efficient antitumor



response. Therefore, there is tremendous demand to develop cancer immunotherapies not only to activate the tumor-specific T-cell response but also to strengthen its force by combatting the immune evasion and suppressive pathways to improve the clinical outcome [2,21,22]. Based on these concepts, wise choices for complementary and synergistic combinations of immunotherapeutic drugs have to be made. Importantly, combinations with more conventional treatments should not be discarded. This selection entails a thorough understanding of the immune-modulating and pharmacological properties as well as the limitations of the agents of choice. Together, this should guide the right combination, dose, and treatment schedule and lead to optimal treatment strategies. Here we provide an overview of the current literature on the timing of therapeutic vaccination in cancer patients. First, timing applies to the most appropriate stage of disease in which an immunotherapeutic modality can be used for optimal clinical effects. Second, timing concerns the sequence and interval of a combination of drugs for immunotherapy.

## **Immunotherapy efficacy at various stages of the disease**

### **Treatment of advanced or end-stage cancer may fail due to immune suppression**

Immunotherapy is often tested in advanced or end-stage cancer patients. These patients have lost responsiveness to earlier therapies, the tumor has grown to larger extent and general immune suppression is more pronounced [2,21]. In preclinical mouse models this is reflected by the increasing failure to control tumor outgrowth when the time period between tumor engraftment and vaccination is increased. This is mainly due to increased frequencies of Tregs and myeloid suppressor cells [24]. In the human setting this is exemplified by the many vaccine trials that have failed to show an effect [2]. Thus, in these late stages the tumor micro-milieu may frustrate the effector arm of the immune system through different mechanisms. First of all, the influx of tumor-specific T-cells may be hampered by abnormal vascularization [25,26]. In both a xenograft transplant model and an immune refractory spontaneous murine model this problem could be overcome by treatment with low dose of gamma irradiation [25], or by targeting VEGF (vascular endothelial growth factor) [27]. However, even when the effector cells are inside the tumor they may encounter several immune suppressive hurdles before they can reach and kill the tumor cells [28]. The tumor microenvironment contains cells that are helping the tumor to expand and to evade the immune system such as cancer-associated fibroblasts, MDSCs, M2 and Tregs [29]. The important role of macrophages in tumor progression and the possibilities to target these cells were reviewed previously [30,31]. Targeting these tumor-resident immune suppressive myeloid cells could be an option to improve immunotherapy [30–32]. Hence, it is no surprise that specifically mono-immunotherapy – focused on reinforcing the tumor-specific T-cell response – as a last resort therapy is often not successful.

## Success of therapy at early stages of cancer or minimal residual disease

Better clinical outcomes are expected if one can treat patients before recurrences develop, in settings of minimal residual disease, or at early (pre-malignant) stages of disease. Indeed, as shown in two independent trials, HPV16-SLP vaccination of patients with high-grade pre-malignant lesions of the vulva resulted in complete regressions of the lesion in almost half of the treated patients [3,33]. Vaccination with a HPV16 E6-E7-L2 fusion protein vaccine in combination with Aldara treatment also achieved clinical success in patients with this disease [34]. Moreover, treatment of high-grade pre-malignant lesions of the cervix was efficacious when the patients received a DNA vaccine targeting the HPV16 oncoproteins [35]. Moreover, vaccination of patients with HER<sup>+</sup> breast ductal carcinoma *in situ* resulted in measurable decreases of residual ductal carcinoma [36]. As can be deduced from above, resection of the tumor mass may alleviate immune suppression allowing the use of immunotherapy to prevent new tumors to arise. Indeed, vaccination of patients with completely resected colorectal cancer metastases showed a significant survival advantage when compared to controls [37], whereas HER2 peptide vaccination in disease-free breast cancer patients was associated with a favourable trend for lower recurrences [38]. Unfortunately, this is not always the case as exemplified by a recent report on patients with surgically resected early stage non-small-cell lung cancer whom were vaccinated with MAGE-A3 but failed to show any improvement in disease free survival [39,40].

## Prevention of cancer for patients at risk

Vaccination of individuals to prevent disease has been one of the major achievements in mankind. Current data on the preventive vaccines for cervical cancer and liver cancer support the notion that prevention is key to success [41,42]. Also for non-virally induced cancers, vaccine strategies are being developed for individuals who are at risk to develop cancer. For instance for individuals with BRCA mutations known to induce breast cancer or for those with Lynch syndrome which is associated with colon cancer [43]. Certainly, there are no cancer-associated hurdles to be overcome when a person is still healthy. This allows the vaccine to induce a protective immune response against the tumor antigens expressed by the type of cancer for which they are at risk [44]. Awareness of the regulatory authorities for this approach is very important to successfully combat cancer [45].

## Correctly timing of therapeutic vaccination in combination with other therapies

Therapeutic vaccination in combination with other therapies can roughly be divided into three differently timed treatment schedules. Treatments that are given before vaccination are generally aimed at removing tumor-associated immune suppression. Modalities provided close to or in combination with vaccination aim to prevent immune regulation following

T-cell activation, thereby improving the quality and efficacy of the vaccine-induced T-cell response. Therapies provided after vaccination generally are to boost the T-cell stimulatory effect of the vaccine or their effector function. An overview of such studies is provided in Table 1.

## **Combinations of therapeutic modalities prior to vaccination**

### *Administration of chemotherapy before vaccination alleviates immune suppression*

It is known that both local and systemic immune parameters in patients with cancer are associated with the prognosis and response to therapy [93]. The composition, phenotype and activation status of the tumor infiltrating T-cells, DCs and macrophages have a strong impact on clinical outcome. In cancer patients with a higher tumor load, the tumor micro-environment merely is pro-tumorigenic and suppressive for the immune effector cells. In a number of cases this is also reflected by the immune cell markers and function of immune cells in the blood of these patients, as measured by flow cytometry and/or functional immune assays [94,95].

Chemotherapy, radiotherapy and surgery used for the treatment of cancer are applied for tumor reduction or eradication. As a direct result they will remove cancer-derived factors known to induce immune suppression. However, even when unsuccessful as monotherapy, a number of chemotherapeutic compounds may also have direct effects on the immune system [96,97], albeit that for many of these compounds the underlying mechanisms still remain to be elucidated. In HPV16<sup>+</sup> TC-1 tumor bearing mice and in advanced stage or recurrent HPV16<sup>+</sup> cervical carcinoma patients the number of circulating myeloid cells, including immunosuppressive myeloid cells, is significantly increased when compared to naïve mice and healthy individuals, respectively [48]. The standard chemotherapy treatment (carboplatin combined with paclitaxel) for these advanced cancer patients resulted in normalization of the different myeloid cells in the peripheral blood, starting 2 weeks after the second chemotherapy cycle and coinciding with a stronger general T-cell response and improved antigen presenting capacity. As this chemotherapeutic treatment not only normalized the circulating myeloid cell population in mice but also altered the intratumoral myeloid cell composition and increased the clinical effect of therapeutic vaccination, it is believed that this will also result in a reduced suppressive microenvironment in patients. Indeed, a single vaccination with HPV16-SLP within the correct time window of 2 weeks after the second cycle of chemotherapy resulted in a much stronger HPV-specific T-cell response than observed before, when vaccination was given after chemotherapy failure [4,48]. In line with this data, a similar time window of 12–14 days after combination chemotherapy with carboplatin and paclitaxel has been observed in a study of advanced ovarian cancer patients [47]. Here, they reported that at this time point the number of Tregs was reduced while there were increased percentages of IFN $\gamma$ -

producing CD8<sup>+</sup> T-cells, T-helper (Th1) cells, CD45RO memory T-cells and NKT-cells. Also in extensive stage small cell lung cancer, vaccination with DCs transduced with full-length wild-type p53 gene delivered via an adenoviral vector at least 8 weeks after the last dose of chemotherapy with carboplatin or cisplatin demonstrated a high rate of objective clinical responses, and this was associated with the induction of vaccine-induced immune responses [46].

An effect on the number and function of Tregs has specifically been reported for the chemotherapeutic agent cyclophosphamide [98,99]. Several studies suggest that the optimal time point for vaccination is 3–7 days after this type of chemotherapy [50–52]. In a randomized phase II trial, administration of a single dose of cyclophosphamide, followed by vaccination 3 days later with IMA901, a vaccine that consists of multiple-tumor associated peptides (TUMAPs) plus granulocyte-macrophage colony-stimulating factor (GM-CSF), reduced the number of Tregs and was associated with prolonged survival in immune responder patients with advanced renal cell cancer [52]. Similarly, peripheral blood mononuclear cells (PBMCs) analysis of stage II–III melanoma patients, who were vaccinated with HLA- A\*0201-modified tumor peptides 7 days after low-dose of cyclophosphamide, showed transient reduction in the frequency of Tregs and an increase in vaccine-induced antigen specific CD8<sup>+</sup> T-cells [50]. Other studies in which cyclophosphamide treatment was used, showed that the depletion of Tregs may be associated with the induction of Th17, Th1 and vaccine-induced CD25<sup>+</sup>CD4<sup>+</sup>Foxp3-negative effector T-cells [65,66]. Also other chemotherapeutic compounds may affect Tregs and immune suppressive myeloid cells. Gemcitabine is known to reduce both Tregs and MDSCs in mice and in patients with ovarian cancer [53,54,80,100,101]. A selective decrease in MDSCs was also observed after treatment with 5-fluorouracil (5-FU) [102]. The combination of cisplatin plus vinorelbine appears to significantly increase the ratio between effector T-cells and Tregs and to reduce the immunosuppressive activity of the latter in the blood of the majority of non-small cell lung cancer patients [103]. Therefore, modulation of immune suppressive cells by chemotherapeutic agents prior to anticancer vaccine could explain the additive or synergistic antitumor effect of combined chemotherapy and immunotherapy.

#### *Other interventions applied before vaccination that reduce immune suppression*

Notably, the reduction of immunosuppressive cells can also be mediated by other methods than chemotherapy. These therapies should also be provided prior to administration of immunotherapy or at the time that immunotherapy induces tumor-specific immune responses [104,105]. For instance, in the CT26 tumor model the antibody mediated depletion of CD25<sup>+</sup> T-cells (including Tregs) before immunization with tumor antigen AH1 resulted in long-lasting memory T-cell responses and even augmented a tumor-induced CD4<sup>+</sup> T-cell response [56]. In another study, vaccination with AH1 tumor antigen in combination with the FOXP3-





Table 1. Classification of different combinatorial strategies based on timing regimen and mechanism

Timing of the intervention	Cancer type	Combined treatment regimen	Efficacy/immunological responses of combined treatments	Mechanisms of intervention	References	Timing of the intervention	Intervention
Prior to treatment							
8 weeks before vaccine	Carboplatin + cisplatin	Extensive stage small cell lung cancer	P53 DC cancer vaccine + carboplatin + cisplatin	High rate of objective clinical responses, Association of clinical response with immunologic response	No proposed mechanism	Counteracting suppressive immunity by reducing immunosuppressive cells	Antonia et al. [46]
2 weeks before vaccine	Carboplatin + paclitaxel	Advanced ovarian cancer	Tumor antigen-loaded DCs + carboplatin + paclitaxel	Immune reconstitution Enhanced antitumor immune response		Decreased percentage of Tregs	Wu et al. [47]
2 weeks before vaccine	Carboplatin + paclitaxel	HPV 16/17 TC-1 tumor model Advanced cervical cancer	HPV16-SLP vaccination + carboplatin + paclitaxel	Decreased immunosuppressive myeloid cells, Increased vaccine-induced T-cell response, Improved overall survival of mice	Myeloid cells depletion		Welters et al. [48]
11 days before vaccine	Irradiation	F10 melanoma tumor model	DC-gp100 tumor vaccine + irradiation	Reduced tumor burden and prolonged mouse survival	Decreased Tregs and increase effector-memory T-cells frequency		Liu et al. [49]
7 days before vaccine	Cyclophosphamide	Stage II-III melanoma cancer	HLA-A*0201-modified tumor peptide vaccine + cyclophosphamide + IL-2	Increased tumor-specific T-cells	Lower frequency of Tregs		Canisasischi et al. [50]
4 days before vaccine	Cyclophosphamide	Gastrointestinal, lung, cervical and colorectal cancer	HLA-A2402-restricted tumor-associated antigen epitope peptides + cyclophosphamide	Association of prolonged survival with TAA-specific T-cell responses, Safety and correlation of immune responses with vaccine-induced T-cell response in phase I clinical trial	Reduced number of Tregs		Murahashi et al. [51]
3 days before vaccine	Cyclophosphamide	Advanced renal cell cancer	Multiple tumor associated peptides (TUMAPs) + cyclophosphamide	Prolonged survival in immune responders' patients	Reduced number of Tregs		Walter et al. [52]
4 and 1 days before treatment	Gemcitabine	Mesothelioma AB12 tumor model	IFN- $\beta$ cytokine immunogene therapy + gemcitabine	Enhanced antitumor efficacy	Decreased myeloid suppressor cells		Suzuki et al. [53]
1 day before vaccine	Gemcitabine	Setting without tumor	Particle-mediated epidermal delivery vaccination against NYESO-1	Improved the efficacy of vaccine	Reduced percentage of Tregs		Reitig et al. [54]
4 days before vaccine	Anti-CD25 antibody	B16 melanoma tumor model	Tumor cell-based vaccine + anti-CTLA-4 + anti-CD25	Increased CTL specific response	Depletion of Tregs		Sutmoller et al. [55]
4 days before prophylactic vaccine	Anti-CD25 antibody	CT26 colorectal carcinoma model	tumor-specific peptide vaccine + anti-CD25	Induction of long-lasting antitumoral immune response	Depletion of Tregs		Caesares et al. [56]
1 day before prophylactic vaccine	Anti-CD25 antibody	B16-F10 tumor model	DC vaccine with stressed tumor cells + anti-CD25	Improved the efficacy of treatment and developed long-lived tumor- protective immune responses	Depletion of Tregs		Prasad et al. [57]

5 days before ACT and vaccine	PLX3397 kinase inhibitor	B16F10 melanoma tumor model	Adoptive transfer of pmel-1 CD8 T-cells and peptide vaccination + PLX3397 Kinase inhibitor	Inhibits CSF-1 R Decreased tumor infiltrating macrophages	Sluijter et al. [58]
4 days before ACT	PLX3397 kinase inhibitor	Syngeneic mouse model of BRAF (V600E)-driven melanoma	Adoptive cell therapy + PLX3397 kinase inhibitor	Enhanced CD8-mediated effect of immunotherapy Increase IFN $\gamma$ production of tumor-specific CD8+ T-cells	Mok et al. [59]
Prior to vaccination	IL-2 diphtheria toxin conjugate DAB389IL-2	Renal cell carcinoma	Tumor RNA-transfected DC vaccine + IL-2 diphtheria toxin conjugate DAB389IL-2	Inhibit CSF-1 R, Decreasing tumor-infiltrating myeloid cells Skewing MHCIIhi macrophages	Dannull et al. [60]
2 weeks before vaccine	Chemoradiation	Esophageal squamous cell carcinoma	Multiple epitopes peptide vaccine + cisplatin+ 5FU + radiotherapy	Deplete Tregs	Iinuma et al. [61]
3 days before vaccine	Gemcitabine	Advanced pancreatic cancer	Antigen-pulsed DCs + lymphokine-activated killer cells stimulated with anti-CD3 (CD3-LAKS) + gemcitabine	Enhancement of the immunogenicity of the cancer cells and antigen presentation of DCs, thereby increasing CTL responses	Hirooka et al. [62]
2 days before vaccine	Docetaxel	Established Lewis lung carcinoma model	GM-CSF-producing tumor vaccine + docetaxel	Induction of tumor antigenspecific CTLs	Chu et al. [63]
2 days before vaccine	Radiation	HPV 16/17 TC-1 tumor model	DNA vaccine encoding calreticulin linked to HPV-E7 + radiation	Enhanced survival of antigen-experienced cells Reduced pre-existing memory cells, Decreased Tregs	Tseng et al. [64]
1 day before ACT	Cyclophosphamide	Friend leukemia	Adoptive transfer of lymphomonocytes from tumorimmunized mice + cyclophosphamide	Enhancement of tumor cell apoptosis by radiotherapy, increased cell-mediated lysis of tumor cells	Moschella et al. [65]
1 day before vaccine	Cyclophosphamide	Advanced melanoma	NY-ESO-1/ISCONATRIX vaccine + low dose cyclophosphamide	Upregulation of various immunomodulatory factors. Induction of Th17, Th1 and activated CD4+	Klein et al. [66]



**Table 1. Continued)**

Timing of the intervention	Intervention	Cancer type	Combined treatment regimen	Efficacy/immunological responses of combined treatments	Mechanisms of intervention	References	Timing of the intervention	Intervention
1 day before vaccine	Cisplatin + 5-FU	MC38 murine colorectal adenocarcinoma tumor model	Intratumoral DCs injection + Low doses of cisplatin + 5-FU	Complete rejection and prolonged survival	Increase cytolytic activity of effector tumor-specific CD8+ T-cells	Tanaka et al. [67]		
1 day before vaccine	Dacarbazine	Melanoma	Vaccine consisting HLA-A2 restricted melanoma antigen A and gp100 analog peptide + dacarbazine	Improved long-lasting memory CD8+ T-cell response	Dacarbazine -induced gene activation involved in cytokine production, Leukocyte activation, immune response and cell motility, Widening of TCR repertoire diversity with high avidity and tumor reactivity	Nistico et al. [68] Palermo et al. [69]		
1 day before vaccine	Cisplatin	HPV 16/17 TC-1 tumor model	HPV16 E6/E7L2 fusion protein (TACIN) with GPI-0100 adjuvant + cisplatin	Reduced tumor out growth and extended survival	Induced tumor antigen-specific CD8+ T-cells	Peng et al. [70]		
5 h before ACT	Cyclophosphamide	Murine lymphomas	Adoptive transfer of tumor immune cells + cyclophosphamide	Enhanced the antitumor efficacy	Migration of tumor-immune lymphocytes to the tumor Promotion of homeostatic proliferation/activation of transferred lymphocytes, Cytokine storm induction	Braconi et al. [71]		
7 days before vaccine	Sumitinib	Colon carcinoma (MC38-CEA)	Poxvirus-based vaccine encoding (CEA) plus 3 costimulatory molecules + sunitinib	Reduced tumor volumes Increased survival	Increased intratumoral infiltration of antigen-specific T-cells Improved type-1 T-cell cytokine response Decreased Tregs and MDSCs	Farsaci et al. [72] and Finke et al. [73]		
4-7 days before vaccine	Cisplatin	HPV 16/17 TC-1 tumor model	DNA vaccine encoding calreticulin linked to HPV-E7 + cisplatin	Induce significant anti-tumor effect Improved survival of tumor bearing mice Increase E7-specific tumor-infiltrating CD8+ T-cells	Increased MHC class I expression by tumor cells upon cisplatin treatment, Increase cell-mediated lysis of tumor cells, Decrease myeloid suppressor cells and Tregs in blood and spleen	Tseng et al.[74]		
4 days before vaccine	Cisplatin	HPV 16/17 TC-1 tumor model	Vaccinia vaccine encoding HPV-16 E7 + cisplatin	Induce significant anti-tumor effect	Increase E7-specific tumor-infiltrating CD8+ T-cells, Increase intratumoral CD11c+ Decrease myeloid suppressor cells in spleen	Lee et al. [75]		

In combination	Concurrent with vaccine	Cyclophosphamide	Advanced ovarian cancer	Surviving HLA class I peptides (DPX-surviva) + metronomic cyclophosphamide	Enhanced T-cell response associated with differentiation of naïve T-cells into central/effector memory and late differentiated polyfunctional antigen-specific T-cells	Enhanced vaccine induced T-cell response	Improvement of the T-cell response	Berinstein et al. [76]
	1 day before vaccine (cyclophosphamide + paclitaxel) and 1 week after vaccine (doxorubicin)	Cyclophosphamide + Paclitaxel + doxorubicin	Mammary tumor model in antigen-specific tolerized neu transgenic mice	GM-CSF-secreting HER-2/neu-expressing whole-cell vaccine + cyclophosphamide + paclitaxel + doxorubicin	Enhanced vaccine anti-tumor effect to delay tumor growth	Enhanced the efficacy of vaccine, increased neu-specific T cells and Th1 response		Machiels et al. [77]
	Concurrent with vaccine	CD27 antibody	Prostate cancer model	Tumor lysate-pulsed DC vaccine + CD27 antibody	Reduced tumor outgrowth	Enhanced T-cell response		Wei et al. [78]
	Concurrent with vaccine	Cyclophosphamide + Paclitaxel + docetaxel	Hepatocellular carcinoma patients	Multi-peptide cocktail including HCV and tumor antigen vaccine + cyclophosphamide + paclitaxel + docetaxel	Enhanced specific T-cell response	Reduced Treg frequency	Counteracting suppressive immunity by reducing immunosuppressive cells	Tagliamonte et al. [79]
	Concurrent with vaccine	Gemcitabine	Platinum-resistant ovarian cancer	p53 SLP vaccine + pegylated IFN- $\alpha$ + gemcitabine	Safe, feasible, immune stimulatory effect of combined treatment	Reduction in MDSCs by gemcitabine and increase in M1 macrophages		Dijkgraaf et al. [80]
	Concurrent with vaccine	Cisplatin	HPV 16/17 TC-1 tumor model	HPV16-SLP vaccination + cisplatin	A synergistic antitumor effect	Sensitize tumor cells to cisplatin-mediated death by TNF $\alpha$ produced by tumor-specific T-cells	Increased tumor cell apoptosis	Van der Sluis et al. [81]
	Concurrent with vaccine	Nivolumab	Resected stage IIIC and IV melanoma	Tumor antigen multi-peptide vaccine + nivolumab	Demonstrated immunologic activity with promising survival	Increased tumor-specific CD8+ T-cells but also CTLA-4+ CD4+ and CD25+ Tregs	Counteracting inhibitory immune regulation	Gibney et al. [82]
	Concurrent with vaccine	Anti-PD-1	B16 melanoma	IFN $\gamma$ -inducing cancer vaccine combined with GM-CSF + TLR agonists + anti-PD-1	Complete tumor regression	Blocking the inhibitory effect of PD-1 induced by vaccine		Fu et al. [83]
	Concurrent with vaccine	Anti-PD-1	Advanced or metastatic HCC patients And RMA lymphoma tumor model	Peptide vaccine + anti-PD-1	Increased tumor specific CTL number and response	Blocking the PD-1 signaling induced by vaccine on specific CTL		Sawada et al. [84]
	Concurrent with vaccine	Anti-PD-1	TC-1 HPV16/17 tumor model	Listeria monocyto genes based vaccine expressing HPV16 E7 + anti PD-1	Tumor outgrowth inhibition and prolonged survival	Increased tumor-specific Tcell response by blocking PD-1/PD-L1 pathway as PDL1 induced by vaccine		Mkritchyian et al. [85]
	Concurrent with vaccine	Anti-CTLA-4	Prostate tumor model	GM-CSF-secreting vaccine (GVAX) + anti-CTLA-4	Increased tumor-specific cells and lytic function	Blocking the inhibitory effect of CTLA-4 induced by vaccine on tumor specific CD8+ T-cells		Wada et al. [86]



Table 1. Continued)

Timing of the intervention	Intervention	Cancer type	Combined treatment regimen	Efficacy/immunological responses of combined treatments	Mechanisms of intervention	References	Timing of the intervention	Intervention
After	Concurrent with vaccine	Anti-IL10R1 monoclonal antibody	Bladder tumor model	Bacillus Calmette-Guérin vaccine + anti-IL10R1 monoclonal antibody	Enhanced anti-bladder cancer immunity and prevention metastasis to lung	Increased CTL specific response	Counteracting suppressive immunity induced by tumor or immunotherapy	Newton et al. [87]
	1 day after vaccine	Anti- 4-1BB	MCA205 and MCA207 fibrosarcomas	DC vaccine pulsed with tumor lysate + anti-4-1BB	Enhanced tumor regression and improve survival	Increased costimulatory signal of 4-1BB enhanced by vaccine on NK, CD4 and CD8 T-cells, Increased T-cell response	Increased costimulatory signals to improve T-cell function	Ito et al. [88]
	2 days after vaccine	Anti-OX40 + anti-4-1-BB	Mammary carcinoma (N202.1A tumor cells in Her-2/ neu mice)	DC vaccine pulsed with apoptotic tumor cells + anti-OX40 + anti-4-1-BB	Tumor reduction and rejection	Enhanced CD4 and CD8 T-cell response		Cuadros et al. [89]
	1 day after vaccine	SM16 (TGFβ blockade)	TC-1 HPV16/17 tumor model	Adenovirus expressing HPV-E7 + SM16	Delayed the tumor outgrowth Increase intratumoral leukocyte infiltration	Increase intratumoral antigen-specific CD8+ T-cells, Increased immunostimulatory cytokines and ICAM-1 Increased the percentage and functional status of CD8+ T-cells	Improvement of the T-cell response	Kim et al. [90]
	3–6 days after vaccine	Radiation	Colon adenocarcinoma tumor cells expressing CEA (MC38-CEA)	Recombinant vaccinia/avipox CEATRICOM vaccine + radiation	Significant Tumor eradication	Upregulation of Fas on tumor cells by radiation Increased infiltration of Tcells to tumor, Induced tumor-specific T-cell response	Induced tumor cell apoptosis and improved T-cell response	Chakraborty et al. [91]
	5 days after vaccine	Radiation	HPV-associated head and neck squamouscell carcinoma	Shiga Toxin B-based HPV vaccine + radiation	Complete tumor clearance	Increased tumor-infiltrating antigen-specific T-cells, Induced CD8+ T-cell memory Enhanced intratumoral vascular permeability	Enhanced intratumoral vascular permeability and improved T-cell response	Mondini et al. [92]

ACT: adoptive cell transfer; CEA: carcinoembryonic antigen; CTLA-4: cytotoxic T-lymphocyte-associated protein 4; CTL: cytotoxic T lymphocytes; CSF-1 R: colony stimulating factor-1 receptor; DC: dendritic cell; GM-CSF: granulocyte-macrophage colony-stimulating factor; gp100: glycoprotein 100; HPV: human papillomavirus; HLA: human leukocyte antigen; HER-2: human epidermal growth factor receptor 2; HCV: hepatitis C virus; HCC: hepatocellular carcinoma; IL-2: interleukin-2; IFN-α: interferon-alpha; IFN-β: interferon beta; IFNγ: interferon gamma; IL-10R1: interleukin 10 receptor 1; MHC: major histocompatibility complex; MDSCs: myeloid-derived suppressor cells; NK: natural killer cells; PD-1: programmed cell death protein 1; PD-L1: programmed death-ligand 1; RNA: ribonucleic acid; SLP: synthetic long peptide; Tregs: regulatory T-cells; TAA: tumor-associated antigens; TDLN: tumor-draining lymph node; Th: T helper cells; TCR: T-cell receptor; TLR: Toll-like receptor; TILs: tumor-infiltrating lymphocytes; TNF-α: tumor necrosis factor alpha.

binding P60 peptide, which reduces the suppressive function of Tregs by preventing the nuclear translocation of FOXP3 and thus its ability to suppress the transcription factor NF- $\kappa$ B and NFAT, efficiently protected mice against CT26 tumor growth [106]. Likewise, antibody-mediated depletion of CD4<sup>+</sup> CD25<sup>+</sup> Tregs before vaccination with DCs loaded with tumor cells, that had been stressed by heat shock and irradiation, resulted in a delayed tumor outgrowth and long-lived tumor-protective immune responses [57]. Also depletion of CD25<sup>+</sup> Tregs prior to tumor cell-based vaccination and CTLA-4 blocking, enhanced the TRP-2-specific CD8<sup>+</sup> cytotoxic T lymphocyte (CTL) response in B16 melanoma tumor model [55]. Similarly, application of the CD25-blocking monoclonal antibody daclizumab to patients with metastatic breast cancer, 1 week before multiple injections with a vaccine (consisting of three peptides derived from human telomerase reverse transcriptase [hTERT], survivin, and pp65 of cytomegalovirus [CMV] as a control), resulted in prolonged Treg suppression and robust vaccine-induced IFN $\gamma$ -producing T-cell responses [107]. However, Treg depletion by using anti-CD25 antibodies may also be performed at the same time with the administration of the vaccine [108]. The elimination of CD4<sup>+</sup> CD25<sup>+</sup> Tregs by using denileukin diftitox, a diphtheria toxin fragment conjugated to recombinant IL-2 (DAB<sub>389</sub>IL-2; also known as ONTAK) that is rapidly internalized upon binding to the IL-2 receptor and then releases the apoptosis inducing toxin, significantly enhanced a tumor RNA-transfected DC vaccine-induced tumor-specific T-cell response in renal cell carcinoma (RCC) patients [60].

Small molecule inhibitors were also shown to decrease immune suppression [73]. In a murine colon carcinoma (MC38-CEA) sequential administration of sunitinib, a tyrosine kinase inhibitor, followed by a poxvirus-based vaccine encoding carcinoembryonic antigen (CEA) plus three costimulatory molecules (B7-1, ICAM-1 and LFA-3) resulted in decreased numbers of intratumoral Tregs and MDSCs as well as an increased influx of antigen-specific T-cells, with as consequence a better tumor control and prolonged survival [72]. Last but not least, low-dose total body irradiation therapy also reduced Tregs and increased effector-memory T-cell frequencies. Administration of a DC-gp100 tumor vaccine 11 days after low dose irradiation reduced tumor outgrowth and increased survival of melanoma-bearing mice [49]. Taken together, altering Treg function or depleting Tregs may improve tumor-specific immune responses and expand the efficacy of immunotherapy (reviewed in [105]).

As already eluded to in the above section, some modalities may also affect MDSC or M2 function and number [109]. However, others are specifically designed to impact on myeloid cells. For instance, the CSF-1 receptor (CSF-1R) is a key regulator for monocyte differentiation from progenitors of the bone marrow and for monocyte activation and migration. It has been shown that macrophages induction by CSF-1 could lead to polarization towards an immunosuppressive and tumor-promoting phenotype [110]. Blocking of CSF-1R signaling by using recombinant CSF-1 antibodies against the ligand and the receptor,

or specific inhibitors of the CSF-1R kinase activity might be effective in combination with other immunotherapies. In the B16F10 mouse melanoma model, inhibition of CSF-1R (PLX3397 kinase) in combination with CD8 T cell-mediated immunotherapy, consisting of the transfusion of pmel-1 CD8<sup>+</sup> T-cells and peptide vaccination, could efficiently remove intratumoral F4/80<sup>+</sup> macrophages, increase IFN $\gamma$  production of tumor-specific CD8<sup>+</sup> T-cells and delay tumor outgrowth [58]. In another study, PLX3397 given 4 days before adoptive T-cell therapy improved the efficacy of this immunotherapy in a syngeneic mouse model of BRAF (V600E)-driven melanoma by decreasing tumor-infiltrating myeloid cells, skewing macrophages towards MHCII<sup>hi</sup> type 1 macrophages (M1) and by increasing the number of IFN $\gamma$ -producing tumor-infiltrating lymphocytes (TIL) [59]. Therefore, targeting myeloid cells either to prevent their recruitment to the tumor or to inhibit their pro-tumor polarization may foster immune control of tumor cells. Such a strategy, used as a standalone therapy or in combination with other immunotherapies has been shown successful to enhance antitumor immune responses [109,111].

#### *Chemoradiation applied prior to vaccination can induce optimal T-cell responses*

Chemotherapy not only acts through the alleviation of immune suppression, but can also have beneficial effects on the immune system through other mechanisms. For example, cyclophosphamide also can induce the infiltration of immune lymphocytes to the tumor as well as promote homeostatic proliferation/activation of B and T lymphocytes due to a cytokine storm (GM-CSF, IL-1B, IL-7, IL-15, IL-2, IL-21 and IFN $\alpha$ ) after drug-induced lymphodepletion [71]. Moreover, many other immunomodulatory factors such as danger signals, pattern recognition receptors, and chemokines receptors are upregulated after cyclophosphamide treatment. These alterations may explain the improved antitumor immunity observed after cyclophosphamide treatment in those cases where an overt effect of cyclophosphamide on the levels and function of Tregs could not be detected [112,113]. The pharmacokinetic analysis of gene and protein expression and anti-tumor efficacy in different therapeutic regimens indicate that the optimal time point to apply adoptive immunotherapy is 1 day after cyclophosphamide treatment [65].

Above all, in cases where the treatment modalities stimulate the functionality or stability of tumor-specific CD8<sup>+</sup> T-cells, administration of immunotherapy following conventional therapy can improve the antitumor immune responses [63,67]. In an established 3LL lung tumor model, administration of docetaxel before but not after vaccination with a GM-CSF-producing tumor vaccine could significantly induce tumor regression and prolonged survival [63]. This is due to the docetaxel-associated enhanced survival of activated antigen-experienced T-cells induced by the vaccine over that of pre-existing memory CD8<sup>+</sup> T-cells and Tregs [63]. Similar results have been observed in melanoma patients who received dacarbazine (DTIC) 1 day before tumor-antigen vaccination [68]. Dacarbazine induces

activation of genes involved in cytokine production, leukocyte activation, immune response and cell motility, thereby enhancing CD8<sup>+</sup> memory T-cell response [68]. It also broadens the TCR repertoire used and this is accompanied by high T-cell avidity and tumor reactivity [69]. Furthermore, in a HPV-induced tumor model, vaccination with HPV16 E6E7L2 fusion protein (TA-CIN) with GPI-0100 adjuvant 1 day after administration of cisplatin reduced tumor outgrowth and extended the survival of TC-1 tumor-bearing mice compared to vaccination alone [70]. In similar studies, cisplatin treatment of mice 4–7 days before vaccination with a DNA vaccine encoding calreticulin linked to HPV16 E7 antigen or with a vaccinia virus vaccine encoding this E7 antigen significantly increased the survival of TC-1 tumor-bearing mice [74,75]. Interestingly, this effect has only been observed when cisplatin was given before and not after the vaccination, emphasizing the importance of timing of the given therapies [74]. The combination induced significantly higher frequencies of E7-specific CD8<sup>+</sup> T-cells, both in blood and tumor, compared to each treatment alone. Reason for this is that cisplatin on one hand increases the expression of MHC class I on tumor cells, thereby enhancing their susceptibility to be lysed by specific CTLs and on the other hand, increases the influx of intratumoral CD11c<sup>+</sup> while decreasing the number of myeloid suppressor cells and Tregs in blood and spleen [74,75]. Similarly, gemcitabine could also increase the percentage of circulating monocytes, M1, and DCs [52,114]. Administration of this chemotherapy alone or in poly-chemotherapy regimens before immunotherapy may also enhance the clinical efficacy through these mechanisms [62,114,115].

Similar observations have been made with low-dose radiation 2 days before vaccination, although the highest frequency of E7-specific CD8<sup>+</sup> T-cells in tumor and spleen was reached when radiation was given in combination with a second DNA vaccination [64]. Moreover, in a phase I clinical study two courses of cisplatin and 5-FU concurrent with radiotherapy and before vaccination with a multiple epitope peptide vaccine increased the vaccine-specific CTL response in patients with unresectable chemo-naïve esophageal squamous cell carcinoma [61]. Thus, both chemotherapy and radiotherapy or their combination (chemoradiation) given prior to vaccination can mediate immune stimulating and clinical effects.

In conclusion, there are a number of modalities that are able to relieve immune suppression as well as to condition the immune system to optimally respond to immunotherapy. Therefore, immunotherapy properly timed after these treatments provides a platform to increase the clinical response of patients to immunotherapy.

## Concurrent combination of therapeutic modalities with vaccination

### *Simultaneous combination of chemotherapy with vaccination increases vaccine efficacy*

Given the immune stimulatory capacity of certain chemotherapeutic agents, administration of these cytotoxic drugs not only before but also during vaccination can result in improved antitumor responses. Concurrent administration of metronomic doses of cyclophosphamide



in combination with an HLA class I-binding survivin peptide vaccine (DPX-Survivac) increased the antigen-specific immune response. This was associated with the differentiation of naïve T-cells into central/effector memory cells (CM/ EM) and late differentiated poly-functional antigen-specific CD8<sup>+</sup> T-cells in advanced ovarian cancer patients [76]. Similarly, metronomic administration of a high dose cocktail of chemotherapeutic agents (including cyclophosphamide, paclitaxel and docetaxel) during vaccination with a multi-peptide cocktail of peptides (comprising hepatitis C virus-derived antigens and tumor-associated antigens) resulted in an enhanced specific T-cell response and a reduced Treg frequency in hepatocellular carcinoma (HCC) patients [79]. Coadministration of gemcitabine with DC-based vaccines in a pancreatic carcinoma model showed a synergistic antitumor effect [116]. Treatment of patients with ovarian cancer with a p53 SLP vaccine in combination with pegINTRON (pegylated IFN $\alpha$ ) 7 days before the first cycle of gemcitabine and repeated at day 22, during gemcitabine treatment, resulted in a strong p53-specific T-cell response. In this study gemcitabine treatment was associated with reduced levels of MDSCs, and increased percentages of M1 macrophages, circulating proliferating CD4<sup>+</sup> and CD8<sup>+</sup> T-cells but not Tregs [80].

In addition, there are some reports suggesting that immunotherapy may provide the correct environment for chemotherapy to become more effective. In a poly-chemotherapy regimen, administration of cyclophosphamide or paclitaxel 1 day before and doxorubicin 7 days after vaccination with GM-CSF-secreting tumor cells, enhanced the antitumor efficacy of these chemotherapeutics in HER-2/neu tolerized mice. Doxorubicin was provided to augment the vaccine-induced antitumor efficacy but the mechanism was unclear [77]. Potentially, immunotherapy operates via increasing the number of cytokine-producing tumor-specific T-cells thereby sensitizing tumor cells for chemotherapy-induced cell death. In a HPV16 preclinical tumor model, vaccination with HPV16 E6 and E7 SLPs combined with cisplatin displayed a synergistic antitumor effect [81]. The vaccination resulted in increased numbers of intratumoral IFN $\gamma$  and TNF $\alpha$  producing CD8<sup>+</sup> T-cells. The TNF $\alpha$  produced by these HPV-specific CD8<sup>+</sup> T-cells not only had a direct effect on tumor cell proliferation but also increased the sensitivity of the tumor cells to cisplatin-induced tumor cell death in a JNK-dependent fashion [81]. Thus, even at this phase there is a place for chemotherapy to improve vaccine-induced antitumor immunity.

#### *Concurrent combination of immunomodulatory antibodies with vaccination to curtail inhibitory immune regulation*

Another reasonable strategy to improve the efficacy and maintenance of tumor-specific T-cell responses is by counteracting immune regulation that acts when effector cells start to express coinhibitory molecules as a normal response to activation. Occasionally immunotherapy can alter the tumor microenvironment or the expression of regulatory molecules in a way

that is not favorable for the therapeutic outcome. Therefore, the appropriate combination of treatments and the correct timing of each treatment modality can be crucial for the final outcome. The demonstration of high numbers of PD-1 and PD-L1 expressing CD8<sup>+</sup> T-cells at the invasive tumor margin and inside tumors of patients with metastatic melanoma, suggested the application of anti-PD-1 therapy in melanoma patients [117]. Indeed, treatment with a multi-peptide tumor-epitope vaccine and PD-1 antibody (nivolumab) was well tolerated in patients with resected high-risk metastatic melanoma. Furthermore, immunological activity, such as increased antigen-specific CD8<sup>+</sup> T-cells but also increased frequencies of CD25<sup>+</sup> or CTLA-4<sup>+</sup> CD4<sup>+</sup> T-cells, was associated with promising survival results [82]. Preclinical evidence has shown that TEGVAX vaccine, which is an IFN $\gamma$ -inducing cancer vaccine combined with GM-CSF and TLR agonists, is associated with DC activation and an increase in the number of tumor-specific IFN $\gamma$ -producing tumor-infiltrating T-cells [83]. However, as a consequence of this influx, cells in the tumor microenvironment upregulate PD-L1 resulting in incomplete tumor cell elimination. Furthermore, analysis of PBMCs following administration of a glypcian-3 (GPC3) peptide vaccine in advanced or metastatic HCC revealed a high expression of PD-1 on peptide-specific CD8<sup>+</sup> T-cells [84]. Similarly, immunotherapy using *Listeria monocytogenes* (Lm)-LLO can be improved by reduction of the Tregs and MDSCs, but as it is also associated with the upregulation of PD-L1 on immune cells, in particular macrophages, the use of antibodies blocking the PD-1:PD-L1 axis is justified [85]. Indeed, administration of the PD-1 blocking antibody in combination with the cancer vaccine caused increased tumor regression. Another example is the combined use of a cell-based GM-CSF-secreting vaccine (GVAX) with CTLA-4 blocking antibody in an auto-chronous prostate cancer model (Pro-TRAMP), which enhanced the tumor antigen-specific CD4<sup>+</sup> and CD8<sup>+</sup> effector T-cells to Treg ratio and the tumor-antigen directed lytic function [86]. Interestingly, the timing of administration of the CTLA-4 blocking antibody greatly influenced the outcome as the maximum effect has been observed when the blocking antibody was applied after, but not before the vaccination. The mechanism behind this crucially timed application of the blocking antibody is that the GVAX vaccine not only increases tumor-specific CD8<sup>+</sup> T-cells but also upregulates the CTLA-4 expression on these effector cells, thus by blocking this inhibitory molecule and its pathway the effector function is not abrogated. Interestingly, in patients with advanced small-cell lung cancer similar results have been observed [118]. Administration of four doses of ipilimumab after two doses of paclitaxel/carboplatin improved the immune-related progression-free survival and overall survival of patients compared to concurrent administration of ipilimumab and paclitaxel/carboplatin [118]. However, the detailed mechanisms still need to be investigated. Thus, vaccination followed by specific treatments to release the brakes on T-cells, instigated by coinhibitory receptors, may form a powerful strategy to improve tumor-specific T-cell efficacy. In addition to coinhibitory receptor regulation, one might also provide antibodies to known



immune regulatory cytokines or other (soluble) factors, which potentially can hamper the induction of or weaken the antitumor immune response. Among them are known tumor-derived factors such as VEGF, transforming growth factor- $\beta$  (TGF $\beta$ ), prostaglandin E<sub>2</sub> (PGE<sub>2</sub>), IL-6, IL-10 and indoleamine-pyrrole 2,3-dioxygenase (IDO). For instance, the combination of the standard therapy - Bacillus Calmette-Guérin (BCG) - with a blocking anti-IL-10 receptor 1 monoclonal antibody (anti-IL10R1) resulted in enhanced antitumor immunity by inducing Th1 immune response in bladder cancer mouse model [87]. Therefore, these strategies to dampen inhibitory immune regulation can be applied in combination or even after vaccination as will be described further in this review.

## **Administration of therapeutic modalities after vaccination**

### *Combination of vaccines and immunomodulatory antibodies enhances the antitumor response*

To enhance antitumor immunity induced by vaccination, other treatments such as agonistic antibodies to costimulatory receptors on T-cells, the provision of cytokines and the stimulation of antigen-presenting cells (APCs) by toll-like receptor (TLR) agonists can play a major role as cotreatments. In these cases the correct timing depends on the mechanism of action of the immunomodulatory compound used, but most likely they will be given in combination or after vaccination. Indeed, immunization with vaccines that stimulate a broad immune response and transfer of costimulatory agonist antibodies potentially improves the antitumor response by enhancing the T-cell response. Using DCs pulsed with apoptotic tumor cells, which stimulate a broad immune response in Her-2/neu mice, in combination with agonist anti-OX40 (CD134) or anti-4-1BB (CD137) monoclonal antibodies showed substantial tumor size reduction [89]. Mechanistically, administration of these agonistic antibodies given 2 days after DC immunization could improve the induced T-cell response as the effect of this combined treatment is abrogated in the absence of CD4<sup>+</sup> and CD8<sup>+</sup> T-cells. Likewise, combination of agonistic anti-4-1BB one day after vaccination with tumor lysate-pulsed DCs following another administration after 3 days enhanced tumor regression in established pulmonary and subcutaneous tumor models [88]. The rationale behind this therapeutic strategy is that tumor lysate-pulsed DC vaccines induce transient upregulation of 4-1BB on T-cells and NK cells in vaccine-primed lymph nodes. Therefore, treatment with agonistic 4-1BB antibody could polarize effector T-cells towards a type 1 (IFN $\gamma$ ) response to tumor antigen in a CD4<sup>+</sup>, CD8<sup>+</sup> and NK cell dependent manner. In a similar fashion, treatment with tumor lysate-pulsed DCs upregulate CD27 on T-cells in RM-1 prostate cancer tumor model and administration of CD27 agonistic antibodies after vaccination with these DCs could reduce tumor outgrowth [78]. Thus, administration of immunomodulatory compounds which stimulate DC or T-cell function, either by providing cytokines or costimulatory signals, following vaccination strategies is a convenient way to promote the vaccine-induced antitumor efficacy.

### *Postvaccination interventions to dampen the immune regulatory response*

Intervention drugs to abrogate the immune suppressive effect of regulatory cytokines or molecules can be applied not only in combination with vaccination but also after immunotherapy. For instance, systemic blocking of TGF $\beta$  signaling after vaccination with adenovirus expressing HPV-E7, or prior to immunotherapy by adenovirus expressing IFN- $\beta$ , increased the antitumor efficacy compared to each treatment alone [90]. TGF $\beta$  receptor blockade enhanced the intratumoral production of immunostimulatory cytokines and chemokines as well as the expression of ICAM-1 and led to the increased infiltration of antigen-specific and functional CD8 $^{+}$  T-cells.

Another example is IDO, which catalyzes essential amino acids such as tryptophan that are required for proliferation and activation of immune cells, in particular T-cells. IDO is overexpressed in tumor cells and tumor-associated APCs. To improve the capacity of a DC-based vaccine, the IDO inhibitor 1-MT was administered after vaccination in a prophylactic Lewis lung carcinoma murine model. Interestingly, IDO was not expressed by tumor cells but only by the myeloid cells within the tumor, tumor draining lymph nodes and spleen. Moreover, a combination of the IDO inhibitor with other modalities such as chemotherapy or blockade of coinhibitory molecules, was shown to potentiate the antitumor efficacy of therapy [119,120].

Postvaccination radiation may also aid by interfering with immune regulating mechanisms. In a mouse colon adenocarcinoma tumor model of CEA, vaccination in a prime-boost strategy with vaccinia and avipox recombinants, expressing CEA and a triad of T-cell costimulatory molecules, in combination with local tumor irradiation induced synergistic antitumor effects [91]. Radiation 3 days after vaccination induced upregulation of the death receptor Fas on tumor cells, leading to Fas/Fas ligand pathway mediated cell death. Therefore, the combined treatment led to increased infiltration of T-cells and CD4 $^{+}$  and CD8 $^{+}$  T-cell responses not only specific for CEA but also for other overexpressed antigens in tumor. Similarly, local radiation 5 days after vaccination with Shiga Toxin B-based HPV vaccine in HPV-associated head and neck squamous cell carcinoma induced synergistic tumor eradication in mice by normalizing the tumor vasculature and thus improving tumor infiltration by immune cells [92]. Thus, to improve the vaccine-induced antitumor response one should also alleviate immune regulatory mechanism that act after the activation of tumor-specific T-cells.

## **Immunoguiding is important for the development of immunotherapeutic strategies**

The increasing reports on the immune modulatory properties of chemotherapy and radiotherapy, the debate on the exact working mechanism of CTLA-4-blocking antibodies



[121–123] and the unexpected outcomes of myeloid cell depletion by CSF1R inhibition during immunotherapy [58,124] exemplify the need for immunomonitoring studies that analyze the effect of drugs on the immune system, and in particular beyond the expected mechanisms of action. This immunological knowledge then can be used to guide the rational design of combination therapies, which in the past were more based on empirical testing [23,95]. It is well known that there are many immunological differences between all the different animal models used – and sometimes even between what used to be the same tumor cell lines – to develop immunotherapy. Moreover, the number of analyses, required to study the many permutations possible, is too high for single consortia to address. Therefore, an important aspect is to ensure that the measurement and reporting of the results obtained are comparable between laboratories so that it is easier to interpret and value the data generated. In the last decade a huge effort, undertaken by the Association of Cancer Immunotherapy's (CIMT's) immunoguiding program [125] and Cancer Immunotherapy Consortium (CIC) [126], has focused on this in the realm of human studies, and this has successfully led to: (i) a strong awareness of the need to harmonize or standardize measurements, (ii) to technical improvements and harmonization of the assays used, and (iii) to more transparent reporting [127–129]. It can be envisaged that similar efforts by scientists performing studies in mouse tumor models will lead to a quicker design of immunotherapeutic strategies, which expedite the translation to the treatment of patients.

## Conclusions

In conclusion, the field is moving rapidly towards understanding the requirements for optimal immunotherapy of cancer. Combinations of treatment modalities are designed and tested to accommodate the most effective tumor-specific immune response. Surgery, chemotherapeutic compounds, radiotherapy schedules, antibodies and targeted therapies have successfully been administered before applying immunotherapy with the aim to reduce immunosuppressive cells, or during and after immunotherapy to potentiate the immune response and to prevent immune regulation. A full understanding of the immunological effects of the compounds used, their pharmacological dynamics, and the optimal sequence during treatment will result in clinical benefit for the majority of patients.

## Expert opinion

Cancer may be cured by immunotherapy but the development of cancer is associated with increased immune suppression. Furthermore, the induction of tumor-specific immunity is difficult and regulated afterwards. Hence, for an optimal antitumor response it is important to provide the most appropriate therapeutic modality at the right time. The different schedules and various modalities, and combinations thereof, have been discussed in this review and

are recapitulated in Figure 1. In our opinion, the prevention of tumor development in high-risk patients, treatment of premalignant lesions or prevention of recurrences after curative treatments, is the ideal time period to stop cancer and vaccines are ideal to induce protective tumor-specific immunity. However, in general practice immunotherapy is applied to cancer patients with more advanced stage of disease, and as such its success is determined by the level of immunosuppression encountered in microenvironment. The treatment of premalignant lesions [3,33], but certainly that of patients with cancer, demonstrates that the increase in general and local immune suppression requires additional modalities to curtail these suppressive mechanisms and to optimally activate and expand tumor-specific T-cells. At this phase a correct sequence and interval of drugs is essential, as it will be required to use prime combinations of several modalities to obtain clinical success in the majority of patients. Based on the observations in mouse tumor models and in patients it is clear that myeloid suppressor cells and Tregs stifle the induction of a strong and effective antitumor response and that alleviation of this immune suppression is required before the activation of the antitumor T-cell response. In addition, extra support is needed to ensure the strong expansion and appropriate effector function of the tumor-specific T-cells. Finally, as the activated effector T-cells will start to express coinhibitory molecules, the ligands of which can be expressed at the tumor site or will be as a consequence of T-cell produced IFN $\gamma$ , there is a need to counteract immune regulation at this point during therapy. As described in this review, for each of the stages (before, during and after vaccination) help can be provided via either surgical tumor reduction, chemotherapy, radiation therapy and/or a number of other immune modulators. However, before such combinations are designed it will be essential to establish the dynamics and exact immune modulatory properties of the agents used. Chemotherapeutic agents may affect different immune cell populations and this effect may be transient [48]. While it seems logical to understand the dynamics and immune modulating properties of chemotherapeutic compounds, this is also required for other compounds such as targeted therapy of macrophages [58,124] and antibodies targeting costimulatory and coinhibitory molecules. This is well illustrated by different timing schedules of anti-CTLA-4 and anti-OX40 in a murine colorectal carcinoma model in combination with radiation therapy [130]. Antibodies against CTLA-4 and OX40 can only improve the survival of tumor bearing mice when applied before and after radiation therapy, respectively. Therefore, not only the mechanism of each immunotherapeutic modality but also the sequence of administration should be tested and considered in the design of the most optimal combined-therapeutic strategy. The drawbacks of this approach of course are the costs and the time needed to perform these interrogations with as result that such well-designed studies are scarce, but they are coming. Immunomonitoring is an extremely important aspect in understanding these matters. It should be applied in the broadest sense, certainly not restricted to the expected mechanism of action, and also take into account (unexpected) negative effects of the treatment. As many of the studies will be performed (only) in mouse models it becomes





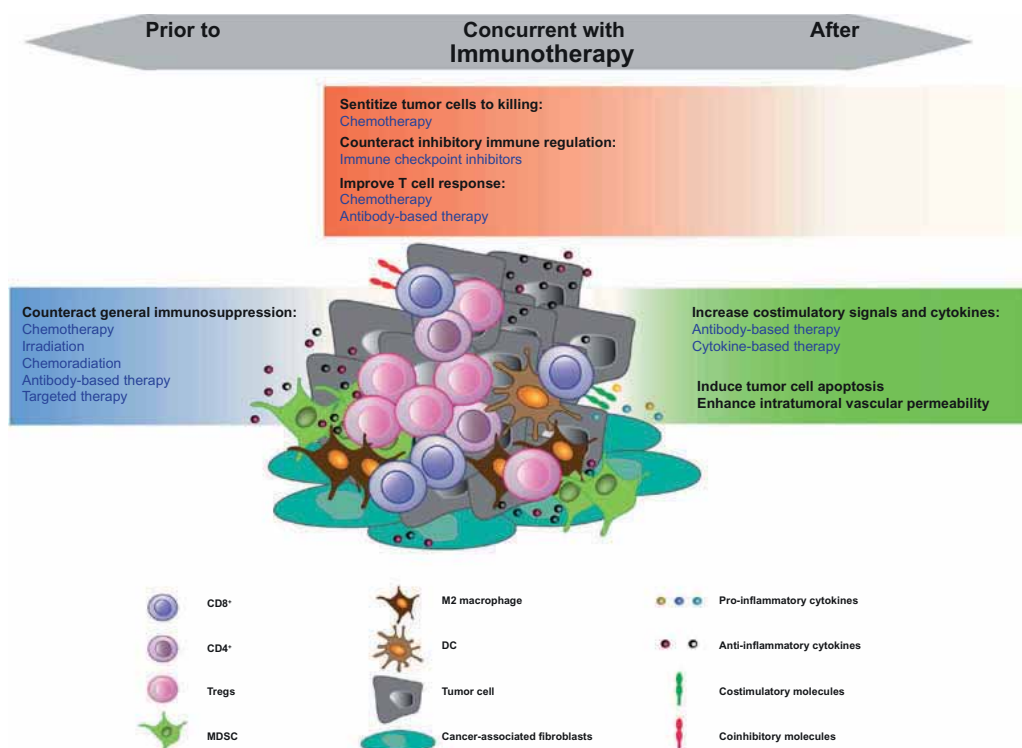


**Figure 1.** Illustration of different timing schedules of various therapies in combination with immunotherapy based on their mechanisms. The individual examples of each combination therapy are summarized in Table 1. The colour gradients show the time points (prior, concurrent and/or after immunotherapy) at which the therapies are mostly applied. The blue box shows the therapies which are mostly applied prior to immunotherapy and less often concurrent with immunotherapy. The orange box shows the therapies which are often applied concurrent with immunotherapy and less after immunotherapy. The green box shows the therapies which are used mainly after immunotherapy and less concurrent with immunotherapy. Abbreviations: Tregs: Regulatory T-cells, MDSC: Myeloid-derived suppressor cells, M2 macrophages: type 2 macrophages, DC: dendritic cell.

important that laboratories using mouse models will focus on increasing the comparability of immunomonitoring and reporting of results, similar to current efforts in the monitoring of human immune responses. Notably, one should be aware that while we can learn a lot from murine experiments, they still not fully reflect the human situation. Therefore, effort should be undertaken to properly investigate the sequence and timing of the most promising combinations in clinical studies. Fortunately, the field is moving forward towards rationally designed combination therapy and a better understanding of the patient population that is to be treated. Finally, we envisage that the ideal combination aims to: (1) increase the number of tumor-specific T-cells; (2) prevent their subsequent regulation in the tumor bed; (3) decrease the number of immune suppressive myeloid cells and Tregs; and (4) activate intratumoral antigen presenting cells. In theory, this should lead to major improvements in clinical outcome, well above the levels that is currently reached.

## Funding

This manuscript is sponsored by the Dutch Cancer Society (2009-4400) and by the Leiden University Medical Center (LUMC).

## Declaration of interest

EB Nejad is sponsored by a PhD grant from the Leiden University Medical Center. SH van der Burg is sponsored by a grant from the Dutch Cancer society. He also received support for his research on vaccines and as an advisor from ISA Pharmaceuticals. Furthermore, MJP Welters is supported by the Dutch Cancer Society while R Arens is sponsored by the Gisela Thier grant from Leiden University Medical Center. The authors have no other relevant affiliations or financial involvement with any organization or entity with a financial interest in or financial conflict with the subject matter or materials discussed in the manuscript apart from those disclosed.





## References

Papers of special note have been highlighted as either of interest (•) or of considerable interest (••) to readers.

1. Melief CJ, van Hall T, Arens R, et al. Therapeutic cancer vaccines. *J Clin Invest.* 2015;125:3401–3412. DOI:10.1172/JCI80009
2. van der Burg SH, Arens R, Ossendorp F, et al. Vaccines for established cancer: overcoming the challenges posed by immune evasion. *Nat Rev Cancer.* 2016;16:219–233. DOI:10.1038/nrc.2016.16.
- **This is a comprehensive review about cancer immune evasion strategies that needs to be considered to design a therapeutic vaccine for established cancer**
3. Kenter GG, Welters MJ, Valentijn AR, et al. Vaccination against HPV-16 oncoproteins for vulvar intraepithelial neoplasia. *N Engl J Med.* 2009;361:1838–1847. DOI:10.1056/NEJMoa0810097
4. van Poelgeest MI, Welters MJ, van Esch EM, et al. HPV16 synthetic long peptide (HPV16-SLP) vaccination therapy of patients with advanced or recurrent HPV16-induced gynecological carcinoma, a phase II trial. *J Transl Med.* 2013;11:88. DOI:10.1186/1479-5876-11-88
5. Kantoff PW, Higano CS, Shore ND, et al. Sipuleucel-T immunotherapy for castration-resistant prostate cancer. *N Engl J Med.* 2010;363:411–422. DOI:10.1056/NEJMoa1001294
6. Rosenberg SA, Yang JC, Sherry RM, et al. Durable complete responses in heavily pretreated patients with metastatic melanoma using T-cell transfer immunotherapy. *Clin Cancer Res.* 2011;17:4550–4557. DOI:10.1158/1078-0432.CCR-11-0116
7. Verdegaal EM. Adoptive cell therapy: a highly successful individualized therapy for melanoma with great potential for other malignancies. *Curr Opin Immunol.* 2016;39:90–95. DOI:10.1016/j.coi.2016.01.004
8. Hodi FS, O'Day SJ, McDermott DF, et al. Improved survival with ipilimumab in patients with metastatic melanoma. *N Engl J Med.* 2010;363:711–723. DOI:10.1056/NEJMoa1003466
9. Ribas A, Kefford R, Marshall MA, et al. Phase III randomized clinical trial comparing tremelimumab with standard-of-care chemotherapy in patients with advanced melanoma. *J Clin Oncol.* 2013;31:616–622. DOI:10.1200/JCO.2012.44.6112
10. Homet MB, Parisi G, Robert L, et al. Anti-PD-1 therapy in melanoma. *Semin Oncol.* 2015;42:466–473. DOI:10.1053/j.seminoncol.2015.02.008
11. Robert C, Schachter J, Long GV, et al. Pembrolizumab versus Ipilimumab in Advanced Melanoma. *N Engl J Med.* 2015;372:2521–2532. DOI:10.1056/NEJMoa1503093
12. Topalian SL, Hodi FS, Brahmer JR, et al. Safety, activity, and immune correlates of anti-PD-1 antibody in cancer. *N Engl J Med.* 2012;366:2443–2454. DOI:10.1056/NEJMoa1200690
13. Wolchok JD, Kluger H, Callahan MK, et al. Nivolumab plus ipilimumab in advanced melanoma. *N Engl J Med.* 2013;369:122–133. DOI:10.1056/NEJMoa1302369
14. Brahmer JR, Tykodi SS, Chow LQ, et al. Safety and activity of anti-PD-L1 antibody in patients with advanced cancer. *N Engl J Med.* 2012;366:2455–2465. DOI:10.1056/NEJMoa1200694
15. Forde PM, Reiss KA, Zeidan AM, et al. What lies within: novel strategies in immunotherapy for non-small cell lung cancer. *Oncologist.* 2013;18:1203–1213. DOI:10.1634/theoncologist.2013-0171
16. Garon EB. Current Perspectives in Immunotherapy for Non-Small Cell Lung Cancer. *Semin Oncol.* 2015;42(Suppl 2):S11–S8. DOI:10.1053/j.seminoncol.2015.09.019
17. Lipson EJ, Forde PM, Hammers HJ, et al. Antagonists of PD-1 and PD-L1 in Cancer Treatment. *Semin Oncol.* 2015;42:587–600. DOI:10.1053/j.seminoncol.2015.05.013



18. Hughes PE, Caenepeel S, Wu LC. Targeted Therapy and Checkpoint Immunotherapy Combinations for the Treatment of Cancer. *Trends Immunol.* 2016;37:462–476. DOI:10.1016/j.it.2016.04.010
19. Chiappinelli KB, Zahnow CA, Ahuja N, et al. Combining Epigenetic and Immunotherapy to Combat Cancer. *Cancer Res.* 2016;76:1683–1689. DOI:10.1158/0008-5472.CAN-15-2125
20. Saleh MH, Wang L, Goldberg MS. Improving cancer immunotherapy with DNA methyltransferase inhibitors. *Cancer Immunol Immunother.* 2016;65:787–796. DOI:10.1007/s00262-015-1776-3
21. Arina A, Corrales L, Bronte V. Enhancing T-cell therapy by overcoming the immunosuppressive tumor microenvironment. *Semin Immunol.* 2016;28:54–63. DOI:10.1016/j.smim.2016.01.002
22. Wolchok JD, Hoos A, O'Day S, et al. Guidelines for the evaluation of immune therapy activity in solid tumors: immune-related response criteria. *Clin Cancer Res.* 2009;15:7412–7420. DOI:10.1158/1078-0432.CCR-09-1624
23. van der Burg SH. Therapeutic vaccines in cancer: moving from immunomonitoring to immunoguiding. *Expert Rev Vaccines.* 2008;7:1–5. DOI:10.1586/14760584.7.1.1
24. Berraondo P, Nouze C, Preville X, et al. Eradication of large tumors in mice by a tritherapy targeting the innate, adaptive, and regulatory components of the immune system. *Cancer Res.* 2007;67:8847–8855. DOI:10.1158/0008-5472.CAN-07-0321
25. Klug F, Prakash H, Huber PE, et al. Low-dose irradiation programs macrophage differentiation to an iNOS(+)/M1 phenotype that orchestrates effective T-cell immunotherapy. *Cancer Cell.* 2013;24:589–602. DOI:10.1016/j.ccr.2013.09.014
26. Motz GT, Santoro SP, Wang LP, et al. Tumor endothelium FasL establishes a selective immune barrier promoting tolerance in tumors. *Nat Med.* 2014;20:607–615. DOI:10.1038/nm.3541
27. Samant RS, Shevde LA. Recent advances in anti-angiogenic therapy of cancer. *Oncotarget.* 2011;2:122–134. DOI:10.18632/oncotarget.234
28. Fox BA, Schendel DJ, Butterfield LH, et al. Defining the critical hurdles in cancer immunotherapy. *J Transl Med.* 2011;9:214. DOI:10.1186/1479-5876-9-214
29. Sharma SH, Thulasingham S, Nagarajan S. Chemopreventive agents targeting tumor microenvironment. *Life Sci.* 2016;145:74–84. DOI:10.1016/j.lfs.2015.12.016
30. Mills CD, Lenz LL, Harris RA. A breakthrough: macrophage-directed cancer immunotherapy. *Cancer Res.* 2016;76:513–516. DOI:10.1158/0008-5472.CAN-15-1737
31. Panni RZ, Linehan DC, DeNardo DG. Targeting tumor-infiltrating macrophages to combat cancer. *Immunotherapy.* 2013;5:1075–1087. DOI:10.2217/imt.13.102
32. Weigert A, Sekar D, Brune B. Tumor-associated macrophages as targets for tumor immunotherapy. *Immunotherapy.* 2009;1:83–95. DOI:10.2217/1750743X.1.1.83
33. van Poelgeest MI, Welters MJ, Vermeij R, et al. Vaccination against oncoproteins of HPV16 for non-invasive vulvar/vaginal lesions: lesion clearance is related to the strength of the T-cell response. *Clin Cancer Res.* 2016. DOI:10.1158/1078-0432.CCR-15-2594
- **Together with reference 35, these studies show clinical efficacy of vaccine in premalignant phase.**
34. Daayana S, Elkord E, Winters U, et al. Phase II trial of imiquimod and HPV therapeutic vaccination in patients with vulval intraepithelial neoplasia. *Br J Cancer.* 2010;102:1129–1136. DOI:10.1038/sj.bjc.6605611
35. Trimble CL, Morrow MP, Kraynyak KA, et al. Safety, efficacy, and immunogenicity of VGX-3100, a therapeutic synthetic DNA vaccine targeting human papillomavirus 16 and 18 E6 and E7 proteins for cervical intraepithelial neoplasia 2/3: a randomised, double-blind, placebo-controlled phase 2b trial. *Lancet.* 2015;386:2078–2088. DOI:10.1016/S0140-6736(15)00239-1.
- **Together with reference 33, these studies show clinical efficacy of vaccine in premalignant phase**

36. Czerniecki BJ, Koski GK, Koldovsky U, et al. Targeting HER-2/neu in early breast cancer development using dendritic cells with staged interleukin-12 burst secretion. *Cancer Res.* 2007;67:1842–1852. DOI:10.1158/0008-5472.CAN-06-4038
37. Morse MA, Niedzwiecki D, Marshall JL, et al. A randomized phase II study of immunization with dendritic cells modified with poxvectors encoding CEA and MUC1 compared with the same poxvectors plus GM-CSF for resected metastatic colorectal cancer. *Ann Surg.* 2013;258:879–886. DOI:10.1097/SLA.0b013e318292919e
38. Holmes JP, Gates JD, Benavides LC, et al. Optimal dose and schedule of an HER-2/neu (E75) peptide vaccine to prevent breast cancer recurrence: from US Military Cancer Institute Clinical Trials Group Study I-01 and I-02. *Cancer.* 2008;113:1666–1675. DOI:10.1002/cncr.23772
- **Together with reference 40, these studies show that the clinical efficacy of vaccination in adjuvant setting varies between studies.**
39. Cuppens K, Vansteenkiste J. Vaccination therapy for non-small-cell lung cancer. *Curr Opin Oncol.* 2014;26:165–170. DOI:10.1097/CCO.0000000000000052
40. Vansteenkiste JF, Cho BC, Vanakesa T, et al. Efficacy of the MAGE-A3 cancer immunotherapeutic as adjuvant therapy in patients with resected MAGE-A3-positive non-small-cell lung cancer (MAGRIT): a randomised, double-blind, placebo-controlled, phase 3 trial. *Lancet Oncol.* 2016;17:822–835. DOI:10.1016/S1470-2045(16)00099-1
- Together with reference 38, these studies show that the clinical efficacy of vaccination in adjuvant setting varies between studies.
41. Chang MH. Hepatitis B virus and cancer prevention. *Recent Results Cancer Res. Fortschritte der Krebsforschung Progres dans les recherches sur le cancer.* 2011;188:75–84. DOI:10.1007/978-3-642-10858-7\_6
42. Chow EP, Danielewski JA, Fehler G, et al. Human papillomavirus in young women with Chlamydia trachomatis infection 7 years after the Australian human papillomavirus vaccination programme: a cross-sectional study. *Lancet Infect Dis.* 2015;15:1314–1323. DOI:10.1016/S1473-3099(15)00055-9
43. Saletta F, Dalla PL, Byrne JA. Genetic causes of cancer predisposition in children and adolescents. *Transl Pediatr.* 2015;4:67–75. DOI:10.3978/j.issn.2224-4336.2015.04.08
44. Finn OJ, Beatty PL. Cancer immunoprevention. *Curr Opin Immunol.* 2016;39:52–58. DOI:10.1016/j.coi.2016.01.002
45. Finn OJ, Khleif SN, Herberman RB. The FDA guidance on therapeutic cancer vaccines: the need for revision to include preventive cancer vaccines or for a new guidance dedicated to them. *Cancer Prev Res (Phila).* 2015;8:1011–1016. DOI:10.1158/1940-6207.CAPR-15-0234
46. Antonia SJ, Mirza N, Fricke I, et al. Combination of p53 cancer vaccine with chemotherapy in patients with extensive stage small cell lung cancer. *Clin Cancer Res.* 2006;12:878–887. DOI:10.1158/1078-0432.CCR-05-2013
47. Wu X, Feng QM, Wang Y, et al. The immunologic aspects in advanced ovarian cancer patients treated with paclitaxel and carboplatin chemotherapy. *Cancer Immunol Immunother.* 2010;59:279–291. DOI:10.1007/s00262-009-0749-9
48. Welters MJ, van der Sluis TC, van Meir H, et al. Vaccination during myeloid cell depletion by cancer chemotherapy fosters robust T-cell responses. *Sci Transl Med.* 2016;8:334ra52. DOI:10.1126/sci-translmed.aaf0746
- **In this study, the vaccination has been given at a specific time point during chemotherapy based on preclinical immunomonitoring of chemotherapeutic impact on immune system.**
49. Liu R, Xiong S, Zhang L, et al. Enhancement of antitumor immunity by low-dose total body irradiation is associated with selectively decreasing the proportion and number of T regulatory cells. *Cell Mol Immunol.* 2010;7:157–162. DOI:10.1038/cmi.2009.117

50. Camisaschi C, Filipazzi P, Tazzari M, et al. Effects of cyclophosphamide and IL-2 on regulatory CD4<sup>+</sup> T-cell frequency and function in melanoma patients vaccinated with HLA-class I peptides: impact on the antigen-specific T-cell response. *Cancer Immunol Immunother.* 2013;62:897–908. DOI:10.1007/s00262-013-1397-7.
- **Together with references 57 and 58, it was shown that the dose and timing of cyclophosphamide administration prior to peptide vaccination to affect regulatory T-cells determines the vaccine-induced immunity and clinical outcome**
51. Murahashi M, Hijikata Y, Yamada K, et al. Phase I clinical trial of a five-peptide cancer vaccine combined with cyclophosphamide in advanced solid tumors. *Clin Immunol.* 2016. DOI:10.1016/j.clim.2016.03.015.
- **Together with references 56 and 58, it was shown that the dose and timing of cyclophosphamide administration prior to peptide vaccination to affect Tregs determines the vaccine-induced immunity and clinical outcome**
52. Walter S, Weinschenk T, Stenzl A, et al. Multi-peptide immune response to cancer vaccine IMA901 after single-dose cyclophosphamide associates with longer patient survival. *Nat Med.* 2012;18:1254–1261. DOI:10.1038/nm.2883.
- **Together with references 56 and 57, it was shown that the dose and timing of cyclophosphamide administration prior to peptide vaccination to affect Tregs determines the vaccine-induced immunity and clinical outcome**
53. Suzuki E, Kapoor V, Jassar AS, et al. Gemcitabine selectively eliminates splenic Gr-1<sup>+</sup>/CD11b<sup>+</sup> myeloid suppressor cells in tumor-bearing animals and enhances antitumor immune activity. *Clin Cancer Res.* 2005;11:6713–6721. DOI:10.1158/1078-0432.CCR-05-0883
54. Rettig L, Seidenberg S, Parvanova I, et al. Gemcitabine depletes regulatory T-cells in human and mice and enhances triggering of vaccine-specific cytotoxic T-cells. *Int J Cancer.* 2011;129:832–838. DOI:10.1002/ijc.25756
55. Suttmüller RP, van Duivenvoorde LM, van Elsas A, et al. Synergism of cytotoxic T lymphocyte-associated antigen 4 blockade and depletion of CD25(+) regulatory T-cells in antitumor therapy reveals alternative pathways for suppression of autoreactive cytotoxic T lymphocyte responses. *J Exp Med.* 2001;194:823–832.
56. Casares N, Arribillaga L, Sarobe P, et al. CD4<sup>+</sup>/CD25<sup>+</sup> regulatory cells inhibit activation of tumor-primed CD4<sup>+</sup> T-cells with IFN- $\gamma$ -dependent antiangiogenic activity, as well as long-lasting tumor immunity elicited by peptide vaccination. *J Immunol.* 2003;171:5931–5939.
57. Prasad SJ, Farrand KJ, Matthews SA, et al. Dendritic cells loaded with stressed tumor cells elicit long-lasting protective tumor immunity in mice depleted of CD4<sup>+</sup>CD25<sup>+</sup> regulatory T-cells. *J Immunol.* 2005;174:90–98.
58. Sluijter M, van der Sluis TC, van der Velden PA, et al. Inhibition of CSF-1R supports T-cell mediated melanoma therapy. *PLoS One.* 2014;9:e104230. DOI:10.1371/journal.pone.0104230
59. Mok S, Koya RC, Tsui C, et al. Inhibition of CSF-1 receptor improves the antitumor efficacy of adoptive cell transfer immunotherapy. *Cancer Res.* 2014;74:153–161. DOI:10.1158/0008-5472.CAN-13-1816
60. Dannull J, Su Z, Rizzieri D, et al. Enhancement of vaccine-mediated antitumor immunity in cancer patients after depletion of regulatory T-cells. *J Clin Invest.* 2005;115:3623–3633. DOI:10.1172/JCI25947
- **This report demonstrates that proper depletion of regulatory T-cells prior to vaccination significantly improved the efficacy of the vaccine in renal cell cancer patients.**
61. Iinuma H, Fukushima R, Inaba T, et al. Phase I clinical study of multiple epitope peptide vaccine combined with chemoradiation therapy in esophageal cancer patients. *J Transl Med.* 2014;12:84. DOI:10.1186/1479-5876-12-84



62. Hirooka Y, Itoh A, Kawashima H, et al. A combination therapy of gemcitabine with immunotherapy for patients with inoperable locally advanced pancreatic cancer. *Pancreas*. 2009;38:e69–e74. DOI:10.1097/MPA.0b013e318197a9e3.
- **Together with references 61 and 97, these studies reveal different mechanisms of gemcitabine all resulting in enhanced efficacy of the immunotherapy**
63. Chu Y, Wang LX, Yang G, et al. Efficacy of GM-CSF-producing tumor vaccine after docetaxel chemotherapy in mice bearing established Lewis lung carcinoma. *J Immunother*. 2006;29:367–380. DOI:10.1097/01.cji.0000199198.43587.ba
64. Tseng CW, Trimble C, Zeng Q, et al. Low-dose radiation enhances therapeutic HPV DNA vaccination in tumor-bearing hosts. *Cancer Immunol Immunother*. 2009;58:737–748. DOI:10.1007/s00262-008-0596-0
65. Moschella F, Valentini M, Arico E, et al. Unraveling cancer chemo-immunotherapy mechanisms by gene and protein expression profiling of responses to cyclophosphamide. *Cancer Res*. 2011;71:3528–3539. DOI:10.1158/0008-5472.CAN-10-4523
66. Klein O, Davis ID, McArthur GA, et al. Low-dose cyclophosphamide enhances antigen-specific CD4(+) T-cell responses to NY-ESO-1/ ISCOMATRIX vaccine in patients with advanced melanoma. *Cancer Immunol Immunother*. 2015;64:507–518. DOI:10.1007/s00262-015-1656-x
67. Tanaka F, Yamaguchi H, Ohta M, et al. Intratumoral injection of dendritic cells after treatment of anticancer drugs induces tumor-specific antitumor effect in vivo. *Int J Cancer*. 2002;101:265–269. DOI:10.1002/ijc.10597
68. Nistico P, Capone I, Palermo B, et al. Chemotherapy enhances vaccine-induced antitumor immunity in melanoma patients. *Int J Cancer*. 2009;124:130–139. DOI:10.1002/ijc.23886.
- **This report demonstrates a chemotherapy-induced enhancement of the vaccine-induced CD8<sup>+</sup> (memory) T-cell immune response**
69. Palermo B, Del BD, Sottini A, et al. Dacarbazine treatment before peptide vaccination enlarges T-cell repertoire diversity of melan-asppecific, tumor-reactive CTL in melanoma patients. *Cancer Res*. 2010;70:7084–7092. DOI:10.1158/0008-5472.CAN-10-1326
70. Peng S, Wang JW, Karanam B, et al. Sequential cisplatin therapy and vaccination with HPV16 E6E7L2 fusion protein in saponin adjuvant GPI-0100 for the treatment of a model HPV16+ cancer. *PLoS One*. 2015;10:e116389. DOI:10.1371/journal.pone.0116389
71. Bracci L, Moschella F, Sestili P, et al. Cyclophosphamide enhances the antitumor efficacy of adoptively transferred immune cells through the induction of cytokine expression, B-cell and T-cell homeostatic proliferation, and specific tumor infiltration. *Clin Cancer Res*. 2007;13:644–653. DOI:10.1158/1078-0432.CCR-06-1209.
- **Next to effect of cyclophosphamide on regulatory T-cells this report shows a different mechanism of enhancing the antitumor response**
72. Farsaci B, Higgins JP, Hodge JW. Consequence of dose scheduling of sunitinib on host immune response elements and vaccine combination therapy. *Int J Cancer*. 2012;130:1948–1959. DOI:10.1002/ijc.26219
73. Finke JH, Rini B, Ireland J, et al. Sunitinib reverses type-1 immune suppression and decreases T-regulatory cells in renal cell carcinoma patients. *Clin Cancer Res*. 2008;14:6674–6682. DOI:10.1158/1078-0432.CCR-07-5212
74. Tseng CW, Hung CF, Alvarez RD, et al. Pretreatment with cisplatin enhances E7-specific CD8<sup>+</sup> T-Cell-mediated antitumor immunity induced by DNA vaccination. *Clin Cancer Res*. 2008;14:3185–3192. DOI:10.1158/1078-0432.CCR-08-0037
75. Lee SY, Kang TH, Knoff J, et al. Intratumoral injection of therapeutic HPV vaccinia vaccine following cisplatin enhances HPV-specific antitumor effects. *Cancer Immunol Immunother*. 2013;62:1175–1185. DOI:10.1007/s00262-013-1421-y

76. Berinstein NL, Karkada M, Oza AM, et al. Survivin-targeted immunotherapy drives robust polyfunctional T-cell generation and differentiation in advanced ovarian cancer patients. *Oncoimmunology*. 2015;4:e1026529. DOI:10.1080/2162402X.2015.1008371
77. Machiels JP, Reilly RT, Emens LA, et al. Cyclophosphamide, doxorubicin, and paclitaxel enhance the antitumor immune response of granulocyte/macrophage-colony stimulating factor-secreting whole-cell vaccines in HER-2/neu tolerized mice. *Cancer Res*. 2001;61:3689–3697.
78. Wei SM, Fei JX, Tao F, et al. Anti-CD27 antibody potentiates anti-tumor effect of dendritic cell-based vaccine in prostate cancer-bearing mice. *Int Surg*. 2015;100:155–163. DOI:10.9738/INTSURG-D-14-00147.1
79. Tagliamonte M, Petrizzo A, Napolitano M, et al. Novel metronomic chemotherapy and cancer vaccine combinatorial strategy for hepatocellular carcinoma in a mouse model. *Cancer Immunol Immunother*. 2015;64:1305–1314. DOI:10.1007/s00262-015-1698-0
80. Dijkgraaf EM, Santeoets SJ, Reyners AK, et al. A phase 1/2 study combining gemcitabine, Pegintron and p53 SLP vaccine in patients with platinum-resistant ovarian cancer. *Oncotarget*. 2015;6:32228–32243. DOI:10.18632/oncotarget.4772.
- **Together with references 95 and 96, these studies reveal different mechanisms of gemcitabine all resulting in enhanced efficacy of the immunotherapy**
81. van der Sluis TC, van Duikeren S, Huppelschoten S, et al. Vaccine-induced tumor necrosis factor-producing T-cells synergize with cisplatin to promote tumor cell death. *Clin Cancer Res*. 2015;21:781–794. DOI:10.1158/1078-0432.CCR-14-2142
82. Gibney GT, Kudchadkar RR, DeConti RC, et al. Safety, correlative markers, and clinical results of adjuvant nivolumab in combination with vaccine in resected high-risk metastatic melanoma. *Clin Cancer Res*. 2015;21:712–720. DOI:10.1158/1078-0432.CCR-14-2468
83. Fu J, Malm IJ, Kadayakkara DK, et al. Preclinical evidence that PD1 blockade cooperates with cancer vaccine TEGVAX to elicit regression of established tumors. *Cancer Res*. 2014;74:4042–4052. DOI:10.1158/0008-5472.CAN-13-2685
84. Sawada Y, Yoshikawa T, Shimomura M, et al. Programmed death-1 blockade enhances the antitumor effects of peptide vaccine-induced peptide-specific cytotoxic T lymphocytes. *Int J Oncol*. 2015;46:28–36. DOI:10.3892/ijo.2014.2737
85. Mkrtichyan M, Chong N, Abu ER, et al. Anti-PD-1 antibody significantly increases therapeutic efficacy of *Listeria monocytogenes* (Lm)-LLO immunotherapy. *J Immunother Cancer*. 2013;1:15. DOI:10.1186/2051-1426-1-15
86. Wada S, Jackson CM, Yoshimura K, et al. Sequencing CTLA-4 blockade with cell-based immunotherapy for prostate cancer. *J Transl Med*. 2013;11:89. DOI:10.1186/1479-5876-11-89
87. Newton MR, Askeland EJ, Andresen ED, et al. Anti-interleukin-10R1 monoclonal antibody in combination with bacillus Calmette–Guerin is protective against bladder cancer metastasis in a murine orthotopic tumour model and demonstrates systemic specific anti-tumour immunity. *Clin Exp Immunol*. 2014;177:261–268. DOI:10.1111/cei.12315
88. Ito F, Li Q, Shreiner AB, et al. Anti-CD137 monoclonal antibody administration augments the antitumor efficacy of dendritic cell-based vaccines. *Cancer Res*. 2004;64:8411–8419. DOI:10.1158/0008-5472.CAN-04-0590
89. Cuadros C, Dominguez AL, Lollini PL, et al. Vaccination with dendritic cells pulsed with apoptotic tumors in combination with anti-OX40 and anti-4-1BB monoclonal antibodies induces T-cell-mediated protective immunity in Her-2/neu transgenic mice. *Int J Cancer*. 2005;116:934–943. DOI:10.1002/ijc.21098
90. Kim S, Buchlis G, Fridlender ZG, et al. Systemic blockade of transforming growth factor-beta signaling augments the efficacy of immunogene therapy. *Cancer Res*. 2008;68:10247–10256. DOI:10.1158/0008-5472.CAN-08-1494



91. Chakraborty M, Abrams SI, Coleman CN, et al. External beam radiation of tumors alters phenotype of tumor cells to render them susceptible to vaccine-mediated T-cell killing. *Cancer Res.* 2004;64:4328–4337. DOI:10.1158/0008-5472.CAN-04-0073
- **Together with reference 120, these studies demonstrate the importance of radiation therapy given after immunotherapy in a mouse model to increase the anti-tumor efficacy.**
92. Mondini M, Nizard M, Tran T, et al. Synergy of Radiotherapy and a Cancer Vaccine for the Treatment of HPV-Associated Head and Neck Cancer. *Mol Cancer Ther.* 2015;14:1336–1345. DOI:10.1158/1535-7163.MCT-14-1015
- **Together with reference 119, these studies demonstrate the importance of radiation therapy given after immunotherapy in a mouse model to increase the antitumor efficacy.**
93. Fridman WH, Pages F, Sautes-Fridman C, et al. The immune contexture in human tumours: impact on clinical outcome. *Nat Rev Cancer.* 2012;12:298–306. DOI:10.1038/nrc3245
94. Gouttefangeas C, Walter S, Welters M, et al. Flow cytometry in cancer immunotherapy: applications, quality assurance and future. In: *Cancer Immunology: Translational Medicine from Bench to Bedside* (N. Rezaei *editor*). Springer-Verlag Berlin Heidelberg. Chapter 25: pages 471–486. DOI: 10.1007/978-3-662-44006-3
95. Welters MJ, Van Der Burg SH. Comprehensive immunomonitoring to guide the development of immunotherapeutic products for cancer. In: Prendergast GC, Jaffee EM, editors. *Cancer Immunotherapy second edition: Immune suppression and tumor growth*. 2013. Elsevier Academic Press London UK, Chapter 16, p. 241–258.
96. Galluzzi L, Buque A, Kepp O, et al. Immunological Effects of Conventional Chemotherapy and Targeted Anticancer Agents. *Cancer Cell.* 2015;28:690–714. DOI:10.1016/j.ccell.2015.10.012
97. Vacchelli E, Aranda F, Eggermont A, et al. Trial watch: chemotherapy with immunogenic cell death inducers. *Oncoimmunology.* 2014;3:e27878. DOI:10.4161/onci.27878
98. Ghiringhelli F, Larmonier N, Schmitt E, et al. CD4+CD25+ regulatory T-cells suppress tumor immunity but are sensitive to cyclophosphamide which allows immunotherapy of established tumors to be curative. *Eur J Immunol.* 2004;34:336–344. DOI:10.1002/eji.200324181
99. Lutsiak ME, Semnani RT, De PR, et al. Inhibition of CD4(+)25+ T regulatory cell function implicated in enhanced immune response by low-dose cyclophosphamide. *Blood.* 2005;105:2862–2868. DOI:10.1182/blood-2004-06-2410
100. Homma Y, Taniguchi K, Nakazawa M, et al. Changes in the immune cell population and cell proliferation in peripheral blood after gemcitabine-based chemotherapy for pancreatic cancer. *Clin Transl Oncol.* 2014;16:330–335. DOI:10.1007/s12094-013-1079-0
101. Shevchenko I, Karakhanova S, Soltek S, et al. Low-dose gemcitabine depletes regulatory T-cells and improves survival in the orthotopic Panc02 model of pancreatic cancer. *Int J Cancer.* 2013;133:98–107. DOI:10.1002/ijc.27990
102. Vincent J, Mignot G, Chalmin F, et al. 5-Fluorouracil selectively kills tumor-associated myeloid-derived suppressor cells resulting in enhanced T-cell-dependent antitumor immunity. *Cancer Res.* 2010;70:3052–3061. DOI:10.1158/0008-5472.CAN-09-3690
103. Roselli M, Cereda V, di Bari MG, et al. Effects of conventional therapeutic interventions on the number and function of regulatory T-cells. *Oncoimmunology.* 2013;2:e27025. DOI:10.4161/onci.27025
104. Vieweg J, Su Z, Dahm P, et al. Reversal of tumor-mediated immunosuppression. *Clin Cancer Res.* 2007;13:727s–32s. DOI:10.1158/1078-0432.CCR-06-1924
105. Welters MJ, Piersma SJ, van der Burg SH. T-regulatory cells in tumour-specific vaccination strategies. *Expert Opin Biol Ther.* 2008;8:1365–1379. DOI:10.1517/14712598.8.9.1365
106. Casares N, Rudilla F, Arribillaga L, et al. A peptide inhibitor of FOXP3 impairs regulatory T-cell activity and improves vaccine efficacy in mice. *J Immunol.* 2010;185:5150–5159. DOI:10.4049/jimmunol.1001114

107. Rech AJ, Mick R, Martin S, et al. CD25 blockade depletes and selectively reprograms regulatory T-cells in concert with immunotherapy in cancer patients. *Sci Transl Med*. 2012;4:134ra62. DOI:10.1126/scitranslmed.3003330
  108. Kudo-Saito C, Schlom J, Camphausen K, et al. The requirement of multimodal therapy (vaccine, local tumor radiation, and reduction of suppressor cells) to eliminate established tumors. *Clin Cancer Res*. 2005;11:4533–4544. DOI:10.1158/1078-0432.CCR-04-2237
  109. Ruffell B, Coussens LM. Macrophages and therapeutic resistance in cancer. *Cancer Cell*. 2015;27:462–472. DOI:10.1016/j.ccell.2015.02.015
  110. Hume DA, MacDonald KP. Therapeutic applications of macrophage colony-stimulating factor-1 (CSF-1) and antagonists of CSF-1 receptor (CSF-1R) signaling. *Blood*. 2012;119:1810–1820. DOI:10.1182/blood-2011-09-379214
  111. Srivastava MK, Dubinett S, Sharma S. Targeting MDSCs enhance therapeutic vaccination responses against lung cancer. *Oncoimmunology*. 2012;1:1650–1651. DOI:10.4161/onci.21970
  112. Moschella F, Torelli GF, Valentini M, et al. Cyclophosphamide induces a type I interferon-associated sterile inflammatory response signature in cancer patients' blood cells: implications for cancer chemoimmunotherapy. *Clin Cancer Res*. 2013;19:4249–4261. DOI:10.1158/1078-0432.CCR-12-3666
  113. Vermeij R, Leffers N, Hoogeboom BN, et al. Potentiation of a p53-SLP vaccine by cyclophosphamide in ovarian cancer: a single-arm phase II study. *Int J Cancer*. 2012;131:E670–E80. DOI:10.1002/ijc.27388
  114. Kaida M, Morita-Hoshi Y, Soeda A, et al. Phase I trial of Wilms tumor 1 (WT1) peptide vaccine and gemcitabine combination therapy in patients with advanced pancreatic or biliary tract cancer. *J Immunother*. 2011;34:92–99. DOI:10.1097/CJI.0b013e3181fb65b9.
- **Together with references 61 and 96, these studies reveal different mechanisms of gemcitabine all resulting in enhanced efficacy of the immunotherapy**
115. Correale P, Cusi MG, Tsang KY, et al. Chemo-immunotherapy of metastatic colorectal carcinoma with gemcitabine plus FOLFOX 4 followed by subcutaneous granulocyte macrophage colony-stimulating factor and interleukin-2 induces strong immunologic and antitumor activity in metastatic colon cancer patients. *J Clin Oncol*. 2005;23:8950–8958. DOI:10.1200/JCO.2005.12.147
  116. Bauer C, Bauernfeind F, Sterzik A, et al. Dendritic cell-based vaccination combined with gemcitabine increases survival in a murine pancreatic carcinoma model. *Gut*. 2007;56:1275–1282. DOI:10.1136/gut.2006.108621
  117. Tumeh PC, Harview CL, Yearley JH, et al. PD-1 blockade induces responses by inhibiting adaptive immune resistance. *Nature*. 2014;515:568–571. DOI:10.1038/nature13954
  118. Reck M, Bondarenko I, Luft A, et al. Ipilimumab in combination with paclitaxel and carboplatin as first-line therapy in extensive-disease small-cell lung cancer: results from a randomized, double-blind, multicenter phase 2 trial. *Ann Oncol*. 2013;24:75–83. DOI:10.1093/annonc/mds213.
- **Not the concurrent administration but chemotherapy prior to checkpoint blockade results in improved clinical outcome**
119. Muller AJ, DuHadaway JB, Donover PS, et al. Inhibition of indoleamine 2,3-dioxygenase, an immunoregulatory target of the cancer suppression gene Bin1, potentiates cancer chemotherapy. *Nat Med*. 2005;11:312–319. DOI:10.1038/nm1196.
  120. Bjoern J, Iversen TZ, Nitschke NJ, et al. Safety, immune and clinical responses in metastatic melanoma patients vaccinated with a long peptide derived from indoleamine 2,3-dioxygenase in combination with ipilimumab. *Cytotherapy*. 2016;18:1043–1055. DOI:10.1016/j.jcyt.2016.05.010
  121. Kvistborg P, Philips D, Kelderman S, et al. Anti-CTLA-4 therapy broadens the melanoma-reactive CD8+ T-cell response. *Sci Transl Med*. 2014;6:254ra128. DOI:10.1126/scitranslmed.3008918
  122. Peggs KS, Quezada SA, Chambers CA, et al. Blockade of CTLA-4 on both effector and regulatory T-cell compartments contributes to the antitumor activity of anti-CTLA-4 antibodies. *J Exp Med*. 2009;206:1717–1725. DOI:10.1084/jem.20082492



123. Romano E, Kusio-Kobialka M, Foukas PG, et al. Ipilimumab-dependent cell-mediated cytotoxicity of regulatory T-cells ex vivo by nonclassical monocytes in melanoma patients. *Proc Natl Acad Sci U S A*. 2015;112:6140–6145. DOI:10.1073/pnas.1417320112
  124. van der Sluis TC, Sluijter M, van Duikeren S, et al. Therapeutic Peptide Vaccine-Induced CD8 T Cells Strongly Modulate Intratumoral Macrophages Required for Tumor Regression. *Cancer Immunol Res*. 2015;3:1042–1051. DOI:10.1158/2326-6066.CIR-15-0052
  125. Association of Cancer Immunotherapy's (CIMT's) immunoguiding program. Available from: <http://www.cimt.eu/workgroups/cip/>
  126. Cancer Immunotherapy Consortium (CIC). <http://www.cancerresearch.org/cic>
  127. Britten CM, Gouttefangeas C, Welters MJ, et al. The CIMT-monitoring panel: a two-step approach to harmonize the enumeration of antigen-specific CD8+ T lymphocytes by structural and functional assays. *Cancer Immunol Immunother*. 2008;57:289–302. DOI:10.1007/s00262-007-0378-0
  128. Filbert H, Attig S, Bidmon N, et al. Serum-free freezing media support high cell quality and excellent ELISPOT assay performance across a wide variety of different assay protocols. *Cancer Immunol Immunother*. 2013;62:615–627. DOI:10.1007/s00262-012-1359-5
  129. Britten CM, Janetzki S, Butterfield LH, et al. T-cell assays and MIATA: the essential minimum for maximum impact. *Immunity*. 2012;37:1–2. DOI:10.1016/j.immuni.2012.07.010
  130. Young KH, Baird JR, Savage T, et al. Optimizing Timing of Immunotherapy Improves Control of Tumors by Hypofractionated Radiation Therapy. *PLoS One*. 2016;11:e0157164. DOI:10.1371/journal.pone.0157164
- **This report shows the importance of specific timing in the combination therapy using agonistic antibody therapy and immune checkpoint blockade.**





# Chapter **7**

## **Summary and general discussion**



Immunotherapy as stand-alone treatment or in combination with other therapies including conventional therapies show promising clinic results. However, durable responses have only been obtained in a minority of patients. Therefore, a better understanding of the role of the immune system and the tumor context in (combination) therapies is needed. This involves comprehensive investigation of the mechanisms underlying the efficacy of therapies, the type of tumor, its microenvironment and the changes induced upon treatment. Recently, the histological sections of tumor biopsies from patients prior to treatment with PD-L1/PD1 were examined for these factors in the context of clinical studies (1-3). Three immune profiles were identified which potentially can predict the response of patients to immunotherapy (4). The first profile, called an immune-inflamed phenotype or “hot” tumor which is characterized by the presence of immune cells in the tumor parenchyma and in close proximity to the tumor cells. This phenotype is often accompanied by detection of proinflammatory and effector cytokines and exhibits pre-existing tumor immunity, which may be impeded by immunosuppression. Therefore, a response is not guaranteed. The second profile reflects an immune-excluded phenotype and is defined by the presence of abundant immune cells in the stroma of which only a few penetrate the tumor parenchyma. The third phenotype lacks tumor-infiltrating immune cells, in particular CD8 T cells, thereby displaying an immune-desert (“cold”) phenotype. The immune-desert phenotype most likely does not respond to immunotherapy. Thus, it is crucial to determine the tumor micro-environmental status before designing an effective anti-cancer therapy. In addition, the changes of the developing tumor in time and during treatment as part of the cancer immunoediting process should be considered in the context of these cancer-immune phenotypes. In **chapter 6**, we discussed the importance of correct timing of immunotherapy in two main categories. First, we discussed the significance of optimal timing of immunotherapy and combination therapy in the context of early and late stage of disease. Secondly, we reviewed the ideal sequential administration of different chemotherapy and immunotherapy approaches, depending on their mechanisms. Therefore, effective immunotherapy or combination therapies can be explained not only based on their mechanisms but also in the context of timing and cancer-immune phenotypes.

## **Making a “cold” tumor “hot” by overcoming immune ignorance and tolerance**

Early stages of tumors are usually immunogenic, and can be potentially targeted by different immunotherapy approaches, thereby converting a cold tumor to hot tumor. However, tumor can become resistant to immunotherapy due to various tumor cell intrinsic and extrinsic mechanisms. Tumor cell intrinsic mechanism includes absence of antigenic protein or antigen presentation, deregulation in expression of certain genes and pathways in tumor cells that inhibit immune cell infiltration or function within the tumor environment such as mitogen-activated protein kinase (MAPK) pathway, PTEN and PI3K signaling, WNT/ $\beta$ -catenin

signaling pathway and loss of IFN $\gamma$  signaling pathway (5). Absence of T cells, inhibitory immune checkpoints or immunosuppressive cells are the different examples of tumor cell extrinsic mechanisms (5). Therefore, it is critical to overcome these resistance mechanisms so that tumor- specific T cells can specifically eradicate the tumor cells.

In **chapter 2** we showed that cisplatin, a chemotherapeutic agent that synergizes with T-cell produced TNF $\alpha$  to kill tumor cells (6), also acts as an agent that converts cold tumors into hot tumors (**Figure 1**). Treatment of TC-1 tumors resulted in a strong influx of the tumors with inflammatory myeloid cells, including CD11c<sup>+</sup>CD11b<sup>+</sup>Ly6C<sup>+</sup> cells. Previously, it has been shown that these myeloid cells were responsible for the immunogenic cell death of tumors when treated with anthracycline chemotherapy (7). CD11c<sup>+</sup>CD11b<sup>+</sup>Ly6C<sup>+</sup> cells were well prepared to engulf apoptotic tumor cells and to present tumor antigen to T cells, thereby increasing anti-tumor immunity. In **chapter 2**, we demonstrated that increasing the activation of professional APCs by danger signals released by chemotherapy-treated tumor cells lead to a higher activation of T cells. Cisplatin treatment of the tumor not only killed the tumor cells but also induced the release of a series of danger signals, including HMGB1 and IFN $\alpha$  in the tumor microenvironment. These APC-activating signals increased the expression of T cell costimulatory signals such as CD80 and CD86 on myeloid cells, especially on inflammatory myeloid cells. As result, a more potent T cell response was induced, as shown by the higher production of cytokines by these cells. Thus, immunotherapy including the chemotherapeutic agents that have immunostimulatory effects can not only target tumor cells but also reshape the tumor microenvironment in a way that is beneficial to anti-tumor immunity. This notion is also depicted in **chapter 3** showing that administration of cisplatin at the time of the regression could prevent the relapse by killing the remaining tumor cells after the first T-cell mediated tumor regression and not altering the intratumoral myeloid composition. However, in the setting in which directly ex-vivo cell sorted of recurrent tumor cells were reinjected into naïve mice and where the tumor cells still retained their resistance to vaccine therapy, cisplatin alone could delay tumor out growth and in combination with peptide vaccination significantly improved the survival of the mice. This effect was based on a restored tumor influx by the inflammatory myeloid cells.

Cancer vaccines, designed to generate and expand the pool of tumor-specific T cells from the naïve repertoire and/or restore the activity of tumor-specific T cells that are already present in a dormant or anergic state, may also be used to induce or activate a strong tumor-specific T cell response. These so- called therapeutic vaccines have been optimized by using optimal antigen selection, proper adjuvants and a suitable mode of delivery (8-10). As yet, the clinical efficacy of most therapeutic vaccines has been /demonstrated in the context of premalignant lesions or minimal residual disease; a clinical setting where the impact of the tumor microenvironment is less underestimated. For example, HPV16 SLP vaccination in



patients with high-grade HPV16-induced vulvar intraepithelial neoplasia (VIN) induced complete and partial regression (11-13). Importantly, the clinical success is correlated with vaccine-induced T cell responses against the tumor antigen (14). Similar success has been achieved in VIN and cervical intraepithelial neoplasia (CIN) patients with other vaccine platforms such as an HPV16 E6-E7-L2 fusion protein vaccine and a DNA vaccine (15, 16). However, in patients with late stage cervical cancer these vaccines were not successful, which may be related to the weaker vaccine-induced T cell response observed in cancer patients (12, 17). We addressed this issue in **chapter 3**, where a suboptimal vaccination strategy for HPV16 SLP vaccination, containing an E7 CTL and Th epitope, was used in mice. In comparison to the optimal vaccination scheme, a much lower percentage of tumor-specific T cells was obtained after vaccination. Under the suboptimal vaccine condition therapeutic vaccination of tumor-bearing mice still induced tumor regression. This, however, was only transient control of TC- 1 tumor burden as the tumors subsequently recurred. Based on the tumor microenvironment, the original tumor is displayed as cold tumor (**Figure 1A**). SLP vaccination in combination with CPG adjuvant, providing increased availability of tumor antigen and its presentation to T cells by APCs, improved the priming and activation of type 1 T cells. These IFN $\gamma$  and TNF $\alpha$  producing tumor-specific CD8 T cells migrated to the tumor where they also attracted inflammatory myeloid cells, together responsible for tumor cell death and full tumor regression but only if the vaccine-induced response was strong enough. Also, vaccination with short synthetic peptide in IFA induces inadequate tumor regression. Vaccination resulted in the transient activation of effector CD8 T cell without the secondary expansion. Most likely this was due to the fact that the minimal CTL epitope also is loaded on non-professional APCs resulting in its presentation to the T cells in non-inflamed lymphoid organs in the absence of appropriate costimulatory signals. Vaccination with a longer version of the CTL peptide epitope in combination with MHC-II-binding Th peptide epitope, resulted in the presentation of the T cell epitopes by professional APCs only, resulting in enhanced duration of *in vivo* epitope presentation in an appropriate context leading to superior CTL responses (18). In **chapter 5**, we showed that vaccination with MCMV-based vaccine vectors expressing the minimal HPV16 E7 CTL epitope in the MCMV IE2 region induced antigen-specific CTL response. In contrast to the minimal CTL epitope peptide vaccine, the antigen-specific CTL responses induced by MCMV-based vaccine vector expanded over time and followed the inflationary response similar to the MCMV viral epitopes. Importantly, defined levels of these tumor- specific T cells prevented the development of tumors and induced tumor outgrowth delay in a therapeutic setting. Thus, potent and optimal vaccination can induce type 1 cytokine producing tumor-specific T cells. Infiltration of these tumor-specific T cells in the tumor microenvironment, accompanied by the influx of other immune cells, can lead to the development of an inflamed-tumor and an effective anti- tumor response (**Figure 1B**). In addition, combination of immunotherapy with other cancer therapeutic strategies such chemotherapy at this stage of tumor microenvironment can induce synergistic anti-tumor effect as shown by us in **chapter 2** and others (6).

## Immune regulation of inflamed tumors

Despite massive immune cell infiltration and subsequent full tumor regression of immunotherapy-induced inflamed tumors, a long-term complete response is not always ensured (**Figure 1C**). Currently, several pathways have been described that may limit the efficacy of tumor-specific T cell responses (5). In the recent years, it has been a major focus on immune checkpoint inhibitors which regulate immune activation and maintain immune homeostasis. Several studies have shown the role of these pathways such as PD-1/PD-L1, CD28/CTLA-4 and the recently discovered NKG2A/Qa-1 axis in escape of tumors from the immune system (19-25). In our preclinical tumor model of HPV-induced cancer, we demonstrated that sub-optimal HPV16 SLP vaccine can induce tumor regression in all the mice although in the end tumor recurrences are observed in all mice (**Chapter 3**). Previously, it has been shown that PD-L1 treatment is most effective in patients with inflamed tumor in which the pre-existing immunity is suppressed (2, 26). Therefore, to prevent immunotherapy-driven recurrence of tumors, we made use of combination therapy of vaccine with immune checkpoint blockade of the PD-1/PD-L1 pathway. In **chapter 6**, we discussed the importance of timing in administration of combination therapy. Therefore, in **chapter 3** we tried the combination therapy of SLP vaccine with PD-1 blocking antibody at two time points; before tumor regression or at the time of regression. Despite expression of PD-L1 on myeloid cells and tumor cells, administration of PD-1 blocking antibodies both before or at the time of regression did not prevent tumor recurrence, showing that this pathway does not play a role in our immunotherapy-driven recurrence tumor model.

It has been shown previously that tumor-infiltrating lymphocytes may display a dysfunctional state such as exhaustion which results in lower efficacy of immunotherapy (27). Exhausted CD8 T cells are defined by several criteria such as overexpression of several inhibitory receptors, alteration in cytokine signaling pathway and genes involved in chemotaxis, adhesion, and migration, expression of a distinct set of transcription factors and lack of metabolic and bioenergetics (28). However, recently a new population of CD8 T cells has been identified in a chronic viral infection and cancer which proliferates after PD-1 blockade pathway (29, 30). This population expresses PD-1 inhibitory receptor but also expresses several costimulatory molecules such as ICOS and CD28 and is characterized by a unique gene signature. Following PD-1 treatment, these cells differentiate to the terminally exhausted CD8 T cells (29). Particularly, the transcription factor TCF1 has a cell-intrinsic and crucial role in the generation of this subset. In **chapter 3**, we have shown that CD8 T cells including tumor-specific CD8 T cells express similar levels of coinhibitory markers such as PD-1, LAG-3 and TIM-3 at the time of the regression compared to the relapse. In addition, T cells at both time points produced equivalent levels of cytokines for instance IFN $\gamma$ , TNF $\alpha$  and IL-2 and even CD4<sup>+</sup> T cells produced higher amount of these cytokines at the time of





relapse. Therefore, it is unlikely that the T cells at the time of relapse underwent exhaustion. Nevertheless, we cannot exclude the possibility if the CD8 T cells at the time of the relapse are the terminally exhausted cells. Thus, further investigation needs to be performed to define the characterization of these less infiltrated T cells. This also has great importance in all the tumor settings to characterize the phenotype and transcription profile of CD8 T cells before applying immunotherapy or combination therapies. This could potentially have major impact in the cost of the immunotherapy.

Another rate-limiting factor which hinders the efficacy of the tumor-specific T cell responses is the immunosuppressive tumor microenvironment. Several mechanisms have been identified which can trigger an immunosuppressive microenvironment leading to a non-inflamed tumor. In this regard, immunosuppressive cells such as Tregs, M2 macrophages and MDSCs as well as immunosuppressive molecules are critical. Immunotherapeutic approaches targeting these immunosuppressive cells or factors, including blocking/depleting antibodies or small molecule inhibitors are well studied in a clinical setting. Treatment modalities such as chemotherapeutic agents that can affect the immunosuppressive tumor microenvironment have been discussed in **chapter 6**. However, sometimes immunotherapy can mediate a double-edged effect. An example of this is shown in **chapter 4**, where the negative effect of IL-6 produced by tumor cells on the composition of the tumor microenvironment was shown. Importantly, IL-6 blockade by administration of IL-6R or IL-6 blocking antibodies from the time of vaccination onwards, did not improve the therapeutic effect of this therapy. IL-6 produced by the tumor cells increase the percentage of CD11b<sup>+</sup> Ly6C<sup>+</sup> myeloid cells and skews the phenotype of these cells to a less immature phenotype. This was observed both under steady state conditions as during therapeutic vaccination. However, blockade of IL-6 pathway had a negative effect probably because both the expansion of vaccine-induced T cells and the full tumoricidal function of the vaccine-driven tumor-infiltrating macrophages required IL-6 signaling during the regression phase of the tumors. Late IL-6 blockade, that is after the initial regression of tumors, improved the clinical outcome of treated tumors. Moreover, we showed that compared to early IL-6 blockade, the administration of IL-6 blocking antibodies after regression led to a stronger influx with type 1 CD4 and CD8 T cells (**Chapter 4**). Similarly, in melanoma tumor model IL-6 blockade increase Th1 response and tumor outgrowth delay. However, it also induces upregulation of PD-L1 on tumor cells. At the same time, blocking PD-L1 increase PD-1<sup>+</sup> TAMs which produce IL-6 and hampered the Th1 response (31). Therefore, this provides a rationale behind combining IL-6 blockade with PD-L1 blocking antibody. Of note, these results stress the importance of correct sequential administration of different immunotherapeutic agents, as discussed in **chapter 6**. Thus, to achieve the most effective anti-tumor response in combination therapies, the timing and effect of each treatment on different immune cells in tumor microenvironment needs to be carefully investigated.

## Non-curative immunotherapy drives shift from inflamed tumors to non-inflamed tumors

HPV16 SLP vaccination of TC-1 tumors result in a strong tumor influx which subsequently attract inflammatory myeloid cells ((32, 33) and **Chapter 3**). As shown in **chapter 3**, this is accompanied by production of a large number of chemokines and cytokines in the tumor microenvironment reflecting this conversion of a cold to an inflamed tumor (**Figure 1B**). However, when a spontaneous anti-tumor response or an immunotherapy induced response does not lead to cure, the tumor microenvironment may be reshaped governed by a variety of genetic and/or environmental factors (34).

In **chapter 3**, we indicated that the recurrence of tumors after non-curative therapeutic vaccination resulted in a plethora of effects including 1) lower production of CXCL9/CXCL10 chemokines, 2) lowered expression of the CXCR3 chemokine receptor on T cells, 3) a tumor influx with classical TAMs. All these effects could have explained subsequent tumor escape in the face of boost vaccine-induced systemic expansion of functional tumor-specific T cells, but in fact were not the reason that the escaped tumors hardly were infiltrated with CD8 T cells (**Figure 1C**). Comparison of differences between the genetic profile of recurrent tumor and untreated untouched TC-1 tumor cells displayed changes in genes associated with the p53, TNF and the epithelial–mesenchymal transition (EMT) pathways (**chapter 3**). The strongest difference was in the genes associated with EMT, including  $\beta$ -catenin and TGF $\beta$ . Recently, it has been shown that EMT signature including TGF $\beta$  signaling, WNT/ $\beta$ -catenin pathway is highly associated with tumor T cell exclusion in different types of cancer (35–38). Indeed, antibody mediated blockade of TGF $\beta$  after initial tumor regression partly prevent tumor recurrence resulting in improved survival of mice. Examining tumors from a large cohort of metastatic urothelial cancer patients demonstrated that response to treatment is highly associated with T cell infiltration and high neoantigen or tumor mutation burden (37). Lack of the response is largely correlated with signature of TGF $\beta$  signaling in fibroblasts accompanied by exclusion of CD8 T cells from tumor. Besides TGF $\beta$ , high expression of *IFNGR1* gene expression was associated in non-responder while increased expression of *IFNG* was observed in responders. Although IFN $\gamma$  is favorable cytokine in anti-tumor immunity, continuous activation of IFN $\gamma$  signaling has been associated with adoptive resistance to immune checkpoint blockade. In **chapter 3**, we have shown that IFN $\gamma$  is highly expressed in the tumor microenvironment of the regressed tumor compared to untreated tumor. Therefore, this in combination with TGF $\beta$  could possibly explain the T cell exclusion and secondary resistance of tumor cells to SLP vaccine at the time of relapse.

Previously, it has been shown that T cells could not infiltrate into  $\beta$ -catenin-expressing tumors, not even when tumor-specific T cells were adoptively transferred (39). The lack of



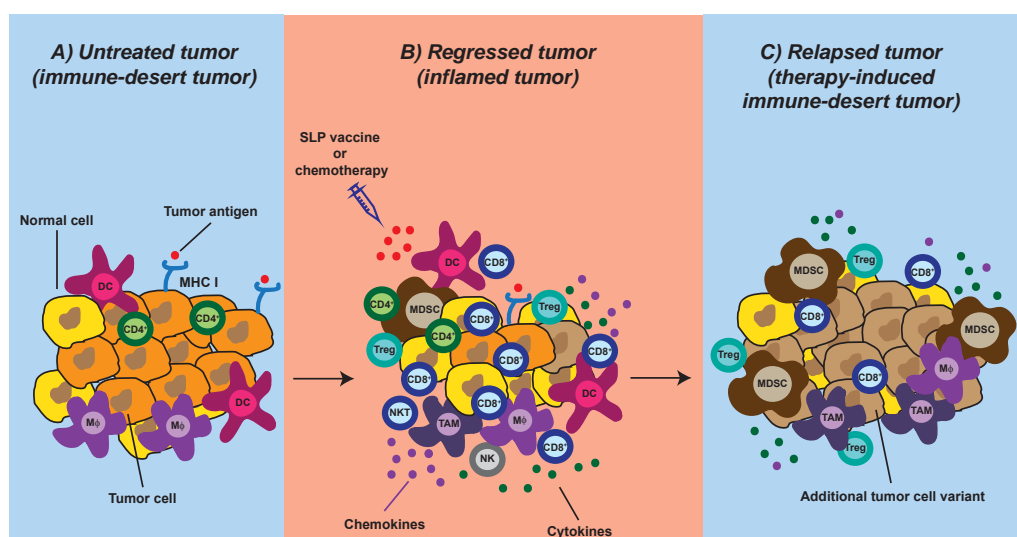


**Figure 1- Cancer-immune phenotypes.**

A) Untreated tumor is initially diagnosed as cold and less immunogenic tumor. At this stage, decrease in tumor burden by using conventional therapies and/or increase infiltration of immune cells in particular tumor specific T cells response is required. B) Immunotherapy approaches such as SLP vaccine and certain chemotherapeutic agents which affect the immune system can enhance the anti-tumor response by different mechanisms, thereby converting the immune-desert tumor to an inflamed tumor. Usually, this leads to the decrease in tumor burden and outgrowth. C) However, due to immunosuppressive tumor microenvironment or resistance mechanisms induced by tumor, tumor relapses. This phenotype of cancer immunity is usually accompanied by the occurrence of additional tumor cell variants which can also be generated during immune selection induced by immunotherapy. Therefore, all these phenomena lead to the relapse of a tumor with an immune-desert phenotype.

T-cell infiltration was due to the absence of the CXCL9/10 chemokines, produced by Batf3-dependent CD103<sup>+</sup> dendritic cells. In **chapter 3**, we also showed that at the time of the tumor recurrence CD8 T cells failed to traffic to the tumor possibly due to lowered production of T-cell attracting chemokines in the tumor microenvironment. Formally, we did not exclude whether the absence of Batf3-dependent CD103<sup>+</sup> DC was the underlying mechanism. However, our unpublished data have shown that CD103 is highly expressed on Ly6C<sup>low</sup> CD11b<sup>+</sup> myeloid cells. In **chapter 3**, we observed that tyrosine kinase inhibitor PLX3397 mainly depleted Ly6C<sup>low</sup> cells in the tumor although depletion of these cells did not affect the tumor regression and the subsequent immune-driven recurrence. Therefore, it is highly plausible that these CD103<sup>+</sup> cells do not play major role in our tumor model and chemokines which produced by other immune cells are adequate for T cell attraction and infiltration to the tumor. However, this concept still needs to be investigated in detail.

A highly interesting observation was that a directly ex-vivo cell sorted pure population of the recurrent tumor cells retained their resistance to vaccine therapy when reinjected into naïve mice but induced a completely different tumor microenvironment than was observed

in the original recurrent tumor, as now high percentages of vaccine-induced tumor-specific T cells infiltrated the tumors. This shows that also the local microenvironment in which tumor cells grow out also has an impact on the shape of the resulting tumor microenvironment. In another study, analysis of immune cell infiltration between primary non- small cell lung carcinomas (NSCLS) and corresponding metastases showed a lower density of CD8 T cells and a lower CD8/CD4 and CD8/CD68 ratio, indicating a differently shaped, more tumor growth- promoting, tumor microenvironment at the metastatic site (40, 41). At the one hand these differences may be due to the seeding of tumor sub-clones, which are also observed in NSCLC (42), fostering the formation of alternative microenvironments. On the other, also the local make-up of the metastatic site may play a role, as suggested by a recent study on the impact of the anatomical location on the tumor microenvironment composition of tumors induced by the same oncogenic pathway (43).

## Concluding remarks

The shortcoming of currently applied anti-cancer treatments is the lack of proper combination therapy based on the immune landscape of the tumor as well as inappropriate timing of the therapies combined.

Better understanding of elements involved in cancer-immune set points and fine-tuning of dynamic interaction between these factors needs to be explored in detail to achieve successful response to immunotherapy. For instance, our laboratory showed that cancer-driven leukocytosis hampered the induction of a strong vaccine-induced tumor-specific T cell response and that this may be overcome by vaccination two weeks after carboplatin-paclitaxel chemotherapy from the 2<sup>nd</sup> cycle onwards (44). This has resulted in a new larger study in patients with advanced HPV16-positive cervical cancer which recently reported clinical benefit for those patients with a strong vaccine-induced immune response (45).



## References

1. Hegde PS, Karanikas V, Evers S. The Where, the When, and the How of Immune Monitoring for Cancer Immunotherapies in the Era of Checkpoint Inhibition. *Clin Cancer Res.* 2016;22(8):1865-74.
2. Herbst RS, Soria JC, Kowanetz M, Fine GD, Hamid O, Gordon MS, et al. Predictive correlates of response to the anti-PD-L1 antibody MPDL3280A in cancer patients. *Nature.* 2014;515(7528):563-7.
3. Kim JM, Chen DS. Immune escape to PD-L1/PD-1 blockade: seven steps to success (or failure). *Ann Oncol.* 2016;27(8):1492-504.
4. Chen DS, Mellman I. Elements of cancer immunity and the cancer-immune set point. *Nature.* 2017;541(7637):321-30.
5. Sharma P, Hu-Lieskovan S, Wargo JA, Ribas A. Primary, Adaptive, and Acquired Resistance to Cancer Immunotherapy. *Cell.* 2017;168(4):707-23.
6. van der Sluis TC, van Duiker S, Huppelschoten S, Jordanova ES, Beyranvand Nejad E, Sloots A, et al. Vaccine-induced tumor necrosis factor-producing T cells synergize with cisplatin to promote tumor cell death. *Clin Cancer Res.* 2015;21(4):781-94.
7. Ma Y, Adjemian S, Mattarollo SR, Yamazaki T, Aymeric L, Yang H, et al. Anticancer chemotherapy-induced intratumoral recruitment and differentiation of antigen-presenting cells. *Immunity.* 2013;38(4):729-41.
8. Melief CJ, van der Burg SH. Immunotherapy of established (pre)malignant disease by synthetic long peptide vaccines. *Nat Rev Cancer.* 2008;8(5):351-60.
9. van der Burg SH. Correlates of immune and clinical activity of novel cancer vaccines. *Semin Immunol.* 2018.
10. van der Burg SH, Arens R, Ossendorp F, van Hall T, Melief CJ. Vaccines for established cancer: overcoming the challenges posed by immune evasion. *Nat Rev Cancer.* 2016;16(4):219-33.
11. Kenter GG, Welters MJ, Valentijn AR, Lowik MJ, Berends-van der Meer DM, Vloon AP, et al. Vaccination against HPV-16 oncoproteins for vulvar intraepithelial neoplasia. *N Engl J Med.* 2009;361(19):1838-47.
12. van Poelgeest MI, Welters MJ, van Esch EM, Stynenbosch LF, Kerpershoek G, van Persijn van Meerten EL, et al. HPV16 synthetic long peptide (HPV16-SLP) vaccination therapy of patients with advanced or recurrent HPV16-induced gynecological carcinoma, a phase II trial. *J Transl Med.* 2013;11:88.
13. Welters MJ, Kenter GG, de Vos van Steenwijk PJ, Lowik MJ, Berends-van der Meer DM, Essahsah F, et al. Success or failure of vaccination for HPV16-positive vulvar lesions correlates with kinetics and phenotype of induced T-cell responses. *Proc Natl Acad Sci U S A.* 2010;107(26):11895-9.
14. van Poelgeest MI, Welters MJ, Vermeij R, Stynenbosch LF, Loof NM, Berends-van der Meer DM, et al. Vaccination against Oncoproteins of HPV16 for Noninvasive Vulvar/Vaginal Lesions: Lesion Clearance Is Related to the Strength of the T-Cell Response. *Clin Cancer Res.* 2016;22(10):2342-50.
15. Daayana S, Elkord E, Winters U, Pawlita M, Roden R, Stern PL, et al. Phase II trial of imiquimod and HPV therapeutic vaccination in patients with vulval intraepithelial neoplasia. *Br J Cancer.* 2010;102(7):1129-36.
16. Trimble CL, Morrow MP, Kraynyak KA, Shen X, Dallas M, Yan J, et al. Safety, efficacy, and immunogenicity of VGX-3100, a therapeutic synthetic DNA vaccine targeting human papillomavirus 16 and 18 E6 and E7 proteins for cervical intraepithelial neoplasia 2/3: a randomised, double-blind, placebo-controlled phase 2b trial. *Lancet.* 2015;386(10008):2078-88.
17. Bagarazzi ML, Yan J, Morrow MP, Shen X, Parker RL, Lee JC, et al. Immunotherapy against HPV16/18 generates potent TH1 and cytotoxic cellular immune responses. *Sci Transl Med.* 2012;4(155):155ra38.

18. Bijker MS, van den Eeden SJ, Franken KL, Melief CJ, Offringa R, van der Burg SH. CD8+ CTL priming by exact peptide epitopes in incomplete Freund's adjuvant induces a vanishing CTL response, whereas long peptides induce sustained CTL reactivity. *J Immunol.* 2007;179(8):5033-40.
19. Iwai Y, Ishida M, Tanaka Y, Okazaki T, Honjo T, Minato N. Involvement of PD-L1 on tumor cells in the escape from host immune system and tumor immunotherapy by PD-L1 blockade. *Proc Natl Acad Sci U S A.* 2002;99(19):12293-7.
20. Brahmer JR, Drake CG, Wollner I, Powderly JD, Picus J, Sharfman WH, et al. Phase I study of single-agent anti-programmed death-1 (MDX-1106) in refractory solid tumors: safety, clinical activity, pharmacodynamics, and immunologic correlates. *J Clin Oncol.* 2010;28(19):3167-75.
21. Brahmer JR, Tykodi SS, Chow LQ, Hwu WJ, Topalian SL, Hwu P, et al. Safety and activity of anti-PD-L1 antibody in patients with advanced cancer. *N Engl J Med.* 2012;366(26):2455-65.
22. Rosenberg JE, Hoffman-Censits J, Powles T, van der Heijden MS, Balar AV, Necchi A, et al. Atezolizumab in patients with locally advanced and metastatic urothelial carcinoma who have progressed following treatment with platinum-based chemotherapy: a single-arm, multicentre, phase 2 trial. *Lancet.* 2016;387(10031):1909-20.
23. Topalian SL, Hodi FS, Brahmer JR, Gettinger SN, Smith DC, McDermott DF, et al. Safety, activity, and immune correlates of anti-PD-1 antibody in cancer. *N Engl J Med.* 2012;366(26):2443-54.
24. Hodi FS, O'Day SJ, McDermott DF, Weber RW, Sosman JA, Haanen JB, et al. Improved survival with ipilimumab in patients with metastatic melanoma. *N Engl J Med.* 2010;363(8):711-23.
25. van Montfoort N, Borst L, Korner MJ, Sluijter M, Marijt KA, Santegoets SJ, et al. NKG2A Blockade Potentiates CD8 T Cell Immunity Induced by Cancer Vaccines. *Cell.* 2018;175(7):1744-55 e15.
26. Tumeh PC, Harview CL, Yearley JH, Shintaku IP, Taylor EJ, Robert L, et al. PD-1 blockade induces responses by inhibiting adaptive immune resistance. *Nature.* 2014;515(7528):568-71.
27. Canale FP, Ramello MC, Nunez N, Araujo Furlan CL, Bossio SN, Gorosito Serran M, et al. CD39 Expression Defines Cell Exhaustion in Tumor-Infiltrating CD8(+) T Cells. *Cancer Res.* 2018;78(1):115-28.
28. Wherry EJ, Ha SJ, Kaech SM, Haining WN, Sarkar S, Kalia V, et al. Molecular signature of CD8+ T cell exhaustion during chronic viral infection. *Immunity.* 2007;27(4):670-84.
29. Im SJ, Hashimoto M, Gerner MY, Lee J, Kissick HT, Burger MC, et al. Defining CD8+ T cells that provide the proliferative burst after PD-1 therapy. *Nature.* 2016;537(7620):417-21.
30. Siddiqui I, Schaeuble K, Chennupati V, Fuertes Marraco SA, Calderon-Copete S, Pais Ferreira D, et al. Intratumoral Tcf1(+)PD-1(+)CD8(+) T Cells with Stem-like Properties Promote Tumor Control in Response to Vaccination and Checkpoint Blockade Immunotherapy. *Immunity.* 2019;50(1):195-211 e10.
31. Tsukamoto H, Fujieda K, Miyashita A, Fukushima S, Ikeda T, Kubo Y, et al. Combined Blockade of IL6 and PD-1/PD-L1 Signaling Abrogates Mutual Regulation of Their Immunosuppressive Effects in the Tumor Microenvironment. *Cancer Res.* 2018;78(17):5011-22.
32. Thoreau M, Penny HL, Tan K, Regnier F, Weiss JM, Lee B, et al. Vaccine-induced tumor regression requires a dynamic cooperation between T cells and myeloid cells at the tumor site. *Oncotarget.* 2015;6(29):27832-46.
33. van der Sluis TC, Sluijter M, van Duikeren S, West BL, Melief CJ, Arens R, et al. Therapeutic Peptide Vaccine-Induced CD8 T Cells Strongly Modulate Intratumoral Macrophages Required for Tumor Regression. *Cancer Immunol Res.* 2015;3(9):1042-51.
34. Rooney MS, Shukla SA, Wu CJ, Getz G, Hacohen N. Molecular and genetic properties of tumors associated with local immune cytolytic activity. *Cell.* 2015;160(1-2):48-61.
35. Chae YK, Chang S, Ko T, Anker J, Agte S, Iams W, et al. Epithelial-mesenchymal transition (EMT) signature is inversely associated with T-cell infiltration in non-small cell lung cancer (NSCLC). *Sci Rep.* 2018;8(1):2918.



36. Lohr J, Ratliff T, Huppertz A, Ge Y, Dictus C, Ahmadi R, et al. Effector T-cell infiltration positively impacts survival of glioblastoma patients and is impaired by tumor-derived TGF-beta. *Clin Cancer Res.* 2011;17(13):4296-308.
37. Mariathasan S, Turley SJ, Nickles D, Castiglioni A, Yuen K, Wang Y, et al. TGFbeta attenuates tumour response to PD-L1 blockade by contributing to exclusion of T cells. *Nature.* 2018;554(7693):544-8.
38. Tauriello DVF, Palomo-Ponce S, Stork D, Berenguer-Llergo A, Badia-Ramentol J, Iglesias M, et al. TGFbeta drives immune evasion in genetically reconstituted colon cancer metastasis. *Nature.* 2018;554(7693):538-43.
39. Spranger S, Dai D, Horton B, Gajewski TF. Tumor-Residing Batf3 Dendritic Cells Are Required for Effector T Cell Trafficking and Adoptive T Cell Therapy. *Cancer Cell.* 2017;31(5):711-23 e4.
40. Baine MK, Turcu G, Zito CR, Adeniran AJ, Camp RL, Chen L, et al. Characterization of tumor infiltrating lymphocytes in paired primary and metastatic renal cell carcinoma specimens. *Oncotarget.* 2015;6(28):24990-5002.
41. Muller P, Rothschild SI, Arnold W, Hirschmann P, Horvath L, Bubendorf L, et al. Metastatic spread in patients with non-small cell lung cancer is associated with a reduced density of tumor-infiltrating T cells. *Cancer Immunol Immunother.* 2016;65(1):1-11.
42. McGranahan N, Furness AJ, Rosenthal R, Ramskov S, Lyngaa R, Saini SK, et al. Clonal neoantigens elicit T cell immunoreactivity and sensitivity to immune checkpoint blockade. *Science.* 2016;351(6280):1463-9.
43. Santegoets SJ, van Ham VJ, Ehsan I, Charoentong P, Duurland CL, van Unen V, et al. The Anatomical Location Shapes the Immune Infiltrate in Tumors of Same Etiology and Affects Survival. *Clin Cancer Res.* 2019;25(1):240-52.
44. Welters MJ, van der Sluis TC, van Meir H, Loof NM, van Ham VJ, van Duikeren S, et al. Vaccination during myeloid cell depletion by cancer chemotherapy fosters robust T cell responses. *Sci Transl Med.* 2016;8(334):334ra52.
45. Melief CJ, Welters MJP, Vergote I, Kroep JR, Kenter GG, Ottevanger PB, et al. Chemo-immunotherapy for advanced cervical cancer is associated with prolonged survival. Submitted. 2019.



## Nederlandse samenvatting

De rol van het immuunsysteem in het controleren van tumorgroei is nu alom geaccepteerd. Het adaptieve immuunsysteem is niet alleen in staat om tumor-geassocieerde antigenen (TAA) en tumor-specifieke antigen (TSA) te herkennen, maar kan ook kankercellen opruimen en langetermijngeheugen genereren dat bescherming biedt tegen het terugkomen van de tumor. Desalniettemin weten veel tumoren toch nog verder te groeien door gebruik te maken van verscheidene strategieën om aan het immuunsysteem te ontsnappen en tumor-specifieke afweerreacties te onderdrukken of te omzeilen. Om deze reden zijn er verschillende kankerbehandelingen ontwikkeld, die gekenmerkt worden door het direct reduceren van tumormassa of het stimuleren van afweerreacties tegen kanker. Conventionele behandelingen zoals chirurgie, radiotherapie en chemotherapie zijn ontworpen om de tumormassa te reduceren en tumorgroei te remmen. Veel recente studies hebben aangetoond dat deze behandelingen bovendien het immuunsysteem kunnen stimuleren. Met het oog op de rol van het immuunsysteem in het controleren van tumorgroei, zijn er verscheidene immunotherapeutische strategieën ontworpen om de afweerreactie tegen tumoren te versterken.

Voor het induceren van goede tumorgroei controlerende afweerreacties is er een interactie tussen verschillende componenten van het immuunsysteem nodig. In dit opzicht spelen antigeen-presenterende cellen (APCs) een cruciale rol door T-cellen die tumorcellen specifiek kunnen elimineren te stimuleren. Voor de stimulatie van antigeen-specifieke T-cellen dienen APCs drie signalen aan T-cellen te geven. Het eerste signaal is de presentatie van antigeen in de context van een MHC-complex aan de T-celreceptor (TCR). Om dit signaal te kunnen geven, dienen peptiden afkomstig van intracellulaire of extracellulaire eiwitten door APCs te worden opgenomen, verwerkt en gepresenteerd door het MHC-complex op deze cellen. De presentatie van exogene antigenen in MHC klasse I moleculen op APCs, een proces genaamd kruispresentatie, leidt tot de activatie van naïeve CD8 T-cellen welke daarop cytotoxische T-lymfocyten (CTL) worden. Om de T-cellen volledig te activeren zijn daarnaast nog twee complementaire signalen vereist. Het tweede signaal wordt gedreven door costimulatie moleculen, zoals CD80 en CD86, die op APCs tot expressie komen en kunnen binden aan hun unieke receptoren op T-cellen. Het derde signaal wordt bezorgd door cytokines zoals IL-12 die door APCs geproduceerd worden en binden aan cytokinereceptoren op T-cellen. Op basis van deze mechanismes zijn verscheidene immunotherapeutische strategieën ontwikkeld om de anti-tumorresponsen te versterken. De ontwikkeling van adoptieve celtherapie (ACT) bijvoorbeeld is gebaseerd op de ex-vivo isolatie en expansie van antigeen-specifieke T-cellen en laat veelbelovende resultaten zien in de behandeling van verschillende soorten kanker. Vaccins inclusief synthetische lange peptiden, virale vectoren, RNA- of DNA-vectoren hebben



als doel de hoeveelheid van tumor-specifieke T-cel respons te vergroten en hun activatie te bewerkstelligen. Een andere aanpak om de tumor-specifieke T-celrespons te verbeteren is de toepassing van agonistische antilichamen gericht tegen costimulatie moleculen. Voorbeelden van costimulatie moleculen waartegen agonistische antilichamen worden gebruikt in kanker-immuuntherapie zijn CD27, CD40L, CD40, 4-1BB, OX40. T-cel reacties kunnen ook worden versterkt door andere immuunmodulatoire stoffen zoals cytokines. Gezien de belangrijke rol van de tumor-micro-omgeving waarin de T cellen hun werk moeten doen is een andere strategie gebaseerd op het tegengaan van immuunsuppressie in deze omgeving.

Coinhibitoire receptoren komen tot expressie op T-cellen om de T-celrespons te verzwakken na de activatie van T-cellen. Echter, zowel tumorcellen als myeloïde cellen in de tumor-micro-omgeving kunnen misbruik maken van deze receptoren door de liganden voor deze receptoren tot expressie te brengen, en zo de anti-tumor T-cel respons te verzwakken. Deze T-cel remmende moleculen, ook wel immuuncheckpoints genoemd, zijn daarom interessante targets voor immuuntherapie. Verscheidene blokkerende antilichamen gericht tegen CTLA-4, PD-1 of diens ligand PD-L1 zijn met succes ontwikkeld om remmende signalen te blokkeren. Naast remmende receptoren worden ook immuunremmende moleculen of cytokines geproduceerd in de tumor-micro-omgeving door tumorcellen of immuunsuppressieve immuuncellen die mogelijk aangepakt kunnen worden.

In de kliniek worden verschillende vormen van immuuntherapie gecombineerd met standaardbehandelingen, inclusief chemotherapie, specifiek voor het type tumor dat wordt behandeld. Verschillende studies hebben de effectiviteit van deze combinatiebehandelingen aangetoond. Desalniettemin hebben de variërende resultaten in patiënten geresulteerd in nieuwe vragen en hypothesen die nog onderzocht moeten worden. De studies beschreven in dit proefschrift beogen deze vragen te beantwoorden teneinde de mechanismes van immuuntherapie te begrijpen en een manier te vinden om de klinische effectiviteit te verbeteren.

Chemotherapeutica zoals cisplatine worden vaak gebruikt om patiënten met immunogene kankers te behandelen en zouden een van de standaardbehandelingen zijn die gebruikt kunnen worden voor combinatie met immuuntherapie. Om deze reden hebben we ons in **hoofdstuk 2** gericht op de immunologische effecten van cisplatine. We tonen aan dat de maximum getolereerde dosis van cisplatine het immuunsysteem nodig heeft voor het definitief genezen van tumordragende muizen. Cisplatine is niet alleen direct toxisch voor tumorcellen, hetgeen de groei van tumorcellen enorm vertraagt, maar stimuleert ook het immuunsysteem. De door het immuunsysteem gemedieerde eliminatie van tumoren door cisplatine vereist myeloïde cellen en T-cellen en is geassocieerd met een veel sterkere intratumorale ontsteking, gekenmerkt door de infiltratie van nieuwe APCs en een hogere expressie van costimulatie

moleculen op T-cellen, als gevolg van het vrijkomen van ontsteking bevorderende eiwitten s als gevolg van tumorcel dood.

Bij de immuunmonitoring van onze klinische trials met therapeutische vaccinatie in patiënten met HPV-geïnduceerde ziektes kwam naar voren dat de vaccin-geïnduceerde immuunrespons zwakker is in patiënten met geavanceerde kanker in een gevorderd stadium. Om deze reden hebben we in **hoofdstuk 3** gebruik gemaakt van suboptimale vaccinatiestrategieën voor HPV16 SLP-vaccinatie in muizen om deze situatie te simuleren. We laten zien dat suboptimale vaccinatie in eerste instantie nog wel in staat is om tumorregressie te induceren en de uitgroei van HPV-geassocieerde tumorcellen te voorkomen, maar uiteindelijk komen de tumoren weer terug en groeien progressief uit. We tonen aan dat een suboptimale anti-tumorrespons resulteert in een verandering van de tumor cellen waardoor zij alsnog resistent worden, zogenaamde secundaire resistentie. Terug groeiende tumoren hebben een deregulatie in genen geassocieerd met de apoptose-signaleringsroute, inclusief P53, en in genen betrokken bij epitheliale-mesenchymale transitie (EMT) zoals TGF $\beta$ ,  $\beta$ -catenine. Dit is geassocieerd met een duidelijke afname van het aantal infiltrerende leukocyten, met name CD8 T-cellen en APCs. De toediening van het chemotherapeutikum cisplatine of blokkade van TGF $\beta$  na initiële regressie kon de terug groei van tumoren voorkomen. We laten zien dat deze terug groeiende tumoren, wanneer zij getransplanteerd worden naar een naïeve muis, niet meer gevoelig waren voor immuuntherapie tenzij ook cisplatine werd gegeven om de immuuninfiltratie van tumoren te verhogen, hetgeen het belang van de tumor-micro-omgeving in combinatiebehandelingen benadrukt om tot succesvolle controle van tumorlast te komen.

Eerdere studies hebben aangetoond dat de resistentie van veel tumoren tegen chemotherapie was geassocieerd met toegenomen productie van IL-6 door tumorcellen. Werk uit onze groep suggereerde dat er geen directe resistentie van tumorcellen tegen chemotherapie was, maar dat de chemoresistentie was gestoeld op differentiatie van myeloïde cellen richting een afweer remmend fenotype als gevolg van blootstelling aan IL-6. In **hoofdstuk 4** laten we zien dat IL-6 geproduceerd door tumorcellen inderdaad de anti-tumor effectiviteit van cisplatine chemotherapie verminderd, en daarnaast ook die van immuuntherapie met het HPV16 SLP vaccin. Resistentie was geassocieerd met sterke IL-6-gemedieerde veranderingen in systemische en lokale myeloïde cel-fenotypes en gepaard ging met een verminderde tumor-specifieke T-cel respons. We hebben verscheidene strategieën bestudeerd om deze IL-6-gemedieerde effecten te blokkeren, maar dit werd bemoeilijkt door het feit dat IL-6 signalering ook benodigd is voor het induceren van een effectieve vaccin-geïnduceerde tumor-specifieke T-celrespons en voor het optimaal functioneren van tumordodende macrofagen tijdens initiële tumorregressie. De timing van de therapieën was cruciaal in dit geval aangezien blokkade van IL-6 na initiële tumorregressie de gevoeligheid van IL-6-producerende tumoren voor immuuntherapie verbeterde.

Om een langdurige effector T-celrespons te induceren, hebben we in **hoofdstuk 5** de potentie van muis cytomegalovirus onderzocht om gebruikt te worden als virale vector voor vaccins. We laten zien dat er gedefinieerde drempels van vaccin-specifieke T-cellen gecorreleerd zijn aan bescherming tegen de tumoren.

Aangezien er in elke fase van de anti-tumor immuunrespons een verschillend type hulp benodigd zou kunnen zijn om maximale therapeutische effectiviteit te bereiken, bespreken we in **hoofdstuk 6** de correcte timing van verschillende soorten chemotherapeutica of afweer modulators, wanneer deze gecombineerd worden met verschillende op T-cellen gerichte immuuntherapieën. Dit hoofdstuk benadrukt ook het belang van immuunmonitoring als essentiële strategie om het juiste behandelingschema voor combinatietherapie te ontwerpen.

Tot slot worden in **hoofdstuk 7** de algemene aspecten en het belang van de in dit proefschrift beschreven experimenten besproken in de context van combinatietherapie. Ook wordt de recente literatuur en het toekomstbeeld van behandelstrategieën voor kanker hier bediscussieerd.

## Acknowledgements

“Life changes you, but you can also change life”. This came to my mind in one of Tumor Immunology group’s lunches during my PhD. At that time, I didn’t know when I am going to finish this chapter of my life, but I was sure I would do that, and I did it! Now that the six-year journey of my PhD life has come to the end, I am taking this opportunity to acknowledge all the people who has been somehow present in this chapter of my life.

This journey started by doing the second internship of my master study in the Tumor immunology group under the supervision of Tetje and Ramon. Dear **Tetje**, I’m happy that I could start my internship with you and later becoming colleague together. Thanks for giving me this opportunity and for all your efforts as my supervisor. Dear **Ramon**, thank you too for granting me the opportunity to pursue my PhD with you and in your group. All this time, I have enjoyed working with you and I have learned a lot from you. Thank you for all the times of fruitful discussions about our projects and papers. And, dear **Sjoerd**, I am profoundly grateful that I have had the chance to work under your supervision and your great leadership. My research would have been impossible without the aid and support of you to start my PhD in IHB and later in Medical Oncology by giving me the chance of doing post-doctoral research on one of my PhD projects. Dear **Thorwald**, although you joined us in the middle of the way I always appreciate your great ideas for my projects, which indeed improved the quality of them greatly.

With all the pains and gains I had during my PhD life, I remember very well the help of two most important persons, my paranimphs, **Suzanne** and **Camilla**. Undeniably, I could not finish all the PhD projects without their invaluable helps. Dear **Suzanne**, thank you for all your great, realistic suggestions for experiments and helps with performing them. Dear **Camilla**, I cannot express how much I’m happy and grateful that you started your job with us on my projects. You made my PhD life in Medical Oncology joyful when I just moved to the department. We both started here, have grown, and together performed impossible experiments on many long-working-hours days. The only thing I can say here is, “*here it is, we did it together*”!

My special thanks go to all my colleagues in the Tumor Immunology group, **Marcel, Anke, Marieke, Jan Willem, Brett, Elena, Guillaume, Esme, Iris, Jeroen**, and former colleagues **Ayse, Suzanne Welten, Gijs**; I’m so thankful of having had this great chance to work with you all. I have always had the feeling that we have not only been colleagues but also more like family members. Dear **Marcel**, you were the best desk-neighbor in the world whom I enjoyed sitting next to for all that years. Thanks for listening and tolerating all my naggings and cursing, and all your support of being always there for me. Certainly, I will never forget

all the dinners, teas and late working hours and activities we did together. Dear **Anke**, I really enjoyed working with you and I will never forget your smile and your positive attitudes when I came to you to ask for help or questions. Dear **Marieke**, it was so nice to have a colleague like you who is so motivational when I was desperate of the PhD and life. You always remind me to focus on finishing my PhD and celebrate my day in a way I like. Dear **Jan Willem**, thank you for all your helpful comments while we were sitting together in one room and discussing my projects both in Tumor Immunology and Medical Oncology. I am grateful that you could help me with the Dutch summary of this publication. Dear **Guillaume**, I remember you joined us at the time when my first paper got accepted after 3 years of my PhD. I have always been impressed by your energy and humor at the occasional times we felt down and desperate. You always give me very good comments about my presentations and you make me more motivated. Dear **Brett, Esme, Elena, Iris** and **Jeroen** thank you all for helping me when I came to your rooms for asking all kind of questions. I always felt welcome among you guys.

I am grateful to work with all the people in Medical Oncology; **Lien, Marij, Els, Saskia, Nadine, Ferenc, Koen, Linda** (Borst), **Marjolein, Vanessa, Nikki, Ilina, Sanne, Marten, Priscilla, Chantal, Linda, Monique** and the recent joined members **Christianne, Marit** and **Jim**. Thanks for all your support. Dear **Lien**, I would like to express my special appreciation to you for all your helps.

Looking back at all the work that has been done, I am also thankful to many other people who helped me. Special thanks to the colleagues in the **FACS facility; Center for Proteomics and Metabolomics** and **peptide facility, animal facility** (PDC and IVD).

And coming to the most important and beloved people in my life; I express my greatest attitude and appreciation to my parents. **Maman** and **Baba**; now with tears in my eyes I am writing these words for you. I am sure I could not achieve and have anything in my life without your support. You have always motivated and encouraged me to study harder and be a useful person for myself and in society. You have done whatever you could to support me for moving to the Netherlands and being successful in my life. Thanks for everything.

Last but not least, I would like to thank a precious person in my life, my brother, **Ashkan**. I am sure I could not have all the things that I have now in my life without him and his support. **Ashki**, thank you for being such a great brother to me. I have always appreciated your support of me for moving to the Netherlands and continuing my study here. During all

these years being far from our parents, you have been the only one with me and supported me in all the aspects of my life. I cannot really express all my feelings in these few words but I'm sure you yourself know how thankful I am to have you in my life.

Elham Beyranvand Nejad  
Leiden, The Netherlands

## List of publications

- **Demarcated thresholds of tumor-specific CD8 T cells elicited by MCMV-based vaccine vectors provide robust correlates of protection.**  
Beyranvand Nejad E, Ratts RB, Panagioti E, Meyer C, Oduro JD, Cicin-Sain L, Früh K, van der Burg SH, Arens R.  
*J Immunother Cancer*. 2019 Jan 31;7(1):25.
- **The importance of correctly timing cancer immunotherapy.**  
Beyranvand Nejad E, Welters MJ, Arens R, van der Burg SH.  
*Expert Opin Biol Ther*. 2017 Jan;17(1):87-103. Review.
- **Tumor Eradication by Cisplatin Is Sustained by CD80/86-Mediated Costimulation of CD8<sup>+</sup> T Cells.**  
Beyranvand Nejad E, van der Sluis TC, van Duikeren S, Yagita H, Janssen GM, van Veelen PA, Melief CJ, van der Burg SH, Arens R.  
*Cancer Res*. 2016 Oct 15;76(20):6017-6029.
- **Vaccine-induced tumor necrosis factor-producing T cells synergize with cisplatin to promote tumor cell death.**  
van der Sluis TC, van Duikeren S, Huppelschoten S, Jordanova ES, Beyranvand Nejad E, Sloots A, Boon L, Smit VT, Welters MJ, Ossendorp F, van de Water B, Arens R, van der Burg SH, Melief CJ.  
*Clin Cancer Res*. 2015 Feb 15;21(4):781-94.

## Curriculum vitae

Elham Beyranvand Nejad was born on August 20<sup>th</sup> 1986, in Tehran, Iran. In 2004, she obtained her diploma in Experimental Sciences at the Farasat high school in Tehran, Iran. In the same year, she started her undergraduate education in Medical Laboratory Science at Shahid Beheshti University of Medical Sciences in Tehran, Iran. After obtaining her associate degree in 2006, she continued her education to bachelor of Medical Laboratory Science in Tehran University Medical Sciences and completed her bachelor degree in 2009 in which she was selected as the third place of talented students. In September 2009, she started her first scientific job as a Laboratory Technician in Endocrinology and Metabolism Research Institute in Tehran, Iran; where she performed various diagnostic tests related to hormonal disorders in patients. In October 2010, she moved to the Netherlands to start her master education in Biomedical Sciences at Leiden University. For this program, she was awarded a Leiden University Excellence Scholarship Bronze (first year) and Ivory (second year). As part of her master study, she carried out five months internship in the department of Infection Disease under supervision of Dr. P.H. Nibbering and Dr. A. de Breij. Later, she performed her second internship for nine months in the Tumor Immunology group under supervision of Dr. R. Arens and Dr. T. van der Sluis; where she investigated the immune stimulatory mechanism(s) underlying chemotherapy. During her master program she was granted a BW-plus master program grant in December 2011 and further to the BW-plus PhD program grant in December in 2012. With the BW-plus PhD program, she started her PhD project in May 2013 in Immunohematology and Blood Transfusion department at the Leiden University Medical Center under the supervision of Dr. R. Arens and Prof. Dr. S.H. van der Burg. The outcome of this work has been published in different articles as described in this dissertation. During her PhD, she participated and presented in the different national and international conferences. She was awarded for the EACR poster prize at the 13<sup>th</sup> international conference of Progress In Vaccination Against Cancer (PIVAC 13) in 2013 and she was nominated for the AIO (PhD) award at the Dutch Tumor Immunology Meeting (DTIM) for the best presentation in 2018. In addition, she received in 2019 a Keystone Symposia scholarship (Cancer Vaccine). Since April 2017, she has been working as a post-doctoral researcher in the group of Prof. Dr. S.H. van der Burg at the Medical Oncology department of LUMC on the role of IL-6 in cancer chemo-immunotherapy.





